(12) INTERNATIONAL APPLICATION PUBLISHED UNDER THE PATENT COOPERATION TREATY (PCT)

(19) World Intellectual Property Organization
International Bureau

(43) International Publication Date
2 June 2016 (02.06.2016)

WIPO | PCT

(10) International Publication Number
WO 2016/086080 A1

(51) International Patent Classification:
C07D 487/04 (2006.01) *A61P 35/00* (2006.01)
A61K 31/407 (2006.01)

(21) International Application Number:
PCT/US2015/062572

(22) International Filing Date:
25 November 2015 (25.11.2015)

(25) Filing Language: English

(26) Publication Language: English

(30) Priority Data:
62/084,652 26 November 2014 (26.11.2014) US

(71) Applicant: **CEPHALON, INC.** [US/US]; 41 Moores Road, PO Box 4011, Frazer, PA 19355 (US).

(72) Inventors: **BIERLMAIER, Stephen, J.**; 246 Thornridge Drive, Thorndale, PA 19372 (US). **HALTIWANGER, Ralph, C.**; 1262 Bridgewater Drive, West Chester, PA 19380 (US). **JACOBS, Martin, J.**; 146 Sugartree Lane, Versailles, KY 40383 (US).

(74) Agents: **VILLACORTA, Gilberto, M.** et al.; Foley and Lardner LLP, 3000 K Street, N.W., 6th Floor, Washington, DC 20007-5109 (US).

(81) Designated States *(unless otherwise indicated, for every kind of national protection available)*: AE, AG, AL, AM, AO, AT, AU, AZ, BA, BB, BG, BH, BN, BR, BW, BY, BZ, CA, CH, CL, CN, CO, CR, CU, CZ, DE, DK, DM, DO, DZ, EC, EE, EG, ES, FI, GB, GD, GE, GH, GM, GT, HN, HR, HU, ID, IL, IN, IR, IS, JP, KE, KG, KN, KP, KR, KZ, LA, LC, LK, LR, LS, LU, LY, MA, MD, ME, MG, MK, MN, MW, MX, MY, MZ, NA, NG, NI, NO, NZ, OM, PA, PE, PG, PH, PL, PT, QA, RO, RS, RU, RW, SA, SC, SD, SE, SG, SK, SL, SM, ST, SV, SY, TH, TJ, TM, TN, TR, TT, TZ, UA, UG, US, UZ, VC, VN, ZA, ZM, ZW.

(84) Designated States *(unless otherwise indicated, for every kind of regional protection available)*: ARIPO (BW, GH, GM, KE, LR, LS, MW, MZ, NA, RW, SD, SL, ST, SZ, TZ, UG, ZM, ZW), Eurasian (AM, AZ, BY, KG, KZ, RU, TJ, TM), European (AL, AT, BE, BG, CH, CY, CZ, DE, DK, EE, ES, FI, FR, GB, GR, HR, HU, IE, IS, IT, LT, LU, LV, MC, MK, MT, NL, NO, PL, PT, RO, RS, SE, SI, SK, SM, TR), OAPI (BF, BJ, CF, CG, CI, CM, GA, GN, GQ, GW, KM, ML, MR, NE, SN, TD, TG).

Published:

— *with international search report (Art. 21(3))*

— *before the expiration of the time limit for amending the claims and to be republished in the event of receipt of amendments (Rule 48.2(h))*

WO 2016/086080 A1

(54) Title: CRYSTALLINE FORMS OF PARP INHIBITORS

(57) Abstract: The present disclosure relates to crystalline forms of 4,5,6,7-tetrahydro-l l-methoxy-2- [(4-methyl-1-piperazinyl)methyl]- 1*H*-cyclopenta[*a*]pyrrolo [3,4-c]carbazole- 1,3 (2*H*)-dione, including salts forms and free base forms.

CRYSTALLINE FORMS OF PARP INHIBITORS

CROSS REFERENCE TO RELATED APPLICATION

[0001] This application claims the benefit of U.S. Provisional Application No. 62/084,652, filed November 26, 2014, the entirety of which is incorporated herein by reference.

TECHNICAL FIELD

[0002] The present disclosure relates to crystalline forms of 4,5,6,7-tetrahydro-11-methoxy-2-[(4-methyl-1-piperazinyl)methyl]-1*H*-cyclopenta[*a*]pyrrolo[3,4-*c*]carbazole-1,3(2*H*)-dione and salts thereof.

BACKGROUND

[0003] Compound A (4,5,6,7-Tetrahydro-11-methoxy-2-[(4-methyl-1-piperazinyl)methyl]-1*H*-cyclopenta[*a*]pyrrolo[3,4-*c*]carbazole-1,3(2*H*)-dione) is a PARP (poly ADP-ribose polymerase) inhibitor for use in the treatment of breast, ovarian, and other cancers, either alone or in conjunction with chemotherapy or radiotherapy. *See, e.g.,* U.S. Patent Nos. 7,122,679; 8,716,493; and 8,633,314.

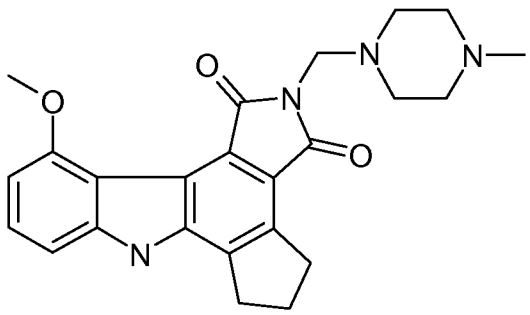

Compound A

[0004] Compound A is a prodrug of Compound B:

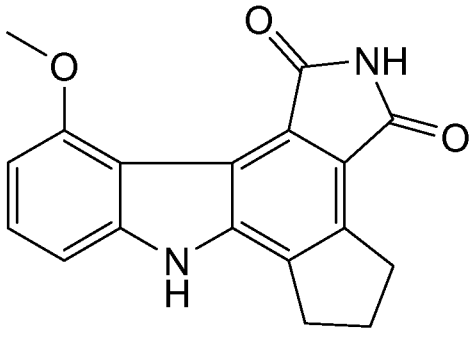

Compound B

[0005] The free base form of Compound A forms hydrates, which are undesirable. In addition, the free base form of Compound A has a low bulk density, impeding manufacturing. Alternative forms of Compound A are needed.

SUMMARY

[0006] The disclosure is directed to Compound A, acetate salt Form $A_{1.5}$; Compound A, glycolate salt hydrate Form A_1; Compound A, L-malate salt Form A_1; Compound A, L-malate salt Form $A_{1.5}$; Compound A, L-pyroglutamate salt Form A_1; Compound A, free base Form C_0; Compound A, hydrochloride salt Form A; Compound A, fumarate salt Form A; and Compound A, p-toluenesulfonate salt Form A. Pharmaceutical compositions comprising one or more of these forms are also described. Methods of using these forms is described, as well.

BRIEF DESCRIPTION OF THE DRAWINGS

[0007] Figure 1 shows an XRPD Pattern for Compound A Free Base, Form A_0.

[0008] Figure 2 shows a DSC/TGA Overlay for Compound A Free Base, Form A_0.

[0009] Figure 3 shows an XRPD Pattern of Compound A Acetate Salt, Form $A_{1.5}$.

[0010] Figure 4 shows VT-XRPD Patterns of Compound A Acetate Salt, Form $A_{1.5}$ - Requested Mode.

[0011] Figure 5 shows VT-XRPD Patterns of Compound A Acetate Salt, Form $A_{1.5}$ - Continuous Mode.

[0012] Figure 6 shows a DSC and TGA Overlay of Compound A Acetate Salt, Form $A_{1.5}$.

[0013] Figure 7 shows a DVS Overlay of Compound A Acetate Salt, Form $A_{1.5}$.

[0014] Figure 8 shows a photomicrograph of Compound A Acetate Salt, Form $A_{1.5}$.

[0015] Figure 9 shows an XRPD Pattern of Compound A Glycolate Salt Hydrate, Form A_1.

[0016] Figure 10 shows thermal XRPD Patterns of Compound A Glycolate Salt Hydrate, Form A_1.

[0017] Figure 11 shows a DSC and TGA Overlay of Compound A Glycolate Salt Hydrate, Form A_1.

[0018] Figure 12 shows a DVS Overlay of Compound A Glycolate Salt Hydrate, Form A_1.

[0019] Figure 13 shows a photomicrograph of Compound A Glycolate Salt Hydrate, Form A_1.

[0020] Figure 14 shows an XRPD Pattern of Compound A L-Malate Salt, Form A_1.

[0021] Figure 15 shows VT-XRPD Patterns of Compound A Malate Salt, Form A_1.

[0022] Figure 16 shows a DSC and TGA Overlay of Compound A L-Malate Salt, Form A_1.

[0023] Figure 17 shows a DVS of Compound A L-Malate Salt, Form A_1.

[0024] Figure 18 shows a photomicrograph of Compound A L-Malate Salt, Form A_1.

[0025] Figure 19 shows an XRPD Pattern of Compound A L-Malate Salt, Form $A_{1.5}$

[0026] Figure 20 shows a DSC and TGA Overlay of Compound A L-Malate Salt, Form $A_{1.5}$.

[0027] Figure 21 shows an XRPD Pattern of Compound A L-Pyroglutamate Salt, Form A_1.

[0028] Figure 22 shows VT-XRPD Patterns of Compound A L-Pyroglutamate Salt, Form A_1.

[0029] Figure 23 shows a DSC and TGA Overlay of Compound A L-Pyroglutamate Salt, Form A_1.

[0030] Figure 24 shows a DVS of Compound A L-Pyroglutamate Salt, Form A_1.

[0031] Figure 25 shows a photomicrograph of Compound A L-Pyroglutamate Salt, Form A_1.

[0032] Figure 26 shows an XRPD Pattern of Compound A Free Base, Form C_0.

[0033] Figure 27 shows thermal XRPD Patterns of Compound A Free Base, Form C_0.

[0034] Figure 28 shows a DSC and TGA Overlay of Compound A Free Base, Form C_0.

[0035] Figure 29 shows a photomicrograph of Compound A A Free Base, Form C_0.

[0036] Figure 30 shows an XRPD Pattern of Compound A Hydrochloride Salt, Form A.

[0037] Figure 31 shows a DSC and TGA Overlay of Compound A Hydrochloride Salt, Form A.

[0038] Figure 32 shows a DVS of Compound A Hydrochloride Salt, Form A.

[0039] Figure 33 shows an XRPD Pattern of Compound A Fumarate Salt, Form A.

[0040] Figure 34 shows a DSC and TGA Overlay of Compound A Fumarate Salt, Form A.

[0041] Figure 35 shows a XRPD Pattern of Compound A p-Toluenesulfonate Salt, Form A.

[0042] Figure 36 shows a DSC and TGA Overlay of Compound A p-Toluenesulfonate Salt, Form A.

[0043] Figure 37 shows plasma levels of Compound B, 1 mg/kg intravenous, Compound A, ascorbic acid salt, 30 mg/kg oral, and Compound A, glycolate hydrate salt, 30 mg/kg oral in rat.

[0044] Figure 38 shows the single crystal structure of Compound A, glycolate hydrate salt.

DETAILED DESCRIPTION OF ILLUSTRATIVE EMBODIMENTS

[0045] The present disclosure addresses a need in the art by providing new forms of Compound A, including new crystalline free base forms of Compound A and new crystalline salt forms of Compound A.

[0046] The disclosure is directed to, among other things, Compound A, acetate salt Form $A_{1.5}$; Compound A, glycolate salt hydrate Form A_1; Compound A, L-malate salt Form A_1; Compound A, L-malate salt Form $A_{1.5}$; Compound A, L-pyroglutamate salt Form A_1; Compound A, free base Form C_0; Compound A, hydrochloride salt Form A; Compound A, fumarate salt Form A; and Compound A, p-toluenesulfonate salt Form A. Pharmaceutical compositions comprising one or more of these forms are also described.

[0047] In one embodiment, the present disclosure pertains to Compound A, acetate salt Form $A_{1.5}$. In one aspect, this crystalline form is characterized by an X-ray diffraction pattern comprising one or more of the following peaks: 6.4, 9.2, 12.7, 13.0, 15.2, 17.4, 18.4, 19.0, 19.3, 21.3, 21.5, 23.1, 24.1, 24.2, and/or 28.2 ± 0.2 degrees 2-theta. In another aspect, this crystalline form comprises at least 3 of the foregoing peaks. In yet another aspect, this crystalline for comprises at least 4, 5, 6, 7, 8, 9, or 10 of the foregoing peaks. In another aspect, this crystalline form has an X-ray powder diffraction pattern substantially as depicted in Figure 3.

[0048] The disclosure is also directed to Compound A, glycolate hydrate salts. These salts can have varying amounts of water within the crystal structure. For example, the ratio of Compound A to water can be from about 1:0.1 to about 1:1. In other embodiments, the ratio of Compound A to water is 1:0.1; 1:0.2; 1:0.3; 1:0.4; 1:0.5; 1:0.6; 1:0.7; 1:0.8; 1:0.9 or 1:1.

[0049] Another embodiment of the present disclosure pertains to Compound A, glycolate hydrate salt Form A_1. In one aspect, this crystalline form is characterized by an X-ray diffraction pattern comprising one or more of the following peaks: 8.1, 8.2, 8.7, 13.9, 14.7, 14.9, 16.3, 17.4, 17.6, 18.2, 18.5, 19.0, 20.2, 20.6, 21.2, 21.4, 23.0, 24.5, 24.7, 26.1, 26.3, 28.0, 30.0,

30.1, 30.2, and/or 32.8±0.2 degrees 2-theta. In another aspect, this crystalline form comprises at least 3 of the foregoing peaks. In yet another aspect, this crystalline for comprises at least 4, 5, 6, 7, 8, 9, or 10 of the foregoing peaks. In another aspect, this crystalline form has an X-ray powder diffraction pattern substantially as depicted in Figure 9.

[0050] Yet another embodiment of the disclosure pertains to Compound A, L-malate salt Form A_1. In one aspect, this crystalline form is characterized by an X-ray diffraction pattern comprising one or more of the following peaks: 8.6, 9.2, 10.1, 10.4, 11.7, 11.9, 14.7, 15.3, 15.6, 17.2, 17.8, 18.5, 20.3, 20.7, 21.2, 22.4, 23.5, 24.3, and/or 27.0 ± 0.2 degrees 2-theta. In another aspect, this crystalline form comprises at least 3 of the foregoing peaks. In yet another aspect, this crystalline for comprises at least 4, 5, 6, 7, 8, 9, or 10 of the foregoing peaks. In another aspect, this crystalline form has an X-ray powder diffraction pattern substantially as depicted in Figure 14.

[0051] In another embodiment, the disclosure pertains to Compound A, L-malate salt Form $A_{1.5}$. In one aspect, this crystalline form is characterized by an X-ray diffraction pattern comprising one or more of the following peaks: 5.5, 6.8, 8.0, 8.4, 8.8, 9.2, 11.8, 12.8, 13.1, 13.6, 14.4, 16.0, 16.7, 18.1, 18.5, 19.4, 20.2, 20.5, 21.1, 21.9, 23.4, and/or 24.6 ± 0.2 degrees 2-theta. In another aspect, this crystalline form comprises at least 3 of the foregoing peaks. In yet another aspect, this crystalline for comprises at least 4, 5, 6, 7, 8, 9, or 10 of the foregoing peaks. In another aspect, this crystalline form has an X-ray powder diffraction pattern substantially as depicted in Figure 19.

[0052] Also described herein is Compound A, L-pyroglutamate salt Form A_1. In one aspect, this crystalline form is characterized by an X-ray diffraction pattern comprising one or more of the following peaks: 6.0, 9.6, 10.3, 10.5, 11.0, 12.0, 13.2, 15.0, 16.7, 17.5, 17.8, 18.0, 19.0, 20.8, 21.0, 21.1, 22.0, 22.1, 23.1, 23.4, 23.5, 24.8, and/or 26.6 ± 0.2 degrees 2-theta. In another aspect, this crystalline form comprises at least 3 of the foregoing peaks. In yet another aspect, this crystalline for comprises at least 4, 5, 6, 7, 8, 9, or 10 of the foregoing peaks. In another aspect, this crystalline form has an X-ray powder diffraction pattern substantially as depicted in Figure 21.

[0053] The present disclosure also pertains to Compound A, free base Form C_0. In one aspect, this crystalline form is characterized by an X-ray diffraction pattern comprising one or more of the following peaks: 8.5, 8.8, 13.9, 14.4, 15.4, 17.6, 18.1, 18.5, 19.2, 19.7, 20.4, 21.1, 21.4, 21.9, 23.6, 24.6, 29.4 and/or 30.1 ± 0.2 degrees 2-theta. In another aspect, this crystalline form comprises at least 3 of the foregoing peaks. In yet another aspect, this crystalline for

comprises at least 4, 5, 6, 7, 8, 9, or 10 of the foregoing peaks. In another aspect, this crystalline form has an X-ray powder diffraction pattern substantially as depicted in Figure 27.

[0054] Another embodiment of the present disclosure pertains to Compound A, hydrochloride salt Form A. In one aspect, this crystalline form is characterized by an X-ray diffraction pattern comprising one or more of the following peaks: 7.5, 8.6, 12.2, 17.1, 18.8, 18.9, 22.3, 24.5, 25.6, 26.1, 33.5, and/or 34.1 ± 0.2 degrees 2-theta. In another aspect, this crystalline form comprises at least 3 of the foregoing peaks. In yet another aspect, this crystalline for comprises at least 4, 5, 6, 7, 8, 9, or 10 of the foregoing peaks. In another aspect, this crystalline form has an X-ray powder diffraction pattern substantially as depicted in Figure 30.

[0055] Yet another embodiment of the present disclosure pertains to Compound A, fumarate salt Form A. In one aspect, this crystalline form is characterized by an X-ray diffraction pattern comprising one or more of the following peaks: 9.0, 10.5, 11.1, 14.9, 17.1, 17.7, 19.3, 21.1, 22.3, 22.9, 23.5, 24.0, 24.2, 25.7, 25.9, 27.3, 29.0, and/or 31.1 ± 0.2 degrees 2-theta. In another aspect, this crystalline form comprises at least 3 of the foregoing peaks. In yet another aspect, this crystalline for comprises at least 4, 5, 6, 7, 8, 9, or 10 of the foregoing peaks. In another aspect, this crystalline form has an X-ray powder diffraction pattern substantially as depicted in Figure 33.

[0056] And yet another embodiment of the present disclosure pertains to Compound A, p-toluenesulfonate salt Form A. In one aspect, this crystalline form is characterized by an X-ray diffraction pattern comprising one or more of the following peaks: 6.0, 9.6, 10.3, 10.5, 11.0, 12.0, 12.9, 13.2, 15.0, 16.7, 17.0, 17.5, 17.8, 18.0, 19.0, 20.8, 21.0, 21.1, 22.1, 22.7, 23.1, 23.4, 23.5, 24.8, , and/or 26.6 ± 0.2 degrees 2-theta. In another aspect, this crystalline form comprises at least 3 of the foregoing peaks. In yet another aspect, this crystalline for comprises at least 4, 5, 6, 7, 8, 9, or 10 of the foregoing peaks. In another aspect, this crystalline form has an X-ray powder diffraction pattern substantially as depicted in Figure 35.

[0057] In some embodiments, the polymorphic forms of the disclosure are substantially free of any other polymorphic forms, or of specified polymorphic forms. In any embodiment of the present invention, by "substantially free" is meant that the forms of the present invention contain 20% (w/w) or less, 10% (w/w) or less, 5% (w/w) or less, 2% (w/w) or less, particularly 1% (w/w) or less, more particularly 0.5% (w/w) or less, and most particularly 0.2% (w/w) or less of either any other polymorphs, or of a specified polymorph or polymorphs. In other embodiments, the polymorphs of the disclosure contain from 1% to 20% (w/w), from 5% to 20%

(w/w), or from 5% to 10% (w/w) of any other polymorphs or of a specified polymorph or polymorphs.

[0058] The salts and solid state forms of the present invention have advantageous properties including at least one of: high crystallinity, solubility, dissolution rate, morphology, thermal and mechanical stability to polymorphic conversion and/or to dehydration, storage stability, low content of residual solvent, a lower degree of hygroscopicity, flowability, and advantageous processing and handling characteristics such as compressibility, and bulk density.

[0059] A crystal form may be referred to herein as being characterized by graphical data "as substantially depicted in" a Figure. Such data include, for example, powder X-ray diffractograms. The skilled person will understand that such graphical representations of data may be subject to small variations, *e.g.,* in peak relative intensities and peak positions due to factors such as variations in instrument response and variations in sample concentration and purity, which are well known to the skilled person. Nonetheless, the skilled person would readily be capable of comparing the graphical data in the Figures herein with graphical data generated for an unknown crystal form and confirm whether the two sets of graphical data are characterizing the same crystal form or two different crystal forms.

[0060] The term “amorphous,” as used herein, means lacking a characteristic crystal shape or crystalline structure.

[0061] The term “crystalline,” as used herein, means having a regularly repeating arrangement of molecules or external face planes.

[0062] The term “crystalline form,” as used in herein, refers to a solid chemical compound or mixture of compounds that provides a characteristic pattern of peaks when analyzed by x-ray powder diffraction; this includes, but is not limited to, polymorphs, solvates, hydrates, co-crystals, and de-solvated solvates.

[0063] The term “polymorphic” or “polymorphism” is defined as the possibility of at least two different crystalline arrangements for the same chemical molecule.

[0064] The term “solution,” as used herein, refers to a mixture containing at least one solvent and at least one compound at least partially dissolved in the solvent.

[0065] The term “pharmaceutically acceptable excipients,” as used herein, includes any and all solvents, dispersion media, coatings, antibacterial and antifungal agents, isotonic and absorption delaying agents and the like. The use of such media and agents for pharmaceutical active substances is well known in the art, such as in Remington: The Science and Practice of Pharmacy, 20th ed.; Gennaro, A. R., Ed.; Lippincott Williams & Wilkins: Philadelphia, Pa.,

2000. Except insofar as any conventional media or agent is incompatible with the active ingredient, its use in the therapeutic compositions is contemplated. Supplementary active ingredients can also be incorporated into the compositions.

[0066] The pharmaceutical compositions of the present invention may be used in a variety of ways, including but not limited to the enhancement of the anti-tumor activity of radiation or DNA-damaging chemotherapeutic agents (Griffin, R. J.; Curtin, N. J.; Newell, D. R.; Golding, B. T.; Durkacz. B. W.; Calvert, A. H. The role of inhibitors of poly(ADP-ribose) polymerase as resistance-modifying agents in cancer therapy. Biochemie 1995, 77, 408).

[0067] For therapeutic purposes, the crystalline forms of the present invention can be administered by any means that results in the contact of the active agent with the agent's site of action in the body of the subject. The crystalline forms may be administered by any conventional means available for use in conjunction with pharmaceuticals, either as individual therapeutic agents or in combination with other therapeutic agents, such as, for example, analgesics. The crystalline forms of the present invention are preferably administered in therapeutically effective amounts for the treatment of the diseases and disorders described herein to a subject in need thereof.

[0068] In therapeutic or prophylactic use, the crystalline forms of the present invention may be administered by any route that drugs are conventionally administered. Such routes of administration include intraperitoneal, intravenous, intramuscular, subcutaneous, intrathecal, intracheal, intraventricular, oral, buccal, rectal, parenteral, intranasal, transdermal or intradermal. Administration may be systemic or localized.

[0069] The crystalline forms described herein may be administered in pure form, combined with other active ingredients, or combined with pharmaceutically acceptable nontoxic excipients or carriers. Oral compositions will generally include an inert diluent carrier or an edible carrier. Pharmaceutically compatible binding agents, and/or adjuvant materials can be included as part of the composition. Tablets, pills, capsules, troches and the like can contain any of the following ingredients, or compounds of a similar nature: a binder such as microcrystalline cellulose, gum tragacanth or gelatin; an excipient such as starch or lactose, a dispersing agent such as alginic acid, Primogel, or corn starch; a lubricant such as magnesium stearate; a glidant such as colloidal silicon dioxide; a sweetening agent such as sucrose or saccharin; or a flavoring agent such as peppermint, methyl salicylate, or orange flavoring. When the dosage unit form is a capsule, it can contain, in addition to material of the above type, a liquid carrier such as a fatty oil. In addition, dosage unit forms can contain various other materials that modify the physical

form of the dosage unit, for example, coatings of sugar, shellac, or enteric agents. Further, a syrup may contain, in addition to the active compounds, sucrose as a sweetening agent and certain preservatives, dyes, colorings, and flavorings.

[0070] Alternative preparations for administration include sterile aqueous or nonaqueous solutions, suspensions, and emulsions. Examples of nonaqueous solvents are dimethylsulfoxide, alcohols, propylene glycol, polyethylene glycol, vegetable oils such as olive oil and injectable organic esters such as ethyl oleate. Aqueous carriers include mixtures of alcohols and water, buffered media, and saline. Intravenous vehicles include fluid and nutrient replenishers, electrolyte replenishers, such as those based on Ringer's dextrose, and the like. Preservatives and other additives may also be present such as, for example, antimicrobials, anti-oxidants, chelating agents, inert gases, and the like.

[0071] Preferred methods of administration of the crystalline forms to mammals include intraperitoneal injection, intramuscular injection, and intravenous infusion. Various liquid formulations are possible for these delivery methods, including saline, alcohol, DMSO, and water based solutions. The concentration may vary according to dose and volume to be delivered and can range from about 1 to about 1000 mg/mL. Other constituents of the liquid formulations can include preservatives, inorganic salts, acids, bases, buffers, nutrients, vitamins, or other pharmaceuticals such as analgesics or additional PARP and kinase inhibitors.

[0072] Having thus described the invention with reference to particular preferred embodiments and illustrative examples, those in the art can appreciate modifications to the invention as described and illustrated that do not depart from the spirit and scope of the invention as disclosed in the specification. The Examples are set forth to aid in understanding the invention but are not intended to, and should not be construed to limit its scope in any way.

EXAMPLES

[0073] Solvents used in the following examples were of reagent-grade quality and were used without further purification. Known forms of Compound A are indicated by A_0 and B_0 for anhydrous material and H_d for hydrate.

X-Ray Powder Diffraction (XRPD)

[0074] **Standard Reflection Mode Measurements:** Powder X-ray diffraction patterns were recorded on a PANalytical X Pert Pro diffractometer equipped with an X'celerator detector using CuK_α radiation at 45 kV and 40 mA. $K_{\alpha 1}$ radiation was obtained with a highly oriented crystal (Ge111) incident beam monochromator. A 10mm beam mask, and fixed (1/4°)

divergence and anti-scatter (1/8°) slits were inserted on the incident beam side. A fixed 5mm receiving slit and a 0.04 radian Soller block were inserted on the diffracted beam side. The X-ray powder pattern scan was collected from ca. 2 to 40° 2θ with a 0.0080° step size and 96.06 sec counting time which resulted in a scan rate of approximately 0.5°/min. The sample was spread on silicon zero background (ZBG) plate for the measurement. The sample was rotated using a PANalytical PW3064 Spinner (15 revolutions / min.).

[0075] Measurement of the Si reference standard before the data collection resulted in values for 2θ and intensity that were well within the tolerances of $28.44 < 2\theta < 28.50$ and significantly greater than the minimum peak height of 150cps.

[0076] **SCXRD - Single Crystal X-ray Diffraction:** For data collection, a piece (0.12 x 0.04 x 0.03 mm3) was broken from a clump of about three or four separate pieces to give an apparently single crystal. The crystal was mounted on a fine glass fiber with the aid of polyisobutene oil (also known as PARATONE) onto a Bruker-Nonius X8 Proteum diffractometer attached to a Nonius FR-591 rotating anode (CuKa) with 'Helios' focusing optics. The crystal was maintained at 90K throughout with a CryoCool LT2 from CryoIndustries of America. Diffraction images for indexing clearly showed split reflections, consistent with either cracking or twinning, but with spot components that were close enough to be integrated together. The relative intensities of pairs of split reflections suggested that cracking was more likely than twinning.

[0077] The crystal was indexed from the reflections found in 72 diffraction images (six sets of twelve 0.5 ° frames). Data collection consisted of 1485 2 ° frames in 15 scans at three detector swing angles (two 360° φ-scans at -40° in 2θ, three 90° ω-scans at -45° in 2θ, four 360° φ-scans at -96° in 2θ and six 90° ω-scans at -96° in 2θ) sufficient to cover reciprocal space for an arbitrarily oriented triclinic crystal to a resolution of 0.83Å with four-fold redundancy. Data were integrated, scaled, averaged and merged using the programs in the APEX2 package from Bruker-AXS. Final cell parameters were derived from the output diagnostics of the integration process. The structure was solved by standard direct methods using SHELXS and refined using SHELXL, both from the SHELX97 package. Diagrams were drawn using XP from the SHELXTL suite and with Mercury from the CCDC. Additional molecular graphics and void calculation were done with Platon.

[0078] Positional and anisotropic displacement parameters of all non-hydrogen atoms were refined. The H atoms were located in a difference Fourier's map, but those attached to carbon atoms were repositioned geometrically. The H atoms were initially refined with soft

restraints on the bond lengths and angles to regularize their geometry (C-H in the range 0.93-0.98 and N-H to 0.86 Å) and Uiso(H) (in the range 1.2-1.5 times Ueq of the parent atom), after which the positions were refined with riding constraints.

[0079] Default Reitveld refinement of the single crystal unit cell parameters against the measured XRPD pattern gave a good fit with no unexplained peaks.

[0080] **Variable Temperature X-Ray Powder Diffraction (VT-XRPD):** Variable temperature studies were performed with an Anton Paar CHC temperature/humidity chamber under computer control through an Anton Paar TCU110 temperature control unit.

[0081] Typically the measurements were done with a nitrogen flow through the camera. Two measurement schemes were used, restricted and continuous. In the restricted mode, measurements were made, only after the CHC chamber reached the requested temperature. In the continuous mode, the sample was heated at 10°C/minute and fast scans were measured as the temperature changed. In both cases, after the requested temperature was reached, the sample was cooled at 35°C/minute and a slow scan was measured at 25°C. The slow 2θ scans were collected from ca. 3 to 30° or 40° with a 0.0080° step size and 100.97 sec counting time which resulted in a scan rate of approximately 0.5°/min. The fast scans were collected from ca. 3 to 30° 2θ with a 0.0167° step size and 1.905 sec counting time which resulted in a scan rate of approximately 44°/min.

[0082] The temperatures chosen were based on DSC results.

[0083] For the diffractometer set-up a 10mm beam mask, 0.04 radian Soller slits, and fixed (1/4°) divergence and anti-scatter (1/8°) slits were inserted on the incident beam side. A fixed 5 mm receiving slit, 0.04 radian Soller slits and a 0.02 mm Nickel filter were inserted on the diffracted beam side.

[0084] **Differential Scanning Calorimetry (DSC):** Thermal curves were acquired using a Perkin-Elmer Sapphire DSC unit equipped with an autosampler running Pyris software version 6.0 calibrated with Indium prior to analysis. Solid samples of 1-10 mg were weighed into 20 µL aluminum pin hole sample pans. The DSC cell was then purged with nitrogen and the temperature heated from 0 to 270°C at 10°C / min. Indium (T_m = 156.6°C; ΔH_{FUS} = 28.45 J g^{-1}) was used for calibration.

[0085] **Modulated Differential Scanning Calorimetry (MDSC)**: Thermal curves were acquired using a TA Q200 Modulated DSC unit. Solid samples of 5-20 mg were weighed into 50 µL aluminum pinhole hermetically sealed pans. The MDSC cell was then purged with

nitrogen and the temperature heated at 2°C/min from 0°C to 350°C at 2°C/min with a modulation amplitude of +/- 1°C over a 60 second period.

[0086] Thermogravimetric Mass Spectrometry (TGA/MS): Thermal curves were acquired using a Perkin-Elmer Pyris 1 TGA unit running Pyris software version 6.0 calibrated with alumel (95% nickel, 2% manganese, 2% aluminum and 1% silicon), nickel and calcium oxalate monohydrate. TGA samples between 1-5 mg were monitored for percent weight loss as heated from 25 to 250°C at 10°C/min in a furnace purged with Helium at ca. 50 mL/min. To simultaneously follow the evolution of the gaseous decomposition products over the temperature range investigated, the thermobalance was connected to a ThermoStar Quadrupole Mass Spectrometer (Asslar, Germany). The transfer line to introduce gaseous decomposition products into the mass spectrometer was a deactivated fused silica capillary (SGE Analytical science, Fused Silica (100% Methyl Deactivated), 220 mm OD, 150 mm ID, Australia) temperature controlled to 200°C to avoid possible condensation of the evolved gases. In this way the TGA weight loss and the mass spectrometric ion intensity curves of the selected ionic species could be recorded simultaneously.

[0087] Dynamic Vapor Sorption (DVS): DVS experiments have been carried out using the DVS-HT instrument (Surface Measurement Systems, London, UK). This instrument measures the uptake and loss of vapor gravimetrically using a recording ultra-microbalance with a mass resolution of ± 0.1 μg. The vapor partial pressure (±1.0%) around the sample is controlled by mixing saturated and dry carrier gas streams using electronic mass flow controllers. The desired temperature is maintained at ± 0.1°C. The samples (1 - 10 mg) were placed into the DVS-HT and DVS-1 instruments at the desired temperature.

[0088] The sample was loaded and unloaded at 40% RH and 25°C (typical room conditions). A moisture sorption isotherm was performed as outlined below (2 scans giving 1 complete cycle). The software uses a least squares minimization procedure together with a model of the mass relaxation, to predict an asymptotic value. The measured mass equilibration value must be within 2% of that predicted by the software before proceeding to the next % RH value. The minimum equilibration time was set to 1 hour and the maximum to 4 hours.

[0089] Optical Microscopy: Microscopic observation of the sample morphology was performed using an Olympus B60 polarized light microscope. Samples were suspended in mineral oil and compressed on a glass slide with a cover slip prior to observation. Images were taken with a FW-24 (PAX CAM) camera. A 10x objective coupled with an additional 10x

magnification from the microscope optics gave a total magnification of 100x. PAX-it software (Version 6.2) was used to capture and analyze the images.

[0090] Nuclear Magnetic Resonance Spectroscopy (^{1}H-NMR): The stoichiometry of the salts were determined by ^{1}H -NMR spectroscopy using a Bruker DPX400 instrument running under conditions optimized to give the best available spectrum for each sample. Each sample (2-4 mg) was dissolved in 0.75 mL DMSO-d6 and spectrum obtained in thin walled glass tubes (4 x14 mm).

Identity, Assay, and Purity by HPLC

[0091] Equipment: Testing was performed on a calibrated and validated Agilent 1200 Rapid Resolution High Performance Liquid Chromatography (HPLC) system designated LC-0430-AD or LC-418-1D. The system comprises a binary SL pump, degasser, high performance autosampler SL with a fraction collector, thermostated column compartment with a 2 valve column switcher, and a DAD SL detector. All standard solutions and samples were prepared in Class A glass volumetric flasks and were placed in autosampler vials. Standard weighings were done using a calibrated Mettler analytical balance. The sample preparations were centrifuged using an Eppendorf microcentrifuge. The primary chromatography data was acquired and integrated using Empower 2 software. Microsoft Office Excel 2003 was used for the calculation of results.

[0092] Reagents: Acetonitrile was obtained from CCI. Trifluoroacetic acid was obtained from EMD. HPLC grade water (18 MΩ·cm) was obtained from the laboratory Barnstead Nanopure system UPW-0403-AD located in laboratory A211. Compounds A and B were prepared as previously described.

[0093] Instrument Parameters:

Column: Zorbax Eclipse XDB-C18, 100 x 3.0 mm ID, 1.8 µ packing		
Detector: UV/vis @ 290 nm		
Column Temperature: 25°C		
Flow Rate: 0.64 mL/min		
Mobile Phase A: 0.1% TFA in water		
Mobile Phase B: 0.1% TFA in ACN		
Gradient:		
Time (min)	Mobile Phase A (%)	Mobile Phase B (%)
0	75	25
10	55	45
12	5	95
13	5	95
13.1	75	25
16.7	75	25

[0094] Solid State Stability of Salts at 40°C and 75% Humidity: Samples of the form to be studied (15-20 mg) were weighed into standard 1.5 mL HPLC vials (32 x 11.6 mm) and stored uncapped for 0, 7, 14 and 28 days in a 40°C and 75% RH stability chamber. Samples were removed on the indicated day and capped. Measurements of XRPD, DSC, TGA and HPLC Identity by Purity and Assay measurements were completed on each time point sample.

[0095] Estimation of Water Solubility: Ten mg portions of the salt forms to be studied were weighed into a standard 1.5 mL HPLC vial (32 x 11.6 mm). A stir bar and 100 µL of water were added to each vial. The samples were capped and stirred for 5-10 minutes. If a clear solution was not obtained by visual inspection, an additional 100-300 µL portion of water was added and stirred. This process was repeated until the sample dissolved or until 1000 µL of water was added. An estimation of solubility was based on the volume of water necessary to dissolve the known weight of sample. The results from these measurements are presented in Table 11.

Table 1. Estimated Water Solubility and HPLC analyses of Salts with One Equivalent of Acid in Acetone by Slow Cooling

Sample	Acid	Estimated Water Solubility	Measured COMPOUND A, %	Calculated Di Salt, %	Calculated Mono Salt, %
13-3	Acetic	50-100mg/mL	72.2	77.0	87.5
13-4	Fumaric	<10 mg/mL	1.9		
13-5	Glycolic	<10 mg/mL[1]	72.0	73.2	84.5
13-6	L-Malic	>100mg/mL	68.3	61.0	75.8
13-7	Phosphoric	50-100mg/mL	5.9	68.4	81.2
13-8	L-Pyroglutamic	>100mg/mL	56.0	61.8	76.4
13-9	p-Toluenesulfonic	<10 mg/mL	42.7	54.9	70.8
13-10	Hydrochloric	10-20mg/mL	39.8	85.1	92.0

Example 1. Salts with Two Equivalents of Acid in Acetone by Maturation

[0096] 200mg of Compound A (0.478 mmoles) was dissolved with warming and stirring in each of five- 20 mL scintillation vials in 15 mL of acetone. 1.95 equivalents of acetic, glycolic, L-malic, or L-malic (1 Eq., 0.48 mmoles) acids were added to the clear Compound A solutions. As soon as these acids were added, the clear solutions became cloudy and began crystallizing. The vials were subject to two cycles of maturation on the HEL unit. Each cycle of maturation consisted of heating to 50° C over a period of one hour, holding at 50°C for four hours, cooling over a period of one hour to 5°C, and holding at 5°C for four hours. The solid was

isolated by suction filtration and solid dried overnight at 50°C and house vacuum (~200 mm) to give yellow solids. The results are presented in Table 2.

Table 2

Sample	Acid	XRPD	DSC, °C	TGA, %	Estimated Water Solubility.
39-1(2)	Acetic	$A_{1.5}$	185.2	24.4	~25 mg/mL
39-2(2)	Glycolic	A_1	68.9, 205.4	4.8	>100 mg/mL
39-3(2)	L-Malic	A_1	186.4	3.6	>100 mg/mL
39-5(2)	L-Malic (1 eq.)	$A_1 + C_0$	186.5	1.0	>100 mg/mL

Example 2. Acid Screening (Two Equivalents) in Acetone using Quick Cooling

[0097] To seven HPLC vials containing a stirring bar and 1.5 mL of Compound A solution (13.3 mg/mL), the quantities of acids to give two equivalents (0.096 mmoles) were weighed or added by pipette. The samples were capped and heated to the boiling point and then chilled overnight in the refrigerator at 2-8 °C. The solid was isolated by suction filtration and solid dried overnight at 50°C and house vacuum (~200mm) to give yellow solids. The results are presented in Table 3.

Table 3

Sample	Acid	XRPD	DSC, °C	TGA, %	Estimated Water Solubility.
31-1	Acetic	$A_{1.5}$	181.3	22.6	~25 mg/mL
31-2	Glycolic	A_1	205.4	4.8	>100 mg/mL
31-3	L-Malic	$A_{1.5}$	160.4	3.6	>100 mg/mL
31-4	L-Pyroglutamic	A_1	196.4	4.4	>100 mg/mL
31-5	L-Malic(1 eq.)	C_0	206.4	2.7	~25 mg/mL

Example 3. Salts with Two Equivalents of Acid in Acetone by Slurry Conversion

[0098] 400mg of Compound A (0.956 mmoles) was slurried with warming and stirring in each of five 20 mL glass scintillation vials with 18 mL of acetone. Two equivalents of acetic, glycolic, L-malic, L-pyroglutamic or L-malic (1 Eq. (0.956 mmoles) acids were added to the COMPOUND A suspension in each vial. These mixtures were capped and warmed to near the boiling point. In all cases a heavy yellow solid was noted. The samples were allowed to cool to ambient temperature on the laboratory bench and chilled overnight in the refrigerator at 2-8 °C. The solid was isolated by suction filtration and the product dried overnight at 50 °C and house vacuum (~200 mm) to give yellow solids. The results are presented in Table 4.

Table 4

Sample	Acid	XRPD	DSC, °C	TGA, %	Estimated Water Solubility.
39-1	Acetic	$A_{1.5}$	185.4, split peak	2.1	~50 mg/mL
39-2	Glycolic	A_1	77.4, 209.0	1.9	<10mg/mL
39-3	L-Malic	A_1	193.3	3.6	>100 mg/mL
39-4	L-Pyroglutamic	A_1	50.4, 198.2	3.5	>100 mg/mL
39-5	L-Malic(1 eq.)	$A_1 + C_0$	192.2	1.0	>100 mg/mL

Example 4. Acid Screening (Two Equivalents) in Acetone - Maturation

[0099] 240 mg of Compound A (0.574 mmoles) in 18 mL of acetone and warmed with stirring by a magnetic stirring bar to dissolve. This solution was dispensed equally to 12 1.5 mL HPLC vials.

[00100] To each of 5 vials containing an aliquot of the Compound A solution and a stirring bar, the quantities of acid to give two equivalents (0.096 mmoles) were weighed or added by pipette. The samples were capped and subject to two cycles of maturation on the HEL unit. Each cycle of maturation consisted of heating to 50° C over a period of one hour, holding at 50° C for four hours, cooling over a period of one hour to 5°C, and holding at 5°C for four hours. The solid was isolated by suction filtration and solid dried overnight at 50°C and house vacuum (~200 mm) to give yellow solids. The results are presented in Table 5.

Table 5

Sample	Acid	XRPD	DSC, °C	TGA, %	Estimated Water Solubility.
30-1	Acetic	$A_{1,5}$	187.7, 334.1	21.7	~20 mg/mL
30-2	Glycolic	A_1	206.6	3.2	>100 mg/mL
30-3	L-Malic	A_1	190.2	1.5	>100 mg/mL
30-4	L-Pyroglutamic	A_1	197.5	1.8	>100 mg/mL
30-5	L-Malic (1 eq.)	C_0	207.3	2.2	~25 mg/mL

Example 5. One Equivalent in Acetone - Slow Cooling

[00101] A solution of 240 mg of Compound A (0.57 mmoles) was prepared in 12 mL of acetone and warmed with stirring to dissolve. Twelve equal aliquots of this solution will give 20 mg (0.0478mmoles) of Compound A in 1 mL of acetone in each vial. The weight of acid corresponding to 1.05 equivalents (0.06 mmoles) of acid was weighed or added by pipette if liquid to 12 1.5 mL HPLC vials. To each vial one of the aliquots of Compound A was added. The vials were capped and warmed with stirring to mix and subject to 2 cycles of slow cooling on the HEL unit. Each cycle of slow cooling on the HEL unit consisted of heating over a period of 1 hour to 80°C holding for 1 hour at 80°C and then cooling over a period of 5 hours to 5°C and

holding at 5°C for 16-18 hours. Solid was isolated by suction filtration and samples were dried at 50°C overnight at house vacuum (~200 mm). The results are presented in Table 6.

Table 6

Sample	Acid	DSC °C	TGA%
1	Acetic	171.6	9.9
2	L-Aspartic	145.8, 191.2, 219.8, 240.5, 258.5	1.3
3	Ethanesulfonic	61.2, 193.6, EXO 199.8, 258.7	0.2
4	Fumaric	177.1	0.4
5	Glycolic	207.0	0.4
6	L-Malic	63.1, 198.6	1.5
7	Phosphoric	54.4	3.6
8	L-Pyroglutamic	199.6	0.4
9	Sulfuric(0.5eq)	69.5, 201.0	3.7
10	L-Tartaric	66.0, 162.4	3.2
11	p-Toluenesulfonic	205.9	0.3
12	Hydrochloric(EtOH)	67.0, 234.3	0.9

* EXO = exotherm

Example 6. Preparation of Ascorbate Salt

[00102] 200 mg of Compound A (0.478 mmoles) was weighed into a 20 mL glass scintillation vial with a stirring bar followed by 88.4mg (0.503 mmoles, 1.05 equivalents) of ascorbic acid (J.T. Baker Anhydrous Lot B36597). 2.5 ml of 2,2,2-trifluoroethanol was added by pipette and the sample was warmed. The slurry that formed was subject to 2 cycles of slow cooling on the HEL unit. Each cycle of slow cooling on the HEL unit consisted of heating over a period of 1 hour to 80°C, holding for 1 hour at 80°C, and then cooling over a period of 5 hours to 5°C and holding at 5°C for 16-18 hours. Solid was isolated by suction filtration and samples were dried at 50°C overnight at house vacuum (~200 mm) to give 142mg of yellow solid (49% yield). The crystalline product was analyzed by HPLC and gave 96.2% of Compound B and 0.8% of Compound A. The structure of the Compound B salt was confirmed by ^{1}H-NMR.

Compound A, Free Base, Form A_0

XRPD

[00103] The XRPD is depicted in Figure 1.

Thermal Analysis

[00104] Thermal data is depicted in Figure 2.

Compound A, Acetate Salt, Form $A_{1.5}$

Preparation

[00105] The salt was prepared according to the procedure in Example 1.

XRPD

[00106] The X-ray diffraction data for the acetate salt, Form $A_{1.5}$, is given in Figure 3 and Table 7. Variable temperature XRPD measurements in requested mode (165°C and 200°C) showed two changes in Form - from the acetate to Form B_0 and then conversion to Form A_0. In continuous mode, using one minute scans from 5.5° to 11.5° and a 1°C/minute temperature ramp, three changes in form were noted, acetate to Freebase B_0, B_0 to A_0 and A_0 to amorphous (Figure 4). The acetate slowly converts to freebase Form B_0 over the temperature range 91°C to 130°C. The form changes from B_0 to A_0 between 197°C and 200°C (Figure 5).

Table 7. XRPD Peaks for the Acetate Salt, Form $A_{1.5}$

No.	Pos. [2θ°]*	d-spacing [Å]	Rel. Int.[%]		No.	Pos. [2θ°]*	d-spacing [Å]	Rel. Int.[%]
1	**6.41**	**13.777**	**100**		15	21.11	4.205	1
2	9.21	9.599	6		16	21.30	4.169	2
3	12.42	7.123	1		17	21.53	4.124	3
4	12.71	6.961	4		18	21.70	4.092	1
5	13.02	6.796	4		19	23.10	3.847	3
6	13.22	6.694	1		20	23.90	3.720	1
7	14.72	6.012	1		21	24.07	3.694	2
8	15.22	5.817	2		22	24.18	3.678	2
9	17.41	5.089	2		23	24.33	3.655	1
10	18.00	4.924	1		24	25.50	3.490	1
11	18.36	4.828	2		25	26.09	3.412	1
12	18.47	4.799	1		26	26.21	3.397	1
13	19.02	4.661	6		27	28.15	3.167	2
14	19.26	4.605	5		28	28.25	3.157	1

*The use of ZBG or glass plates typically introduces a positive sample height displacement and results in small (0.05° to 0.2°) offset in 2θ values. The highest peak (intensity 100%) is set in bold letters.

Thermal Analysis

[00107] The DSC curve of the acetate salt, Form $A_{1.5}$, shows the presence of one endothermic/degradation peak; at 185.4°C having a ΔH_{Fus} of 172.0 J/g (Figure 6). The acetate salt had a weight loss of 29.5% between 25 and 150°C.

Water Sorption

[00108] The DVS plot in Figure 7 indicates that the sample appears to be saturated from the onset. There is a steady weight loss during the drying curves with no equilibration reached. The sample was dried at 0%RH for 4 hours for each cycle. There were 4 cycles run, showing a continuing weight loss. The experiment was repeated on another DVS unit and showed similar results.

^{1}H-NMR Spectoscopy

[00109] The ^{1}H-NMR spectrum showed all of the peaks expected for Compound A. The peak at about 7.5 ppm was normalized to the one aromatic proton expected to absorb in this region. The remainder of the peaks associated with Compound A then followed in the proper ratio. For the acetate salt, only one peak is expected at 1.9-2.0 ppm. This peak should integrate for 3 protons. Instead, it showed about 4.5 protons, about 1.5 acetic acid molecules per Compound A molecule.

Stability

[00110] The data is given in Table 8 for the aging of the acetate salt, Form $A_{1.5}$, at 40° C and 75% RH. The XRPD, changes throughout the 28 day test period. The TGA and Compound A Assay values are probably reflecting loss of acetic acid as seen in the thermal and XRPD work cited above. DSC, HPLC Purity and Compound B assay are relatively constant during the study. A monoacetate salt should assay as 87.5% Compound A. A diacetate salt should Assay as 77.7% Compound A. The values in Table 8, suggest that the salt is changing composition as it aged. The ^{1}H-NMR measured 1.5 molecules of acetic acid per molecule of Compound A. The XRPD pattern showed peaks for a hydrate Compound A Free Base, Form H_d. Possibly as the sample aged the excess acetic acid volatilized. The volatility of acetic acid and the changing XRPD pattern suggest that another candidate be chosen.

Table 8. Stability at 40°C and 75% RH of the Acetate Salt, Form $A_{1.5}$

Day	XRPD	DSC, °C	TGA, %	COMPOUND A Assay, %	COMPOUND B Assay, %	HPLC Purity, %
0	$A_{1.5}$	54.7, 180.3 Split Peak	21.5	78.1	0.2	99.7
7	Shows hydrate forming	117.4° 179.9	20.0	70.2	0.1	99.6
14	Shows hydrate forming	132.6, 181.5	16.1	84.2	0.2	99.5
28	Shows hydrate,H_d forming	126.4, 163.6, 197.9	9.6	90.9	0.3	99.6

Optical Microscopy

[00111] The sample as shown in Figure 8 presented agglomerates of irregular shaped crystals. The sampled showed birefringence under plane-polarized light.

Compound A, Glycolate Salt Hydrate, Form A_1

Preparation

[00112] The salt was prepared according to Example 1.

XRPD

[00113] The X-ray diffraction data for the glycolate hydrate salt, Form A_1, is given in Figure 9 and Table 9. Overlaid scans for variable temperature XRPD measurements are shown in Figure 10. The initial XRPD pattern compared to glycolate hydrate Form A_1. There was no change on exposure to a dry N_2 atmosphere. During the one hour slow scan measurement at 175°C, the pattern changed. There is an increase in peak intensities on heating from 175°C to 225°C. It did not compare to known Compound A freebase patterns. The sample on the plate at the end of the measurements was a dark brown powder which did not have the appearance of passing through a melt. The patterns observed after heating to 175°C and 225°C partially compares to Compound B. This is consistent with the DSC which shows changes after 130°C and a melt at 205°C. Both the VT-XRPD and the DSC were consistent with the loss of glycolic acid and conversion to Compound B.

Table 9. XRPD Peaks for the Glycolate Hydrate Salt, Form A_1

Pos. [°2θ]	Position calc.	h	k	l	d-spacing [Å]	Height [cts]	Rel. Int. [%]
8.12	8.13	0	0	1	10.8850	781	8.7
8.24	8.25	0	1	0	10.7261	5010	55.9
8.68	8.69	0	1	1	10.1821	6898	77.0
11.96	11.98	1	1	1	7.3925	501	5.6
13.62	13.63	1	1	0	6.4987	275	3.1
13.90	13.91	0	1	-1	6.3683	4729	52.8
14.62	14.63	1	0	-1	6.0549	581	6.5
14.68	14.70	0	1	2	6.0279	692	7.7
14.89	14.90	0	2	1	5.9468	456	5.1
16.29	16.30	0	0	2	5.4374	321	3.6
17.42	17.44	0	2	2	5.0866	3502	39.1
17.59	17.61	1	2	1	5.0367	994	11.1
18.20	18.22	1	-2	-1	4.8706	557	6.2
18.48	18.50	1	2	2	4.7970	927	10.3
18.98	18.99	2	0	1	4.6728	252	2.8
19.84	19.85	2	0	0	4.4719	328	3.7
20.23	20.24	2	1	1	4.3864	1426	15.9

Pos. [°2θ]	Position calc.	h	k	l	d-spacing [Å]	Height [cts]	Rel. Int. [%]
20.58	20.59	2	-1	0	4.3131	1969	22.0
21.21	21.22	2	-1	1	4.1864	3681	41.1
21.30	21.32	0	1	-2	4.1681	1097	12.2
21.44	21.46	1	1	3	4.1409	926	10.3
21.48	21.49	2	0	2	4.1337	2196	24.5
21.54	21.56	1	-2	-2	4.1216	273	3.0
21.66	21.68	1	-2	1	4.0988	240	2.7
22.82	22.84	0	2	3	3.8938	297	3.3
23.04	23.06	0	3	2	3.8571	2250	25.1
23.07	23.08	2	-1	-1	3.8523	1182	13.2
23.71	23.73	2	0	-1	3.7491	239	2.7
24.45	24.47	2	2	1	3.6373	464	5.2
24.73	24.75	2	-1	2	3.5969	8960	100.0
25.95	25.96	1	-3	-2	3.4310	312	3.5
26.07	26.09	2	-2	1	3.4148	209	2.3
26.27	26.28	0	3	3	3.3900	267	3.0
26.41	26.43	1	3	3	3.3716	308	3.4
27.08	27.09	2	1	-1	3.2907	249	2.8
27.90	27.92	2	-1	-2	3.1952	271	3.0
27.96	27.98	1	3	0	3.1881	219	2.4
28.53	28.55	1	2	4	3.1260	206	2.3
29.96	29.97	3	0	0	2.9805	486	5.4
30.05	30.06	0	4	2	2.9718	224	2.5
30.08	30.10	2	-2	2	2.9682	1322	14.7
30.13	30.14	3	-1	0	2.9639	546	6.1
30.21	30.23	2	-1	3	2.9557	1534	17.1
31.57	31.58	3	-1	2	2.8318	240	2.7
32.01	32.03	3	2	2	2.7934	298	3.3
32.76	32.77	1	4	1	2.7319	202	2.3
33.11	33.12	3	2	1	2.7038	276	3.1
33.51	33.53	3	0	-1	2.6721	371	4.1
34.01	34.02	2	-2	-3	2.6343	249	2.8
37.51	37.52	0	1	-4	2.3960	240	2.7

*The use of ZBG or glass plates typically introduces a positive sample height displacement and results in small (0.05° to 0.2°) offset in 2θ values. The highest peak (intensity 100%) is set in bold letters.

Single Crystal Structure

[00114] The single crystal X-ray structure confirmed the presence of the glycolate anion and showed that the piperazine nitrogen atom carries the hydrogen atom. The molecule is shown in Figure 38. The structure also shows a water molecule which is present at 60% occupancy, that is, the ratio of Compound A to water is 1:0.6. Structural details are given in the below table.

Variable		**Value**
System		Triclinic
Space Group		P-1
Temperature (°K)	90.0(2)	298(3)
a, Å	9.3613(2)	9.3957(5)
b, Å	11.8453(2)	11.9911(8)
c, Å	12.4918(2)	12.6433(8)
α	64.9920(1)	65.2827(2)
β	73.2080(1)	73.0954(1)
γ	88.2480(1)	88.7671(1)
Volume, Å^3	1195.08(4)	1229.8
Density, g/ml		1.404
λ, Å		1.54178
μ, mm^{-1}		0.846
Absorption Correction Method		multi-scan
Absorption Correction Minimum		0.781
Absorption Correction Maximum		0.963
Reflections (total)		16031
Reflections (Unique)		4237
Reflections (Observed, > 2σ)		3388
R_{merge} (internal agreement)		0.043
R		0.0409
wR		0.1043
Minimum Residual Density, e$^-$/mm^3		0.31(5)
Maximum Residual Density, e$^-$/mm^3		-0.20(5)

[00115] Fractional coordinates and isotropic displacement parameters for nonhydrogen atoms of Compound A glycolate hydrate are below.

Atom	x/a	y/b	z/c	Ueq or Uiso
N(1)	-257(2)	-899(1)	12193(1)	20(1)
N(2)	5139(2)	694(1)	7829(1)	20(1)
N(3)	6756(2)	2109(1)	5718(1)	19(1)
N(4)	6028(2)	3909(1)	3603(1)	20(1)
O(1)	3205(2)	2569(1)	10538(1)	28(1)
O(2)	4938(2)	2063(1)	8709(1)	29(1)
O(3)	4772(1)	-997(1)	7440(1)	24(1)
C(1)	125(2)	99(2)	12375(2)	19(1)
C(2)	-591(2)	359(2)	13379(2)	24(1)
C(3)	17(2)	1385(2)	13408(2)	26(1)
C(4)	1276(2)	2140(2)	12470(2)	25(1)
C(5)	1979(2)	1871(2)	11474(2)	21(1)
C(6)	1426(2)	814(2)	11409(2)	18(1)
C(7)	1877(2)	171(2)	10607(2)	18(1)
C(8)	3033(2)	251(2)	9554(2)	18(1)
C(9)	3028(2)	-663(2)	9123(2)	18(1)
C(10)	1928(2)	-1682(2)	9680(2)	18(1)
C(11)	1733(2)	-2727(2)	9343(2)	21(1)
C(12)	438(2)	-3632(2)	10444(2)	32(1)
C(13)	-315(2)	-2918(2)	11209(2)	22(1)
C(14)	786(2)	-1790(2)	10718(2)	18(1)
C(15)	769(2)	-890(2)	11162(2)	18(1)
C(16)	3936(2)	3508(2)	10681(2)	29(1)
C(17)	4427(2)	1141(2)	8708(2)	20(1)
C(18)	4362(2)	-404(2)	8046(2)	19(1)
C(19)	6654(2)	1170(2)	6943(2)	20(1)
C(20)	6273(2)	3305(2)	5683(2)	19(1)
C(21)	6719(2)	4290(2)	4353(2)	20(1)
C(22)	6426(2)	2644(2)	3709(2)	24(1)
C(23)	6001(2)	1698(2)	5052(2)	21(1)
C(24)	6476(2)	4852(2)	2287(2)	25(1)
C(1G)	539(2)	3469(2)	4989(2)	28(1)
O(1G)	335(2)	4218(1)	3828(1)	36(1)
C(2G)	2165(2)	3395(2)	4961(2)	22(1)

Atom	x/a	y/b	z/c	Ueq or Uiso
O(2G)	3132(1)	4059(1)	3938(1)	28(1)
O(3G)	2455(1)	2720(1)	5939(1)	26(1)
O(1W)	2887(3)	5938(2)	1816(2)	33(1)

[00116] Fractional coordinates and isotropic displacement parameters for hydrogen atoms of Compound A glycolate hydrate are below.

Atom	x/a	y/b	z/c	Ueq or Uiso
H(1N)	-1000(20)	-1530(20)	12750(20)	24
H(4N)	4940(30)	3842(19)	3953(19)	23
H(2)	-1457	-148	14013	29
H(3)	-433	1583	14085	31
H(4)	1659	2849	12512	30
H(11A)	2661	-3146	9246	26
H(11B)	1469	-2413	8561	26
H(12A)	830	-4388	10960	38
H(12B)	-296	-3897	10139	38
H(13A)	-1292	-2670	11078	26
H(13B)	-472	-3436	12105	26
H(16A)	3290	4181	10650	44
H(16B)	4885	3850	10010	44
H(16C)	4137	3140	11482	44
H(19A)	7229	1522	7305	24
H(19B)	7157	450	6862	24
H(20A)	6749	3560	6170	23
H(20B)	5171	3219	6054	23
H(21A)	6384	5100	4325	24
H(21B)	7825	4402	3996	24
H(22A)	7518	2687	3319	28
H(22B)	5895	2376	3262	28
H(23A)	4900	1613	5432	25
H(23B)	6297	871	5108	25
H(24A)	6170	5666	2242	38
H(24B)	5986	4590	1822	38
H(24C)	7567	4923	1929	38

Atom	x/a	y/b	z/c	Ueq or Uiso
H(1G1)	58	2611	5299	33
H(1G2)	21	3808	5583	33
H(1G)	1112	4714	3360	53
H(1W)	3200(50)	5350(40)	2430(40)	42(11)
H(2W)	3340(60)	6690(40)	1640(40)	70(16)

Thermal Analysis

[00117] The DSC curve of the glycolate hydrate salt, Form A_1, shows the presence of two different endothermic peaks; one at 77.4°C having a ΔH_{Fus} of 63.4 J/g and a second peak at 209.0°C and a ΔH_{Fus} of 170.9 J/g (Figure 11). The glycolate hydrate salt had a weight loss of 1.9% between 25 and 150°C.

Water Sorption

[00118] The DVS plot in Figure 12 indicated that there was surface adsorption with limited bulk absorption throughout the entire RH range. The total uptake in moisture at 90% RH is ~3.5%.

^{1}H-NMR Spectroscopy

[00119] The spectrum gives all of the peaks necessary for Compound A. After normalization of the integration to one proton in the aromatic region at about 7.5 ppm for Compound A, there is a two proton singlet at about 3.9 ppm for the two protons associated with the methylene group of glycolic acid. This indicated a 1:1 mole ratio of Compound A to glycolic acid in the salt.

Stability

[00120] The data given in Table 10 indicate that this salt is fairly stable to the test conditions. A modest increase in Compound B is noted after 28 days. A monoglycolate salt, as the ^{1}H- NMR indicated, should have a Compound A Assay of 84.5% Compound A. Increasing loss in TGA suggests increasing water content, for example, 3.5% loss would be expected for a water to Compound A ratio of 1:1.

Table 10. Stability at 40 °C and 75% RH of Glycolate Salt Hydrate, Form A_1

Day	XRPD	DSC,°C	TGA, %	COMPOUND A Assay, %	COMPOUND B Assay, %	HPLC Purity, %
0	A1	69.7, 207.9	2.1	69.9	0.1	99.8
7	No change	208.3	2.3	68.4	0.1	99.6
14	No change	68.8, 207.3	2.6	73.2	0.2	99.7
28	No change	207.4	3.5	66.8	0.6	99.5

Optical Microscopy

[00121] In Figure 13, the sample presented individual and agglomerates of crystals. The sample showed birefringence under plane polarized light.

Compound A, L-Malate Salt, Form A_1

Preparation

[00122] The salt was prepared according to Example 1.

XRPD

[00123] The X-ray diffraction data for the malate salt, Form A_1, is given in Figure 14 and Table 11. Overlaid slow scans for a VT-XRPD study are shown in Figure 15.

[00124] The initial XRPD pattern is as expected. There is no change in form on exposure to a dry N2 atmosphere (Figure 15). There is a change when the sample is held at 175°C for an hour. The fast scan measured when 175°C was first reached compares to the starting pattern. The crystalinity is almost completely gone in the fast scan measured after 175°C. The slow scan pattern observed for this sample after heating to 175°C and cooling to 25°C partially compares to the pattern for Compound B. This observation is consistent with thermal decomposition to Compound B.

Table 11. XRPD Peaks for Malate Salt, Form A_1

No.	Pos. [2θ°]*	d-spacing [Å]	Rel. Int.[%]		No.	Pos. [2θ°]*	d-spacing [Å]	Rel. Int.[%]
1	8.60	10.269	51		21	21.22	4.184	53
2	9.18	9.631	25		22	21.59	4.112	3
3	10.06	8.789	36		**23**	**22.36**	**3.972**	**100**
4	10.40	8.496	25		24	23.45	3.791	17
5	11.74	7.529	14		25	24.08	3.692	2
6	11.87	7.450	27		26	24.27	3.664	10
7	12.85	6.885	3		27	24.52	3.627	3
8	13.33	6.635	6		28	24.99	3.560	2
9	13.97	6.334	5		29	25.76	3.455	3

No.	Pos. [2θ°]*	d-spacing [Å]	Rel. Int.[%]		No.	Pos. [2θ°]*	d-spacing [Å]	Rel. Int.[%]
10	14.46	6.120	6		30	25.87	3.442	3
11	14.70	6.021	18		31	26.99	3.301	15
12	15.27	5.797	12		32	27.38	3.254	3
13	15.56	5.690	9		33	27.79	3.208	3
14	17.19	5.156	47		34	27.96	3.188	4
15	17.76	4.991	17		35	28.12	3.171	2
16	17.98	4.930	5		36	29.11	3.066	4
17	18.54	4.781	28		37	29.60	3.016	2
18	19.29	4.597	5		38	30.22	2.955	2
19	20.27	4.376	14		39	30.42	2.936	3
20	20.65	4.297	9		40	30.75	2.905	5

*The use of ZBG or glass plates typically introduces a positive sample height displacement and results in small (0.05° to 0.2°) offset in 2θ values. The highest peak (intensity 100%) is set in bold letters.

Thermal Analysis

[00125] The DSC curve of the malate salt, Form A_1 shows the presence of one endothermic peak; at 186.4°C having a ΔH_{Fus} of 75.7 J/g (Figure 16). The malate salt had a weight loss of 1.0% between 25 and 150°C.

Water Sorption

[00126] The DVS plot in (Figure 17) indicated there was very little water absorption during the first cycle from 40%RH to 70%RH. Only surface adsorption is occurring. At 80%RH is an increase in water uptake. The large hysteresis gap is due to bulk absorption. The total uptake is ~2%. The isotherm is irreversible.

^{1}H-NMR Spectroscopy

[00127] All of the peaks expected for Compound A are present. After normalization of the one aromatic proton at 7.5 ppm, there is a one proton triplet at about 4.05ppm that is consistent with L- malic acid. This established the 1:1 stoichiometry for the Compound A L-malic acid salt in Form A_1.

Stability

[00128] The data in Table 12 show that the L-malate salt is stable to the test conditions with a constant XRPD, DSC, TGA and HPLC Purity values (MJJ3331-49). An increase in Compound B is observed after 28 days. As with the glycolate hydrate salt, the L-malate Assay value for Compound A is lower than the 75.8% value expected.

Table 12. Stability at 40°C and 75% RH of the L-Malate Salt, Form A_1

Day	XRPD	DSC	TGA	COMPOUND A Assay	COMPOUND B Assay	HPLC Purity
0	A_1	193.0°C	0.1%	69.9%	0.2%	99.5%
7	No change	192.0°C	0.2%	71.8%	0.4%	99.3%
14	No change	191.4°C	0.8%	72.0%	0.5%	98.8%
28	No change	191.1°C	0.3%	71.7%	0.8%	98.4%

Optical Microscopy

[00129] In Figure 18, the sample showed individual crystals and agglomerates of irregular shaped crystals. The sample showed birefringence under plane polarized light.

Compound A, L-Malate Salt, Form $A_{1.5}$

Preparation

[00130] The salt was prepared according to Example 2.

XRPD

[00131] The X-ray diffraction data for the malate salt, Form $A_{1.5}$, is given in Figure 19 and Table 13.

Table 13. XRPD Peaks for Malate Salt, Form $A_{1.5}$

No.	Pos. [2θ°]*	d-spacing [Å]	Rel. Int.[%]		No.	Pos. [2θ°]*	d-spacing [Å]	Rel. Int.[%]
1	5.53	15.978	63		21	20.16	4.401	16
2	6.80	12.985	53		22	20.53	4.322	15
3	7.97	11.085	26		23	21.13	4.201	20
4	**8.43**	**10.478**	**100**		24	21.37	4.154	11
5	8.76	10.084	35		25	21.86	4.063	20
6	9.23	9.577	23		26	22.84	3.890	10
7	11.79	7.500	28		27	23.14	3.841	24
8	12.44	7.108	10		28	23.63	3.762	14
9	12.78	6.923	17		29	24.04	3.698	10
10	13.05	6.778	17		30	24.60	3.615	29
11	13.64	6.489	15		31	25.16	3.536	13
12	13.92	6.355	11		32	25.66	3.469	9
13	14.44	6.131	61		33	28.20	3.162	7
14	15.99	5.538	44		34	29.00	3.076	3
15	16.66	5.316	72		35	30.05	2.971	5
16	17.12	5.175	7		36	30.43	2.936	6
17	18.12	4.891	31		37	32.25	2.774	2
18	18.46	4.802	40		38	33.11	2.704	2
19	18.79	4.720	7		39	36.66	2.449	3
20	19.44	4.562	17		40	39.38	2.286	3

*The use of ZBG or glass plates typically introduces a positive sample height displacement and results in small (0.05° to 0.2°) offset in 2θ values. The highest peak (intensity 100%) is set in bold letters.

Thermal Analysis

[00132] The DSC curve of the L-malate salt, Form $A_{1.5}$, shows the presence of one endothermic peak; at 160.4°C having a ΔH_{Fus} of 39.2 J/g (Figure 20). The L-malate salt had a weight loss of 3.6% between 25 and 150°C. This Form melts at a much lower temperature and has a larger weight loss than the malate salt, Form A_1.

^{1}H-NMR Spectroscopy

[00133] The ^{1}H-NMR spectrum of the L-malate salt, Form $A_{1.5}$ showed all of the peaks were present for Compound A and the normalized integration showed about 3 moles of L-malic acid for two moles of Compound A. This preparation represented a new form for Compound A L-malate salt.

Compound A, L-Pyroglutamate Salt, Form A_1

Preparation

[00134] The sale was prepared according to Example 3.

XRPD

[00135] The X-ray diffraction data for the L-pyroglutamate salt, Form A_1 is given in Table 14 and Figure 21. The XRPD pattern showed a highly crystalline solid.

[00136] Variable temperature XRPD measurements are shown in Figure 22. The initial XRPD pattern is as expected. There is no change in form on heating to 175°C. At the end of the experiment a black glass was left on the ZBG plate. Comparison of the expected pattern for Compound B and the sample after heating to 210°C shows small differences. This suggests conversion of Compound A to Compound B and a possible second component.

Table 14. XRPD Peaks for L-Pyroglutamate Salt, Form A_1

No.	Pos. [2θ°]*	d-spacing [Å]	Rel. Int.[%]		No.	Pos. [2θ°]*	d-spacing [Å]	Rel. Int.[%]
1	6.02	14.669	74		21	20.98	4.231	34
2	9.56	9.242	43		22	21.14	4.199	29
3	10.31	8.573	61		23	21.36	4.156	9
4	10.54	8.391	25		24	21.67	4.097	10
5	11.03	8.017	96		25	21.96	4.045	33
6	**12.01**	**7.364**	**100**		26	22.11	4.017	23
7	12.89	6.864	21		27	22.70	3.914	21
8	13.22	6.693	33		28	23.13	3.842	23

No.	Pos. [2θ°]*	d-spacing [Å]	Rel. Int.[%]		No.	Pos. [2θ°]*	d-spacing [Å]	Rel. Int.[%]
9	14.32	6.180	12		29	23.39	3.800	84
10	15.00	5.900	24		30	23.51	3.781	56
11	16.71	5.301	36		31	24.11	3.689	14
12	17.02	5.206	22		32	24.53	3.626	8
13	17.51	5.061	59		33	24.84	3.582	54
14	17.79	4.983	68		34	25.08	3.547	9
15	18.02	4.919	78		35	26.56	3.353	33
16	18.68	4.747	19		36	27.57	3.232	8
17	18.98	4.672	29		37	28.15	3.168	13
18	19.37	4.578	7		38	28.78	3.099	9
19	20.22	4.388	7		39	30.22	2.955	11
20	20.76	4.276	35		40	30.43	2.935	9

*The use of ZBG or glass plates typically introduces a positive sample height displacement and results in small (0.05° to 0.2°) offset in 2θ values. The highest peak (intensity 100%) is set in bold letters.

Thermal Analysis

[00137] The DSC curve of the L-pyroglutamate salt, Form A_1, shows the presence of two endothermic peaks; at 50.4°C having a ΔH_{Fus} of 35.6 J/g and 198.2°C having a ΔH_{Fu} of 76.8 J/g (Figure 23). The pyroglutamate salt had a weight loss of 3.5% between 25 and 150°C.

Water Sorption

[00138] In the DVS Plot (Figure 24) indicated that during the first cycle there is very little water absorption over the RH range of 40-75% (~2%). Only surface adsorption is occurring. At 80% RH there is a massive uptake in moisture. The large hysteresis gap at 50-90% RH is due to bulk absorption with a possible hydrate formation. The total uptake is ~27%.

^{1}H-NMR Spectroscopy

[00139] All of the peaks are present for Compound A. After normalization of the integration for one proton for the aromatic peak in Compound A at about 7.5 ppm, there is an additional one proton singlet at about 7.85ppm for the hydrogen atom on the amide nitrogen in pyroglutamic acid. In addition, there is an additional one proton multiplet at about 4.05 ppm from the one hydrogen atom attached to the carbon atom adjacent to the carboxylic acid group. This establishes this salt as a mono L-pyroglutamate salt of Compound A.

Stability

[00140] This salt was stable over a 28 day test period, except for a slow increase in Compound B content (Table 15).

Table 15. Stability at 40°C and 75% RH of the L-Pyroglutamate Salt, Form A_1 (Prepared with Two Equivalents of Acid)

Day	XRPD	DSC,	TGA, %	COMPOUND A Assay, %	COMPOUND B Assay, %	HPLC Purity, %
0	A_1	198.2	0.49	65.5	0.6	98.6
7	No change	199.0	0.54	71.4	0.6	98.7
14	No change	198.3	0.64	60.2	0.8	98.2
28	No change	198.4	0..11	64.0	1.2	97.2

Optical Microscopy

[00141] The sample presented agglomerates of irregular shaped crystals as shown in Figure 25. The sample showed birefringence under plane polarized light.

Comparison of Salts

[00142] In Table 16, glycolate hydrate Form A_1, L-malate Form A_1 and the one and two equivalent preparations of L-pyroglutamate Form A_1 are compared. The glycolate hydrate salt, Form A_1, generated the least amount of Compound B during 40° C and 75% RH stability testing. The glycolate hydrate exhibited a preference for water absorption since the TGA value increased to 3.5 % during stability testing (Table 10).

Table 16. Comparison of Compound A Salts

Property	Glycolate (2 Eq.)	L-malate (2 Eq.)	L-pyroglu-tamate (2 Eq.)	L-pyroglu-tamate (1 Eq.)
Crystallinity	Form A_1	Form A_1	Form A_1	Form A_1
DSC	69.7, 207.9	193.0	198.2	201.7
TGA	2.1%	0.1%	0.5%	0.2%
DVS	Reversible	Irreversible	Irreversible	Not measured
TGA After 40/75:				
COMPOUND A Initial	69.9%	71.3%	65.5%	75.5%
COMPOUND B Initial	0.1%	0.2%	0.6%	0.5%
COMPOUND B After 40/75	0.6%	1.2%	1.2%	1.3%
Est. Water Solubility	>100 mg/mL	>100 mg/mL	>100 mg/mL	>100 mg/mL
% Active in Salt	85%	76%	76%	76%
Desiccant Required	Yes	Yes	Yes	Yes
Acid Classification	Class 1	Class 1	Class 2	Class 2

Compound A, Free Base, Form C_0

Preparation

[00143] The free base was prepared according to Example 4.

XRPD

[00144] The X-ray diffraction data for free base, Form C_0, is given in Figure 26 and Table 17. The XRPD pattern showed a crystalline solid.

[00145] Variable temperature XRPD measurements are shown in Figure 27. The initial XRPD pattern compares to the expected pattern for Form C_0. There is no change in form on exposure to a dry N2 atmosphere. There is no change in form after heating to 175°C. After heating to 235°C the XRPD pattern is changed and is similar to, but not the same as, the pattern observed for Compound B. Similar patterns have been seen for other VT samples. There seem to be two components present in this decomposition product.

Table 17. XRPD Peaks for Free Base, Form C_0

No.	Pos. [2θ°]*	d-spacing [Å]	Rel. Int.[%]		No.	Pos. [2θ°]*	d-spacing [Å]	Rel. Int.[%]
1	2.03	43.473	5		21	23.56	3.773	6
2	7.96	11.104	4		22	24.59	3.618	67
3	8.49	10.411	86		23	25.64	3.471	5
4	**8.77**	**10.078**	**100**		24	26.02	3.422	2
5	10.66	8.293	2		25	27.01	3.299	1
6	13.92	6.358	33		26	27.75	3.212	2
7	14.44	6.130	12		27	29.40	3.036	7
8	15.15	5.845	6		28	30.07	2.969	5
9	15.39	5.752	11		29	31.26	2.859	1
10	15.93	5.560	5		30	31.63	2.826	2
11	17.56	5.045	19		31	32.13	2.784	2
12	18.13	4.890	20		32	32.63	2.742	1
13	18.47	4.801	18		33	33.37	2.683	1
14	19.15	4.632	14		34	34.06	2.630	2
15	19.74	4.493	10		35	34.32	2.611	1
16	20.27	4.377	8		36	34.88	2.570	1
17	20.42	4.346	17		37	35.12	2.553	1
18	21.10	4.208	30		38	35.44	2.531	1
19	21.36	4.157	27		39	35.88	2.501	1
20	21.86	4.063	45		40	38.64	2.329	1

Thermal Analysis

[00146] The DSC curve of the free base, Form C_0, shows the presence of one endothermic peak; at 207.3°C having a ΔH_{Fus} of 71.4 J/g (Figure 28). Form C_0 had a weight loss of 2.3% between 25 and 150°C.

Optical Microscopy

[00147] In Figure 29, the sample presented agglomerates and individual irregular shaped crystals. The sample showed birefringence under plane polarized light.

Compound A, Hydrochloride Salt, Form A

Preparation

[00148] The salt was prepared according to Example 5.

XRPD

[00149] The X-ray diffraction data for the chloride salt, Form A, is given in Figure 30 and Table 18.

Table 18. XRPD Peaks for the Hydrochloride Salt, Form A

No.	Pos. [2θ°]*	d-spacing [Å]	Rel. Int.[%]		No.	Pos. [2θ°]*	d-spacing [Å]	Rel. Int.[%]
1	6.13	14.403	2		20	22.30	3.983	12
2	**7.45**	**11.863**	**100**		21	23.58	3.770	0
3	7.95	11.108	3		22	24.49	3.631	9
4	8.55	10.337	25		23	24.88	3.576	3
5	10.51	8.409	1		24	25.57	3.481	8
6	12.20	7.248	42		25	26.08	3.414	8
7	12.94	6.837	4		26	27.14	3.283	0
8	13.55	6.532	0		27	27.75	3.213	3
9	14.94	5.926	2		28	28.34	3.147	3
10	15.90	5.569	1		29	30.81	2.900	3
11	16.21	5.463	2		30	31.06	2.877	3
12	17.12	5.175	16		31	31.80	2.812	2
13	17.95	4.937	2		32	33.46	2.676	4
14	18.34	4.833	1		33	34.13	2.625	4
15	18.83	4.710	37		34	34.89	2.570	2
16	18.87	4.700	29		35	36.22	2.478	1
17	19.26	4.606	4		36	37.44	2.400	1
18	20.24	4.383	1		37	39.42	2.284	1
19	21.27	4.174	1		28			

*The use of ZBG or glass plates typically introduces a positive sample height displacement and results in small (0.05° to 0.2°) offset in 2θ values. The highest peak (intensity 100%) is set in bold letters.

Thermal Analysis

[00150] The DSC curve of the hydrochloride salt, Form A, shows one endothermic peak at 247.3°C having a ΔH_{Fus} of 41.6 J/g (Figure 31). The hydrochloride salt, Form A, had a weight loss of 0.2% between 25 and 150°C.

Water Sorption

[00151] The DVS Plot (Figure 32) indicated there is surface adsorption with limited bulk absorption throughout the entire RH range. The total uptake in moisture is ~2.25%.

Stability

[00152] The data in Table 19 show a relatively constant XRPD pattern and DSC value with modest changes in TGA value. The HPLC values are quite different with Assay value decreasing to nearly half after 28 days of testing. Also noted was a steady decline in HPLC purity and an increase in Compound B content to 1.5%. The theoretical value for Compound A content in a Compound A monohydrochloride salt is 92.0%.

Table 19. Stability at 40°C and 75% RH of the Hydrochloride Form A

Day	XRPD	DSC °C	TGA%	COMPOUND A Assay	COMPOUND B Assay	HPLC Purity
0	A	244.8	0.1	39.9	0.3	99.1
7	No change	247.6	1.5	22.3	0.7	96.3
14	No change	245.9	1.1	21.6	1.1	94.0
28	No change	245.5	0.9	19.6	1.5	91.1

Compound A, Fumarate Salt, Form A

Preparation

[0100] The salt was prepared according to Example 5.

XRPD

[00153] The X-ray diffraction data for Compound A Fumarate Salt, Form A, is given in Figure 33 and Table 20.

Table 20. XRPD Peaks for the Fumarate Salt, Form A

No.	Pos. [20°]*	d-spacing [Å]	Rel. Int.[%]		No.	Pos. [20°]*	d-spacing [Å]	Rel. Int.[%]

No.	Pos. [2θ°]*	d-spacing [Å]	Rel. Int.[%]		No.	Pos. [2θ°]*	d-spacing [Å]	Rel. Int.[%]
1	**8.98**	**9.842**	**100**		21	22.88	3.884	8
2	10.54	8.388	26		22	23.50	3.783	16
3	11.06	7.994	11		23	24.04	3.699	22
4	12.94	6.835	4		24	24.19	3.677	15
5	14.86	5.958	20		25	25.36	3.509	4
6	15.44	5.734	2		26	25.45	3.497	2
7	15.55	5.694	5		27	25.59	3.479	2
8	16.19	5.469	5		28	25.71	3.463	8
9	17.07	5.190	37		29	25.90	3.437	8
10	17.69	5.008	20		30	26.08	3.415	4
11	18.20	4.871	3		31	26.24	3.393	4
12	18.74	4.732	4		32	26.51	3.360	2
13	19.04	4.657	3		33	26.75	3.329	4
14	19.13	4.637	7		34	27.29	3.266	7
15	19.34	4.585	24		35	28.95	3.082	11
16	19.68	4.508	5		36	29.92	2.984	4
17	20.72	4.284	4		37	30.78	2.902	3
18	21.09	4.209	24		38	30.99	2.884	3
19	21.80	4.074	2		39	31.09	2.874	6
20	22.32	3.980	8		40	36.83	2.438	2

*The use of ZBG or glass plates typically introduces a positive sample height displacement and results in small (0.05° to 0.2°) offset in 2θ values. The highest peak (intensity 100%) is set in bold letters.

Thermal Analysis

[00154] The DSC curve of the fumarate salt, Form A, showed the presence of one endothermic peak; at 231.3°C having a ΔH_{Fus} of 106.9 J/g (Figure 34). Form A had a weight loss of 0.2% between 25 and 150°C.

Compound A, p-Toluenesulfonate Salt, Form A

Preparation

[00155] The salt was prepared according to Example 5.

XRPD

[00156] Characterization of the p-Toluenesulfonate Salt, Form A is depicted in Figure 35 and Table 21.

Table 21. XRPD Peaks for the p-Toluenesulfonate Salt, Form A

No.	Pos. [2θ°]*	d-spacing [Å]	Rel. Int.[%]		No.	Pos. [2θ°]*	d-spacing [Å]	Rel. Int.[%]
1	6.02	14.669	74		21	20.98	4.231	34
2	9.56	9.242	43		22	21.14	4.199	29
3	10.31	8.573	61		23	21.36	4.156	9
4	10.54	8.391	25		24	21.67	4.097	10
5	11.03	8.017	96		25	21.96	4.045	33
6	**12.01**	**7.364**	**100**		26	22.11	4.017	23
7	12.89	6.864	21		27	22.70	3.914	21
8	13.22	6.693	33		28	23.13	3.842	23
9	14.32	6.180	12		29	23.39	3.800	84
10	15.00	5.900	24		30	23.51	3.781	56
11	16.71	5.301	36		31	24.11	3.689	14
12	17.02	5.206	22		32	24.53	3.626	8
13	17.51	5.061	59		33	24.84	3.582	54
14	17.79	4.983	68		34	25.08	3.547	9
15	18.02	4.919	78		35	26.56	3.353	33
16	18.68	4.747	19		36	27.57	3.232	8
17	18.98	4.672	29		37	28.15	3.168	13
18	19.37	4.578	7		38	28.78	3.099	9
19	20.22	4.388	7		39	30.22	2.955	11
20	20.76	4.276	35		40	30.43	2.935	9

*The use of ZBG or glass plates typically introduces a positive sample height displacement and results in small (0.05° to 0.2°) offset in 2θ values. The highest peak (intensity 100%) is set in bold letters.

Thermal Analysis

[00157] The DSC curve of the p-toluenesulfonate salt, Form A, shows the presence of one endothermic peak; at 239.6°C having a ΔH_{Fus} of 38.5 J/g (Figure 36). Form A had a weight loss of 0.04% between 25 and 150°C.

What is Claimed:

1. A crystalline form of 4,5,6,7-tetrahydro-11-methoxy-2-[(4-methyl-1-piperazinyl)methyl]-1*H*-cyclopenta[*a*]pyrrolo[3,4-*c*]carbazole-1,3(2*H*)-dione (Compound A)

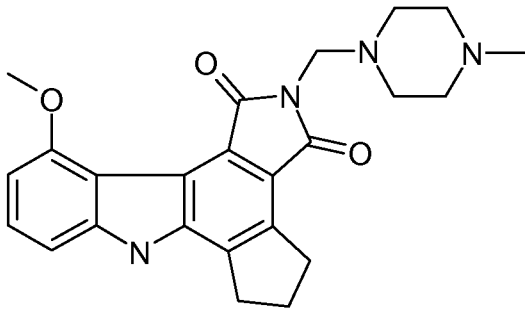

Compound A

that is

Compound A, acetate salt Form $A_{1.5}$;

Compound A, glycolate salt hydrate Form A_1;

Compound A, L-malate salt Form A_1;

Compound A, L-malate salt Form $A_{1.5}$;

Compound A, L-pyroglutamate salt Form A_1;

Compound A, free base Form C_0;

Compound A, hydrochloride salt Form A;

Compound A, fumarate salt Form A; or

Compound A, p-toluenesulfonate salt Form A.

2. The crystalline form of claim 1 that is Compound A, glycolate salt hydrate Form A_1.

3. The crystalline form of claim 2, characterized by an X-ray powder diffraction pattern having at least three peaks selected from the group consisting of 8.2, 8.7, 13.8, 14.9, 16.4, 17.5, 18.2, 18.5, 20.2, 20.6, 21.2, 21.4, 23.0, 24.6, 27.8, 29.9, 30.1, and 30.5 degrees two theta ± 0.2 degrees two theta.

4. The crystalline form of claim 2 or claim 3, further characterized by an X-ray powder diffraction pattern substantially as depicted in Figure 9 or Figure 10.

5. The crystalline form of any one of claims 2 to 4, further characterized by an X-ray powder diffraction pattern substantially as depicted in Figure 9.

6. The crystalline form of any one of claims 2 to 5, further characterized by a DSC substantially as depicted in Figure 11.

7. The crystalline form of any one of claims 2 to 6, further characterized by a DVS substantially as depicted in Figure 12.

8. The crystalline form of claim 1 that is Compound A, acetate salt Form $A_{1.5}$.

9. The crystalline form of claim 8, characterized by an X-ray powder diffraction pattern having at least three peaks selected from the group consisting of 6.4, 9.2, 12.7, 13.0, 15.2, 17.4, 18.4, 19.0, 19.3, 21.3, 21.5, 23.1, 24.1, 24.2, and 28.2 ± 0.2 degrees 2-theta.

10. The crystalline form of claim 8 or claim 9, further characterized by an X-ray powder diffraction pattern substantially as depicted in Figure 3, Figure 4, or Figure 5.

11. The crystalline form of any one of claims 8 to 10, further characterized by a DSC substantially as depicted in Figure 6.

12. The crystalline form of any one of claims 8 to 11, further characterized by a DVS substantially as depicted in Figure 7.

13. The crystalline form of claim 1 that is Compound A, L-malate salt Form A_1.

14. The crystalline form of claim 13, characterized by an X-ray powder diffraction pattern having at least three peaks selected from the group consisting of 8.6, 9.2, 10.1, 10.4, 11.7, 11.9, 14.7, 15.3, 15.6, 17.2, 17.8, 18.5, 20.3, 20.7, 21.2, 22.4, 23.5, 24.3, and 27.0 ± 0.2 degrees 2-theta.

15. The crystalline form of claim 13 or claim 14, further characterized by an X-ray powder diffraction pattern substantially as depicted in Figure 14 or Figure 15.

16. The crystalline form of any one of claims 13 to 15, further characterized by a DSC substantially as depicted in Figure 16.

17. The crystalline form of any one of claims 13 to 16, further characterized by a DVS substantially as depicted in Figure 17.

18. The crystalline form of claim 1 that is Compound A, L-malate salt Form $A_{1.5}$.

19. The crystalline form of claim 18, characterized by an X-ray powder diffraction pattern having at least three peaks selected from the group consisting of 5.5, 6.8, 8.0, 8.4, 8.8, 9.2, 11.8, 12.8, 13.1, 13.6, 14.4, 16.0, 16.7, 18.1, 18.5, 19.4, 20.2, 20.5, 21.1, 21.9, 23.4, and 24.6 ± 0.2 degrees 2-theta.

20. The crystalline form of claim 18 or claim 19, further characterized by an X-ray powder diffraction pattern substantially as depicted in Figure 19.

21. The crystalline form of any one of claims 18 to 20, further characterized by a DSC substantially as depicted in Figure 20.

22. The crystalline form of claim 1 that is Compound A, L-pyroglutamate salt Form A_1.

23. The crystalline form of claim 22, characterized by an X-ray powder diffraction pattern having at least three peaks selected from the group consisting of 6.0, 9.6, 10.3, 10.5, 11.0, 12.0, 13.2, 15.0, 16.7, 17.5, 17.8, 18.0, 19.0, 20.8, 21.0, 21.1, 22.0, 22.1, 23.1, 23.4, 23.5, 24.8, and 26.6 ± 0.2 degrees 2-theta.

24. The crystalline form of claim 22 or claim 23, further characterized by an X-ray powder diffraction pattern substantially as depicted in Figure 21 or Figure 22.

25. The crystalline form of any one of claims 22 to 24, further characterized by a DSC substantially as depicted in Figure 23.

26. The crystalline form of any one of claims 22 to 25, further characterized by a DVS substantially as depicted in Figure 24.

27. The crystalline form of claim 1 that is Compound A, free base Form C_0.

28. The crystalline form of claim 27, characterized by an X-ray powder diffraction pattern having at least three peaks selected from the group consisting of 8.5, 8.8, 13.9, 14.4, 15.4, 17.6, 18.1, 18.5, 19.2, 19.7, 20.4, 21.1, 21.4, 21.9, 23.6, 24.6, 29.4 and 30.1 ± 0.2 degrees 2-theta.

29. The crystalline form of claim 27 or claim 28, further characterized by an X-ray powder diffraction pattern substantially as depicted in Figure 26 or Figure 27.

30. The crystalline form of any one of claims 27 to 29, further characterized by a DSC substantially as depicted in Figure 28.

31. The crystalline form of claim 1 that is Compound A, hydrochloride salt Form A.

32. The crystalline form of claim 31, characterized by an X-ray powder diffraction pattern having at least three peaks selected from the group consisting of 7.5, 8.6, 12.2, 17.1, 18.8, 18.9, 22.3, 24.5, 25.6, 26.1, 33.5, and 34.1 ± 0.2 degrees 2-theta.

33. The crystalline form of claim 31 or claim 32, further characterized by an X-ray powder diffraction pattern substantially as depicted in Figure 30.

34. The crystalline form of any one of claims 31 to 33, further characterized by a DSC substantially as depicted in Figure 31.

35. The crystalline form of any one of claims 31 to 34, further characterized by a DVS substantially as depicted in Figure 32.

36. The crystalline form of claim 1 that is Compound A, fumarate salt Form A.

37. The crystalline form of claim 36, characterized by an X-ray powder diffraction pattern having at least three peaks selected from the group consisting of 9.0, 10.5, 11.1, 14.9, 17.1, 17.7, 19.3, 21.1, 22.3, 22.9, 23.5, 24.0, 24.2, 25.7, 25.9, 27.3, 29.0, and 31.1 ± 0.2 degrees 2-theta.

38. The crystalline form of claim 36 or claim 37, further characterized by an X-ray powder diffraction pattern substantially as depicted in Figure 33.

39. The crystalline form of any one of claims 36 to 38, further characterized by a DSC substantially as depicted in Figure 34.

40. The crystalline form of claim 1 that is Compound A, p-toluenesulfonate salt Form A.

41. The crystalline form of claim 40, characterized by an X-ray powder diffraction pattern having at least three peaks selected from the group consisting of 6.0, 9.6, 10.3, 10.5, 11.0, 12.0, 12.9, 13.2, 15.0, 16.7, 17.0, 17.5, 17.8, 18.0, 19.0, 20.8, 21.0, 21.1, 22.1, 22.7, 23.1, 23.4, 23.5, 24.8, , and 26.6 ± 0.2 degrees 2-theta.

42. The crystalline form of claim 40 or claim 41, further characterized by an X-ray powder diffraction pattern substantially as depicted in Figure 35.

43. The crystalline form of any one of claims 40 to 42, further characterized by a DSC substantially as depicted in Figure 36.

44. A pharmaceutical composition comprising the crystalline form of any one of the preceding claims and at least one pharmaceutically acceptable excipient.

45. A method of treating cancer in a patient comprising administering to the patient a crystalline form of 4,5,6,7-tetrahydro-11-methoxy-2-[(4-methyl-1-piperazinyl)methyl]-1*H*-cyclopenta[*a*]pyrrolo[3,4-*c*]carbazole-1,3(2*H*)-dione (Compound A) according to any one of claims 1 to 43.

46. The method of claim 45, wherein the cancer is breast cancer or ovarian cancer.

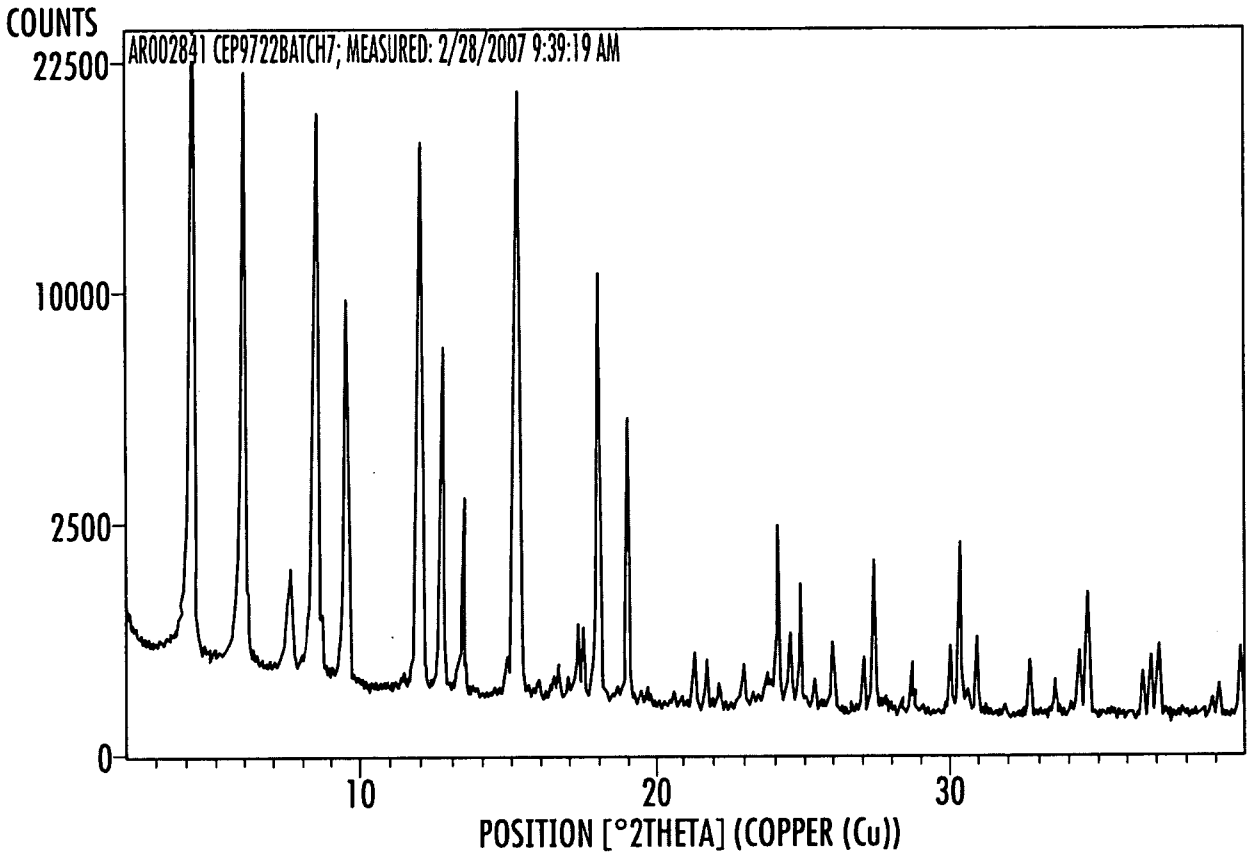

XRPD PATTERN FOR A COMPOUND A FREE BASE, FORM A_0

FIG. 1

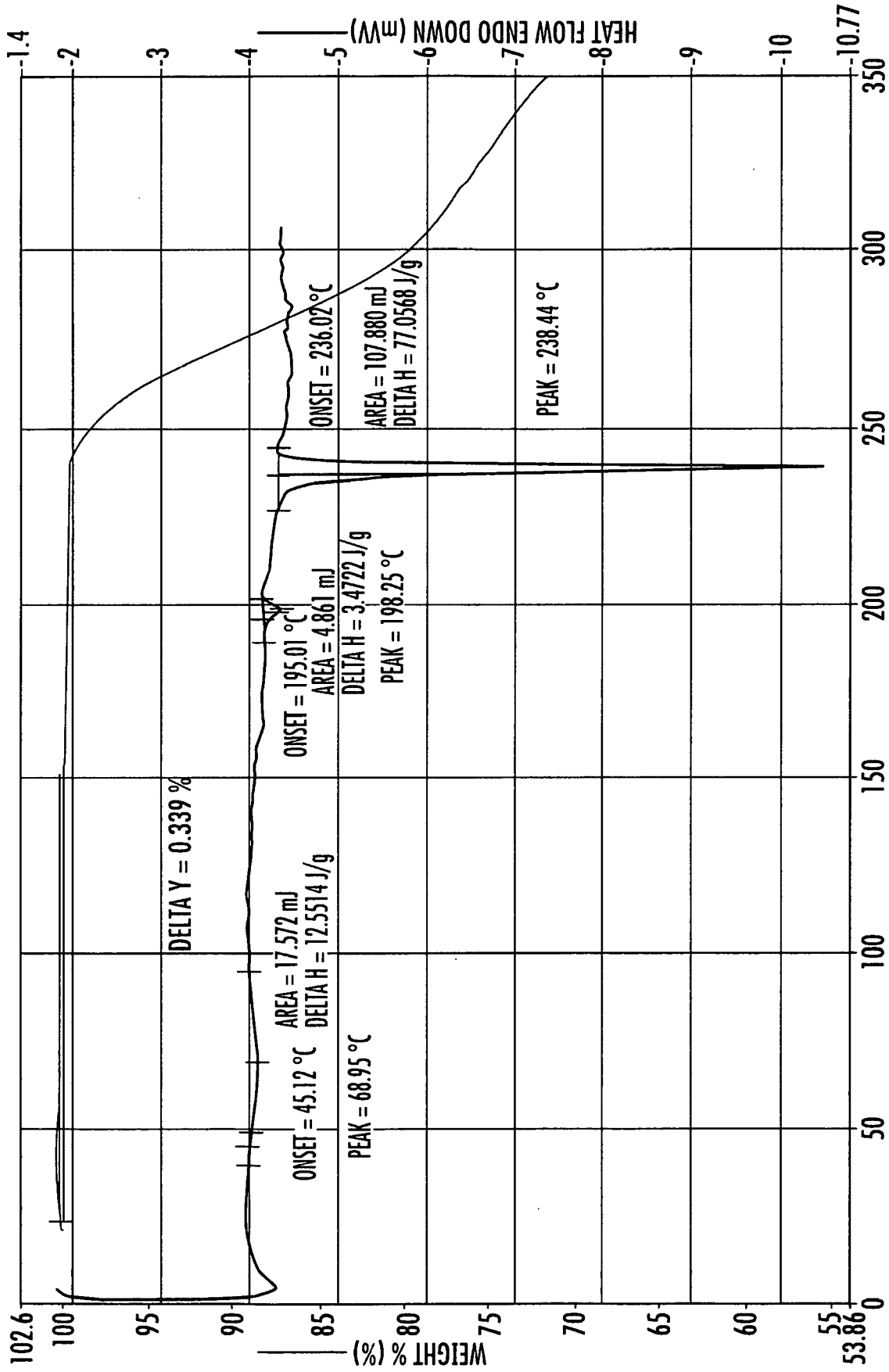

DSC/TGA OVERLAY FOR COMPOUND A FREE BASE, FORM A_0

FIG. 2

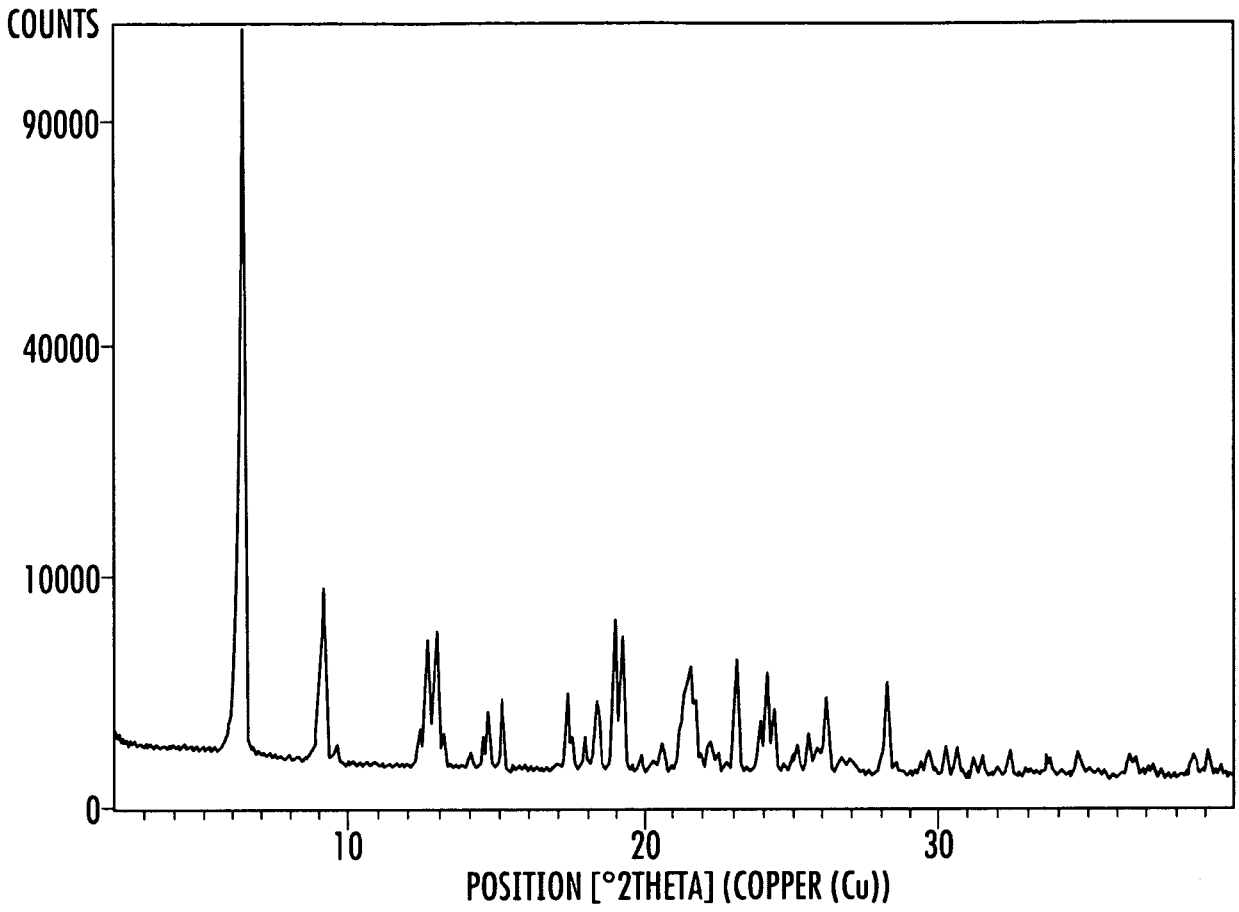

XRPD PATTERN OF COMPOUND A ACETATE SALT, FORM $A_{1.5}$

FIG. 3

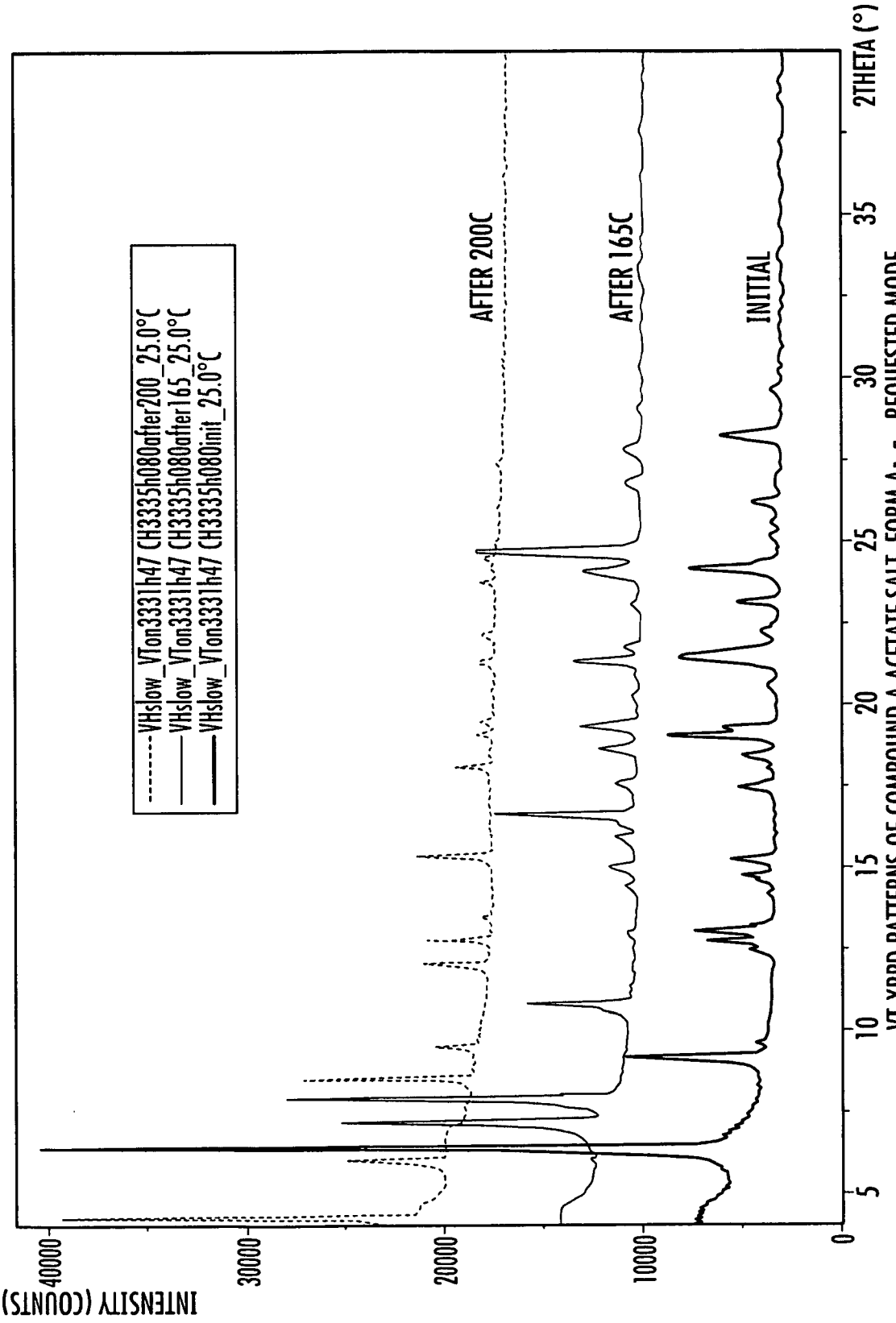

VT-XRPD PATTERNS OF COMPOUND A ACETATE SALT, FORM $A_{1.5}$ - REQUESTED MODE

FIG. 4

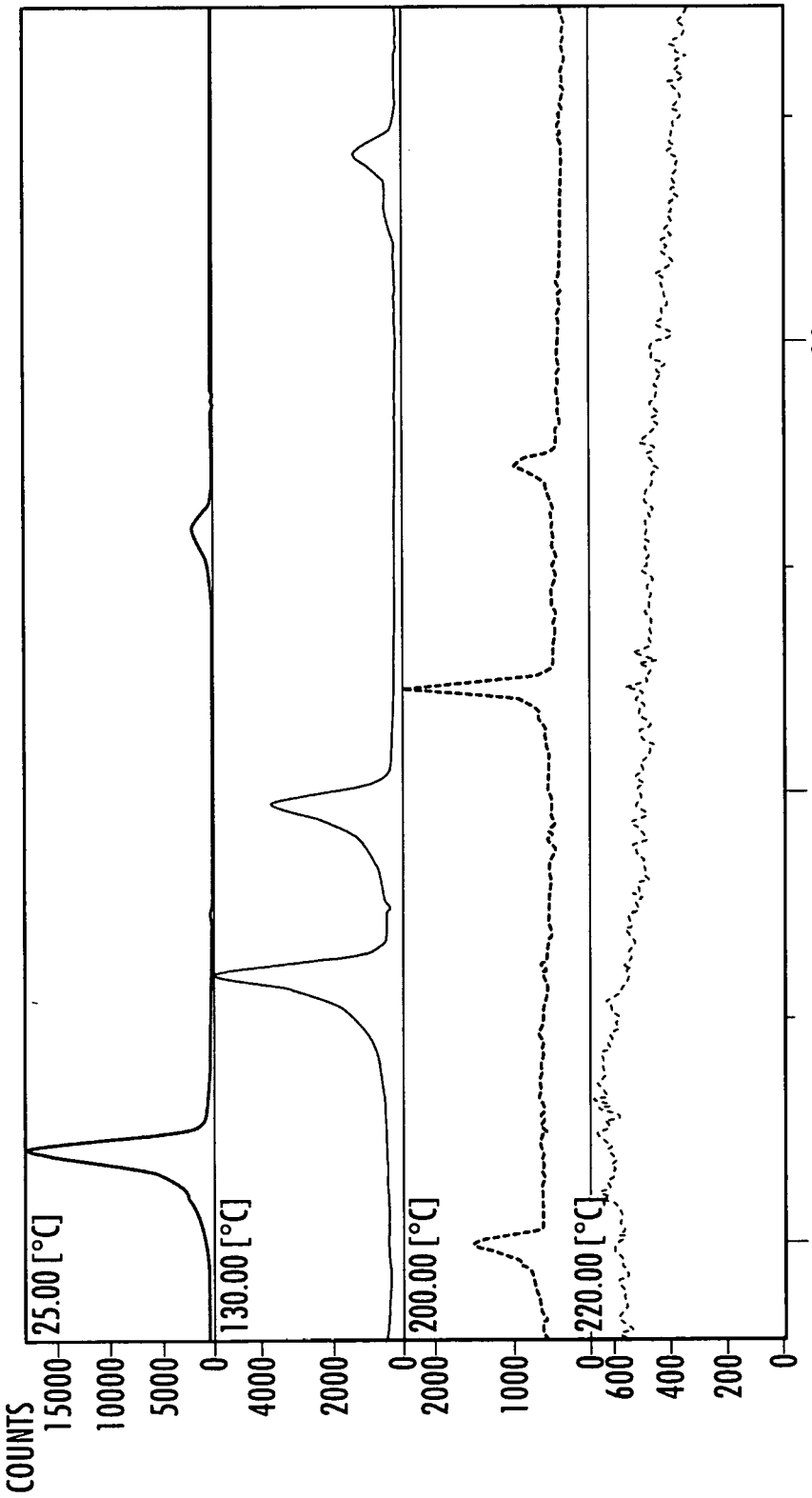

VT-XRPD PATTERNS OF COMPOUND A ACETATE SALT, FORM $A_{1.5}$ - CONTINUOUS MODE

FIG. 5

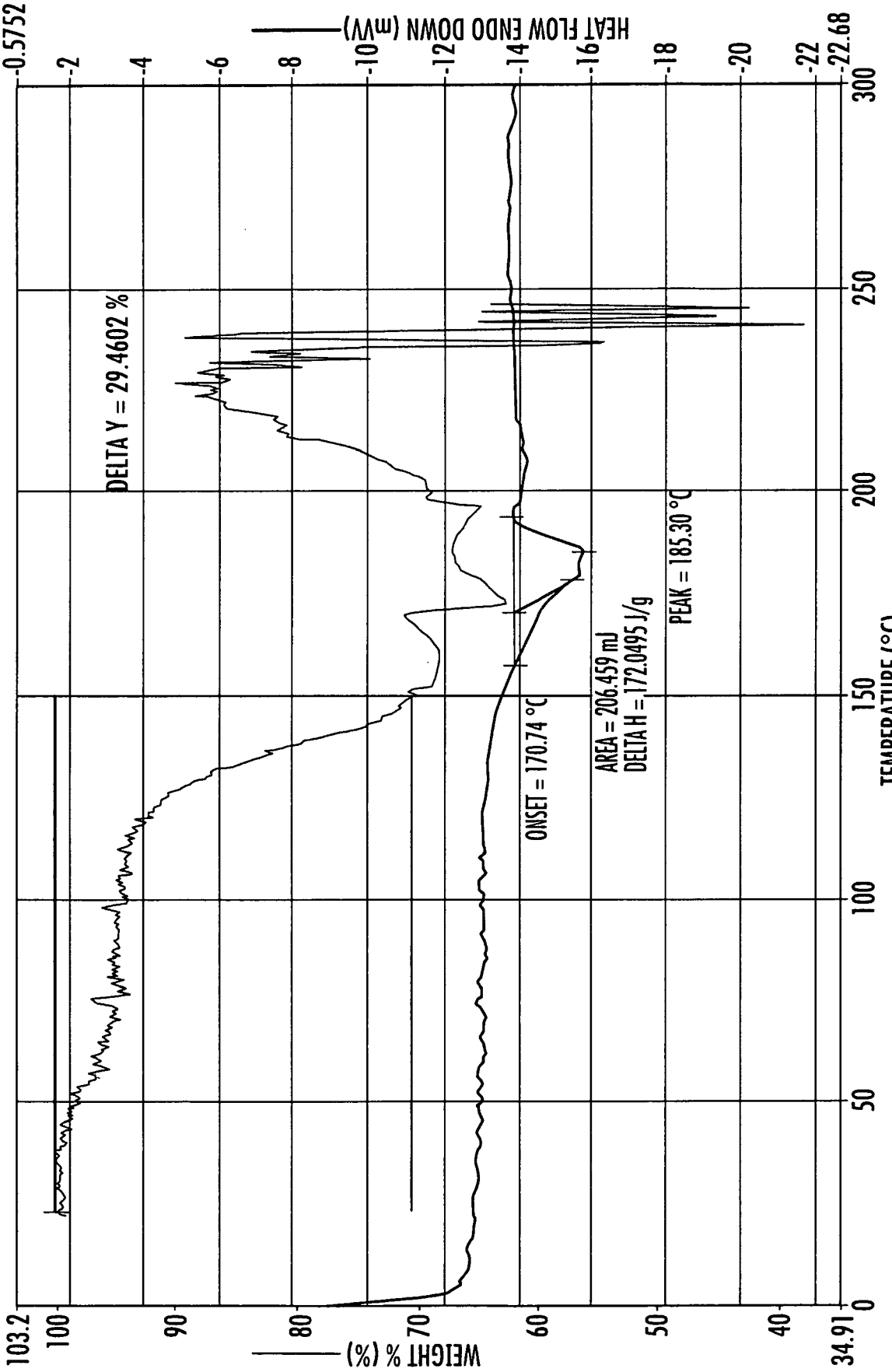

DSC AND TGA OVERLAY OF COMPOUND A ACETATE SALT, FORM $A_{1.5}$

FIG. 6

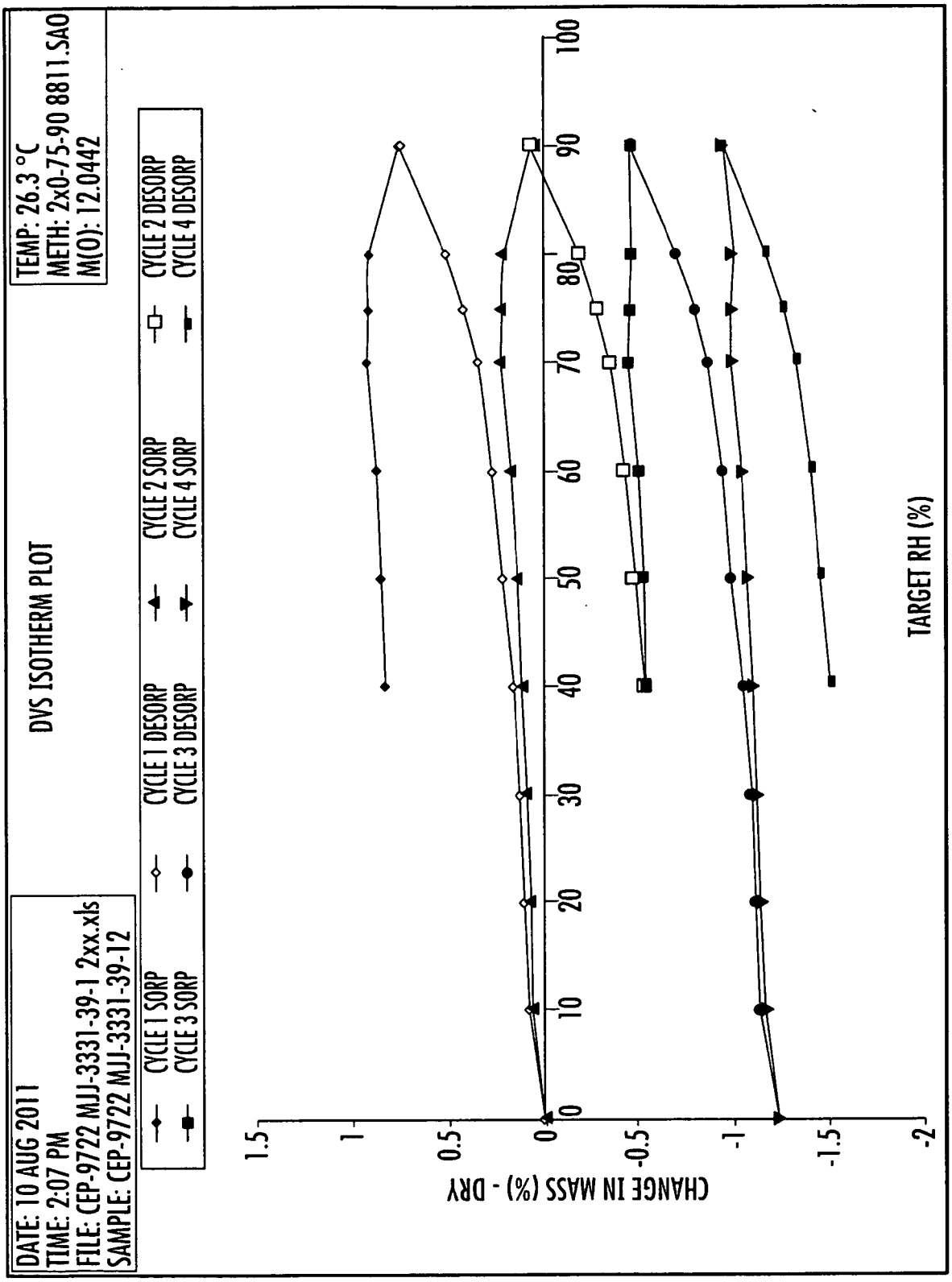

DVS OVERLAY OF COMPOUND A ACETATE SALT, FORM $A_{1.5}$

FIG. 7

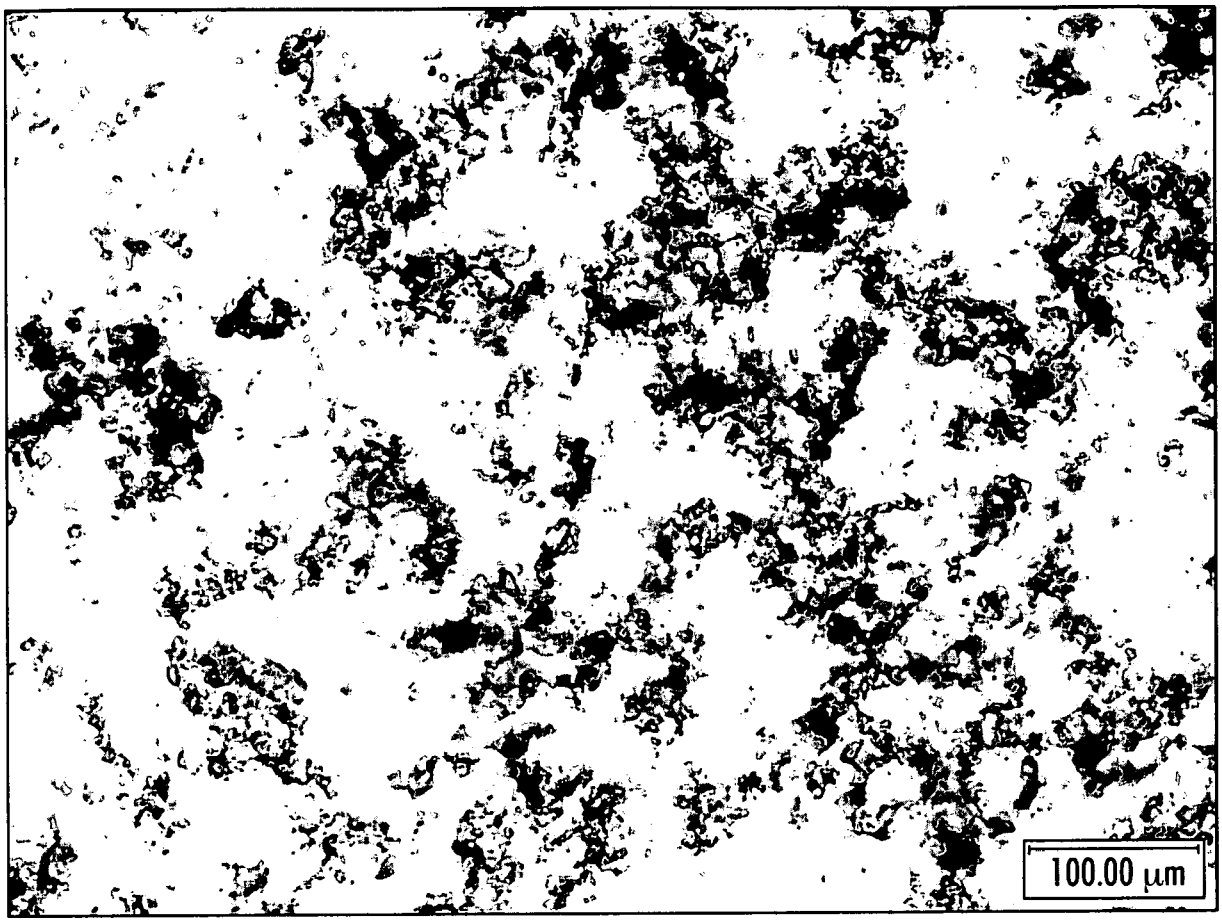

PHOTOMICROGRAPH OF COMPOUND A ACETATE SALT, FORM $A_{1.5}$

FIG. 8

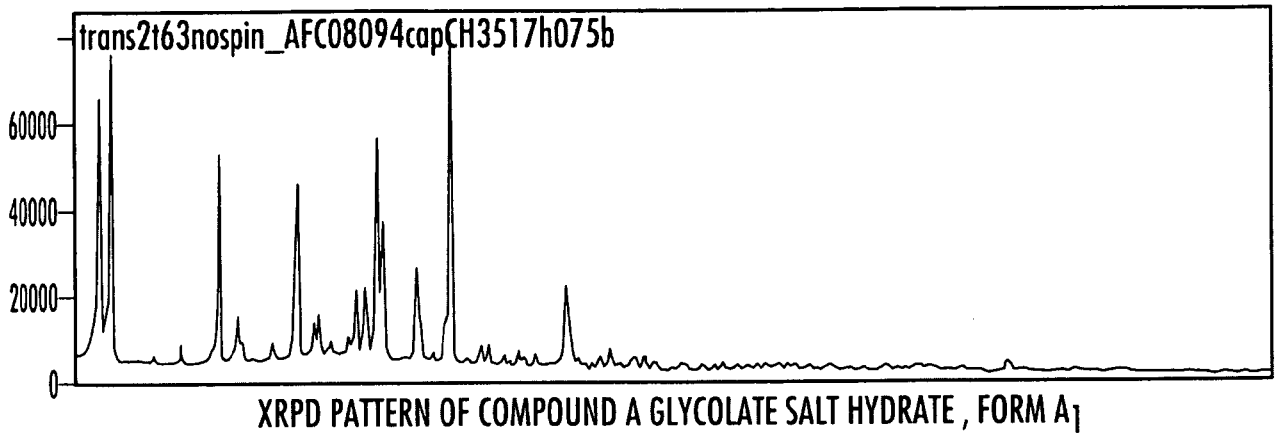

XRPD PATTERN OF COMPOUND A GLYCOLATE SALT HYDRATE , FORM A_1

FIG. 9

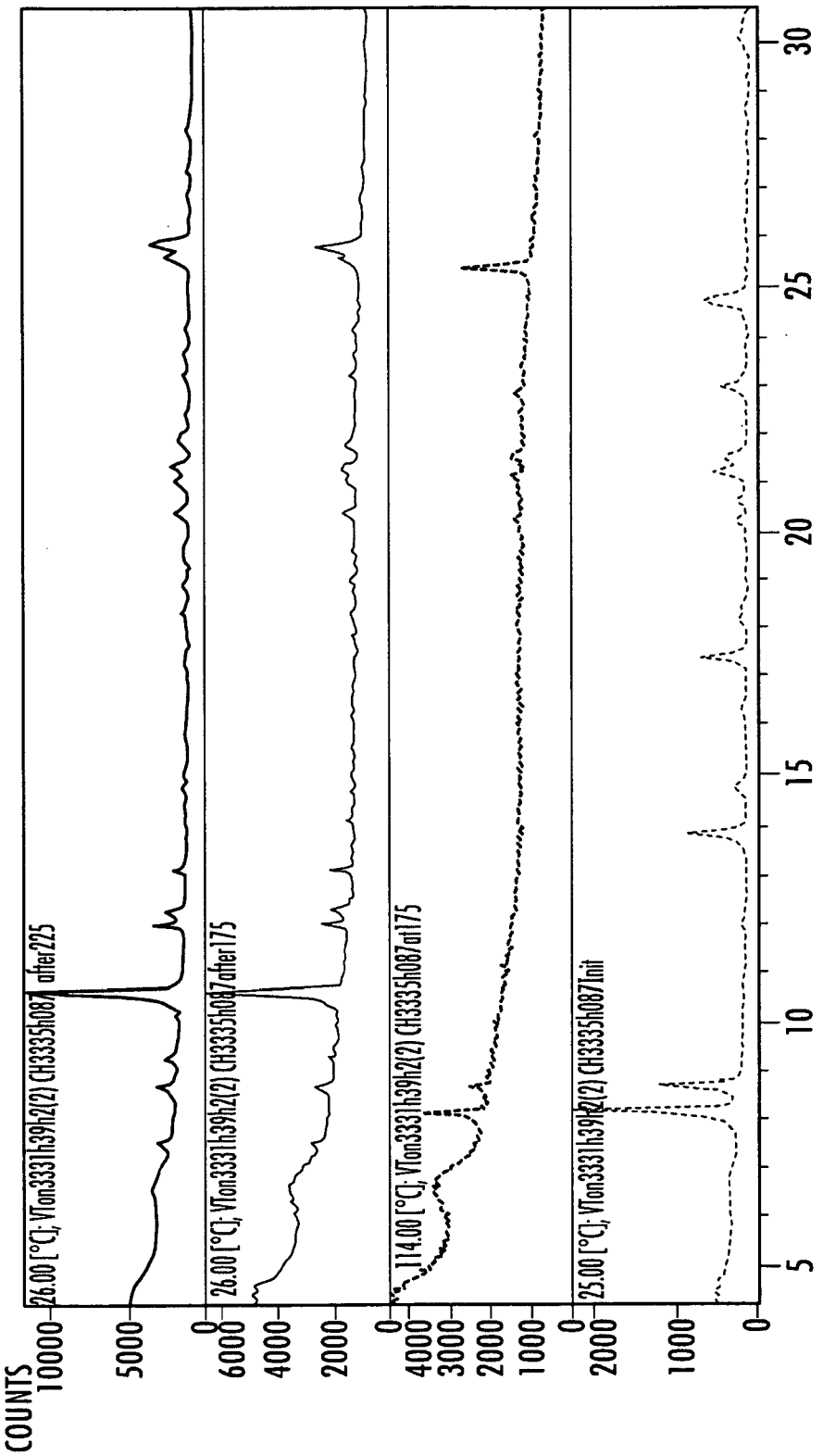

THERMAL XRPD PATTERNS OF COMPOUND A GLYCOLATE HYDRATE SALT, FORM A_1

FIG. 10

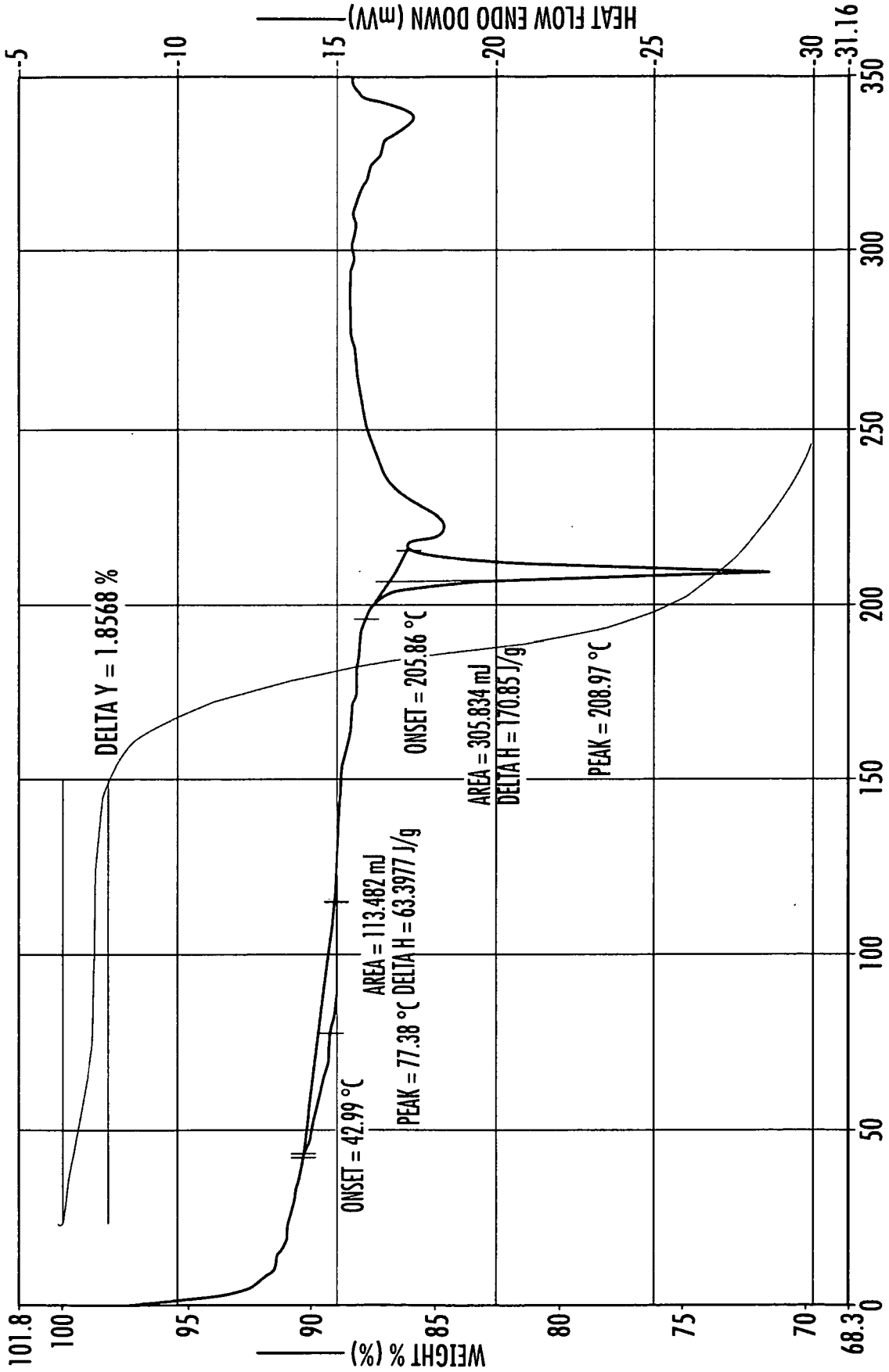

FIG. 11

DSC AND TGA OVERLAY FOR A COMPOUND A GLYCOLATE HYDRATE SALT, FORM A_1

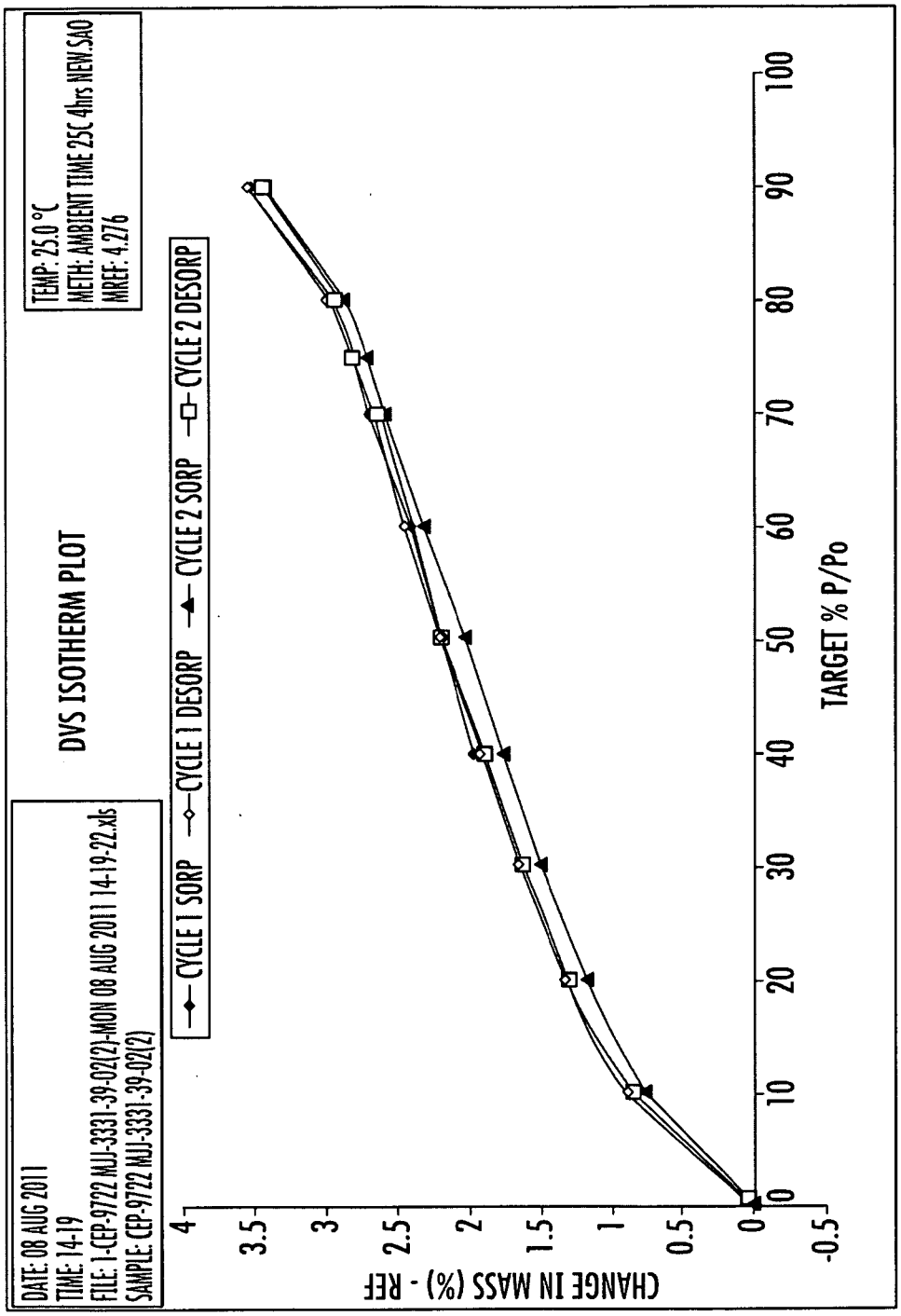

40% RH UPTAKE		75% RH UPTAKE		TOTAL UPTAKE 90% RH		ISOTHERM
CYCLE 1	CYCLE 2	CYCLE 1	CYCLE 2	CYCLE 2	CYCLE 1	REVERSIBLE
1.98	1.77	2.82	2.75	3.53	3.43	

DVS OVERLAY OF COMPOUND A GLYCOLATE HYDRATE SALT, FORM A_1

FIG. 12

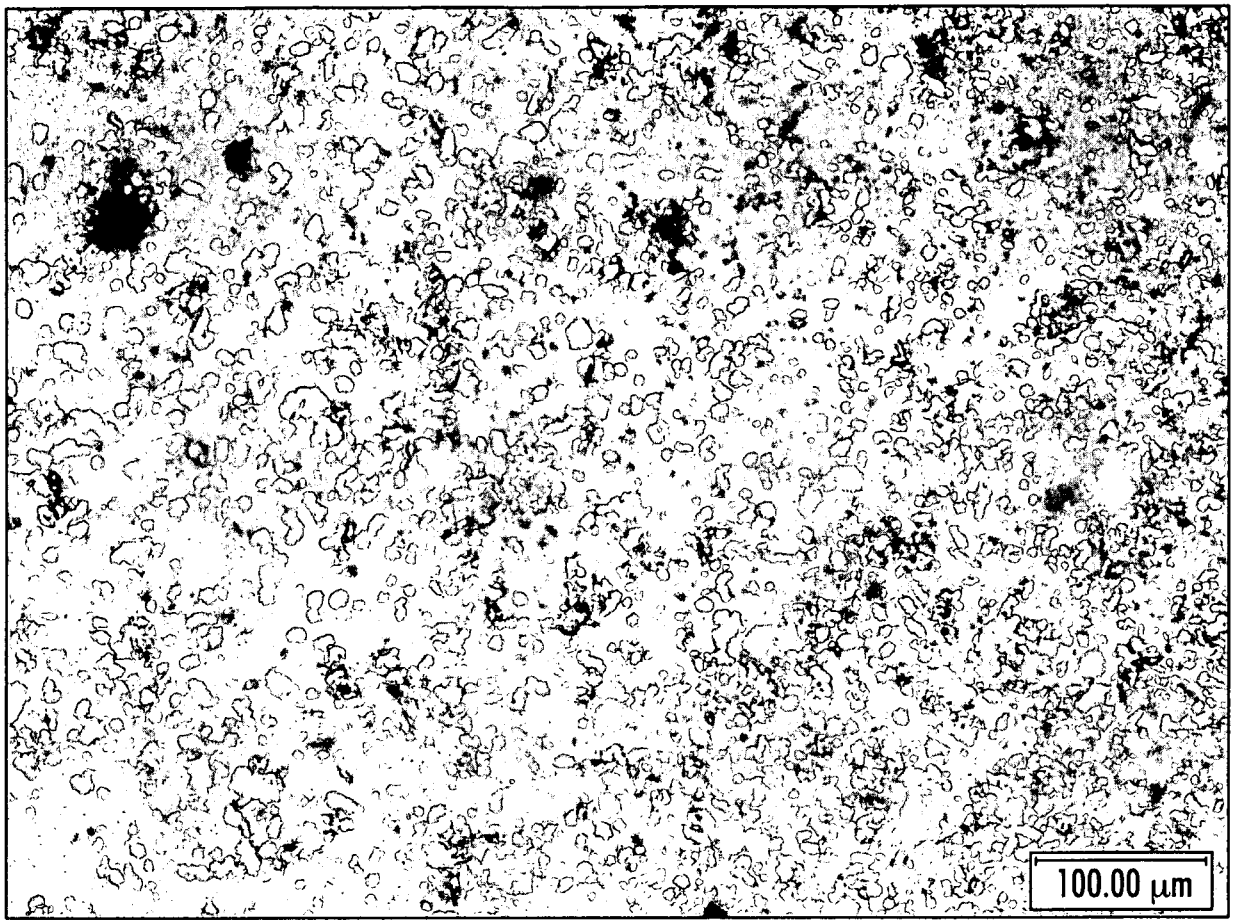

PHOTOMICROGRAPH OF COMPOUND A GLYCOLATE HYDRATE SALT, FORM A_1

FIG. 13

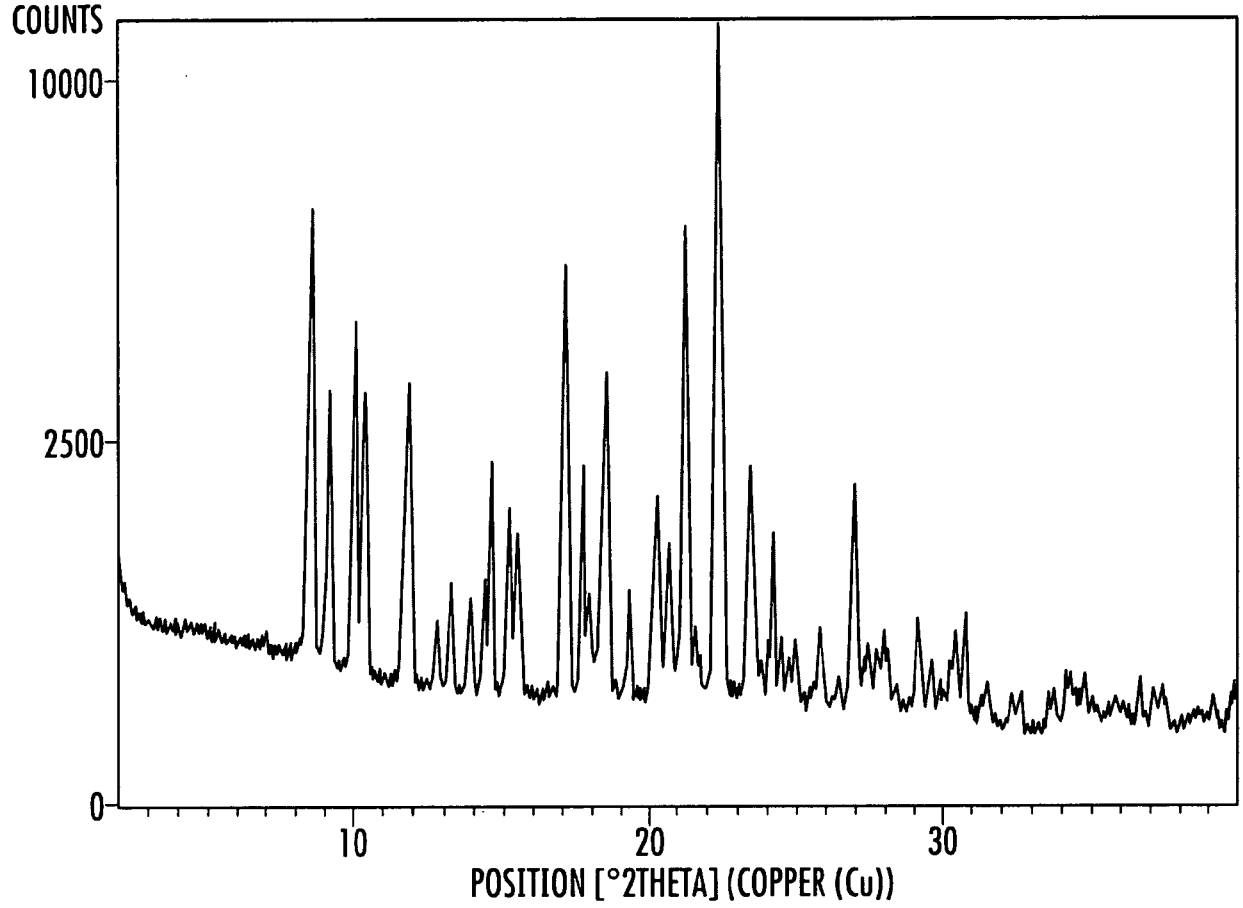

XRPD PATTERN OF COMPOUND A L-MALATE SALT, FORM A_1

FIG. 14

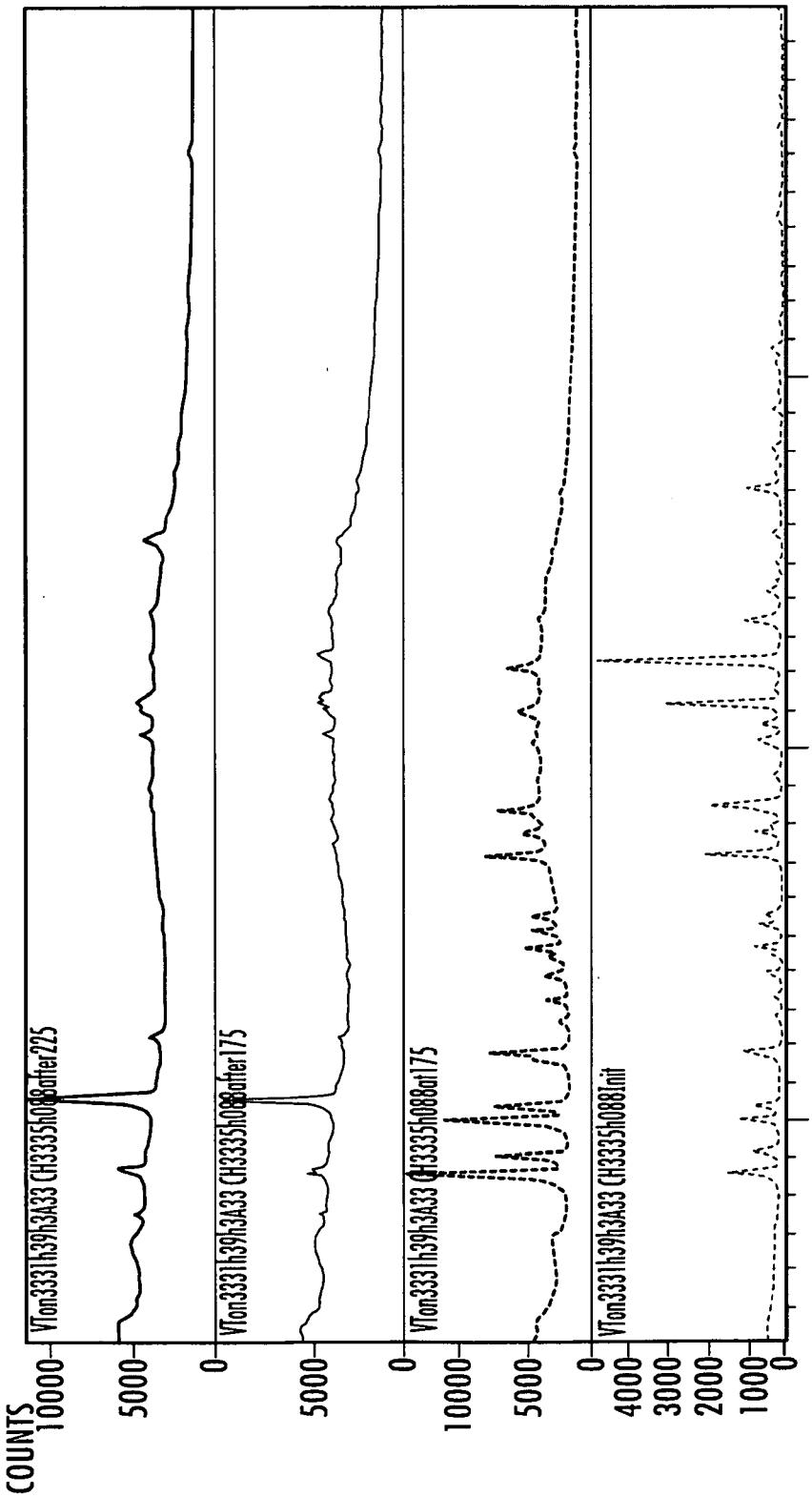

VT-XRPD PATTERNS OF COMPOUND A MALATE SALT, FORM A_1

FIG. 15

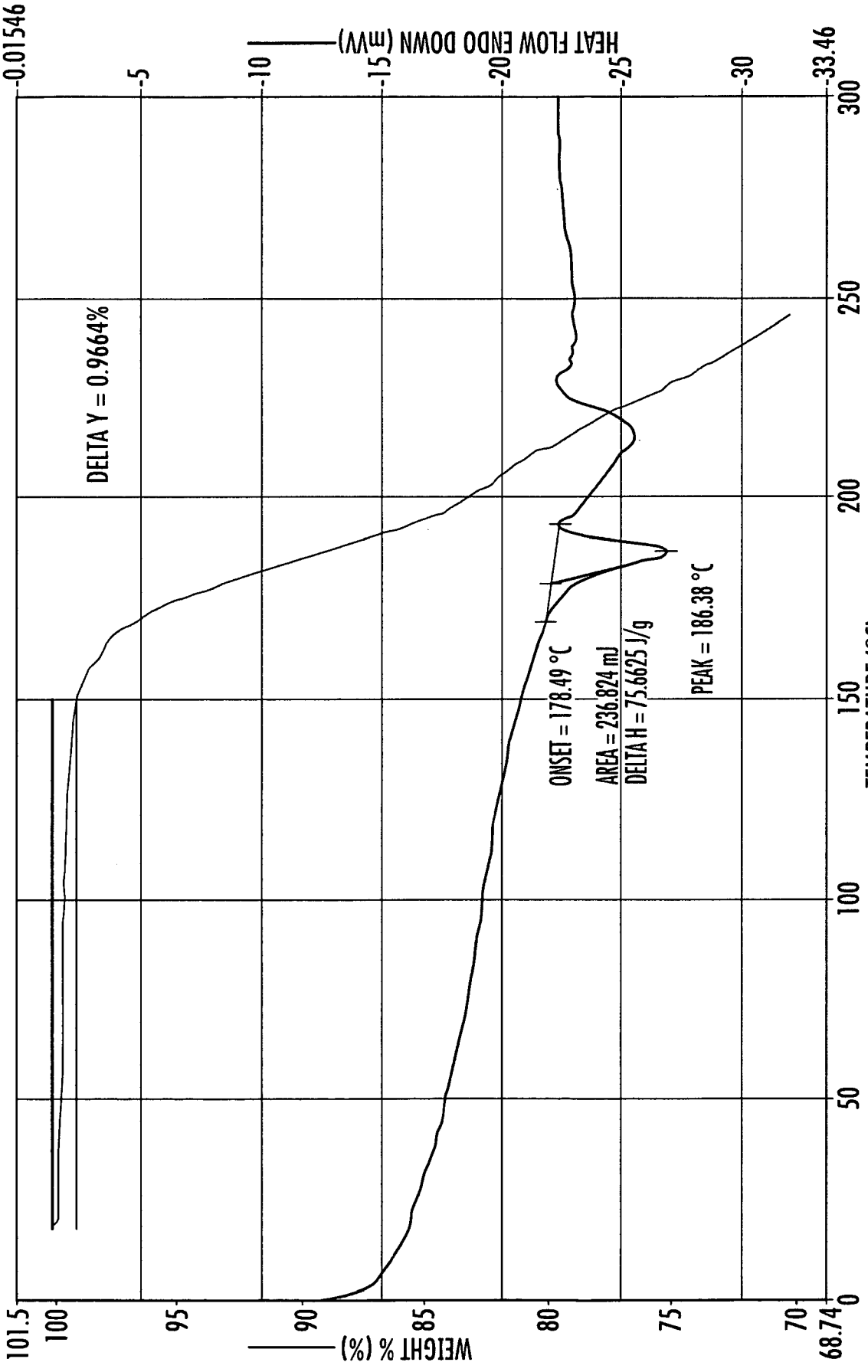

DSC AND TGA OVERLAY OF COMPOUND A L-MALATE SALT, FORM A1

FIG. 16

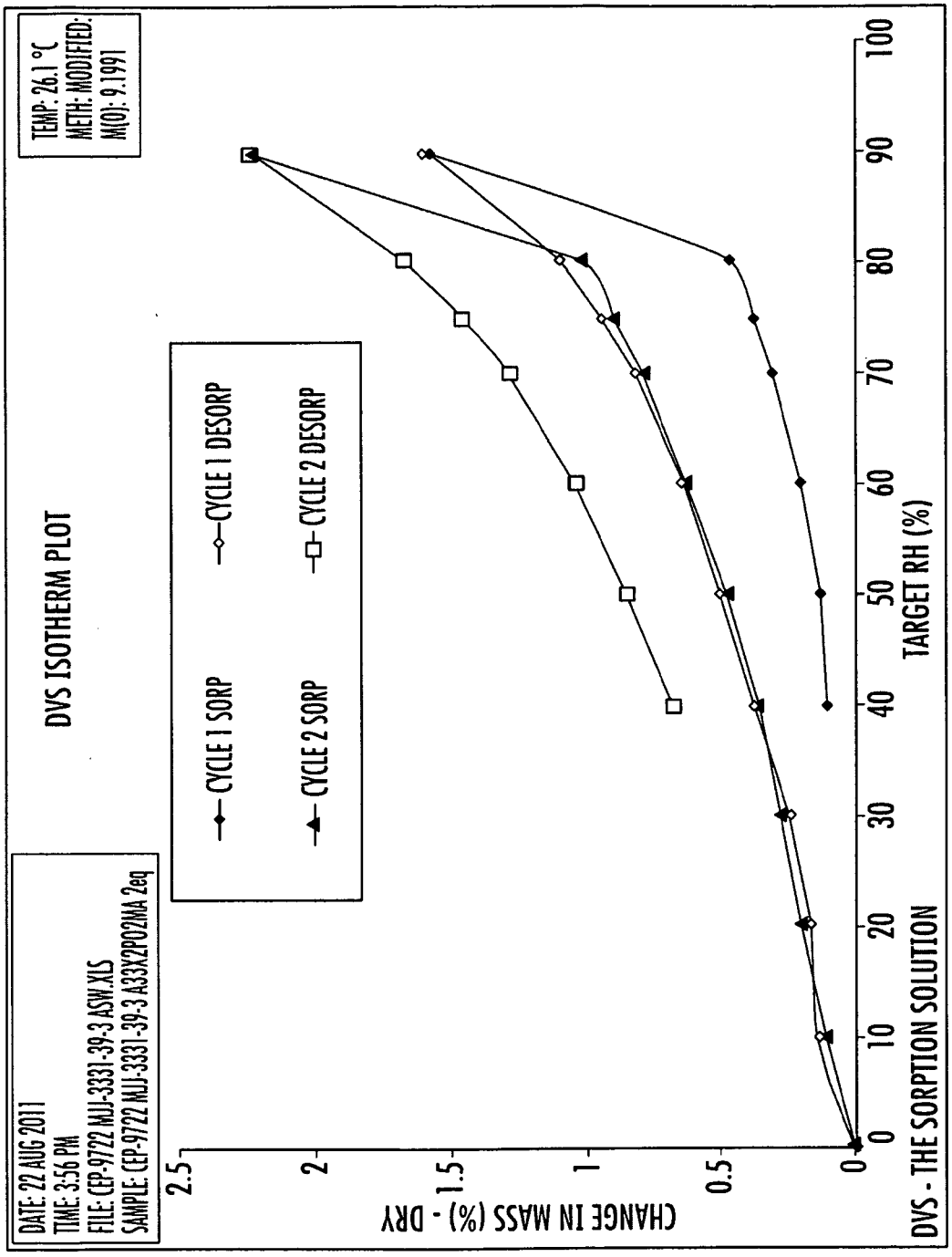
DVS ISOTHERM PLOT
DATE: 22 AUG 2011
TIME: 3:56 PM
FILE: CEP-9722 MJJ-3331-39-3 ASW.XLS
SAMPLE: CEP-9722 MJJ-3331-39-3 A33X2P02MA 2eq
TEMP: 26.1 °C
METH: MODIFIED:
M(0): 9.1991
CYCLE 1 SORP
CYCLE 1 DESORP
CYCLE 2 SORP
CYCLE 2 DESORP
CHANGE IN MASS (%) - DRY
TARGET RH (%)
DVS - THE SORPTION SOLUTION
40% RH UPTAKE
75% RH UPTAKE
TOTAL UPTAKE 90% RH
ISOTHERM
CYCLE 1 CYCLE 2 CYCLE 1 CYCLE 2 CYCLE 2 CYCLE 1 IREVERSIBLE
0.11 0.37 0.38 0.90 1.59 2.23
DVS OF COMPOUND A L-MALATE SALT, FORM A1

FIG. 17

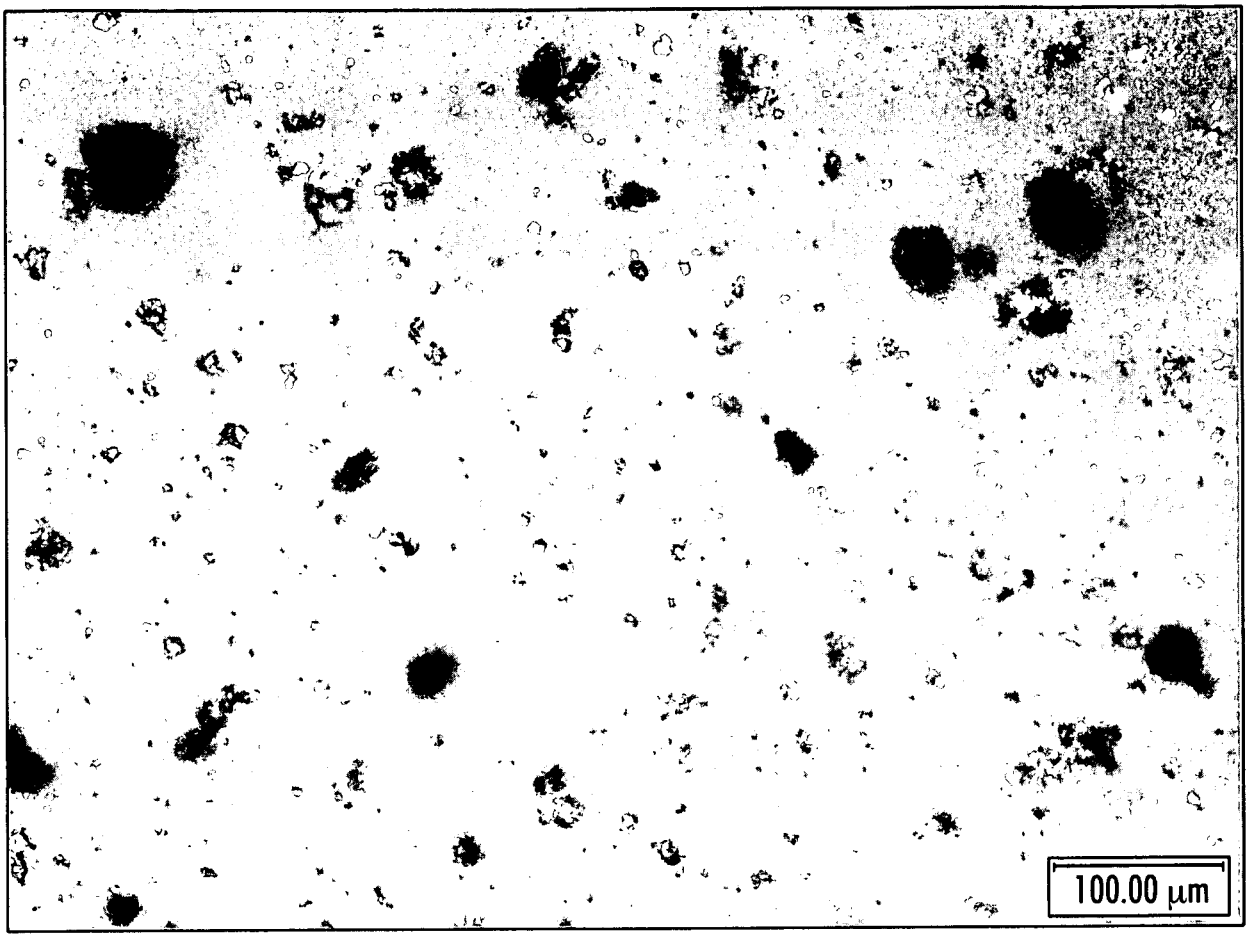

PHOTOMICROGRAPH OF COMPOUND A L-MALATE SALT, FORM A_1

FIG. 18

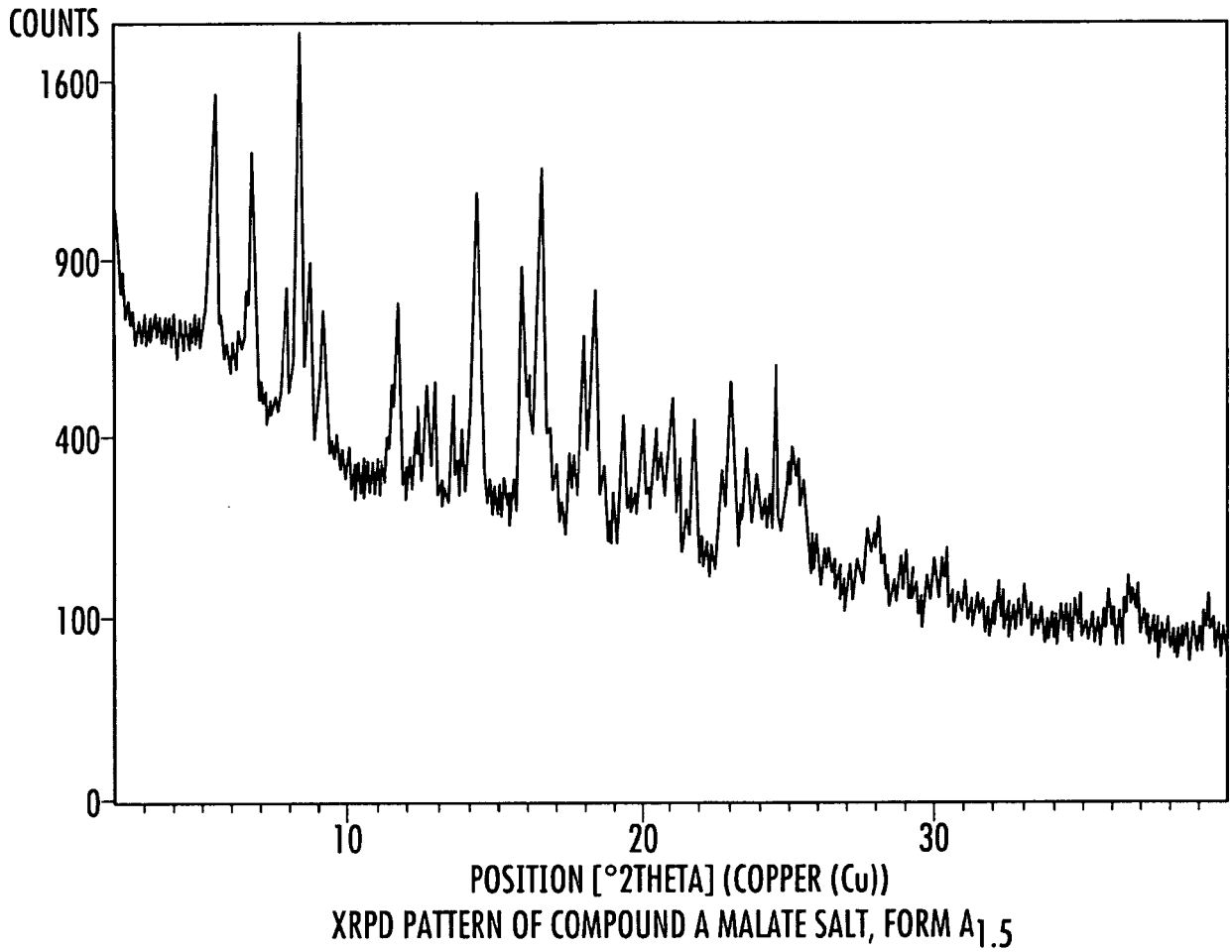

XRPD PATTERN OF COMPOUND A MALATE SALT, FORM $A_{1.5}$

FIG. 19

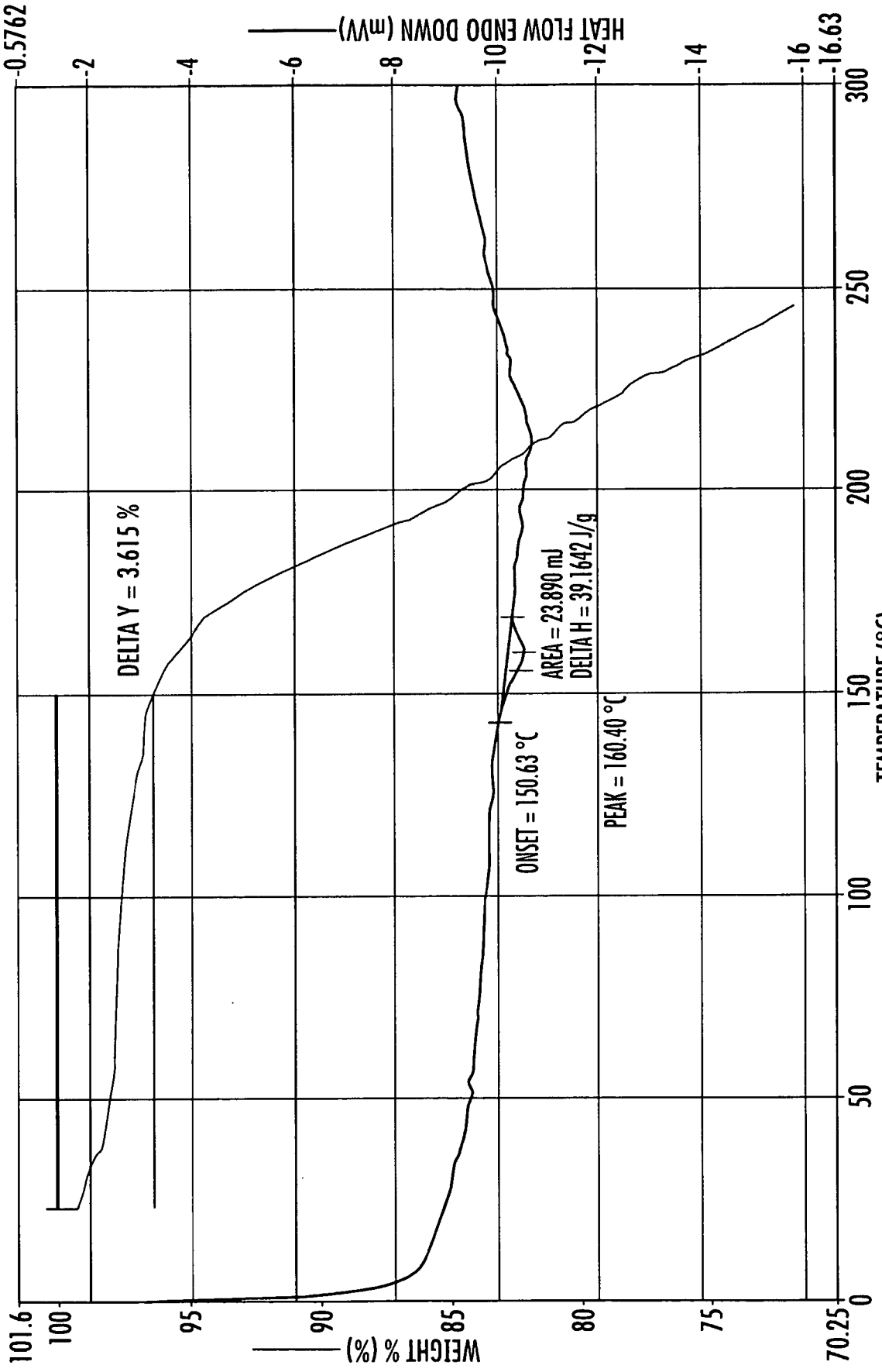

DSC AND TGA OVERLAY OF COMPOUND A L-MALATE SALT, FORM $A_{1.5}$

FIG. 20

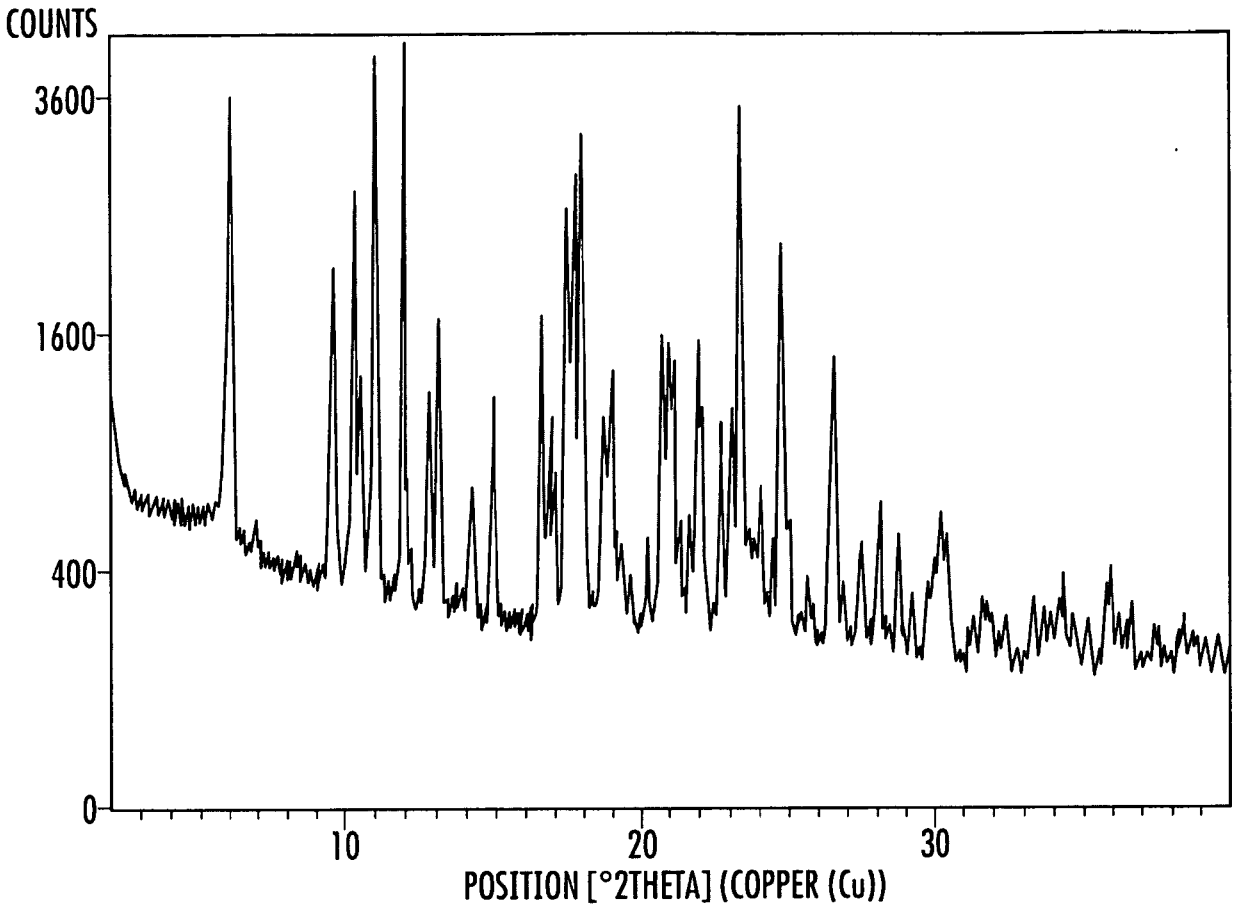

XRPD PATTERN OF COMPOUND A L-PYROGLUTAMATE SALT, FORM A_1

FIG. 21

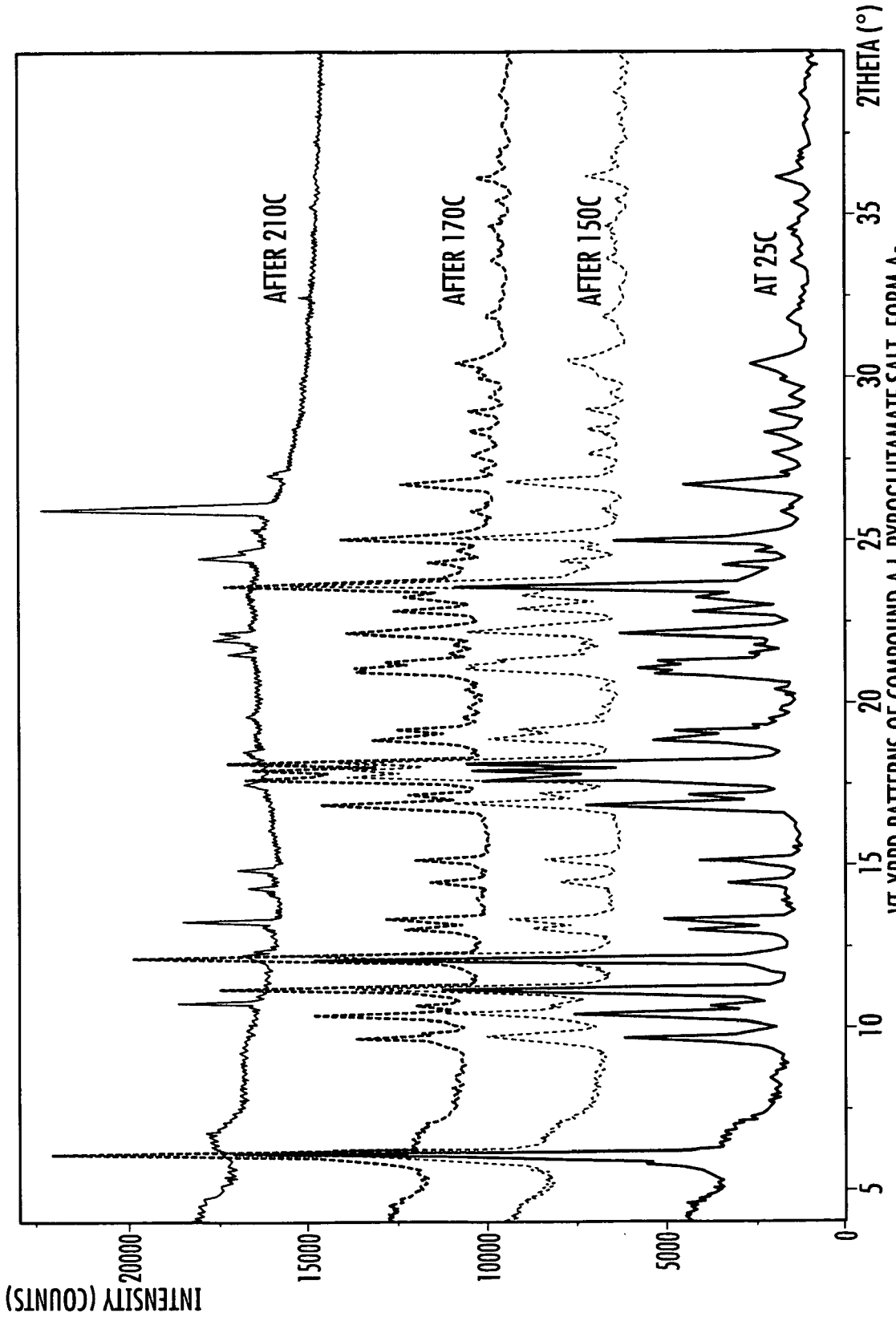

FIG. 22

VT-XRPD PATTERNS OF COMPOUND A L-PYROGLUTAMATE SALT, FORM A1

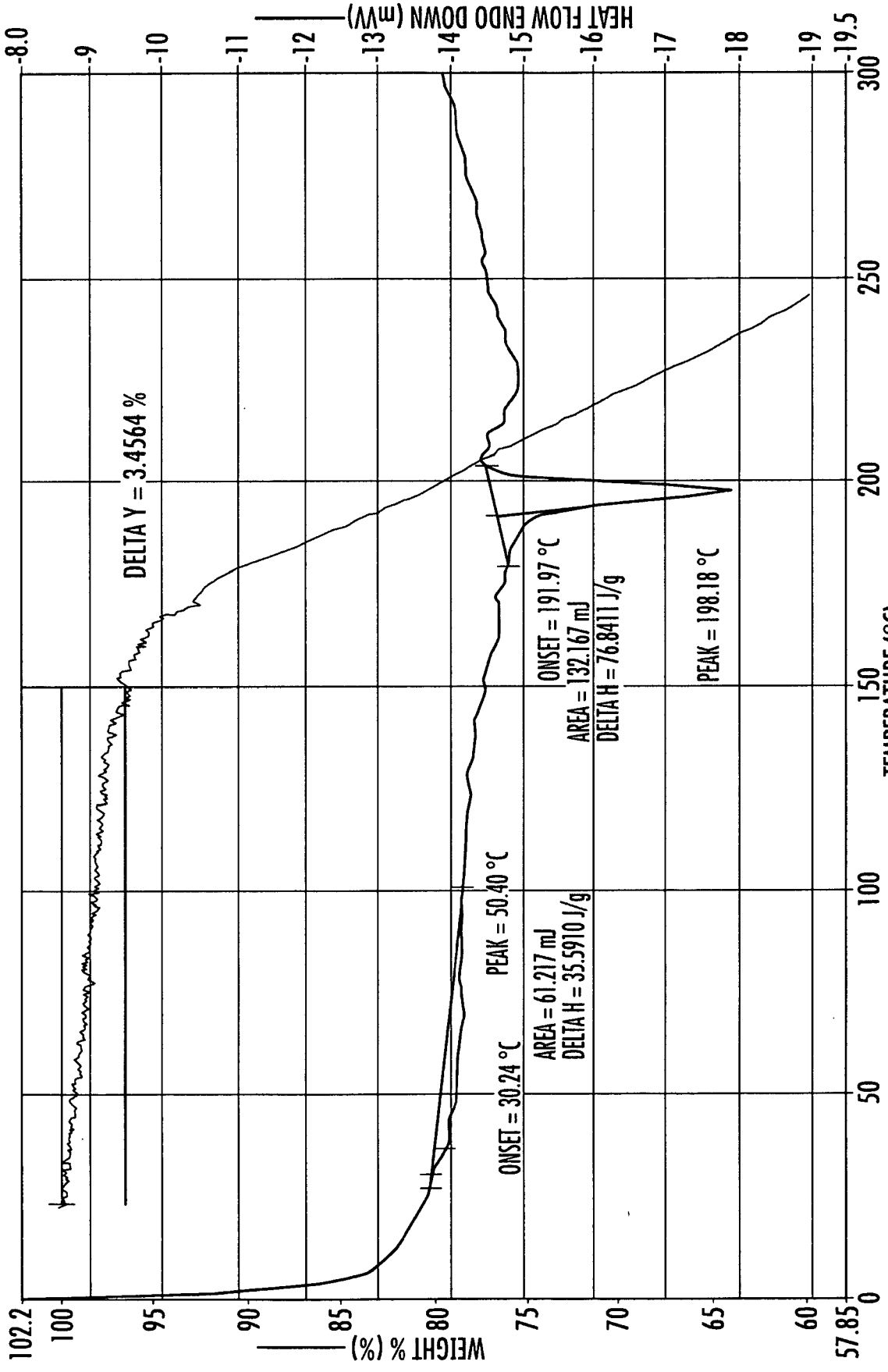

DSC AND TGA OVERLAY OF COMPOUND A L-PYROGLUTAMATE SALT, FORM A1

FIG. 23

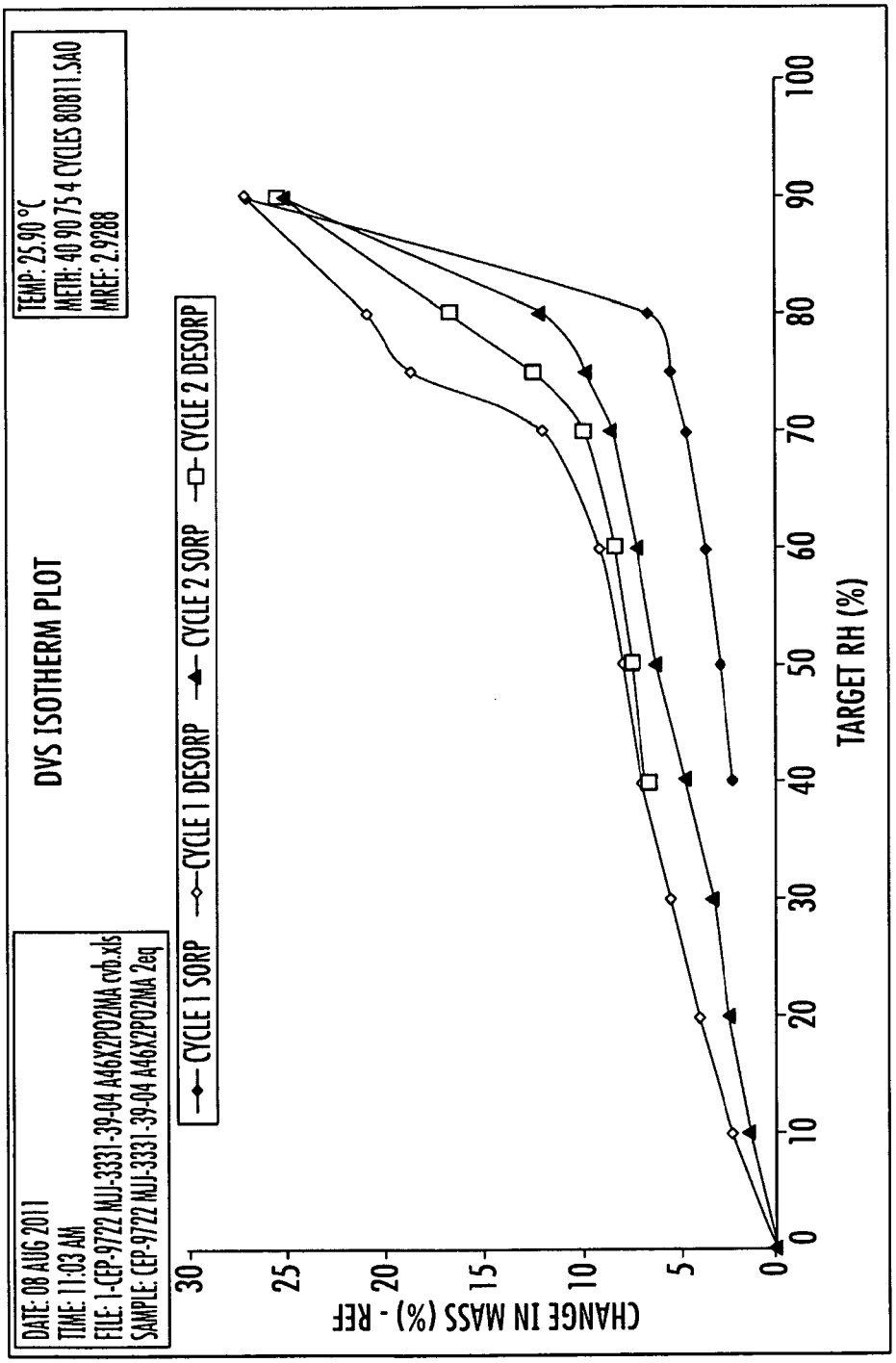

40% RH UPTAKE		75% RH UPTAKE		TOTAL UPTAKE 90% RH		ISOTHERM
CYCLE 1	CYCLE 2	CYCLE 1	CYCLE 2	CYCLE 2	CYCLE 1	IRREVERSIBLE
2.28	4.65	5.50	9.83	27.07	25.42	

DVS OF COMPOUND A L-PYROGLUTAMATEATE SALT, FORM A1

FIG. 24

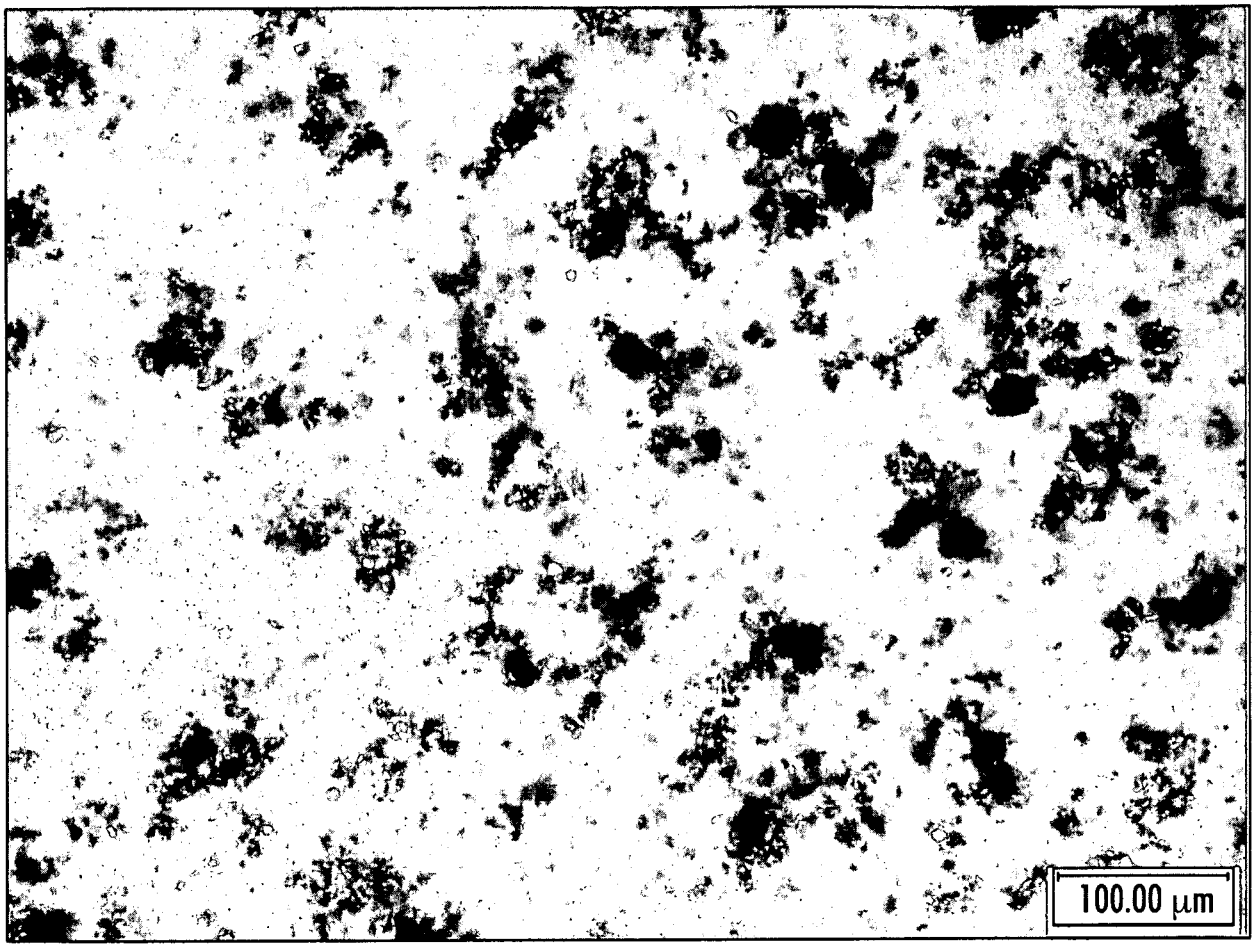

PHOTOMICROGRAPH OF COMPOUND A L-PYROGLUTAMATE SALT, FORM A_1

FIG. 25

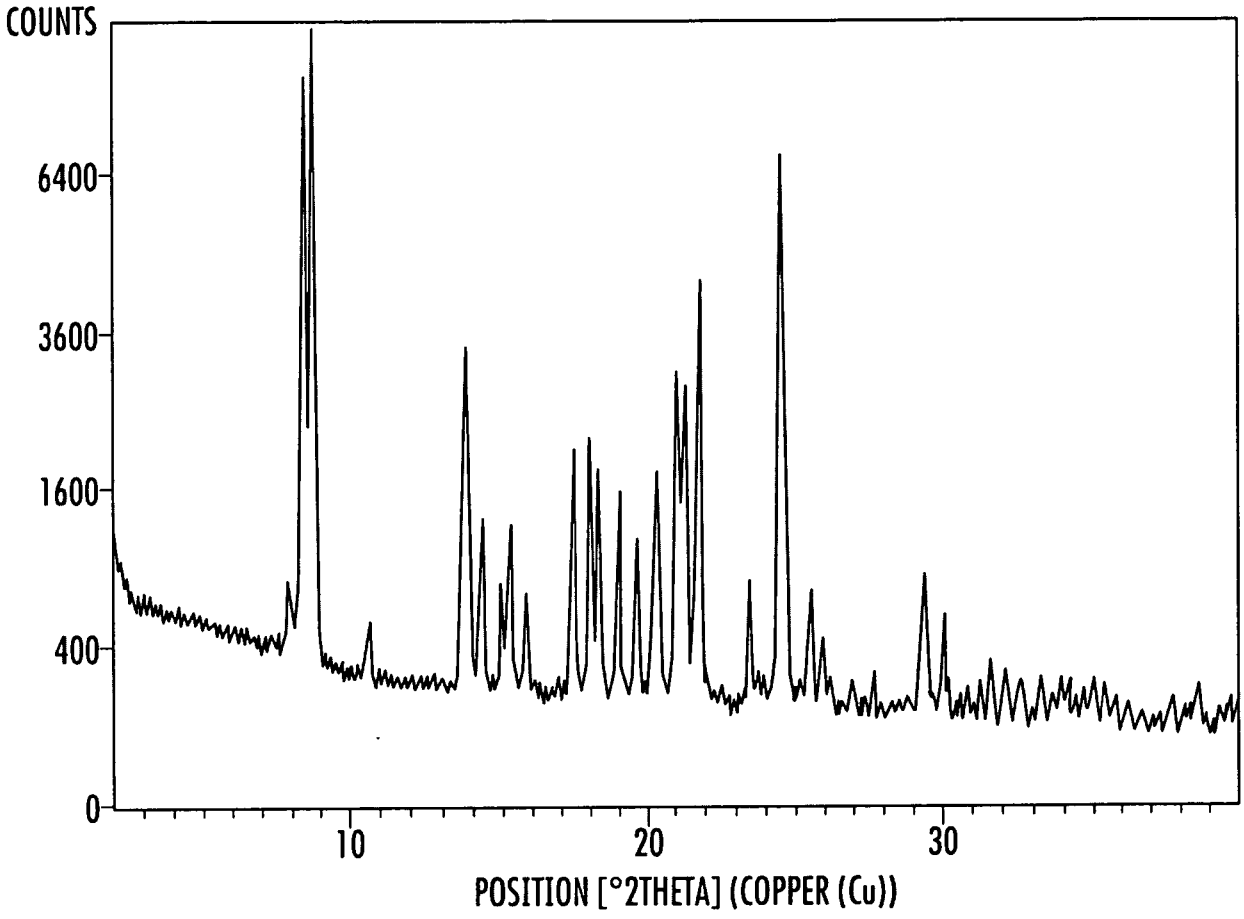

XRPD PATTERN OF COMPOUND A FREE BASE, FORM C_0

FIG. 26

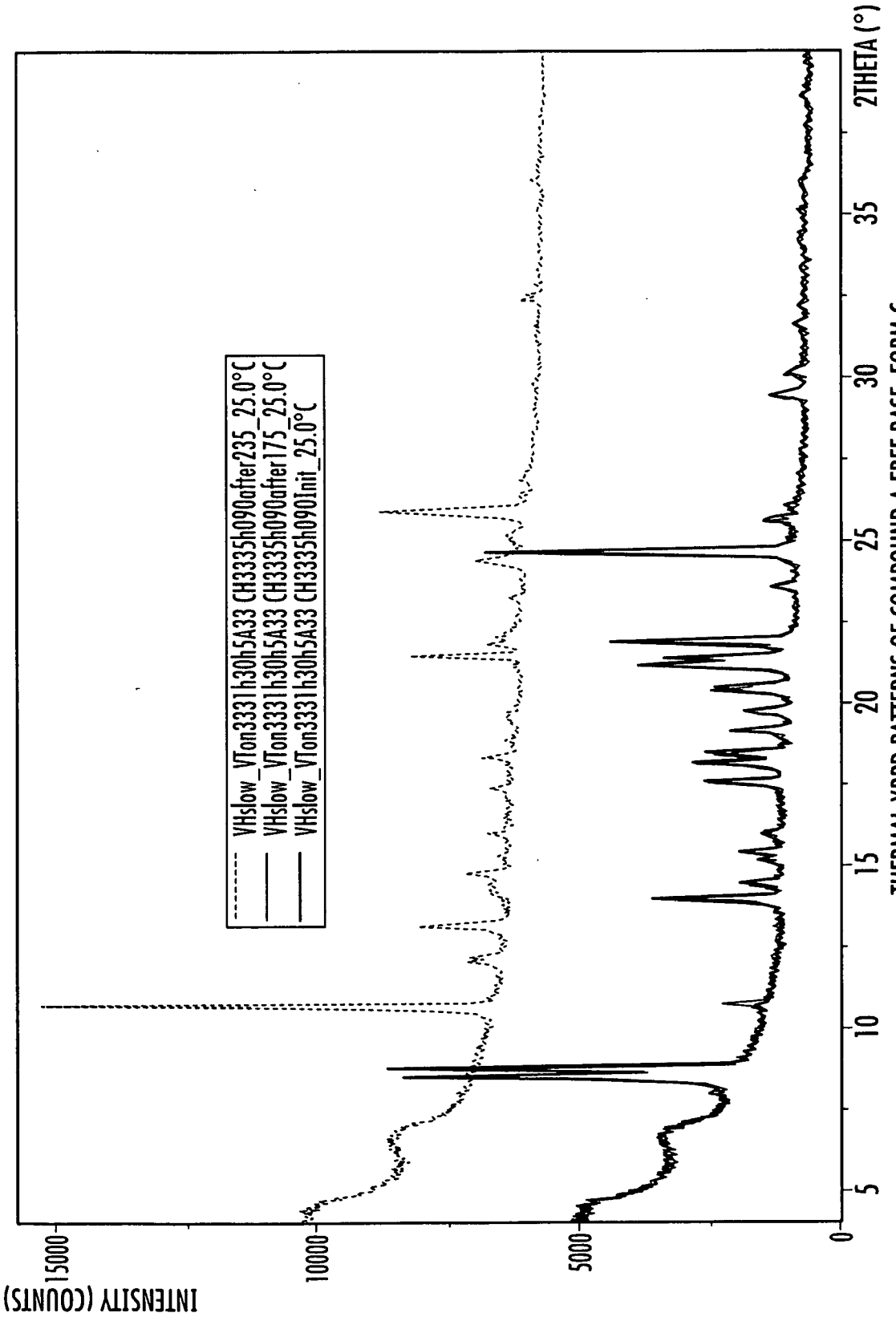

THERMAL XRPD PATTERNS OF COMPOUND A FREE BASE, FORM C_0

FIG. 27

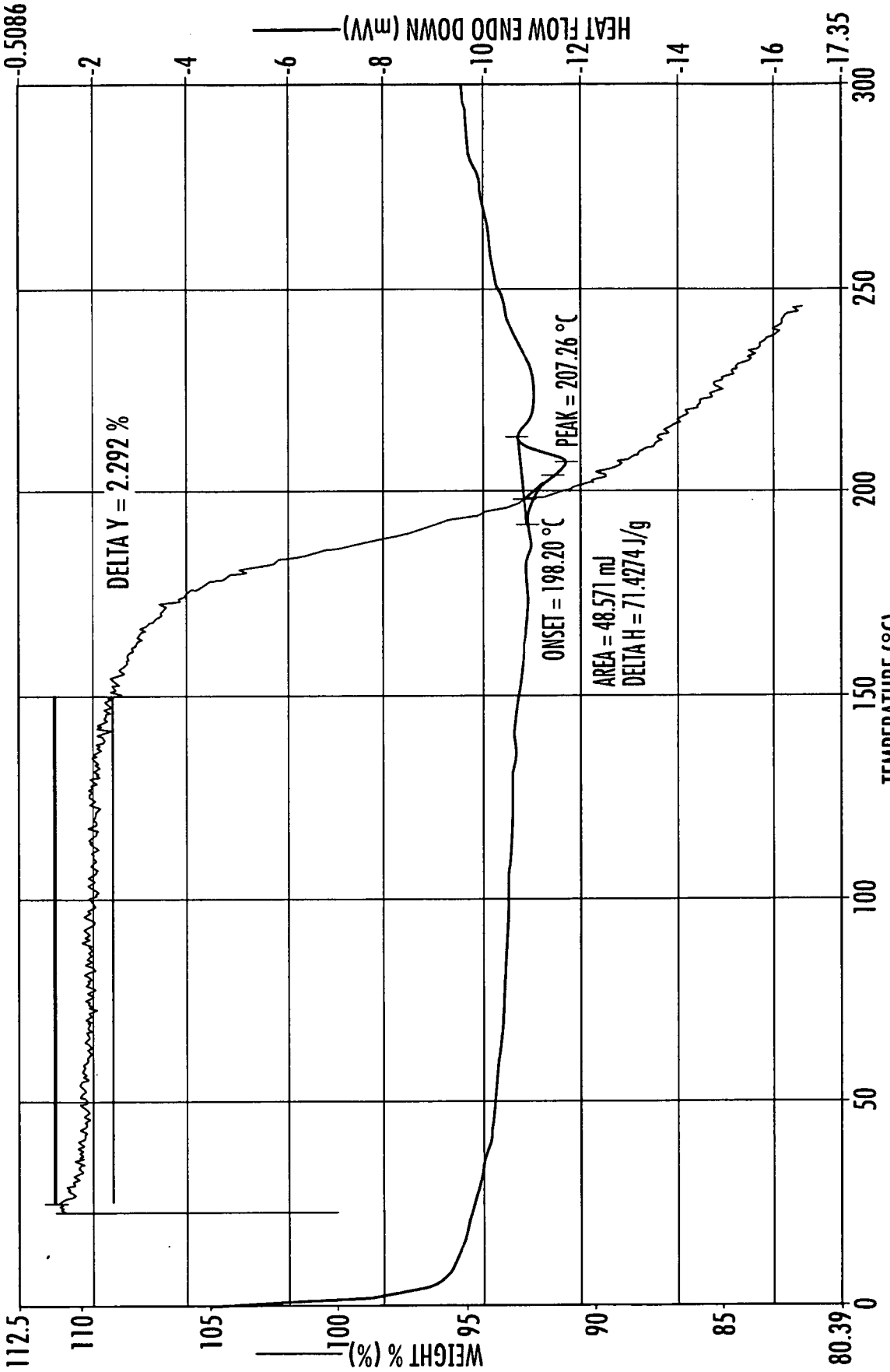

DSC AND TGA OVERLAY OF COMPOUND A FREE BASE, FORM C_0

FIG. 28

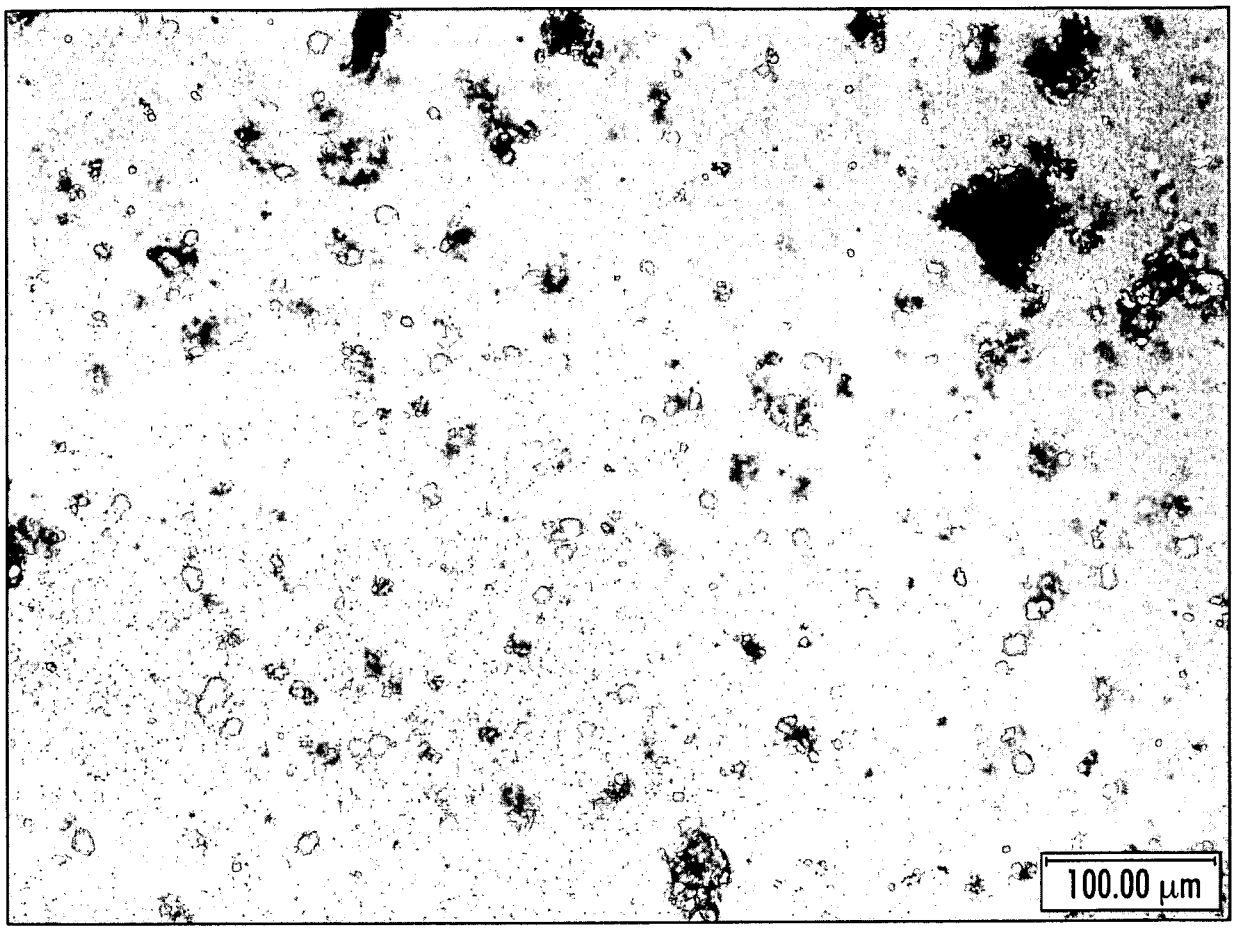

PHOTOMICROGRAPH OF COMPOUND A FREE BASE, FORM C_0

FIG. 29

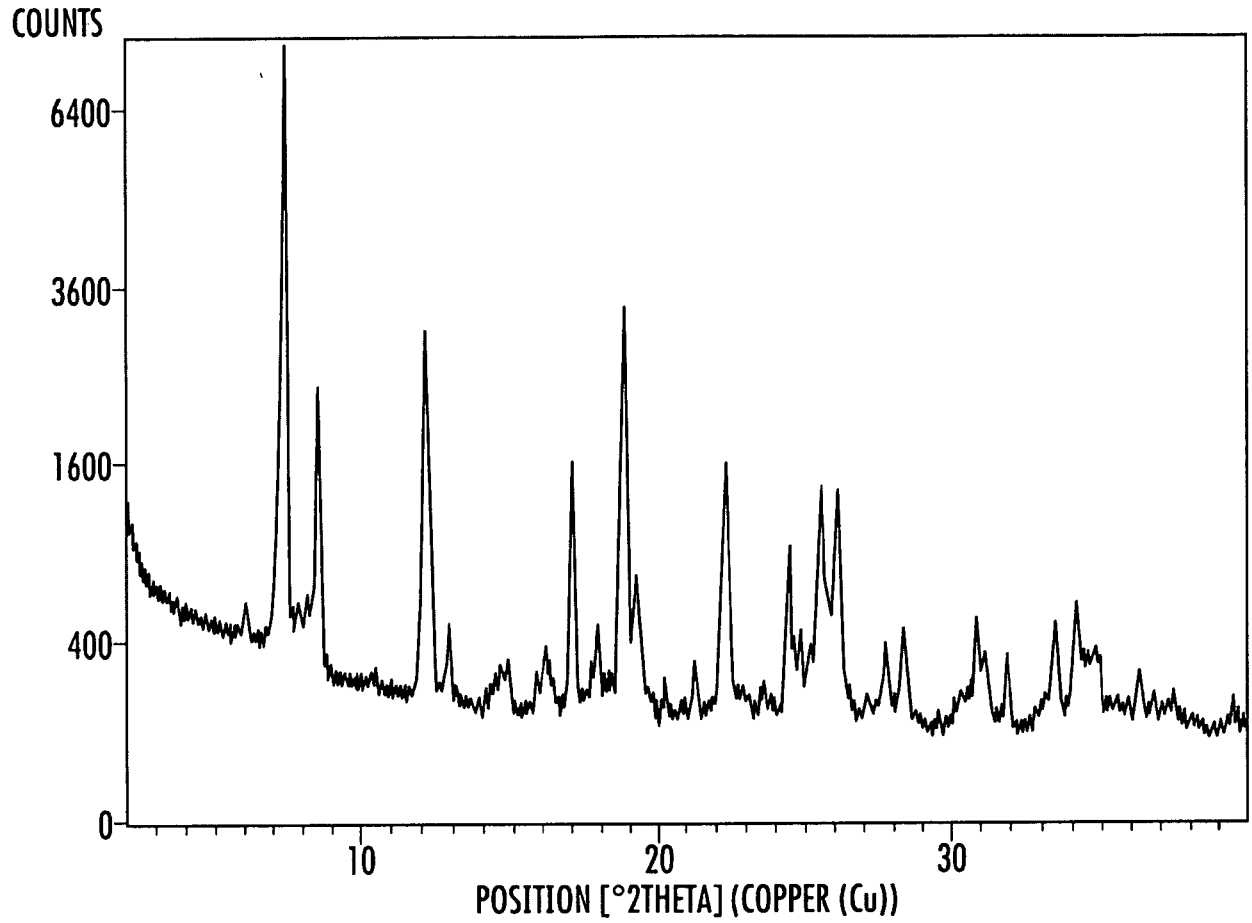

XRPD PATTERN OF COMPOUND A HYDROCHLORIDE SALT, FORM A

FIG. 30

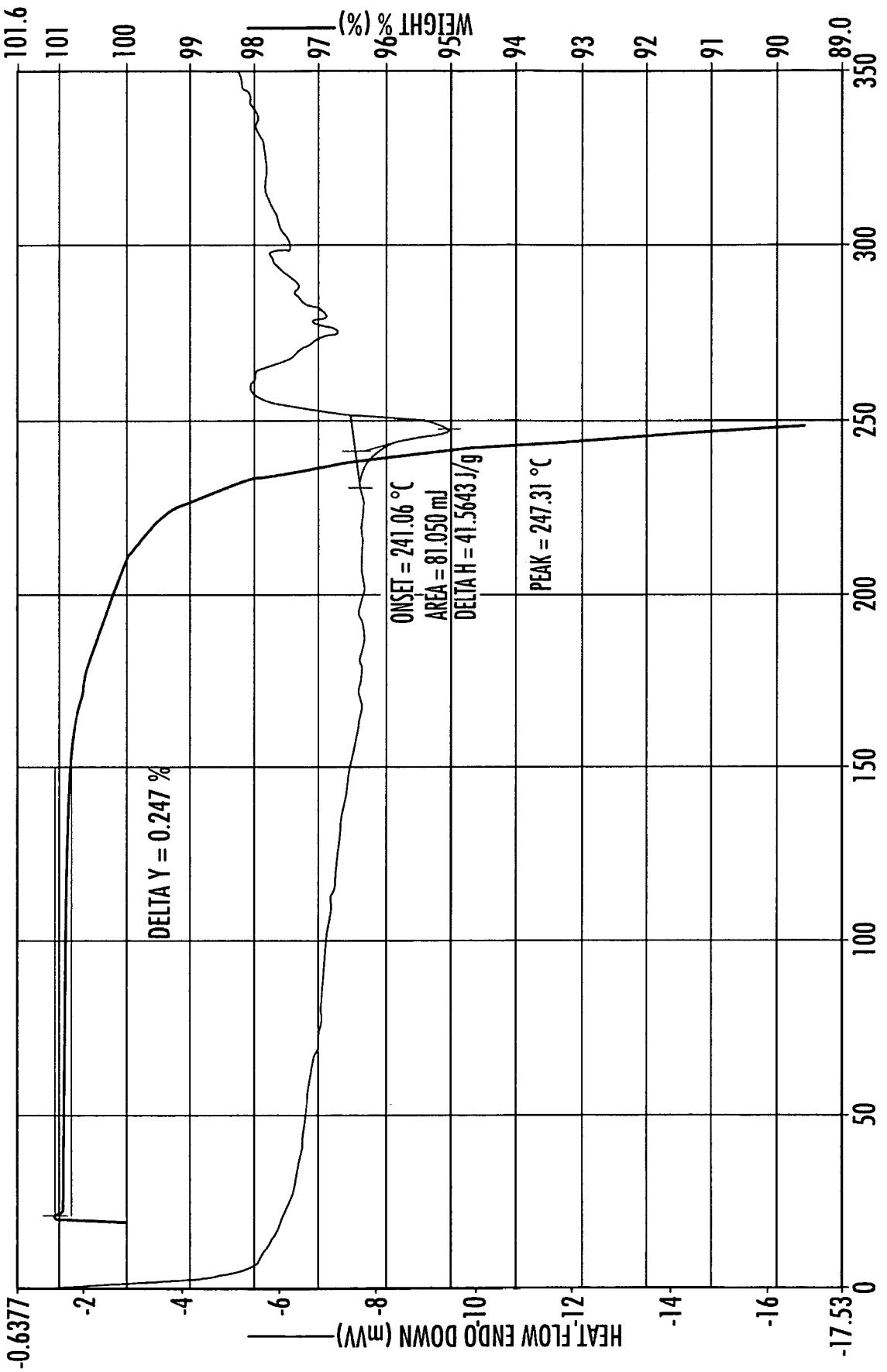

DSC AND TGA OVERLAY OF COMPOUND A HYDROCHLORIDE SALT, FORM A

FIG. 31

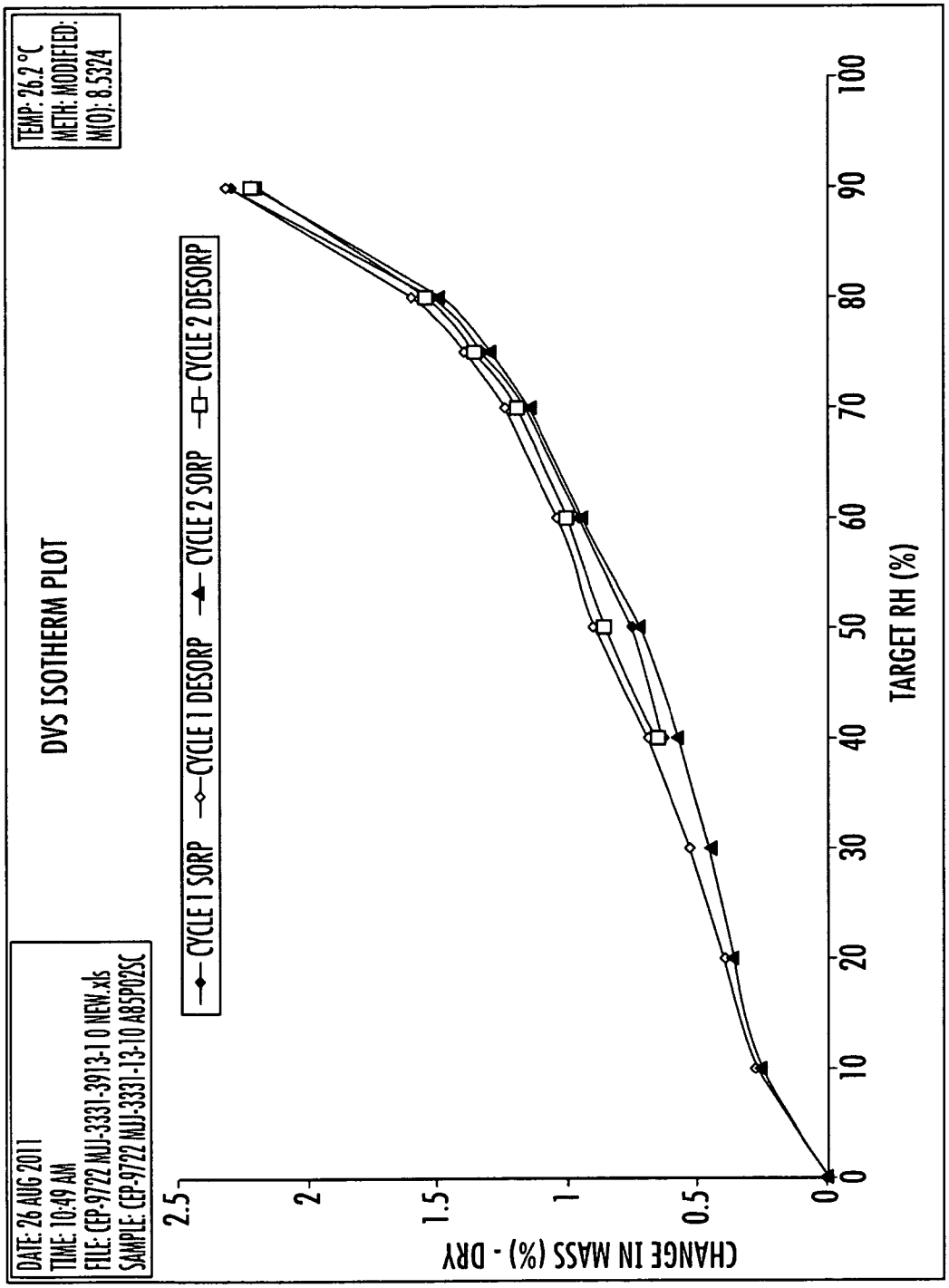

DVS OF THE OF COMPOUND A HYDROCHLORIDE SALT, FORM A

FIG. 32

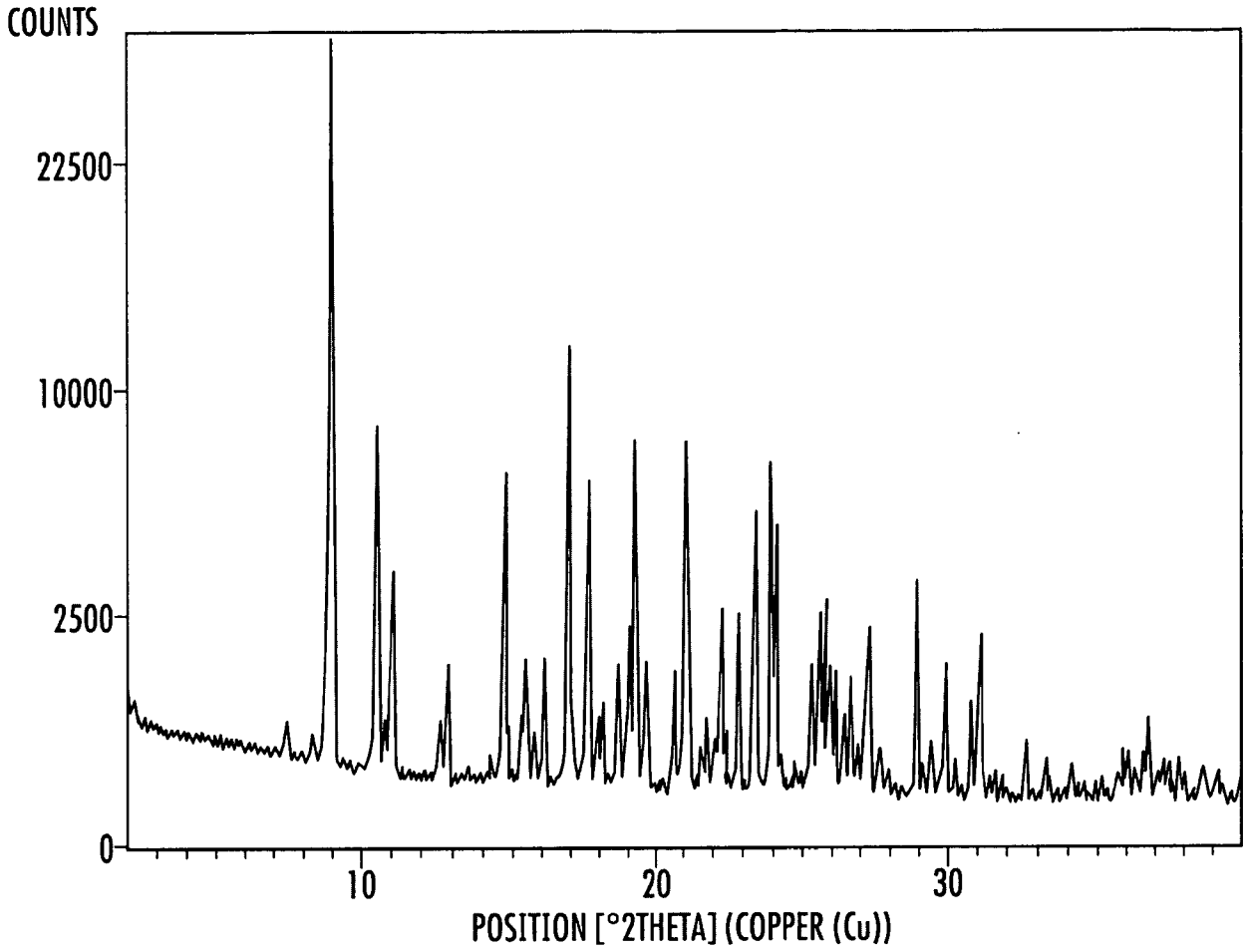

XRPD PATTERN OF COMPOUND A FUMARATE SALT, FORM A

FIG. 33

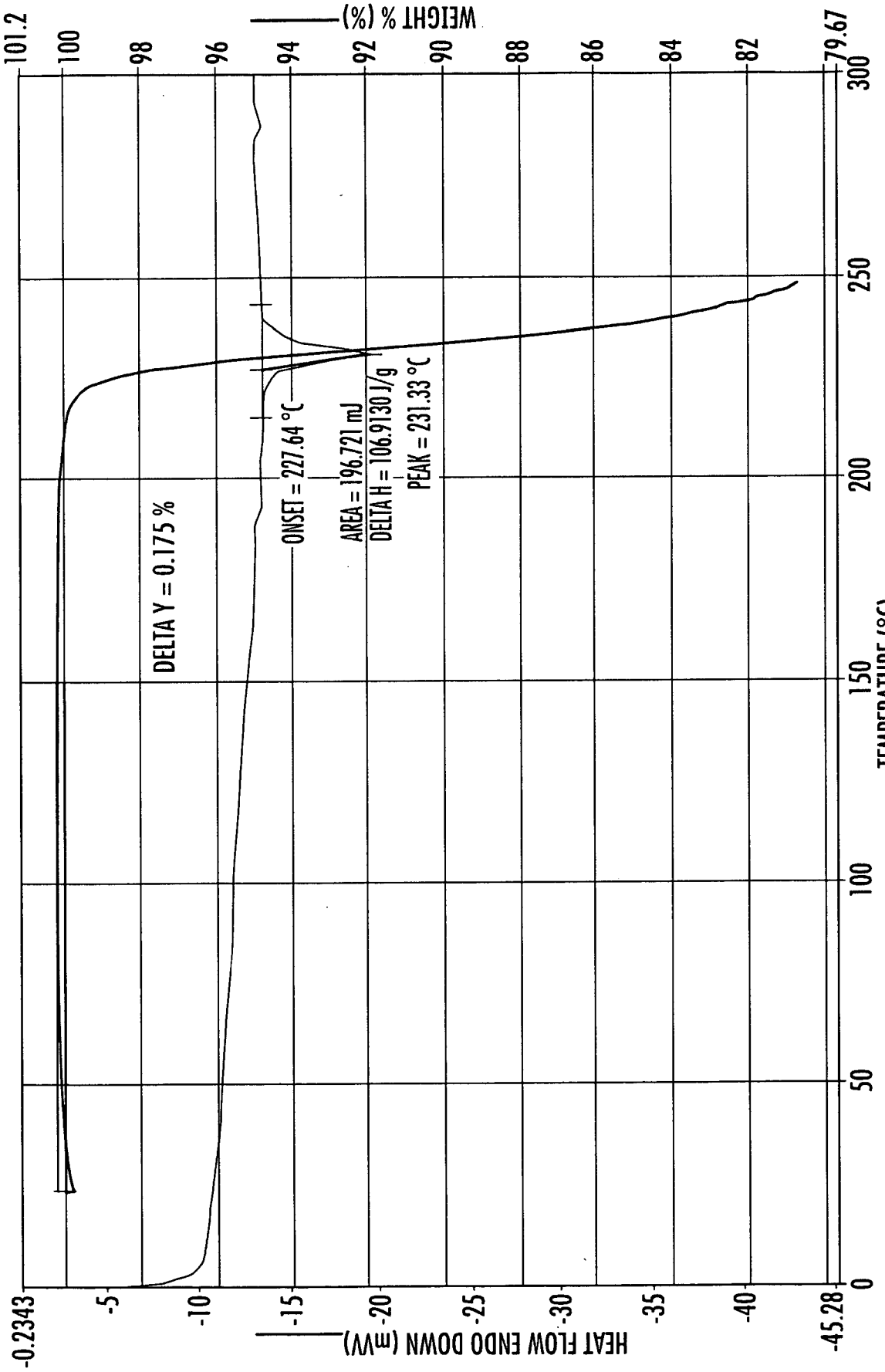

DSC AND TGA OVERLAY OF COMPOUND A FUMARATE SALT, FORM A

FIG. 34

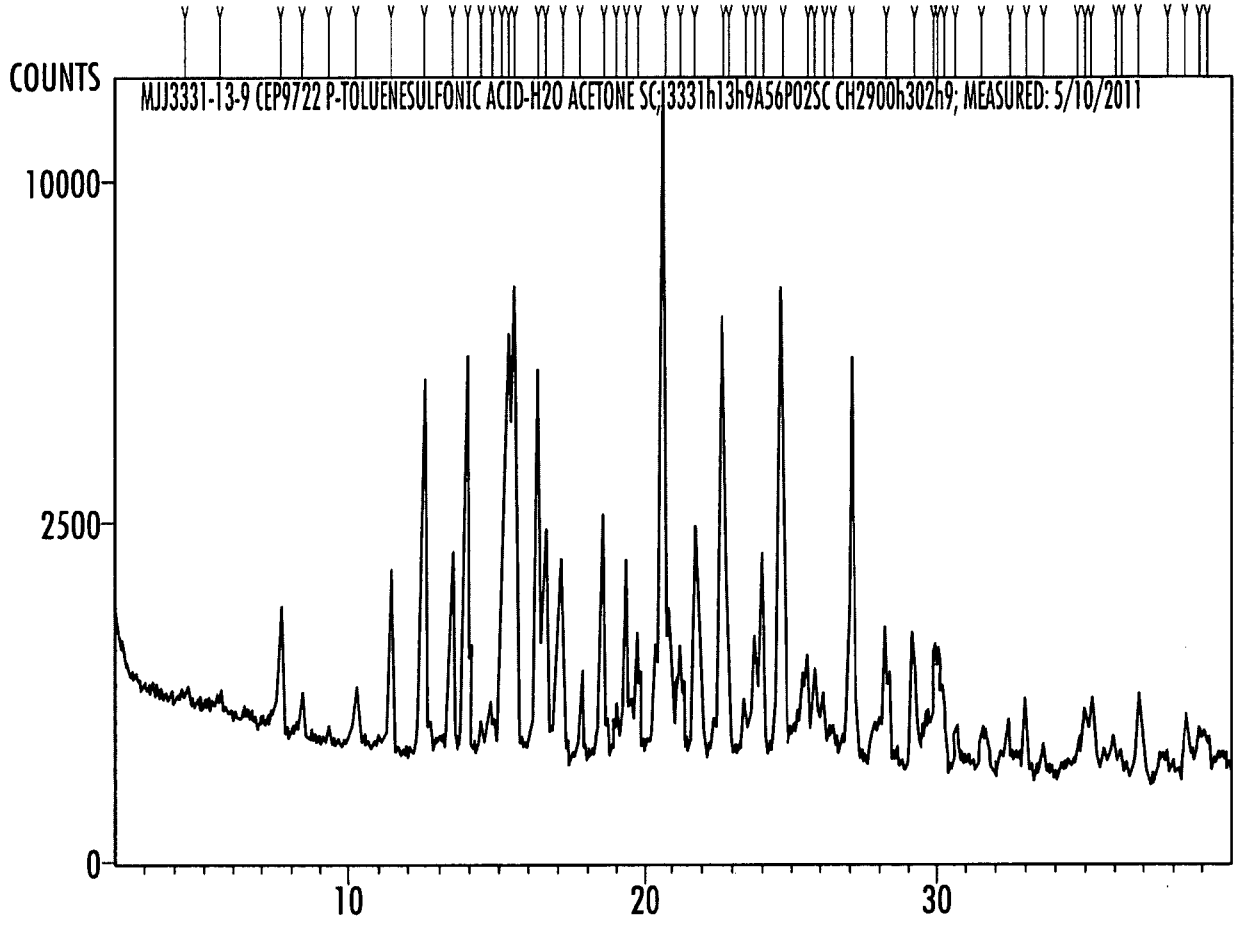

XRPD PATTERN OF COMPOUND A p-TOLUENESULFONATE SALT, FORM A

FIG. 35

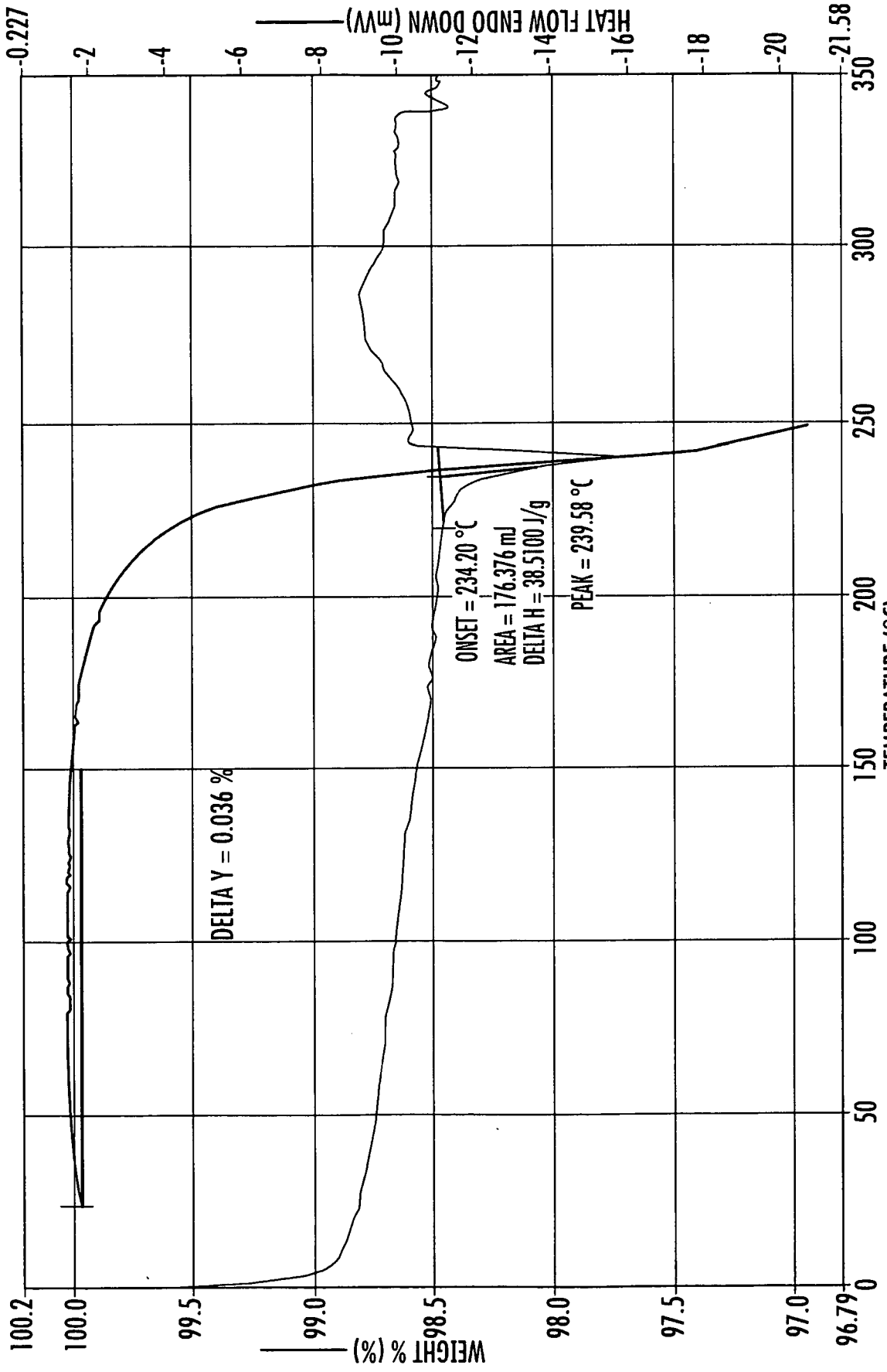

DSC AND TGA OVERLAY OF COMPOUND A p-TOLUENESULFONATE SALT, FORM A

FIG. 36

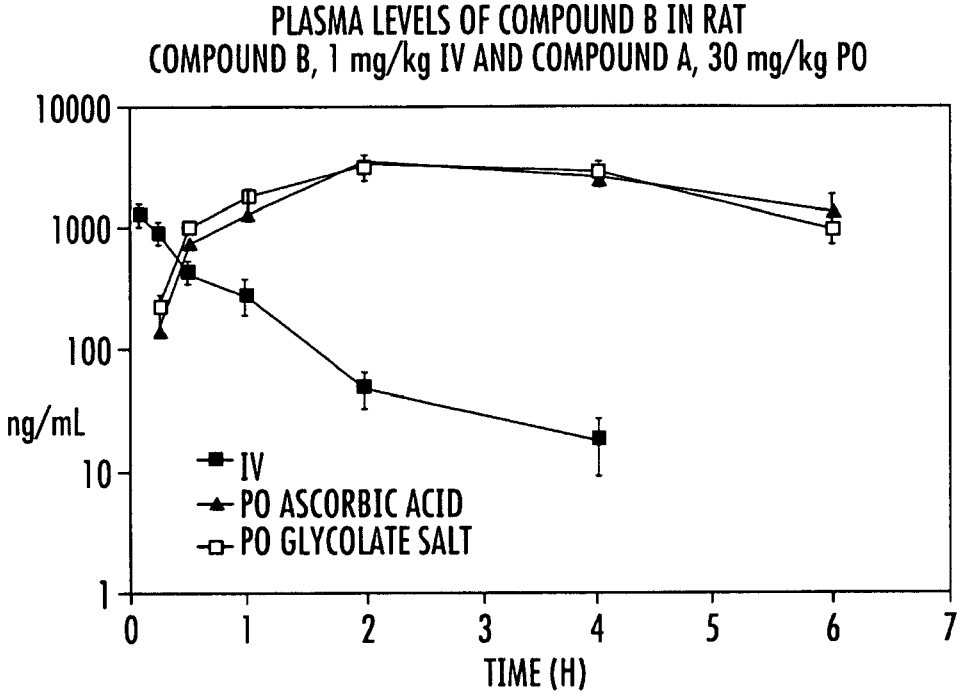

COMPOUND B	1 mg/kg I.V.	30 mg/kg P.O.	ASCORBIC ACID	GLYCOLATE SALT
$t_{1/2}$, h	0.7 ± 0.2	C_{max}, ng/mL	3450 ± 377	3538 ± 809
AUC_{0-6} ng*h/mL	889 ± 220	t_{max}h	2.3 ± 0.3	2.5 ± 0.5
AUC_{0-m},ng*h/hmL	905 ± 224	AUC_{0-6} ng*h/mL	13365 ± 1754	13559 ± 2639
Vd, L/kg	1.2 ± 0.1	AUC_{0-m},ng*h/hmL	ND	ND
CL, mL/min/kg	23 ± 4	$t_{1/2}$, h	ND	ND

PLASMA LEVELS OF COMPOUND B, 1 mg/kg INTRAVENOUS, COMPOUND A, ASCORBIC ACID SALT, 30 mg/kg ORAL, AND COMPOUND A, GLYCOLATE HYDRATE SALT, 30 mg/kg ORAL IN RAT.

FIG. 37

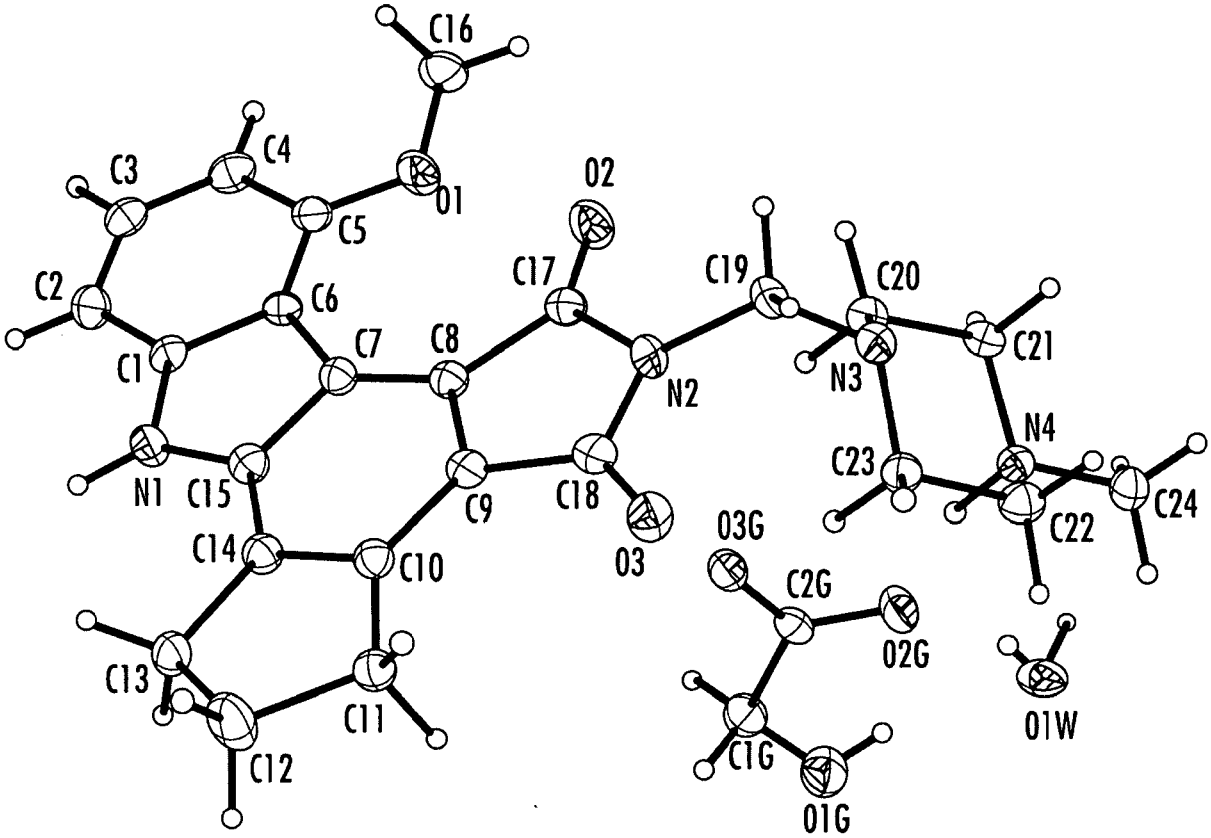

SINGLE CRYSTAL STRUCTURE OF COMPOUND A, GLYCOLATE HYDRATE SALT

FIG. 38

INTERNATIONAL SEARCH REPORT

International application No
PCT/US2015/062572

A. CLASSIFICATION OF SUBJECT MATTER
INV. C07D487/04 A61K31/407 A61P35/00
ADD.

According to International Patent Classification (IPC) or to both national classification and IPC

B. FIELDS SEARCHED

Minimum documentation searched (classification system followed by classification symbols)
C07D

Documentation searched other than minimum documentation to the extent that such documents are included in the fields searched

Electronic data base consulted during the international search (name of data base and, where practicable, search terms used)
EPO-Internal, WPI Data

C. DOCUMENTS CONSIDERED TO BE RELEVANT

Category*	Citation of document, with indication, where appropriate, of the relevant passages	Relevant to claim No.
Y	US 8 633 314 B2 (BIERLMAIER STEPHEN [US] ET AL) 21 January 2014 (2014-01-21) cited in the application	1,8-12, 44-46
A	column 1, lines 13-15; figure 1-	2-7

Y	WO 2008/063644 A1 (CEPHALON INC) 29 May 2008 (2008-05-29)	1,8-12, 44-46
A	page 17, lines 9-15; example 7	2-7

Y	P H Stahl ET AL: "Electronic Supplementary Material for CrytEngComm", CrytEngComm, 1 January 2005 (2005-01-01), XP055246124, Retrieved from the Internet: URL:http://www.rsc.org/suppdata/ce/b5/b503309h/b503309h.doc [retrieved on 2016-01-29] the whole document	1,8-12, 44-46

☐ Further documents are listed in the continuation of Box C.

☒ See patent family annex.

* Special categories of cited documents :

"A" document defining the general state of the art which is not considered to be of particular relevance

"E" earlier application or patent but published on or after the international filing date

"L" document which may throw doubts on priority claim(s) or which is cited to establish the publication date of another citation or other special reason (as specified)

"O" document referring to an oral disclosure, use, exhibition or other means

"P" document published prior to the international filing date but later than the priority date claimed

"T" later document published after the international filing date or priority date and not in conflict with the application but cited to understand the principle or theory underlying the invention

"X" document of particular relevance; the claimed invention cannot be considered novel or cannot be considered to involve an inventive step when the document is taken alone

"Y" document of particular relevance; the claimed invention cannot be considered to involve an inventive step when the document is combined with one or more other such documents, such combination being obvious to a person skilled in the art

"&" document member of the same patent family

Date of the actual completion of the international search	Date of mailing of the international search report
5 February 2016	26/04/2016

Name and mailing address of the ISA/	Authorized officer
European Patent Office, P.B. 5818 Patentlaan 2 NL - 2280 HV Rijswijk Tel. (+31-70) 340-2040, Fax: (+31-70) 340-3016	Grassi, Damian

INTERNATIONAL SEARCH REPORT

International application No.
PCT/US2015/062572

Box No. II Observations where certain claims were found unsearchable (Continuation of item 2 of first sheet)

This international search report has not been established in respect of certain claims under Article 17(2)(a) for the following reasons:

1. ☐ Claims Nos.:
because they relate to subject matter not required to be searched by this Authority, namely:

2. ☐ Claims Nos.:
because they relate to parts of the international application that do not comply with the prescribed requirements to such an extent that no meaningful international search can be carried out, specifically:

3. ☐ Claims Nos.:
because they are dependent claims and are not drafted in accordance with the second and third sentences of Rule 6.4(a).

Box No. III Observations where unity of invention is lacking (Continuation of item 3 of first sheet)

This International Searching Authority found multiple inventions in this international application, as follows:

see additional sheet

1. ☐ As all required additional search fees were timely paid by the applicant, this international search report covers all searchable claims.

2. ☐ As all searchable claims could be searched without effort justifying an additional fees, this Authority did not invite payment of additional fees.

3. ☐ As only some of the required additional search fees were timely paid by the applicant, this international search report covers only those claims for which fees were paid, specifically claims Nos.:

4. ☒ No required additional search fees were timely paid by the applicant. Consequently, this international search report is restricted to the invention first mentioned in the claims; it is covered by claims Nos.:

2-12(completely); 1, 44-46(partially)

Remark on Protest

☐ The additional search fees were accompanied by the applicant's protest and, where applicable, the payment of a protest fee.

☐ The additional search fees were accompanied by the applicant's protest but the applicable protest fee was not paid within the time limit specified in the invitation.

☐ No protest accompanied the payment of additional search fees.

INTERNATIONAL SEARCH REPORT

Information on patent family members

International application No
PCT/US2015/062572

Patent document cited in search report	Publication date	Patent family member(s)	Publication date
US 8633314 B2	21-01-2014	AU 2010289746 A1	12-04-2012
		CA 2772328 A1	10-03-2011
		CN 102482282 A	30-05-2012
		EA 201270315 A1	30-08-2012
		EP 2470540 A1	04-07-2012
		JP 2013503173 A	31-01-2013
		JP 2016014029 A	28-01-2016
		KR 20120092100 A	20-08-2012
		NZ 598883 A	26-09-2014
		SG 178852 A1	27-04-2012
		US 2012214998 A1	23-08-2012
		WO 2011028580 A1	10-03-2011
WO 2008063644 A1	29-05-2008	AR 063869 A1	25-02-2009
		AT 483456 T	15-10-2010
		AU 2007321987 A1	29-05-2008
		CA 2671517 A1	29-05-2008
		CL 2007003331 A1	04-07-2008
		CN 101784268 A	21-07-2010
		EP 2086525 A1	12-08-2009
		ES 2352817 T3	23-02-2011
		HK 1137347 A1	29-07-2011
		IL 198519 A	31-07-2014
		JP 5542444 B2	09-07-2014
		JP 2010510312 A	02-04-2010
		NZ 576693 A	22-12-2011
		NZ 595522 A	26-04-2013
		PT 2086525 E	09-12-2010
		TW 200829276 A	16-07-2008
		TW 201601762 A	16-01-2016
		US 2008146556 A1	19-06-2008
		WO 2008063644 A1	29-05-2008

FURTHER INFORMATION CONTINUED FROM PCT/ISA/ 210

This International Searching Authority found multiple (groups of) inventions in this international application, as follows:

1. claims: 2-12(completely); 1, 44-46(partially)

   Crystalline acetate salt Form A1.5 or glycolate salt hydrate Form A1 of compound A (the group is still not unitary).

   ---

2. claims: 13-21, 36-39(completely); 1, 44-46(partially)

   Crystalline L-malate salt Form A1 or A1.5 or crystalline fumarate salt Form A of compound A (the group is still not unitary).

   ---

3. claims: 22-26(completely); 1, 44-46(partially)

   Crystalline L-pyroglutamate salt Form A1 of compound A.

   ---

4. claims: 27-30(completely); 1, 44-46(partially)

   Crystalline free base Form C0 of compound A.

   ---

5. claims: 31-35(completely); 1, 44-46(partially)

   Crystalline hydrochloride salt Form A of compound A.

   ---

6. claims: 40-43(completely); 1, 44-46(partially)

   Crystalline p-toluenesulfonate salt Form A of compound A.

   ---

(19)中华人民共和国国家知识产权局

(12)发明专利申请

(10)申请公布号 CN 107207511 A
(43)申请公布日 2017.09.26

(21)申请号 201580063386.3
(22)申请日 2015.11.25
(30)优先权数据
62/084,652 2014.11.26 US
(85)PCT国际申请进入国家阶段日
2017.05.22
(86)PCT国际申请的申请数据
PCT/US2015/062572 2015.11.25
(87)PCT国际申请的公布数据
WO2016/086080 EN 2016.06.02
(71)申请人 赛福伦公司
地址 美国宾夕法尼亚州
(72)发明人 斯蒂芬·J·比尔迈耶
拉尔夫·C·霍尔蒂万格
马丁·J·雅各布斯
(74)专利代理机构 北京东方亿思知识产权代理有限责任公司 11258
代理人 肖善强
(51)Int.Cl.
C07D 487/04(2006.01)
A61K 31/496(2006.01)
A61P 35/00(2006.01)

权利要求书3页 说明书29页 附图37页

(54)发明名称

PARP抑制剂的结晶形式

(57)摘要

本公开涉及4,5,6,7-四氢-11-甲氧基-2-[(4-甲基-1-哌嗪基)甲基]-1H-环戊[a]吡咯并[3,4-c]咔唑-1,3(2H)-二酮的结晶形式,包括盐形式和游离碱形式。

CN 107207511 A

1.4,5,6,7-四氢-11-甲氧基-2-[(4-甲基-1-哌嗪基)甲基]-1H-环戊[a]吡咯并[3,4-c]咔唑-1,3(2H)-二酮(化合物A)的结晶形式

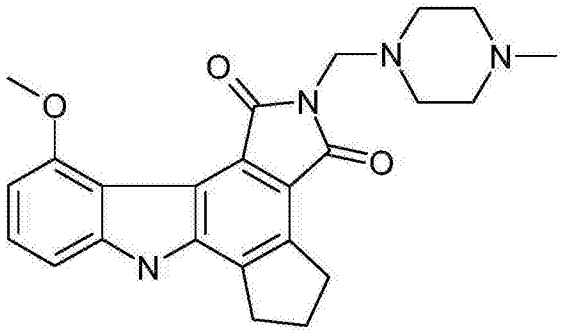

化合物A

其为

化合物A乙酸盐形式$A_{1.5}$;

化合物A乙醇酸盐水合物形式A_1;

化合物A L-苹果酸盐形式A_1;

化合物A L-苹果酸盐形式$A_{1.5}$;

化合物A L-焦谷氨酸盐形式A_1;

化合物A游离碱形式C_0;

化合物A盐酸盐形式A;

化合物A富马酸盐形式A;或

化合物A对甲苯磺酸盐形式A。

2.根据权利要求1所述的结晶形式,其为化合物A乙醇酸盐水合物形式A_1。

3.根据权利要求2所述的结晶形式,其通过具有至少三个选自8.2、8.7、13.8、14.9、16.4、17.5、18.2、18.5、20.2、20.6、21.2、21.4、23.0、24.6、27.8、29.9、30.1和30.5度2θ±0.2度2θ的峰的X射线粉末衍射图案来表征。

4.根据权利要求2或权利要求3所述的结晶形式,其还通过基本上如图9或图10中所描绘的X射线粉末衍射图案来表征。

5.根据权利要求2至4中任一项所述的结晶形式,其还通过基本上如图9中所描绘的X射线粉末衍射图案来表征。

6.根据权利要求2至5中任一项所述的结晶形式,其还通过基本上如图11中所描绘的DSC来表征。

7.根据权利要求2至6中任一项所述的结晶形式,其还通过基本上如图12中所描绘的DVS来表征。

8.根据权利要求1所述的结晶形式,其为化合物A乙酸盐形式$A_{1.5}$。

9.根据权利要求8所述的结晶形式,其通过具有至少三个选自6.4、9.2、12.7、13.0、15.2、17.4、18.4、19.0、19.3、21.3、21.5、23.1、24.1、24.2和28.2±0.2度2-θ的峰的X射线粉末衍射图案来表征。

10.根据权利要求8或权利要求9所述的结晶形式,其还通过基本上如图3、图4或图5中所描绘的X射线粉末衍射图案来表征。

11.根据权利要求8至10中任一项所述的结晶形式，其还通过基本上如图6中所描绘的DSC来表征。

12.根据权利要求8至11中任一项所述的结晶形式，其还通过基本上如图7中所描绘的DVS来表征。

13.根据权利要求1所述的结晶形式，其为化合物A L-苹果酸盐形式A_1。

14.根据权利要求13所述的结晶形式，其通过具有至少三个选自8.6、9.2、10.1、10.4、11.7、11.9、14.7、15.3、15.6、17.2、17.8、18.5、20.3、20.7、21.2、22.4、23.5、24.3和27.0±0.2度2-θ的峰的X射线粉末衍射图案来表征。

15.根据权利要求13或权利要求14所述的结晶形式，其还通过基本上如图14或图15中所描绘的X射线粉末衍射图案来表征。

16.根据权利要求13至15中任一项所述的结晶形式，其还通过基本上如图16中所描绘的DSC来表征。

17.根据权利要求13至16中任一项所述的结晶形式，其还通过基本上如图17中所描绘的DVS来表征。

18.根据权利要求1所述的结晶形式，其为化合物A L-苹果酸盐形式$A_{1.5}$。

19.根据权利要求18所述的结晶形式，其通过具有至少三个选自5.5、6.8、8.0、8.4、8.8、9.2、11.8、12.8、13.1、13.6、14.4、16.0、16.7、18.1、18.5、19.4、20.2、20.5、21.1、21.9、23.4和24.6±0.2度2-θ的峰的X射线粉末衍射图案来表征。

20.根据权利要求18或权利要求19所述的结晶形式，其还通过基本上如图19中所描绘的X射线粉末衍射图案来表征。

21.根据权利要求18至20中任一项所述的结晶形式，其还通过基本上如图20中所描绘的DSC来表征。

22.根据权利要求1所述的结晶形式，其为化合物A L-焦谷氨酸盐形式A_1。

23.根据权利要求22所述的结晶形式，其通过具有至少三个选自6.0、9.6、10.3、10.5、11.0、12.0、13.2、15.0、16.7、17.5、17.8、18.0、19.0、20.8、21.0、21.1、22.0、22.1、23.1、23.4、23.5、24.8和26.6±0.2度2-θ的峰的X射线粉末衍射图案来表征。

24.根据权利要求22或权利要求23所述的结晶形式，其还通过基本上如图21或图22中所描绘的X射线粉末衍射图案来表征。

25.根据权利要求22至24中任一项所述的结晶形式，其还通过基本上如图23中所描绘的DSC来表征。

26.根据权利要求22至25中任一项所述的结晶形式，其还通过基本上如图24中所描绘的DVS来表征。

27.根据权利要求1所述的结晶形式，其为化合物A游离碱形式C_0。

28.根据权利要求27所述的结晶形式，其通过具有至少三个选自8.5、8.8、13.9、14.4、15.4、17.6、18.1、18.5、19.2、19.7、20.4、21.1、21.4、21.9、23.6、24.6、29.4和30.1±0.2度2-θ的峰的X射线粉末衍射图案来表征。

29.根据权利要求27或权利要求28所述的结晶形式，其还通过基本上如图26或图27中所描绘的X射线粉末衍射图案来表征。

30.根据权利要求27至29中任一项所述的结晶形式，其还通过基本上如图28中所描绘

的DSC来表征。

31.根据权利要求1所述的结晶形式，其为化合物A盐酸盐形式A。

32.根据权利要求31所述的结晶形式，其通过具有至少三个选自7.5、8.6、12.2、17.1、18.8、18.9、22.3、24.5、25.6、26.1、33.5和34.1±0.2度2-θ的峰的X射线粉末衍射图案来表征。

33.根据权利要求31或权利要求32所述的结晶形式，其还通过基本上如图30中所描绘的X射线粉末衍射图案来表征。

34.根据权利要求31至33中任一项所述的结晶形式，其还通过基本上如图31中所描绘的DSC来表征。

35.根据权利要求31至34中任一项所述的结晶形式，其还通过基本上如图32中所描绘的DVS来表征。

36.根据权利要求1所述的结晶形式，其为化合物A富马酸盐形式A。

37.根据权利要求36所述的结晶形式，其通过具有至少三个选自9.0、10.5、11.1、14.9、17.1、17.7、19.3、21.1、22.3、22.9、23.5、24.0、24.2、25.7、25.9、27.3、29.0和31.1±0.2度2-θ的峰的X射线粉末衍射图案来表征。

38.根据权利要求36或权利要求37所述的结晶形式，其还通过基本上如图33中所描绘的X射线粉末衍射图案来表征。

39.根据权利要求36至38中任一项所述的结晶形式，其还通过基本上如图34中所描绘的DSC来表征。

40.根据权利要求1所述的结晶形式，其为化合物A对甲苯磺酸盐形式A。

41.根据权利要求40所述的结晶形式，其通过具有至少三个选自6.0、9.6、10.3、10.5、11.0、12.0、12.9、13.2、15.0、16.7、17.0、17.5、17.8、18.0、19.0、20.8、21.0、21.1、22.1、22.7、23.1、23.4、23.5、24.8和26.6±0.2度2-θ的峰的X射线粉末衍射图案来表征。

42.根据权利要求40或权利要求41所述的结晶形式，其还通过基本上如图35中所描绘的X射线粉末衍射图案来表征。

43.根据权利要求40至42中任一项所述的结晶形式，其还通过基本上如图36中所描绘的DSC来表征。

44.一种药物组合物，其包含根据前述权利要求中任一项所述的结晶形式和至少一种药学上可接受的赋形剂。

45.一种治疗患者中的癌症的方法，其包括向所述患者施用根据权利要求1至43中任一项所述的4,5,6,7-四氢-11-甲氧基-2-[(4-甲基-1-哌嗪基)甲基]-1H-环戊[a]吡咯并[3,4-c]咔唑-1,3(2H)-二酮(化合物A)的结晶形式。

46.根据权利要求45所述的方法，其中所述癌症是乳腺癌或卵巢癌。

PARP抑制剂的结晶形式

[0001] 相关申请的交叉引用

[0002] 本申请要求2014年11月26日提交的美国临时申请No.62/084,652的权益，该临时申请的整个内容以引用方式并入本文。

技术领域

[0003] 本公开涉及4,5,6,7-四氢-11-甲氧基-2-[(4-甲基-1-哌嗪基)甲基]-1H-环戊[a]吡咯并[3,4-c]咔唑-1,3(2H)-二酮及其盐的结晶形式。

背景技术

[0004] 化合物A(4,5,6,7-四氢-11-甲氧基-2-[(4-甲基-1-哌嗪基)甲基]-1H-环戊[a]吡咯并[3,4-c]咔唑-1,3(2H)-二酮)是用于单独地或联合化疗或放疗来治疗乳腺癌、卵巢癌和其他癌症的PARP(多聚ADP-核糖聚合酶)抑制剂。参见例如美国专利No.7,122,679、8,716,493和8,633,314。

[0005] 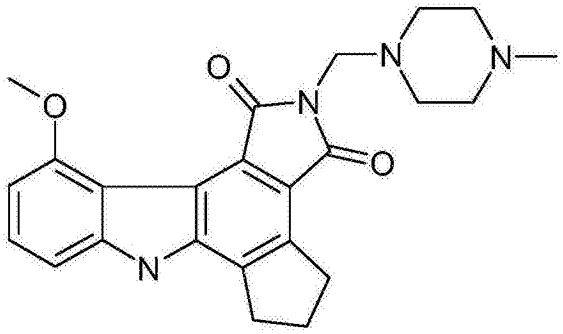

化合物A

[0006] 化合物A是化合物B的前药：

[0007] 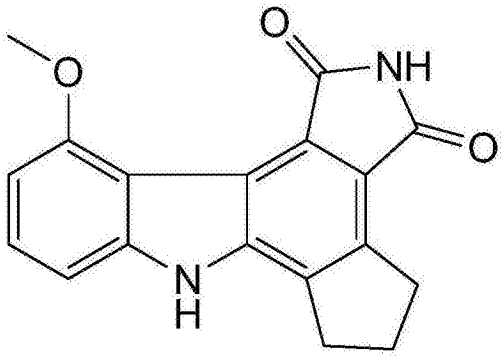

化合物B

[0008] 化合物A的游离碱形式形成水合物，这是不可取的。此外，化合物A的游离碱形式具有低堆积密度，使得不便于制造。需要化合物A的替代形式。

发明内容

[0009] 本公开涉及化合物A乙酸盐形式$A_{1.5}$、化合物A乙醇酸盐水合物形式A_1、化合物A L-苹果酸盐形式A_1、化合物A L-苹果酸盐形式$A_{1.5}$、化合物A L-焦谷氨酸盐形式A_1、化合物A游离碱形式C_0、化合物A盐酸盐形式A、化合物A富马酸盐形式A和化合物A对甲苯磺酸盐形式A。还描述了包含这些形式中的一种或多种的药物组合物。也描述了使用这些形式的方法。

附图说明

[0010] 图1显示化合物A游离碱形式A_0的XRPD图案。

[0011] 图2显示化合物A游离碱形式A_0的DSC/TGA重叠图。

[0012] 图3显示化合物A乙酸盐形式$A_{1.5}$的XRPD图案。

[0013] 图4显示化合物A乙酸盐形式$A_{1.5}$的VT-XRPD图案-请求模式(Requested Mode)。

[0014] 图5显示化合物A乙酸盐形式$A_{1.5}$的VT-XRPD图案-连续模式(Continuous Mode)。

[0015] 图6显示化合物A乙酸盐形式$A_{1.5}$的DSC和TGA重叠图。

[0016] 图7显示化合物A乙酸盐形式$A_{1.5}$的DVS重叠图。

[0017] 图8显示化合物A乙酸盐形式$A_{1.5}$的显微照片。

[0018] 图9显示化合物A乙醇酸盐水合物形式A_1的XRPD图案。

[0019] 图10显示化合物A乙醇酸盐水合物形式A_1的热XRPD图案。

[0020] 图11显示化合物A乙醇酸盐水合物形式A_1的DSC和TGA重叠图。

[0021] 图12显示化合物A乙醇酸盐水合物形式A_1的DVS重叠图。

[0022] 图13显示化合物A乙醇酸盐水合物形式A_1的显微照片。

[0023] 图14显示化合物A L-苹果酸盐形式A_1的XRPD图案。

[0024] 图15显示化合物A苹果酸盐形式A_1的VT-XRPD图案。

[0025] 图16显示化合物A L-苹果酸盐形式A_1的DSC和TGA重叠图。

[0026] 图17显示化合物A L-苹果酸盐形式A_1的DVS。

[0027] 图18显示化合物A L-苹果酸盐形式A_1的显微照片。

[0028] 图19显示化合物A L-苹果酸盐形式$A_{1.5}$的XRPD图案。

[0029] 图20显示化合物A L-苹果酸盐形式$A_{1.5}$的DSC和TGA重叠图。

[0030] 图21显示化合物A L-焦谷氨酸盐形式A_1的XRPD图案。

[0031] 图22显示化合物A L-焦谷氨酸盐形式A_1的VT-XRPD图案。

[0032] 图23显示化合物A L-焦谷氨酸盐形式A_1的DSC和TGA重叠图。

[0033] 图24显示化合物A L-焦谷氨酸盐形式A_1的DVS。

[0034] 图25显示化合物A L-焦谷氨酸盐形式A_1的显微照片。

[0035] 图26显示化合物A游离碱形式C_0的XRPD图案。

[0036] 图27显示化合物A游离碱形式C_0的热XRPD图案。

[0037] 图28显示化合物A游离碱形式C_0的DSC和TGA重叠图。

[0038] 图29显示化合物A A游离碱形式C_0的显微照片。

[0039] 图30显示化合物A盐酸盐形式A的XRPD图案。

[0040] 图31显示化合物A盐酸盐形式A的DSC和TGA重叠图。

[0041] 图32显示化合物A盐酸盐形式A的DVS。

[0042] 图33显示化合物A富马酸盐形式A的XRPD图案。

[0043] 图34显示化合物A富马酸盐形式A的DSC和TGA重叠图。

[0044] 图35显示化合物A对甲苯磺酸盐形式A的XRPD图案。

[0045] 图36显示化合物A对甲苯磺酸盐形式A的DSC和TGA重叠图。

[0046] 图37显示化合物B(1mg/kg静脉内)、化合物A抗坏血酸盐(30mg/kg口服)和化合物A乙醇酸水合盐(30mg/kg口服)在大鼠中的血浆水平。

[0047] 图38显示化合物A乙醇酸水合盐的单晶结构。

具体实施方式

[0048] 本公开通过提供化合物A的新形式(包括化合物A的新结晶游离碱形式和化合物A的新结晶盐形式)而解决本领域中的需求。

[0049] 本公开尤其涉及化合物A乙酸盐形式$A_{1.5}$、化合物A乙醇酸盐水合物形式A_1、化合物A L-苹果酸盐形式A_1、化合物A L-苹果酸盐形式$A_{1.5}$、化合物A L-焦谷氨酸盐形式A_1、化合物A游离碱形式C_0、化合物A盐酸盐形式A、化合物A富马酸盐形式A和化合物A对甲苯磺酸盐形式A。还描述了包含这些形式中的一种或多种的药物组合物。

[0050] 在一个实施方案中,本公开涉及化合物A乙酸盐形式$A_{1.5}$。在一个方面,该结晶形式通过包括以下峰中的一个或多个的X射线衍射图案来表征:6.4、9.2、12.7、13.0、15.2、17.4、18.4、19.0、19.3、21.3、21.5、23.1、24.1、24.2和/或28.2±0.2度2-θ。在另一个方面,该结晶形式包括前述峰中的至少3个。在又一个方面,该结晶形式包括前述峰中的至少4、5、6、7、8、9或10个。在另一个方面,该结晶形式具有基本上如图3中所描绘的X射线粉末衍射图案。

[0051] 本公开还涉及化合物A乙醇酸水合盐。这些盐可在晶体结构中具有不同量的水。例如,化合物A与水的比率可为从约1:0.1至约1:1。在其他实施方案中,化合物A与水的比率为1:0.1、1:0.2、1:0.3、1:0.4、1:0.5、1:0.6、1:0.7、1:0.8、1:0.9或1:1。

[0052] 本公开的另一个实施方案涉及化合物A乙醇酸水合盐形式A_1。在一个方面,该结晶形式通过包括以下峰中的一个或多个的X射线衍射图案来表征:8.1、8.2、8.7、13.9、14.7、14.9、16.3、17.4、17.6、18.2、18.5、19.0、20.2、20.6、21.2、21.4、23.0、24.5、24.7、26.1、26.3、28.0、30.0、30.1、30.2和/或32.8±0.2度2-θ。在另一个方面,该结晶形式包括前述峰中的至少3个。在又一个方面,该结晶形式包括前述峰中的至少4、5、6、7、8、9或10个。在另一个方面,该结晶形式具有基本上如图9中所描绘的X射线粉末衍射图案。

[0053] 本公开的又一个实施方案涉及化合物A L-苹果酸盐形式A_1。在一个方面,该结晶形式通过包括以下峰中的一个或多个的X射线衍射图案来表征:8.6、9.2、10.1、10.4、11.7、11.9、14.7、15.3、15.6、17.2、17.8、18.5、20.3、20.7、21.2、22.4、23.5、24.3和/或27.0±0.2度2-θ。在另一个方面,该结晶形式包括前述峰中的至少3个。在又一个方面,该结晶形式包括前述峰中的至少4、5、6、7、8、9或10个。在另一个方面,该结晶形式具有基本上如图14中所描绘的X射线粉末衍射图案。

[0054] 在另一个实施方案中,本公开涉及化合物AL-苹果酸盐形式$A_{1.5}$。在一个方面,该结晶形式通过包括以下峰中的一个或多个的X射线衍射图案来表征:5.5、6.8、8.0、8.4、8.8、9.2、11.8、12.8、13.1、13.6、14.4、16.0、16.7、18.1、18.5、19.4、20.2、20.5、21.1、21.9、23.4和/或24.6±0.2度2-θ。在另一个方面,该结晶形式包括前述峰中的至少3个。在又一个

方面，该结晶形式包括前述峰中的至少4、5、6、7、8、9或10个。在另一个方面，该结晶形式具有基本上如图19中所描绘的X射线粉末衍射图案。

[0055] 本文还描述化合物A L-焦谷氨酸盐形式A_1。在一个方面，该结晶形式通过包括以下峰中的一个或多个的X射线衍射图案来表征：6.0、9.6、10.3、10.5、11.0、12.0、13.2、15.0、16.7、17.5、17.8、18.0、19.0、20.8、21.0、21.1、22.0、22.1、23.1、23.4、23.5、24.8和/或26.6±0.2度2-θ。在另一个方面，该结晶形式包括前述峰中的至少3个。在又一个方面，该结晶形式包括前述峰中的至少4、5、6、7、8、9或10个。在另一个方面，该结晶形式具有基本上如图21中所描绘的X射线粉末衍射图案。

[0056] 本公开还涉及化合物A游离碱形式C_0。在一个方面，该结晶形式通过包括以下峰中的一个或多个的X射线衍射图案来表征：8.5、8.8、13.9、14.4、15.4、17.6、18.1、18.5、19.2、19.7、20.4、21.1、21.4、21.9、23.6、24.6、29.4和/或30.1±0.2度2-θ。在另一个方面，该结晶形式包括前述峰中的至少3个。在又一个方面，该结晶形式包括前述峰中的至少4、5、6、7、8、9或10个。在另一个方面，该结晶形式具有基本上如图27中所描绘的X射线粉末衍射图案。

[0057] 本公开的另一个实施方案涉及化合物A盐酸盐形式A。在一个方面，该结晶形式通过包括以下峰中的一个或多个的X射线衍射图案来表征：7.5、8.6、12.2、17.1、18.8、18.9、22.3、24.5、25.6、26.1、33.5和/或34.1±0.2度2-θ。在另一个方面，该结晶形式包括前述峰中的至少3个。在又一个方面，该结晶形式包括前述峰中的至少4、5、6、7、8、9或10个。在另一个方面，该结晶形式具有基本上如图30中所描绘的X射线粉末衍射图案。

[0058] 本公开的再一个实施方案涉及化合物A富马酸盐形式A。在一个方面，该结晶形式通过包括以下峰中的一个或多个的X射线衍射图案来表征：9.0、10.5、11.1、14.9、17.1、17.7、19.3、21.1、22.3、22.9、23.5、24.0、24.2、25.7、25.9、27.3、29.0和/或31.1±0.2度2-θ。在另一个方面，该结晶形式包括前述峰中的至少3个。在又一个方面，该结晶形式包括前述峰中的至少4、5、6、7、8、9或10个。在另一个方面，该结晶形式具有基本上如图33中所描绘的X射线粉末衍射图案。

[0059] 本公开的还一个实施方案涉及化合物A对甲苯磺酸盐形式A。在一个方面，该结晶形式通过包括以下峰中的一个或多个的X射线衍射图案来表征：6.0、9.6、10.3、10.5、11.0、12.0、12.9、13.2、15.0、16.7、17.0、17.5、17.8、18.0、19.0、20.8、21.0、21.1、22.1、22.7、23.1、23.4、23.5、24.8和/或26.6±0.2度2-θ。在另一个方面，该结晶形式包括前述峰中的至少3个。在又一个方面，该结晶形式包括前述峰中的至少4、5、6、7、8、9或10个。在另一个方面，该结晶形式具有基本上如图35中所描绘的X射线粉末衍射图案。

[0060] 在一些实施方案中，本公开的多晶型形式基本上不含任何其他多晶型形式或指定的多晶型形式。在本发明的任何实施方案中，所谓“基本上不含”是指本发明的所述形式含有20％(w/w)或以下、10％(w/w)或以下、5％(w/w)或以下、2％(w/w)或以下、尤其是1％(w/w)或以下、更尤其是0.5％(w/w)或以下且最尤其是0.2％(w/w)或以下的任何其他多晶型物或指定的一种或多种多晶型物。在其他实施方案中，本公开的多晶型物含有从1％至20％(w/w)、从5％至20％(w/w)或从5％至10％(w/w)的任何其他多晶型物或指定的一种或多种多晶型物。

[0061] 本发明的盐和固态形式具有有利的性质，包括以下至少一种：高结晶度、溶解度、溶解速率、形态、针对多晶型转化和/或针对脱水的热和机械稳定性、储存稳定性、低残余溶

剂含量、较低的吸湿度、流动性以及有利的加工和处理特性，诸如可压缩性和堆积密度。

[0062] 晶型在本文中可称为通过“基本上如图中所描绘的”图形数据来表征。这些数据包括例如粉末X射线衍射图。技术人员将理解的是，数据的此类图形表示可以发生小的变化，例如在峰相对强度和峰位置上，原因是诸如仪器响应中的变化和样品浓度及纯度中的变化等因素，这对于技术人员而言是熟知的。尽管如此，技术人员将能够容易地比较本文图中的图形数据与针对未知晶型产生的图形数据并确认两组图形数据是表征相同的晶型还是两种不同的晶型。

[0063] 如本文所用的术语“无定形的”是指缺乏特征性晶体形状或结晶结构。

[0064] 如本文所用的术语“结晶的”是指具有规则性重复的分子排列或外晶面平面(external face plane)。

[0065] 如本文所用的术语“结晶形式”是指一种固体化合物或多种化合物的混合物，当通过X射线粉末衍射对其分析时，这种物质提供特征性峰图案；这种物质包括但不局限于多晶型物、溶剂化物、水合物、共晶和去溶剂化的溶剂化物。

[0066] 术语“多晶型的”或“多晶型现象”被定义为对于相同的化学分子有至少两种不同的结晶排列的可能性。

[0067] 如本文所用的术语“溶液”是指含有至少一种溶剂以及至少一种化合物的混合物，该化合物在该溶剂中至少部分地溶解。

[0068] 如本文所用的术语“药学上可接受的赋形剂”包括任何及所有的溶剂、分散介质、包衣、抗细菌剂和抗真菌剂、等渗剂和吸收延迟剂等。对于药物活性物质而言，此类介质和药剂的使用在本领域中是熟知的，诸如在Remington:The Science and Practice of Pharmacy，第20版；Gennaro,A.R.编，Lippincott Williams &Wilkins:Philadelphia,Pa.，2000中。除非在任何常规介质或药剂与活性成分不相容的情况下，否则考虑了它在治疗性组合物中的使用。还可以将补充性活性成分掺入这些组合物中。

[0069] 本发明的药物组合物可以多种方式使用，包括但不限于增强辐照或DNA损伤性化疗剂的抗肿瘤活性(Griffin,R.J.;Curtin,N.J.;Newell,D.R.;Golding,B.T.;Durkacz.B.W.;Calvert,A.H.The role of inhibitors of poly(ADP-ribose)polymerase as resistance-modifying agents in cancer therapy.Biochemie 1995,77,408)。

[0070] 出于治疗性目的，本发明的结晶形式可以通过导致活性剂与受试者体内的药剂作用位点相接触的任何手段来施用。结晶形式可以通过可用于与药物结合使用的任何常规手段作为单独的治疗剂或与其他治疗剂比如止痛剂联合来施用。本发明的结晶形式优选地以用于治疗本文所述的疾病和病症的治疗有效量施用给对其有需要的受试者。

[0071] 在治疗性或预防性用途中，本发明的结晶形式可以通过通常施用药物的任何途径来施用。此类施用途径包括腹膜内、静脉内、肌内、皮下、鞘内、气管内、心室内、口、颊、直肠、肠胃外、鼻内、透皮或真皮内。施用可以是全身或局部的。

[0072] 本文所述的结晶形式可以采取纯的形式、与其他活性成分组合、或与药学上可接受的无毒赋形剂或载体组合施用。口服组合物一般将包含惰性稀释载体或可食用载体。可以包含药学上相容的粘合剂和/或佐剂材料作为组合物的一部分。片剂、丸剂、胶囊、锭剂等可以含有任何下述成分或性质类似的化合物：粘合剂，诸如微晶纤维素、黄蓍胶或明胶；赋形剂，诸如淀粉或乳糖；分散剂，诸如藻酸、Primogel或玉米淀粉；润滑剂，诸如硬脂酸镁；助

流剂，诸如胶体二氧化硅；甜味剂，诸如蔗糖或糖精；或调味剂，诸如胡椒薄荷、水杨酸甲酯或橙香精。当剂量单位形式是胶囊时，除了上述类型的材料之外，它还可以含有液体载体，诸如脂肪油。此外，剂量单位形式可以含有改变剂量单位的物理形式的各种其他材料，例如糖、虫胶或肠溶试剂的包衣。此外，除了活性化合物之外，糖浆还可以含有作为甜味剂的蔗糖以及某些防腐剂、色素、着色剂和调味剂。

[0073] 用于施用的备选制剂包括无菌水性或非水性溶液、悬浮液和乳液。非水性溶剂的实例是二甲基亚砜、醇类、丙二醇、聚乙二醇、植物油诸如橄榄油和注射用有机酯诸如油酸乙酯。水性载体包括醇类与水的混合物、缓冲介质和盐水。静脉内溶媒包括流体和营养补充剂、电解质补充剂，诸如基于林格氏(Ringer's)葡萄糖等的那些。也可以存在防腐剂和其他添加剂，比如抗微生物剂、抗氧化剂、螯合剂、惰性气体等。

[0074] 结晶形式向哺乳动物施用的优选方法包括腹膜内注射、肌内注射和静脉内输注。各种液体制剂可能用于这些递送方法，包括盐水、醇、DMSO和水基溶液。浓度可以根据待递送的剂量和体积而变化，并且可以在从约1至约1000mg/mL的范围内。液体制剂的其他成分可以包括防腐剂、无机盐、酸、碱、缓冲剂、营养剂、维生素或其他药物诸如止痛剂或另外的PARP和激酶抑制剂。

[0075] 因此，已经参照了特定的优选实施方案和示例性实例描述了本发明，但是本领域的技术人员可以认识到不脱离如说明书中所公开的本发明精神和范围的对所描述和例示的发明的适当修改。示出实施例以有助于理解本发明，但无意且不应被视为以任何方式限制本发明的范围。

[0076] 实施例

[0077] 以下实施例中所用的溶剂具有试剂级质量且无需进一步纯化即使用。化合物A的已知形式用A_0和B_0来表示无水材料，用H_d来表示水合物。

[0078] X-射线粉末衍射(XRPD)

[0079] 标准反射模式测量：在45kV和40mA下使用CuK_α辐射在配有X'celerator检测器的PANalytical X Pert Pro衍射仪上记录粉末X射线衍射图案。$K_{\alpha 1}$辐射使用高度取向的晶体(Ge111)入射光束单色仪获得。将10mm光束掩模以及固定的(1/4°)发散和防散射(1/8°)狭缝插到入射光束一侧上。将固定的5mm接收狭缝和0.04弧度Soller块插到衍射光束一侧上。X射线粉末图案扫描从约2至40°2θ以0.0080°的步长和96.06秒的计数时间(这导致约0.5°/min的扫描速率)来收集。在硅零背景(ZBG)板上展开样品以用于测量。用PANalytical PW3064旋转器(15转/分钟)旋转样品。

[0080] 在收集数据之前对Si参比标准进行的测量得到了2θ以及强度的值，这些值完全处于$28.44<2\theta<28.50$的容限内并且显著大于150cps的最小峰高。

[0081] SCXRD-单晶X射线衍射：对于数据收集，从由约三或四个单独块构成的团块脱落下一块(0.12×0.04×0.03mm3)以得到看起来为单晶的晶体。借助聚异丁烯油(也称为PARATONE)将晶体安装到Bruker-Nonius X8Proteum衍射仪上的细玻璃纤维上，衍射仪附连到Nonius FR-591旋转阳极(CuKa)，该阳极具有'Helios'聚焦光学器件。将晶体通过得自CryoIndustries of America的CryoCool LT2自始至终维持在90K。用于索引的衍射图像清楚地显示出分裂反射(split reflection)，与开裂(cracking)或孪晶(twinning)相符，但是具有靠得足够近而融合在一起的光斑分量(spot component)。数对分裂反射的相对强度

表明开裂比孪晶的可能性更大。

[0082] 从存在于72个衍射图像(六组,每组12个0.5°的帧)中的反射来索引晶体。数据采集包括以三个检测器偏转角在15次扫描中获得的1485个2°的帧(以2θ在-40°进行的两个360° φ-扫描,以2θ在-45°进行的三个90°ω-扫描,以2θ在-96°进行的四个360° φ-扫描,以及以2θ在-96°进行的六个90°ω-扫描),其足够以四倍冗余度覆盖任意取向的三斜晶体的倒易空间,达到0.83Å的分辨率。使用得自Bruker-AXS的APEX2包中的程序,对数据进行积分、换算、平均化和合并。最终的晶胞参数来源于积分过程的输出诊断。结构通过标准直接方法使用SHELXS进行解析,并使用SHELXL进行精修,两者均得自SHELX97包。使用得自SHELXTL套装的XP和得自CCDC的Mercury绘图。通过Platon进行了另外的分子图形和空间计算。

[0083] 对所有非氢原子的位置和各向异性位移参数进行了精修。H原子位于差分傅里叶图谱(difference Fourier's map)中,但附连到碳原子的那些氢原子在几何上重新定位。H原子最初通过软约束(soft restraint)在键长和角度上进行精修,以调整它们的几何(N-H和0.93-0.98范围内的C-H至0.86 Å)和Uiso(H)(在1.2-1.5倍母原子Ueq的范围内),之后,通过跨骑约束(riding constraint)对位置进行精修。

[0084] 单晶单元晶胞参数针对测得的XPRD图案进行默认Reitveld精修得到了良好的拟合,没有无法解释的峰。

[0085] 变温X射线粉末衍射(VT-XRPD):通过Anton Paar CHC温度/湿度箱在通过Anton Paar TCU110温度控制单元进行的计算机控制下执行变温研究。

[0086] 一般来讲,在氮气流过照相机的情况下进行测量。使用了两个测量方案:受限和连续。在受限模式中,仅在CHC箱达到请求温度后才进行测量。在连续模式中,将样品以10℃/分钟加热,并随着温度的变化进行快速扫描。在两种情况下,在达到请求的温度后,将样品以35℃/分钟冷却,并在25℃进行缓慢扫描。从约3至30°或40°采集缓慢2θ扫描,步长为0.0080°,计数时间为100.97秒,这导致0.5°/min的扫描速率。从约3至30°2θ采集快速扫描,步长为0.0167°,计数时间为1.905秒,这导致约44°/min的扫描速率。

[0087] 所选的温度基于DSC结果。

[0088] 对于衍射仪设置,将10mm光束掩模、0.04弧度Soller狭缝以及固定的(1/4°)发散和防散射(1/8°)狭缝插到入射光束一侧上。将固定的5mm接收狭缝、0.04弧度的Soller狭缝和0.02mm的镍滤光片插到衍射光束一侧上。

[0089] 差示扫描热量法(DSC):热曲线使用在分析之前用铟校准的运行Pyris软件6.0版的Perkin-Elmer Sapphire DSC单元获得,该DSC单元配有自动进样器。称取1-10mg的固体样品加到20μL的铝质针孔样品盘中。然后将DSC单元用氮气吹扫并且将温度以10℃/min从0℃加热到270℃。将铟(T_m=156.6℃,ΔH_{FUS}=28.45J g^{-1})用于校准。

[0090] 调制式差示扫描量热法(MDSC):使用TA Q200调制DSC单元采集热曲线。称取5-20mg固体样品加到50μL铝针孔气密封盘中。然后将MDSC单元用氮气吹扫,并将温度以2℃/min从0℃加热至350℃,加热速率为2℃/min,在60秒周期内的调制幅度为+/-1℃。

[0091] 热重量质谱法(TGA/MS):使用由亚铝美(alumel)(95%镍、2%锰、2%铝和1%硅)、镍和草酸钙一水合物校准的运行Pyris软件6.0版的Perkin-Elmer Pyris 1TGA单元来获得热曲线。随着在用氦气以约50mL/min吹扫的炉中以10℃/min从25℃加热至250℃,对1-5mg

之间的TGA样品进行百分比重量损失的监测。为了同时跟踪在所研究的温度范围内气体分解产物的释放，将热天平连接到ThermoStar四极杆质谱仪(Asslar,Germany)。将气态分解产物引入到质谱仪中的传输管线是温度控制到200℃以避免可能的所释放气体的冷凝的去活化熔融石英毛细管(SGE Analytical science,熔融石英(100％甲基去活化),220mm OD,150mm ID,Australia)。以此方式，可以同时记录所选离子种类的质谱离子强度曲线和TGA重量损失。

[0092] 动态蒸汽吸附(DVS)：使用DVS-HT仪器(Surface Measurement Systems,London,UK)进行了GVS实验。该仪器使用质量分辨率为±0.1μg的记录超微量天平来在重量上测量蒸汽的吸收和损失。通过使用电子质量流量控制器混合饱和的干燥载气流来控制样品周围的蒸汽分压(±1.0％)。将期望的温度保持在±0.1℃。在该期望的温度下，将样品(1至10mg)置于DVS-HT和DVS-1仪器中。

[0093] 在40％RH和25℃下(典型的室内条件)加载和卸载样品。如下所列(给出1个完整循环的2次扫描)进行水分吸着等温线绘制。软件使用最小二乘法最小化程序以及质量松弛模型来预测渐进值。测得的质量平衡值在转到下一个％RH值之前必须在由软件预测的值的2％之内。将最小平衡时间设为1小时，最大平衡时间设为4小时。

[0094] 光学显微术：使用Olympus B60偏光显微镜来进行样品形态的显微观察。将样品悬于矿物油中并在观察之前用盖玻片压在载玻片上。使用FW-24(PAX CAM)照相机来采集图像。10x物镜加上来自显微镜光学器件的另外10x放大给出100x的总放大。使用PAX-it软件(6.2版)来捕获并分析图像。

[0095] 核磁共振光谱法(^{1}H-NMR)：通过^{1}H-NMR光谱法测定盐的化学计量，其中使用在针对每个样品进行了优化以得到可能最佳的光谱的条件下运行的Bruker DPX400仪器。将每个样品(2-4mg)溶于0.75mL DMSO-d6，并在薄壁玻璃管(4×14mm)中获得光谱。

[0096] 通过HPLC进行鉴定、分析和纯度测定

[0097] 设备：测试在经过校准和验证的名为LC-0430-AD或LC-418-1D的Agilent1200快速分离高效液相色谱(HPLC)系统上进行。系统包括二元SL泵、脱气器、具有级分收集器的高效自动进样器SL、具有双阀柱切换器的恒温柱温箱和DADSL检测器。所有标准溶液和样品均在A类玻璃容量瓶中配制并置于自动进样器小瓶中。使用经校准的Mettler分析天平进行标准称量。使用Eppendorf微量离心机对制备样进行离心。采集原始色谱数据，并使用Empower 2软件积分。将Microsoft Office Excel 2003用于计算结果。

[0098] 试剂：乙腈得自CCI。三氟乙酸得自EMD。HPLC级水(18MΩ·cm)得自位于实验室A211的实验室Barnstead Nanopure系统UPW-0403-AD。如之前所述制备化合物A和B。

[0099] 仪器参数：

[0100]

柱：Zorbax Eclipse XDB-C18，100×3.0 mm ID，1.8 μ 填充		
检测器：UV/vis @ 290 nm		
柱温：25℃		
流速：0.64 mL/min		
流动相 A：0.1%的 TFA 水溶液		
流动相 B：0.1% TFA 的 ACN 溶液		
梯度：		
时间（分钟）	流动相 A (%)	流动相 B (%)
0	75	25
10	55	45
12	5	95
13	5	95
13.1	75	25
16.7	75	25

[0101] 盐在40℃和75％湿度下的固态稳定性：称取待研究形式的样品(15-20mg)加到标准1.5mL HPLC小瓶(32×11.6mm)中，不加盖在40℃和75％RH的稳定箱中储存0、7、14和28天。在指定的天数取出样品并盖上。对每个时间点的样品通过纯度和分析测量法完成了XRPD、DSC、TGA和HPLC鉴定测量。

[0102] 水溶性估计：称取多份十毫克待研究的盐形式加到标准1.5mL HPLC小瓶(32×11.6mm)中。将搅拌棒和100μL水加到每只小瓶中。将样品盖上并搅拌5-10分钟。如果目测未得到透明溶液，则添加另外100-300μL部分的水并搅拌。重复该过程，直到样品溶解或直到添加了1000μL水。基于溶解已知重量的样品所必需的水的体积来估计溶解性。得自这些测量的结果在表11中给出。

[0103] 表1.通过缓慢冷却在丙酮中形成的具有一当量酸的盐的估计水溶性和HPLC分析

[0104]

样品	酸	估计的水溶性	测得的化合物 A，%	计算的二盐，%	计算的单盐，%
13-3	乙酸	50-100mg/mL	72.2	77.0	87.5
13-4	富马酸	<10 mg/mL	1.9		
13-5	乙醇酸	<10 mg/mL	72.0	73.2	84.5
13-6	L-苹果酸	>100mg/mL	68.3	61.0	75.8
13-7	磷酸	50-100mg/mL	5.9	68.4	81.2
13-8	L-焦谷氨酸	>100mg/mL	56.0	61.8	76.4
13-9	对甲苯磺酸	<10 mg/mL	42.7	54.9	70.8
13-10	盐酸	10-20mg/mL	39.8	85.1	92.0

[0105] 实施例1.通过成熟在丙酮中形成具有两当量酸的盐

[0106] 在五只20mL闪烁小瓶中的每一只的15mL丙酮中，将200mg化合物A(0.478毫摩尔)通过温热和搅拌而溶解。将1.95当量的乙酸、乙醇酸、L-苹果酸或L苹果酸(1当量，0.48毫摩尔)加到透明的化合物A溶液中。添加完这些酸后，透明溶液就变浑浊且开始结晶。使小瓶在HEL单元上接受两个成熟循环。每个成熟循环包括在一小时的时间段内加热到50℃，在50℃保持四小时，在一小时的时间段内冷却到5℃，并在5℃保持四小时。通过抽吸过滤而分离固体，将固体在50℃和清扫真空(house vacuum)(～200mm)下干燥过夜得到黄色固体。结果在表2中给出。

[0107] 表2

[0108]

样品	酸	XRPD	DSC,℃	TGA,%	估计的水溶性
39-1(2)	乙酸	$A_{1.5}$	185.2	24.4	～25mg/mL
39-2(2)	乙醇酸	A_1	68.9,205.4	4.8	>100mg/mL
39-3(2)	L-苹果酸	A_1	186.4	3.6	>100mg/mL
39-5(2)	L-苹果酸(1当量)	A_1+C_0	186.5	1.0	>100mg/mL

[0109] 实施例2.使用快速冷却在丙酮中进行酸筛选(两当量)

[0110] 向七只容纳有搅拌棒和1.5mL化合物A溶液(13.3mg/mL)的HPLC小瓶中,称取将得到两当量(0.096毫摩尔)的酸量,或通过移液器添加。将样品盖上并加热到沸点,然后在2-8℃的冰箱中冷却过夜。通过抽吸过滤而分离固体,将固体在50℃和清扫真空(～200mm)下干燥过夜得到黄色固体。结果在表3中给出。

[0111] 表3

[0112]

样品	酸	XRPD	DSC，℃	TGA，%	估计的水溶性
31-1	乙酸	$A_{1.5}$	181.3	22.6	~25 mg/mL
31-2	乙醇酸	A_1	205.4	4.8	>100 mg/mL

[0113]

31-3	L-苹果酸	$A_{1.5}$	160.4	3.6	>100 mg/mL
31-4	L-焦谷氨酸	A_1	196.4	4.4	>100 mg/mL
31-5	L-苹果酸（1 当量）	C_0	206.4	2.7	~25 mg/mL

[0114] 实施例3.通过浆液转化在丙酮中形成具有两当量酸的盐

[0115] 在五只具有18mL丙酮的20mL玻璃闪烁小瓶的每一只中,将400mg化合物A(0.956毫摩尔)温热并搅拌而浆液化。将两当量的乙酸、乙醇酸、L-苹果酸、L-焦谷氨酸或L-苹果酸(1当量,0.956毫摩尔)加到每只小瓶中的化合物A悬浮液中。将这些混合物盖上并温热至接近沸点。在所有情况下,均注意到厚重的黄色固体。使样品在试验台上冷却至环境温度,然后在2-8℃的冰箱中冷却过夜。通过抽吸过滤而分离固体,将产物在50℃和清扫真空(～200mm)下干燥过夜得到黄色固体。结果在表4中给出。

[0116] 表4

[0117]

样品	酸	XRPD	DSC,℃	TGA,%	估计的水溶性
39-1	乙酸	$A_{1.5}$	185.4,分裂峰	2.1	～50mg/mL
39-2	乙醇酸	A_1	77.4,209.0	1.9	<10mg/mL
39-3	L-苹果酸	A_1	193.3	3.6	>100mg/mL
39-4	L-焦谷氨酸	A_1	50.4,198.2	3.5	>100mg/mL
39-5	L-苹果酸(1当量)	A_1+C_0	192.2	1.0	>100mg/mL

[0118] 实施例4.在丙酮中进行酸筛选(两当量)-成熟

[0119] 通过在磁力搅拌棒搅拌下温热,在18mL丙酮中溶解240mg化合物A(0.574毫摩尔)。将该溶液等量分配到12只1.5mL HPLC小瓶中。

[0120] 向5只容纳有化合物A溶液的等分试样和搅拌棒的小瓶的每一只中,称取将得到两

当量(0.096毫摩尔)的酸量,或通过移液器添加。将样品盖上,并使样品在HEL单元上接受两个成熟循环。每个成熟循环包括在一小时的时间段内加热到50℃,在50℃保持四小时,在一小时的时间段内冷却到5℃,并在5℃保持四小时。通过抽吸过滤而分离固体,将固体在50℃和清扫真空(~200mm)下干燥过夜得到黄色固体。结果在表5中给出。

[0121] 表5

[0122]

样品	酸	XRPD	DSC,℃	TGA,%	估计的水溶性
30-1	乙酸	$A_{1,5}$	187.7,334.1	21.7	~20mg/mL
30-2	乙醇酸	A_1	206.6	3.2	>100mg/mL
30-3	L-苹果酸	A_1	190.2	1.5	>100mg/mL
30-4	L-焦谷氨酸	A_1	197.5	1.8	>100mg/mL
30-5	L-苹果酸(1当量)	C_0	207.3	2.2	~25mg/mL

[0123] 实施例5.丙酮中一当量-缓慢冷却

[0124] 在12mL丙酮中配制240mg化合物A(0.57毫摩尔)的溶液,并在搅拌下温热以溶解。十二个该溶液的均等等分试样将在每只小瓶中的1mL丙酮中将得到20mg(0.0478毫摩尔)化合物A。称取对应于1.05当量(0.06毫摩尔)酸的酸重量加到12只1.5mL HPLC小瓶中,或如果为液体则通过移液器添加。向每只小瓶中,添加化合物A的一个等分式样。将小瓶盖上并在搅拌下温热以混合,然后在HEL单元上接受2个缓慢冷却循环。HEL单元上的每个缓慢冷却循环包括:在1小时的时间段内加热到80℃,在80℃下保持1小时,然后在5小时的时间段内冷却到5℃,并在5℃下保持16-18小时。通过抽吸过滤而分离固体,将样品在50℃和清扫真空(~200mm)下干燥过夜。结果在表6中给出。

[0125] 表6

[0126]

样品	酸	DSC ℃	TGA%
1	乙酸	171.6	9.9
2	L-天冬氨酸	145.8, 191.2, 219.8, 240.5, 258.5	1.3
3	乙磺酸	61.2, 193.6, EXO 199.8, 258.7	0.2
4	富马酸	177.1	0.4
5	乙醇酸	207.0	0.4
6	L-苹果酸	63.1, 198.6	1.5
7	磷酸	54.4	3.6
8	L-焦谷氨酸	199.6	0.4
9	硫酸 (0.5 当量)	69.5, 201.0	3.7
10	L-酒石酸	66.0, 162.4	3.2
11	对甲苯磺酸	205.9	0.3
12	盐酸(EtOH)	67.0, 234.3	0.9

[0127] *EXO=放热

[0128] 实施例6.制备抗坏血酸盐

[0129] 称取200mg化合物A(0.478毫摩尔)在搅拌棒搅拌下加到20mL玻璃闪烁小瓶中,然后添加88.4mg(0.503毫摩尔,1.05当量)抗坏血酸(J.T.Baker,无水,批号B36597)。通过移液器添加2.5ml 2,2,2-三氟乙醇,并将样品温热。使所形成的浆液在HEL单元上接受2个缓慢冷却循环。HEL单元上的每个缓慢冷却循环包括:在1小时的时间段内加热到80℃,在80℃

下保持1小时，然后在5小时的时间段内冷却到5℃，并在5℃下保持16-18小时。通过抽吸过滤而分离固体，将样品在50℃和清扫真空(～200mm)下干燥过夜得到142mg黄色固体(49％收率)。通过HPLC分析结晶产物，得到96.2％的化合物B和0.8％的化合物A。化合物B盐的结构通过^{1}H-NMR确认。

[0130] 化合物A游离碱形式A_0

[0131] XRPD

[0132] XRPD在图1中描绘。

[0133] 热分析

[0134] 热数据在图2中描绘。

[0135] 化合物A乙酸盐形式$A_{1.5}$

[0136] 制备

[0137] 根据实施例1中的程序制备盐。

[0138] XRPD

[0139] 乙酸盐形式$A_{1.5}$的X射线衍射数据在图3和表7中给出。以请求模式(165℃和200℃)进行的变温XRPD测量显示出形式上的两个变化-从乙酸盐到形式B_0，然后转化成形式A_0。在连续模式中，使用从5.5°至11.5°的一分钟扫描和1℃/分钟温度斜坡，注意到形式上的三个变化：乙酸盐到游离碱B_0、B_0到A_0以及A_0到无定形(图4)。乙酸盐在从91℃至130℃的温度范围内缓慢转化成游离碱形式B_0。形式在197℃与200℃之间从B_0变成A_0(图5)。

[0140] 表7.乙酸盐形式$A_{1.5}$的XRPD峰

[0141]

编号	位置 [2θ°]*	晶面间距[Å]	相对强度[%]		编号	位置 [2θ°]*	晶面间距[Å]	相对 强度[%]
1	**6.41**	**13.777**	**100**		15	21.11	4.205	1
2	9.21	9.599	6		16	21.30	4.169	2
3	12.42	7.123	1		17	21.53	4.124	3
4	12.71	6.961	4		18	21.70	4.092	1
5	13.02	6.796	4		19	23.10	3.847	3
6	13.22	6.694	1		20	23.90	3.720	1
7	14.72	6.012	1		21	24.07	3.694	2
8	15.22	5.817	2		22	24.18	3.678	2
9	17.41	5.089	2		23	24.33	3.655	1
10	18.00	4.924	1		24	25.50	3.490	1
11	18.36	4.828	2		25	26.09	3.412	1
12	18.47	4.799	1		26	26.21	3.397	1
13	19.02	4.661	6		27	28.15	3.167	2
14	19.26	4.605	5		28	28.25	3.157	1

[0142] *使用ZBG或玻璃板通常引入正样品高度位移并导致2θ值的小(0.05°至0.2°)偏移。最高的峰(强度100％)以黑体字母示出。

[0143] 热分析

[0144] 乙酸盐形式$A_{1.5}$的DSC曲线显示出在185.4℃处存在一个吸热/降解峰，ΔH_{Fus}为172.0J/g(图6)。乙酸盐在25与150℃之间具有29.5％的重量损失。

[0145] 吸水

[0146] 图7中的DVS图线表明样品似乎从开始就饱和。在干燥曲线中存在稳定的重量损失，未达到平衡。对于每个循环，将样品在0％RH下干燥4小时。运行了4个循环，显示出连续的重量损失。在另一DVS单元上重复实验，显示出类似的结果。

[0147] ^{1}H-NMR光谱

[0148] ^{1}H-NMR光谱显示出化合物A预期的所有峰。将在约7.5ppm处的峰归一化到预期在该区域中吸收的一个芳族质子。与化合物相关的其余峰然后遵循正确的比率。对于乙酸盐，预期仅有一个在1.9-2.0ppm处的峰。该峰应该集成了3个质子。相反，其显示出约4.5个质子，每个化合物A分子约1.5个乙酸分子。

[0149] 稳定性

[0150] 表8中给出了乙酸盐形式$A_{1.5}$在40℃和75％RH下老化的数据。XRPD在整个28天的测试期中发生变化。TGA和化合物A分析值可能反映乙酸的损失，如在上述热和XRPD研究中所见。DSC、HPLC纯度和化合物B分析在研究中相对恒定。单乙酸盐应分析为87.5％的化合物A。二乙酸盐应分析为77.7％的化合物A。表8中的值表明盐随着老化而改变组成。^{1}H-NMR测得每分子化合物A具有1.5分子乙酸。XRPD图案显示出水合物化合物A游离碱形式H_d的峰。可能的是，随着样品老化，过量的乙酸挥发。乙酸的挥发性和变化的XRPD图案表明要选择另一种候选物。

[0151] 表8.乙酸盐形式$A_{1.5}$在40℃和75％RH下的稳定性

[0152]

天	XRPD	DSC，℃	TGA，%	化合物A分析，%	化合物B分析，%	HPLC纯度，%
0	$A_{1.5}$	54.7, 180.3 分裂峰	21.5	78.1	0.2	99.7
7	显示水合物形成	117.4° 179.9	20.0	70.2	0.1	99.6
14	显示水合物形成	132.6, 181.5	16.1	84.2	0.2	99.5
28	显示水合物 H_d 形成	126.4, 163.6, 197.9	9.6	90.9	0.3	99.6

[0153] 光学显微术

[0154] 如图8中所示的样品展示出不规则形状的晶体的团聚体。样品在平面偏振光下显示出双折射。

[0155] 化合物A乙醇酸盐水合物形式A_1

[0156] 制备

[0157] 根据实施例1制备盐。

[0158] XRPD

[0159] 乙醇酸水合盐形式A_1的X射线衍射数据在图9和表9中给出。变温XRPD测量的重叠图扫描在图10中示出。初始XRPD图案与乙醇酸盐水合物形式A_1进行比较。在暴露于干燥N_2气氛后无变化。在175℃下的一个小时缓慢扫描测量期间，图案发生变化。在从175℃加热至225℃后，峰强度增加。未与已知的化合物A游离碱图案进行比较。在测量结束时板上的样品

为深棕色粉末，其并无发生熔化的外观。在加热到175℃和225℃后观察到的图案与化合物B进行部分比较。这与显示出在130℃后变化并在205℃时熔化的DSC相符。VT-XRPD和DSC均与乙醇酸损失且转化成化合物B相符。

[0160] 表9.乙醇酸水合盐形式A_1的XRPD峰

[0161]

位置 [°2θ]	计算的位置	h	k	l	晶面间距[Å]	高度[cts]	相对 强度[%]
8.12	8.13	0	0	1	10.8850	781	8.7
8.24	8.25	0	1	0	10.7261	5010	55.9
8.68	8.69	0	1	1	10.1821	6898	77.0
11.96	11.98	1	1	1	7.3925	501	5.6
13.62	13.63	1	1	0	6.4987	275	3.1
13.90	13.91	0	1	-1	6.3683	4729	52.8
14.62	14.63	1	0	-1	6.0549	581	6.5
14.68	14.70	0	1	2	6.0279	692	7.7
14.89	14.90	0	2	1	5.9468	456	5.1
16.29	16.30	0	0	2	5.4374	321	3.6
17.42	17.44	0	2	2	5.0866	3502	39.1
17.59	17.61	1	2	1	5.0367	994	11.1
18.20	18.22	1	-2	-1	4.8706	557	6.2
18.48	18.50	1	2	2	4.7970	927	10.3
18.98	18.99	2	0	1	4.6728	252	2.8
19.84	19.85	2	0	0	4.4719	328	3.7
20.23	20.24	2	1	1	4.3864	1426	15.9

[0162]

位置 [°2θ]	计算的位置	h	k	l	晶面间距[Å]	高度[cts]	相对 强度[%]
20.58	20.59	2	-1	0	4.3131	1969	22.0
21.21	21.22	2	-1	1	4.1864	3681	41.1
21.30	21.32	0	1	-2	4.1681	1097	12.2
21.44	21.46	1	1	3	4.1409	926	10.3
21.48	21.49	2	0	2	4.1337	2196	24.5
21.54	21.56	1	-2	-2	4.1216	273	3.0
21.66	21.68	1	-2	1	4.0988	240	2.7
22.82	22.84	0	2	3	3.8938	297	3.3
23.04	23.06	0	3	2	3.8571	2250	25.1
23.07	23.08	2	-1	-1	3.8523	1182	13.2
23.71	23.73	2	0	-1	3.7491	239	2.7
24.45	24.47	2	2	1	3.6373	464	5.2
24.73	24.75	2	-1	2	3.5969	8960	100.0
25.95	25.96	1	-3	-2	3.4310	312	3.5
26.07	26.09	2	-2	1	3.4148	209	2.3
26.27	26.28	0	3	3	3.3900	267	3.0
26.41	26.43	1	3	3	3.3716	308	3.4
27.08	27.09	2	1	-1	3.2907	249	2.8
27.90	27.92	2	-1	-2	3.1952	271	3.0
27.96	27.98	1	3	0	3.1881	219	2.4
28.53	28.55	1	2	4	3.1260	206	2.3
29.96	29.97	3	0	0	2.9805	486	5.4
30.05	30.06	0	4	2	2.9718	224	2.5
30.08	30.10	2	-2	2	2.9682	1322	14.7
30.13	30.14	3	-1	0	2.9639	546	6.1
30.21	30.23	2	-1	3	2.9557	1534	17.1
31.57	31.58	3	-1	2	2.8318	240	2.7
32.01	32.03	3	2	2	2.7934	298	3.3
32.76	32.77	1	4	1	2.7319	202	2.3
33.11	33.12	3	2	1	2.7038	276	3.1
33.51	33.53	3	0	-1	2.6721	371	4.1
34.01	34.02	2	-2	-3	2.6343	249	2.8
37.51	37.52	0	1	-4	2.3960	240	2.7

[0163] *使用ZBG或玻璃板通常引入正样品高度位移并导致2θ值的小(0.05°至0.2°)偏移。最高的峰(强度100%)以黑体字母示出。

[0164] 单晶结构

[0165] 单晶X射线结构确认了存在乙醇酸根阴离子,并表明哌嗪氮原子携带氢原子。分子在图38中示出。结构还显示以60%的占比存在的水分子,也就是说,化合物A与水的比率为1:0.6。结构细节在下表中给出。

[0166]

变量	**值**	
系统		三斜晶系
空间群		P-1
温度(°K)	90.0(2)	298(3)
a, Å	9.3613(2)	9.3957(5)
b, Å	11.8453(2)	11.9911(8)
c, Å	12.4918(2)	12.6433(8)
α	64.9920(1)	65.2827(2)
β	73.2080(1)	73.0954(1)
γ	88.2480(1)	88.7671(1)
体积, $Å^3$	1195.08(4)	1229.8
密度, g/ml		1.404
λ, Å		1.54178
μ, mm^{-1}		0.846
吸收校正法		多重扫瞄
吸收校正最小值		0.781
吸收校正最大值		0.963
反射(总计)		16031
反射(唯一)		4237
反射(观测值,>2σ)		3388
$R_{合并}$(内部符合)		0.043
R		0.0409
wR		0.1043
最小剩余密度, e^-/mm^3		0.31(5)
最大剩余密度, e^-/mm^3		-0.20(5)

[0167] 化合物A乙醇酸盐水合物的非氢原子的分数坐标和各向同性位移参数见下。

[0168]

原子	x/a	y/b	z/c	Ueq 或 Uiso
N(1)	-257(2)	-899(1)	12193(1)	20(1)
N(2)	5139(2)	694(1)	7829(1)	20(1)
N(3)	6756(2)	2109(1)	5718(1)	19(1)

[0169]

原子	x/a	y/b	z/c	Ueq 或 Uiso
N(4)	6028(2)	3909(1)	3603(1)	20(1)
O(1)	3205(2)	2569(1)	10538(1)	28(1)
O(2)	4938(2)	2063(1)	8709(1)	29(1)
O(3)	4772(1)	-997(1)	7440(1)	24(1)
C(1)	125(2)	99(2)	12375(2)	19(1)
C(2)	-591(2)	359(2)	13379(2)	24(1)
C(3)	17(2)	1385(2)	13408(2)	26(1)
C(4)	1276(2)	2140(2)	12470(2)	25(1)
C(5)	1979(2)	1871(2)	11474(2)	21(1)
C(6)	1426(2)	814(2)	11409(2)	18(1)
C(7)	1877(2)	171(2)	10607(2)	18(1)
C(8)	3033(2)	251(2)	9554(2)	18(1)
C(9)	3028(2)	-663(2)	9123(2)	18(1)
C(10)	1928(2)	-1682(2)	9680(2)	18(1)
C(11)	1733(2)	-2727(2)	9343(2)	21(1)
C(12)	438(2)	-3632(2)	10444(2)	32(1)
C(13)	-315(2)	-2918(2)	11209(2)	22(1)
C(14)	786(2)	-1790(2)	10718(2)	18(1)
C(15)	769(2)	-890(2)	11162(2)	18(1)
C(16)	3936(2)	3508(2)	10681(2)	29(1)
C(17)	4427(2)	1141(2)	8708(2)	20(1)
C(18)	4362(2)	-404(2)	8046(2)	19(1)
C(19)	6654(2)	1170(2)	6943(2)	20(1)
C(20)	6273(2)	3305(2)	5683(2)	19(1)
C(21)	6719(2)	4290(2)	4353(2)	20(1)
C(22)	6426(2)	2644(2)	3709(2)	24(1)
C(23)	6001(2)	1698(2)	5052(2)	21(1)
C(24)	6476(2)	4852(2)	2287(2)	25(1)
C(1G)	539(2)	3469(2)	4989(2)	28(1)
O(1G)	335(2)	4218(1)	3828(1)	36(1)
C(2G)	2165(2)	3395(2)	4961(2)	22(1)
O(2G)	3132(1)	4059(1)	3938(1)	28(1)
O(3G)	2455(1)	2720(1)	5939(1)	26(1)
O(1W)	2887(3)	5938(2)	1816(2)	33(1)

[0170] 化合物A乙醇酸盐水合物的氢原子的分数坐标和各向同性位移参数见下。

[0171]

原子	x/a	y/b	z/c	Ueq 或 Uiso
H(1N)	-1000(20)	-1530(20)	12750(20)	24

[0172]

原子	x/a	y/b	z/c	Ueq 或 Uiso
H(4N)	4940(30)	3842(19)	3953(19)	23
H(2)	-1457	-148	14013	29
H(3)	-433	1583	14085	31
H(4)	1659	2849	12512	30
H(11A)	2661	-3146	9246	26
H(11B)	1469	-2413	8561	26
H(12A)	830	-4388	10960	38
H(12B)	-296	-3897	10139	38
H(13A)	-1292	-2670	11078	26
H(13B)	-472	-3436	12105	26
H(16A)	3290	4181	10650	44
H(16B)	4885	3850	10010	44
H(16C)	4137	3140	11482	44
H(19A)	7229	1522	7305	24
H(19B)	7157	450	6862	24
H(20A)	6749	3560	6170	23
H(20B)	5171	3219	6054	23
H(21A)	6384	5100	4325	24
H(21B)	7825	4402	3996	24
H(22A)	7518	2687	3319	28
H(22B)	5895	2376	3262	28
H(23A)	4900	1613	5432	25
H(23B)	6297	871	5108	25
H(24A)	6170	5666	2242	38
H(24B)	5986	4590	1822	38
H(24C)	7567	4923	1929	38
H(1G1)	58	2611	5299	33
H(1G2)	21	3808	5583	33
H(1G)	1112	4714	3360	53
H(1W)	3200(50)	5350(40)	2430(40)	42(11)
H(2W)	3340(60)	6690(40)	1640(40)	70(16)

[0173] 热分析

[0174] 乙醇酸水合盐形式A_1的DSC曲线显示存在两个不同的吸热峰：一个在77.4℃处，ΔH_{Fus}为63.4J/g；第二个峰在209.0℃处，ΔH_{Fus}为170.9J/g(图11)。乙醇酸水合盐在25与150℃之间具有1.9％的重量损失。

[0175] 吸水

[0176] 图12中的DVS图线表明在整个RH范围内存在表面吸附，而体吸收有限。在90％RH下总的水分吸收为～3.5％。

[0177] ^{1}H-NMR光谱

[0178] 光谱给出化合物A所有必要的峰。在将积分归一化到化合物A在约7.5ppm处的芳族区中的一个质子后，在约3.9ppm处存在一个双质子单重峰，其对应于与乙醇酸的亚甲基基团相关的两个质子。这表明盐中化合物A与乙醇酸的摩尔比为1:1。

[0179] 稳定性

[0180] 表10中给出的数据表明该盐对测试条件相当稳定。在28天后注意到化合物B中的适度增加。如^{1}H-NMR所表明，单乙醇酸盐应具有84.5％化合物A的化合物A分析结果。TGA中增加的损失表明含水量的增加，例如，对于1:1的水与化合物A比率，预期将有3.5％的损失。

[0181] 表10.乙醇酸盐水合物形式A_1在40℃和75％RH下的稳定性

[0182]

天	XRPD	DSC,℃	TGA，%	化合物A分析，%	化合物B分析，%	HPLC纯度，%
0	A1	69.7, 207.9	2.1	69.9	0.1	99.8
7	不变	208.3	2.3	68.4	0.1	99.6
14	不变	68.8, 207.3	2.6	73.2	0.2	99.7
28	不变	207.4	3.5	66.8	0.6	99.5

[0183] 光学显微术

[0184] 在图13中，样品展示出单独的晶体和晶体的团聚体。样品在平面偏振光下显示出双折射。

[0185] 化合物A L-苹果酸盐形式A_1

[0186] 制备

[0187] 根据实施例1制备盐。

[0188] XRPD

[0189] 苹果酸盐形式A_1的X射线衍射数据在图14和表11中给出。VT-XRPD研究的重叠图缓慢扫描在图15中示出。

[0190] 初始XRPD图案如预期一样。在暴露于干燥N2气氛后形式上无变化(图15)。当将样品在175℃下保持一小时时，存在变化。在首次达到175℃时进行的快速扫描与开始图案进行比较。在175℃后进行的快速扫描中，结晶几乎完全消失。在加热到175℃并冷却到25℃后该样品所观察到的缓慢扫描图案与化合物B的图案进行部分比较。该观察结果与化合物B的热分解相符。

[0191] 表11.苹果酸盐形式A_1的XRPD峰

[0192]

编号	位置 [2θ°]*	晶面间距[Å]	相对 强度[%]		编号	位置 [2θ°]*	晶面间距[Å]	相对 强度[%]
1	8.60	10.269	51		21	21.22	4.184	53
2	9.18	9.631	25		22	21.59	4.112	3
3	10.06	8.789	36		**23**	**22.36**	**3.972**	**100**
4	10.40	8.496	25		24	23.45	3.791	17
5	11.74	7.529	14		25	24.08	3.692	2
6	11.87	7.450	27		26	24.27	3.664	10
7	12.85	6.885	3		27	24.52	3.627	3
8	13.33	6.635	6		28	24.99	3.560	2
9	13.97	6.334	5		29	25.76	3.455	3
10	14.46	6.120	6		30	25.87	3.442	3
11	14.70	6.021	18		31	26.99	3.301	15
12	15.27	5.797	12		32	27.38	3.254	3
13	15.56	5.690	9		33	27.79	3.208	3
14	17.19	5.156	47		34	27.96	3.188	4
15	17.76	4.991	17		35	28.12	3.171	2
16	17.98	4.930	5		36	29.11	3.066	4
17	18.54	4.781	28		37	29.60	3.016	2
18	19.29	4.597	5		38	30.22	2.955	2
19	20.27	4.376	14		39	30.42	2.936	3
20	20.65	4.297	9		40	30.75	2.905	5

[0193] *使用ZBG或玻璃板通常引入正样品高度位移并导致2θ值的小(0.05°至0.2°)偏移。最高的峰(强度100%)以黑体字母示出。

[0194] 热分析

[0195] 苹果酸盐形式A_1的DSC曲线显示出在186.4℃处存在一个吸热峰，ΔH_{Fus}为75.7J/g(图16)。马来酸盐在25与150℃之间具有1.0%的重量损失。

[0196] 吸水

[0197] 图17中的DVS图线表明在从40%RH至70%RH的第一轮循环中存在极少的吸水。仅发生表面吸附。在80%RH下，吸水增加。由于体吸收存在大的滞后间隙(hysteresis gap)。总吸收为～2%。等温线不可逆。

[0198] ^{1}H-NMR光谱

[0199] 存在化合物A预期的所有峰。在7.5ppm处的一个芳族质子的归一化后，在约4.05ppm处存在一个单质子三重峰，与L-苹果酸一致。这确立了呈形式A_1的化合物AL-苹果酸盐的1:1化学计量。

[0200] 稳定性

[0201] 表12中的数据显示，L-苹果酸盐对测试条件稳定，具有恒定的XRPD、DSC、TGA和HPLC纯度值(MJJ3331-49)。在28天后观察到化合物B中的增加。与乙醇酸水合盐一样，化合物A的L-苹果酸盐分析值低于75.8%的预期值。

[0202] 表12.L-苹果酸盐形式A_1在40℃和75％RH下的稳定性

[0203]

天	XRPD	DSC	TGA	化合物A分析	化合物B分析	HPLC纯度
0	A_1	193.0℃	0.1%	69.9%	0.2%	99.5%
7	不变	192.0℃	0.2%	71.8%	0.4%	99.3%
14	不变	191.4℃	0.8%	72.0%	0.5%	98.8%
28	不变	191.1℃	0.3%	71.7%	0.8%	98.4%

[0204] 光学显微术

[0205] 在图18中，样品显示出单独的晶体和不规则形状的晶体的团聚体。样品在平面偏振光下显示出双折射。

[0206] 化合物A L-苹果酸盐形式$A_{1.5}$

[0207] 制备

[0208] 根据实施例2制备盐。

[0209] XRPD

[0210] 苹果酸盐形式$A_{1.5}$的X射线衍射数据在图19和表13中给出。

[0211] 表13.苹果酸盐形式$A_{1.5}$的XRPD峰

[0212]

编号	位置 [2θ°]*	晶面间距[Å]	相对 强度[%]		编号	位置 [2θ°]*	晶面间距[Å]	相对 强度[%]
1	5.53	15.978	63		21	20.16	4.401	16
2	6.80	12.985	53		22	20.53	4.322	15
3	7.97	11.085	26		23	21.13	4.201	20
4	**8.43**	**10.478**	**100**		24	21.37	4.154	11
5	8.76	10.084	35		25	21.86	4.063	20
6	9.23	9.577	23		26	22.84	3.890	10
7	11.79	7.500	28		27	23.14	3.841	24
8	12.44	7.108	10		28	23.63	3.762	14
9	12.78	6.923	17		29	24.04	3.698	10
10	13.05	6.778	17		30	24.60	3.615	29
11	13.64	6.489	15		31	25.16	3.536	13
12	13.92	6.355	11		32	25.66	3.469	9
13	14.44	6.131	61		33	28.20	3.162	7
14	15.99	5.538	44		34	29.00	3.076	3
15	16.66	5.316	72		35	30.05	2.971	5
16	17.12	5.175	7		36	30.43	2.936	6
17	18.12	4.891	31		37	32.25	2.774	2
18	18.46	4.802	40		38	33.11	2.704	2

[0213]

编号	位置 [2θ°]*	晶面间距[Å]	相对 强度[%]		编号	位置 [2θ°]*	晶面间距[Å]	相对 强度[%]
19	18.79	4.720	7		39	36.66	2.449	3
20	19.44	4.562	17		40	39.38	2.286	3

[0214] *使用ZBG或玻璃板通常引入正样品高度位移并导致2θ值的小(0.05°至0.2°)偏移。最高的峰(强度100%)以黑体字母示出。

[0215] 热分析

[0216] L-苹果酸盐形式$A_{1.5}$的DSC曲线显示出在160.4℃处存在一个吸热峰，ΔH_{Fus}为39.2J/g(图20)。L-苹果酸盐在25与150℃之间具有3.6%的重量损失。该形式在低得多的温度下熔化并具有比苹果酸盐形式A_1更大的重量损失。

[0217] ^{1}H-NMR光谱

[0218] L-苹果酸盐形式$A_{1.5}$的^{1}H-NMR光谱表明存在化合物A的所有峰，并且归一化积分表明两分子的化合物A存在约3分子的L-苹果酸。该制备代表了化合物AL-苹果酸盐的新形式。

[0219] 化合物A L-焦谷氨酸盐形式A_1

[0220] 制备

[0221] 根据实施例3制备盐。

[0222] XRPD

[0223] L-焦谷氨酸盐形式A_1的X射线衍射数据在表14和图21中给出。XRPD图案表明高度结晶的固体。

[0224] 变温XRPD测量结果在图22中示出。初始XRPD图案如预期一样。在加热到175℃后形式上无变化。在实验结束时，将黑色玻璃留在ZBG板上。对化合物B的预期图案与加热到210℃后的样品进行比较显示出小的差异。这表明化合物A转化成了化合物B和可能的第二组分。

[0225] 表14.L-焦谷氨酸盐形式A_1的XRPD峰

[0226]

编号	位置 [2θ°]*	晶面间距[Å]	相对 强度[%]		编号	位置 [2θ°]*	晶面间距[Å]	相对 强度[%]
1	6.02	14.669	74		21	20.98	4.231	34
2	9.56	9.242	43		22	21.14	4.199	29
3	10.31	8.573	61		23	21.36	4.156	9
4	10.54	8.391	25		24	21.67	4.097	10
5	11.03	8.017	96		25	21.96	4.045	33
6	**12.01**	**7.364**	**100**		26	22.11	4.017	23
7	12.89	6.864	21		27	22.70	3.914	21
8	13.22	6.693	33		28	23.13	3.842	23

[0227]

编号	位 置 [2θ°]*	晶面间距 [Å]	相对 强度 [%]		编号	位 置 [2θ°]*	晶面间距[Å]	相 对 强 度 [%]
9	14.32	6.180	12		29	23.39	3.800	84
10	15.00	5.900	24		30	23.51	3.781	56
11	16.71	5.301	36		31	24.11	3.689	14
12	17.02	5.206	22		32	24.53	3.626	8
13	17.51	5.061	59		33	24.84	3.582	54
14	17.79	4.983	68		34	25.08	3.547	9
15	18.02	4.919	78		35	26.56	3.353	33
16	18.68	4.747	19		36	27.57	3.232	8
17	18.98	4.672	29		37	28.15	3.168	13
18	19.37	4.578	7		38	28.78	3.099	9
19	20.22	4.388	7		39	30.22	2.955	11
20	20.76	4.276	35		40	30.43	2.935	9

[0228] *使用ZBG或玻璃板通常引入正样品高度位移并导致2θ值的小(0.05°至0.2°)偏移。最高的峰(强度100%)以黑体字母示出。

[0229] 热分析

[0230] L-焦谷氨酸盐形式A_1的DSC曲线显示存在两个吸热峰:一个在50.4℃处,ΔH_{Fus}为35.6J/g,一个在198.2℃处,ΔH_{Fu}为76.8J/g(图23)。焦谷氨酸盐在25与150℃之间具有3.5%的重量损失。

[0231] 吸水

[0232] 在DVS图线(图24)中,表明在第一个循环中,在40-75%的RH范围内存在极少的吸水(~2%)。仅发生表面吸附。在80%RH下,存在大量的吸水。在50-90%RH下的大的滞后间隙是由于体吸收而可能形成了水合物。总吸收为~27%。

[0233] ^{1}H-NMR光谱

[0234] 存在化合物A的所有峰。在将积分归一化到化合物A在约7.5ppm处的芳族峰中的一个质子后,在约7.85ppm处存在另外一个单质子单重峰,其对应于焦谷氨酸中的酰胺氮上的氢原子。此外,在约4.05ppm处存在另外一个单质子多重峰,其来自附连到与羧酸基团相邻的碳原子上的一个氢原子。这确立了该盐为化合物A的单L-焦谷氨酸盐。

[0235] 稳定性

[0236] 该盐在28天的测试期中稳定,但化合物B含量缓慢增加(表15)。

[0237] 表15.L-焦谷氨酸盐形式A_1(用两当量的酸制备)在40℃和75%RH下的稳定性

[0238]

天	XRPD	DSC,	TGA, %	化合物 A 分析, %	化合物 B 分析, %	HPLC 纯度, %
0	A_1	198.2	0.49	65.5	0.6	98.6
7	不变	199.0	0.54	71.4	0.6	98.7
14	不变	198.3	0.64	60.2	0.8	98.2
28	不变	198.4	0..11	64.0	1.2	97.2

[0239] 光学显微术

[0240] 如图25中所示，样品展示出不规则形状的晶体的团聚体。样品在平面偏振光下显示出双折射。

[0241] 盐的比较

[0242] 在表16中，比较了乙醇酸盐水合物形式A_1、L-苹果酸盐形式A_1以及L-焦谷氨酸盐形式A_1的一当量和两当量制备物。乙醇酸水合盐形式A_1在40℃和75％RH稳定性测试期间生成了最少量的化合物B。乙醇酸盐水合物表现出偏向于吸水，因为在稳定性测试期间TGA值增至3.5％(表10)。

[0243] 表16.化合物A盐的比较

[0244]

属性	乙醇酸盐（2 当量）	L-苹果酸盐（2 当量）	L-焦谷氨酸盐（2 当量）	L-焦谷氨酸盐（1 当量）
结晶度	形式 A_1	形式 A_1	形式 A_1	形式 A_1
DSC	69.7, 207.9	193.0	198.2	201.7
TGA	2.1%	0.1%	0.5%	0.2%
DVS	可逆	不可逆	不可逆	未测量
40/75 后的 TGA：				
初始化合物 A	69.9%	71.3%	65.5%	75.5%
初始化合物 B	0.1%	0.2%	0.6%	0.5%
40/75 后的化合物 B	0.6%	1.2%	1.2%	1.3%
估计的 水溶性	>100 mg/mL	>100 mg/mL	>100 mg/mL	>100 mg/mL
盐形式的活性剂%	85%	76%	76%	76%
需要干燥剂	是	是	是	是
酸分类	1 类	1 类	2 类	2 类

[0245] 化合物A游离碱形式C_0

[0246] 制备

[0247] 根据实例4制备游离碱。

[0248] XRPD

[0249] 游离碱形式C_0的X射线衍射数据在图26和表17中给出。XRPD图案显示出结晶固体。

[0250] 变温XRPD测量结果在图27中示出。初始XRPD图案与形式C_0的预期图案进行比较。在暴露于干燥N2气氛后形式上无变化。在加热到175℃后形式上无变化。在加热到235℃后，XRPD图案发生变化并类似于但不同于化合物B观察到的图案。对于其他VT样品，看见了相似的图案。似乎在在该分解产物中存在两种组分。

[0251] 表17.游离碱形式C_0的XRPD峰

[0252]

编号	位置 [2θ°]*	晶面间距[Å]	相对 强度[%]		编号	位置 [2θ°]*	晶面间距[Å]	相对强度[%]
1	2.03	43.473	5		21	23.56	3.773	6
2	7.96	11.104	4		22	24.59	3.618	67
3	8.49	10.411	86		23	25.64	3.471	5
4	**8.77**	**10.078**	**100**		24	26.02	3.422	2
5	10.66	8.293	2		25	27.01	3.299	1
6	13.92	6.358	33		26	27.75	3.212	2
7	14.44	6.130	12		27	29.40	3.036	7
8	15.15	5.845	6		28	30.07	2.969	5
9	15.39	5.752	11		29	31.26	2.859	1
10	15.93	5.560	5		30	31.63	2.826	2
11	17.56	5.045	19		31	32.13	2.784	2
12	18.13	4.890	20		32	32.63	2.742	1
13	18.47	4.801	18		33	33.37	2.683	1
14	19.15	4.632	14		34	34.06	2.630	2
15	19.74	4.493	10		35	34.32	2.611	1
16	20.27	4.377	8		36	34.88	2.570	1
17	20.42	4.346	17		37	35.12	2.553	1
18	21.10	4.208	30		38	35.44	2.531	1
19	21.36	4.157	27		39	35.88	2.501	1
20	21.86	4.063	45		40	38.64	2.329	1

[0253] 热分析

[0254] 游离碱形式C_0的DSC曲线显示出在207.3℃处存在一个吸热峰，ΔH_{Fus}为71.4J/g(图28)。形式C_0在25与150℃之间具有2.3%的重量损失。

[0255] 光学显微术

[0256] 在图29中，样品展示出团聚体和单独的不规则形状的晶体。样品在平面偏振光下显示出双折射。

[0257] 化合物A盐酸盐形式A

[0258] 制备

[0259] 根据实施例5制备盐。

[0260] XRPD

[0261] 氯化盐形式A的X射线衍射数据在图30和表18中给出。

[0262] 表18.盐酸盐形式A的XRPD峰

[0263]

编号	位置 [2θ°]*	晶面间距[Å]	相对 强度[%]		编号	位置 [2θ°]*	晶面间距[Å]	相对 强度[%]
1	6.13	14.403	2		20	22.30	3.983	12
2	**7.45**	**11.863**	**100**		21	23.58	3.770	0
3	7.95	11.108	3		22	24.49	3.631	9
4	8.55	10.337	25		23	24.88	3.576	3
5	10.51	8.409	1		24	25.57	3.481	8
6	12.20	7.248	42		25	26.08	3.414	8
7	12.94	6.837	4		26	27.14	3.283	0
8	13.55	6.532	0		27	27.75	3.213	3
9	14.94	5.926	2		28	28.34	3.147	3
10	15.90	5.569	1		29	30.81	2.900	3
11	16.21	5.463	2		30	31.06	2.877	3
12	17.12	5.175	16		31	31.80	2.812	2
13	17.95	4.937	2		32	33.46	2.676	4
14	18.34	4.833	1		33	34.13	2.625	4
15	18.83	4.710	37		34	34.89	2.570	2
16	18.87	4.700	29		35	36.22	2.478	1
17	19.26	4.606	4		36	37.44	2.400	1
18	20.24	4.383	1		37	39.42	2.284	1
19	21.27	4.174	1		28			

[0264] *使用ZBG或玻璃板通常引入正样品高度位移并导致2θ值的小(0.05°至0.2°)偏移。最高的峰(强度100%)以黑体字母示出。

[0265] 热分析

[0266] 盐酸盐形式A的DSC曲线显示出在247.3℃处存在一个吸热峰，ΔH_{Fus}为41.6J/g(图31)。盐酸盐形式A在25与150℃之间具有0.2%的重量损失。

[0267] 吸水

[0268] DVS图线(图32)表明在整个RH范围内存在表面吸附，而体吸收有限。总的水分吸收为～2.25%。

[0269] 稳定性

[0270] 表19中的数据显示相对恒定的XRPD图案和DSC值，TGA值适度变化。HPLC值与分析值大不相同，在28天测试后降至近一半。还注意到HPLC纯度的平稳下降，且化合物B含量增至1.5%。化合物A单盐酸盐中的化合物A含量的理论值为92.0%。

[0271] 表19.盐酸盐形式A在40℃和75%RH下的稳定性

[0272]

天	XRPD	DSC ℃	TGA%	化合物 A 分析	化合物 B 分析	HPLC 纯度

[0273]

0	A	244.8	0.1	39.9	0.3	99.1
7	不变	247.6	1.5	22.3	0.7	96.3
14	不变	245.9	1.1	21.6	1.1	94.0
28	不变	245.5	0.9	19.6	1.5	91.1

[0274] 化合物A富马酸盐形式A

[0275] 制备

[0276] 根据实施例5制备盐。

[0277] XRPD

[0278] 化合物A富马酸盐形式A的X射线衍射数据在图33和表20中给出。

[0279] 表20.富马酸盐形式A的XRPD峰

[0280]

编号	位置 [2θ°]*	晶面间距[Å]	相对 强度[%]		编号	位置 [2θ°]*	晶面间距[Å]	相对强度[%]
1	**8.98**	**9.842**	**100**		21	22.88	3.884	8
2	10.54	8.388	26		22	23.50	3.783	16
3	11.06	7.994	11		23	24.04	3.699	22
4	12.94	6.835	4		24	24.19	3.677	15
5	14.86	5.958	20		25	25.36	3.509	4
6	15.44	5.734	2		26	25.45	3.497	2
7	15.55	5.694	5		27	25.59	3.479	2
8	16.19	5.469	5		28	25.71	3.463	8
9	17.07	5.190	37		29	25.90	3.437	8
10	17.69	5.008	20		30	26.08	3.415	4
11	18.20	4.871	3		31	26.24	3.393	4
12	18.74	4.732	4		32	26.51	3.360	2
13	19.04	4.657	3		33	26.75	3.329	4
14	19.13	4.637	7		34	27.29	3.266	7
15	19.34	4.585	24		35	28.95	3.082	11
16	19.68	4.508	5		36	29.92	2.984	4
17	20.72	4.284	4		37	30.78	2.902	3
18	21.09	4.209	24		38	30.99	2.884	3
19	21.80	4.074	2		39	31.09	2.874	6
20	22.32	3.980	8		40	36.83	2.438	2

[0281] *使用ZBG或玻璃板通常引入正样品高度位移并导致2θ值的小(0.05°至0.2°)偏移。最高的峰(强度100%)以黑体字母示出。

[0282] 热分析

[0283] 富马酸盐形式A的DSC曲线显示出在231.3℃处存在一个吸热峰，ΔH_{Fus}为106.9J/g(图34)。形式A在25与150℃之间具有0.2%的重量损失。

[0284] 化合物A对甲苯磺酸盐形式A

[0285] 制备

[0286] 根据实施例5制备盐。

[0287] XRPD

[0288] 对甲苯磺酸盐形式A的表征在图35和表21中描绘。

[0289] 表21.对甲苯磺酸盐形式A的XRPD峰

[0290]

编号	位置 [2θ°]*	晶面间距[Å]	相对 强度[%]		编号	位置 [2θ°]*	晶面间距[Å]	相对 强度[%]
1	6.02	14.669	74		21	20.98	4.231	34
2	9.56	9.242	43		22	21.14	4.199	29
3	10.31	8.573	61		23	21.36	4.156	9
4	10.54	8.391	25		24	21.67	4.097	10
5	11.03	8.017	96		25	21.96	4.045	33
6	**12.01**	**7.364**	**100**		26	22.11	4.017	23
7	12.89	6.864	21		27	22.70	3.914	21
8	13.22	6.693	33		28	23.13	3.842	23
9	14.32	6.180	12		29	23.39	3.800	84
10	15.00	5.900	24		30	23.51	3.781	56
11	16.71	5.301	36		31	24.11	3.689	14
12	17.02	5.206	22		32	24.53	3.626	8
13	17.51	5.061	59		33	24.84	3.582	54
14	17.79	4.983	68		34	25.08	3.547	9
15	18.02	4.919	78		35	26.56	3.353	33
16	18.68	4.747	19		36	27.57	3.232	8
17	18.98	4.672	29		37	28.15	3.168	13
18	19.37	4.578	7		38	28.78	3.099	9
19	20.22	4.388	7		39	30.22	2.955	11
20	20.76	4.276	35		40	30.43	2.935	9

[0291] *使用ZBG或玻璃板通常引入正样品高度位移并导致2θ值的小(0.05°至0.2°)偏移。最高的峰(强度100%)以黑体字母示出。

[0292] 热分析

[0293] 对甲苯磺酸盐形式A的DSC曲线显示出在239.6℃处存在一个吸热峰，ΔH_{Fus}为38.5J/g(图36)。形式A在25与150℃之间具有0.04%的重量损失。

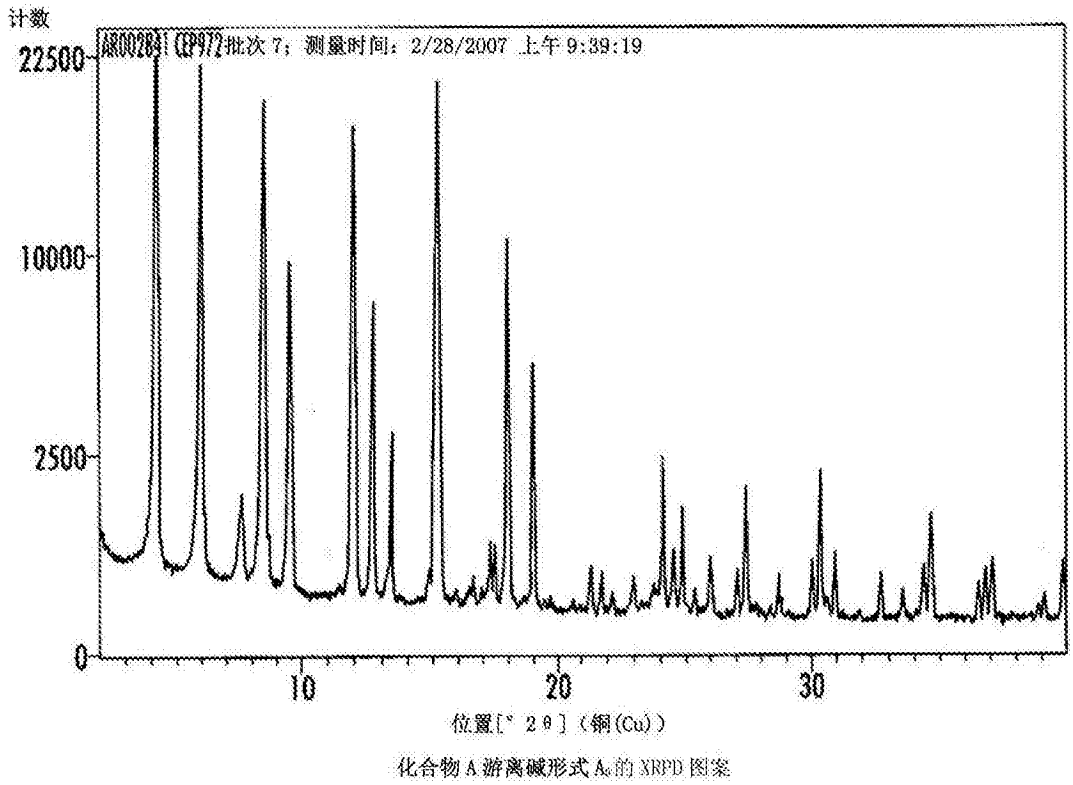

化合物 A 游离碱形式 A_0 的 XRPD 图案

图1

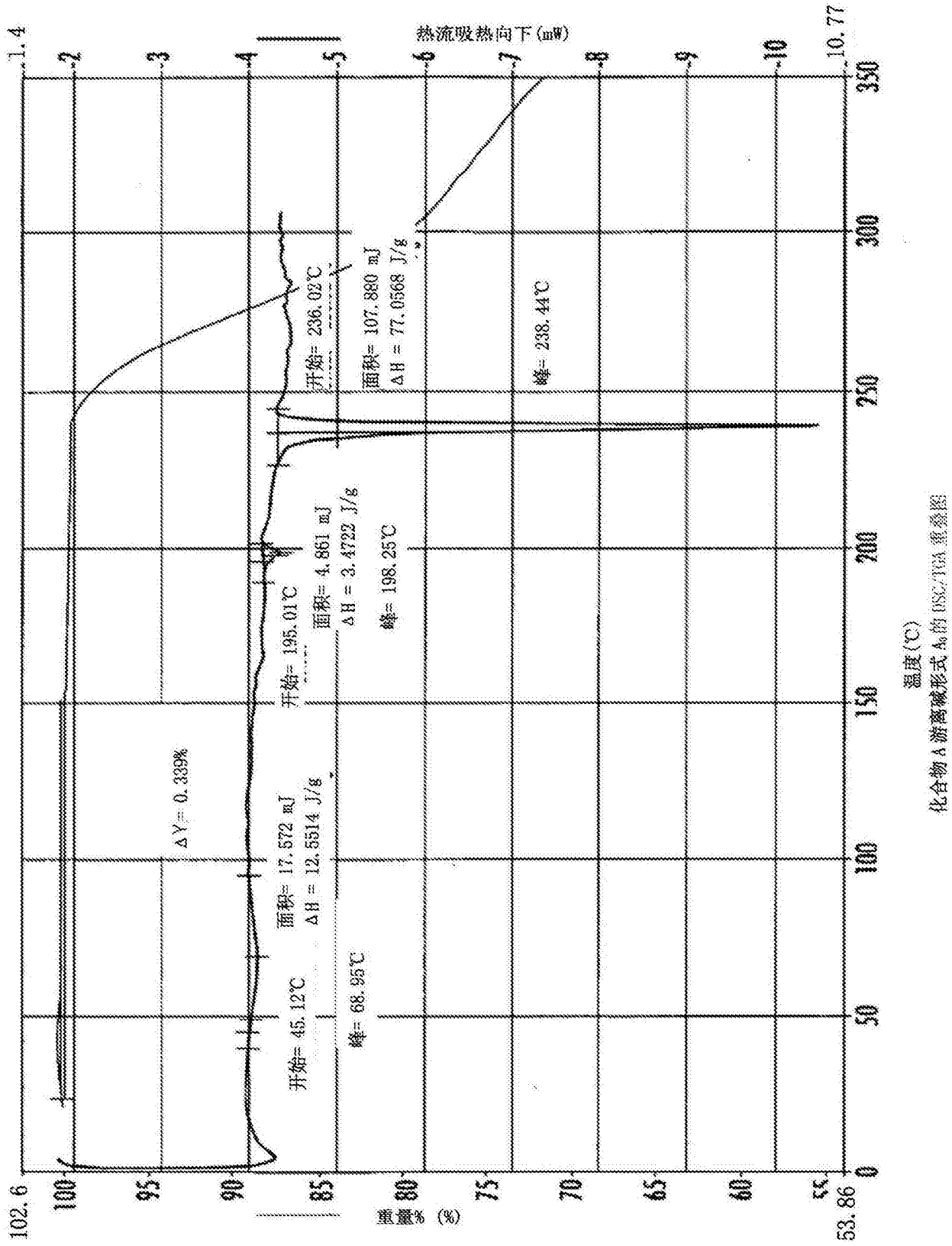
热流吸热向下(mW)
重量% (%)
温度(℃)
ΔY= 0.339%
面积= 17.572 mJ
ΔH = 12.5514 J/g
开始= 45.12℃
峰= 68.95℃
开始= 195.01℃
面积= 4.861 mJ
ΔH = 3.4722 J/g
峰= 198.25℃
开始= 236.02℃
面积= 107.880 mJ
ΔH = 77.0568 J/g
峰= 238.44℃
化合物A游离碱形式A6的DSC/TGA重叠图

图2

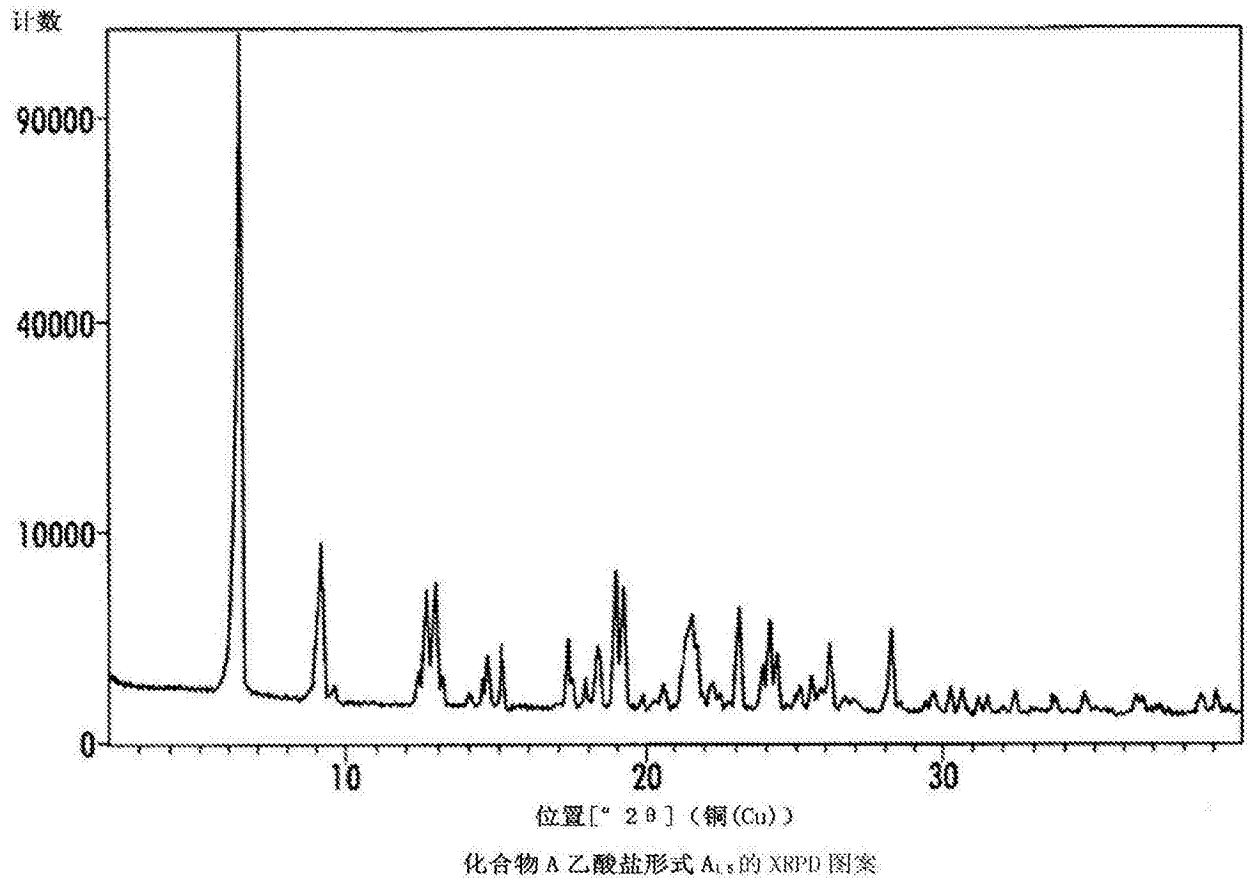

化合物 A 乙酸盐形式 A_{ES} 的 XRPD 图案

图3

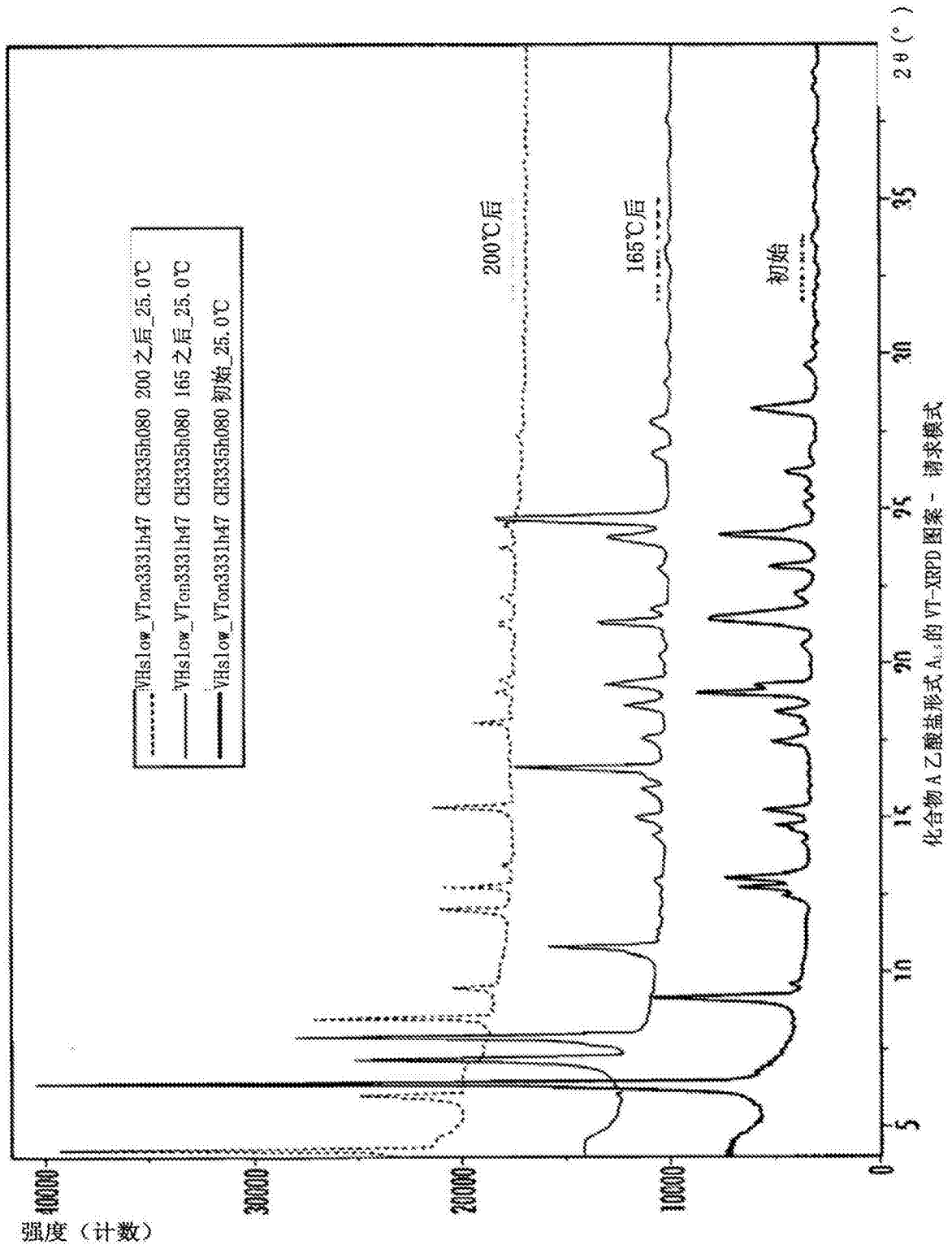
VHslow_VTon3331h47 CH3335h080 200 之后_25.0℃
VHslow_VTon3331h47 CH3335h080 165 之后_25.0℃
VHslow_VTon3331h47 CH3335h080 初始_25.0℃
200℃后
165℃后
初始
强度（计数）
40000
30000
20000
10000
0
5
10
15
20
25
30
35
2θ(°)
化合物A乙酸盐形式A...的VT-XRPD图案 - 请求模式

图4

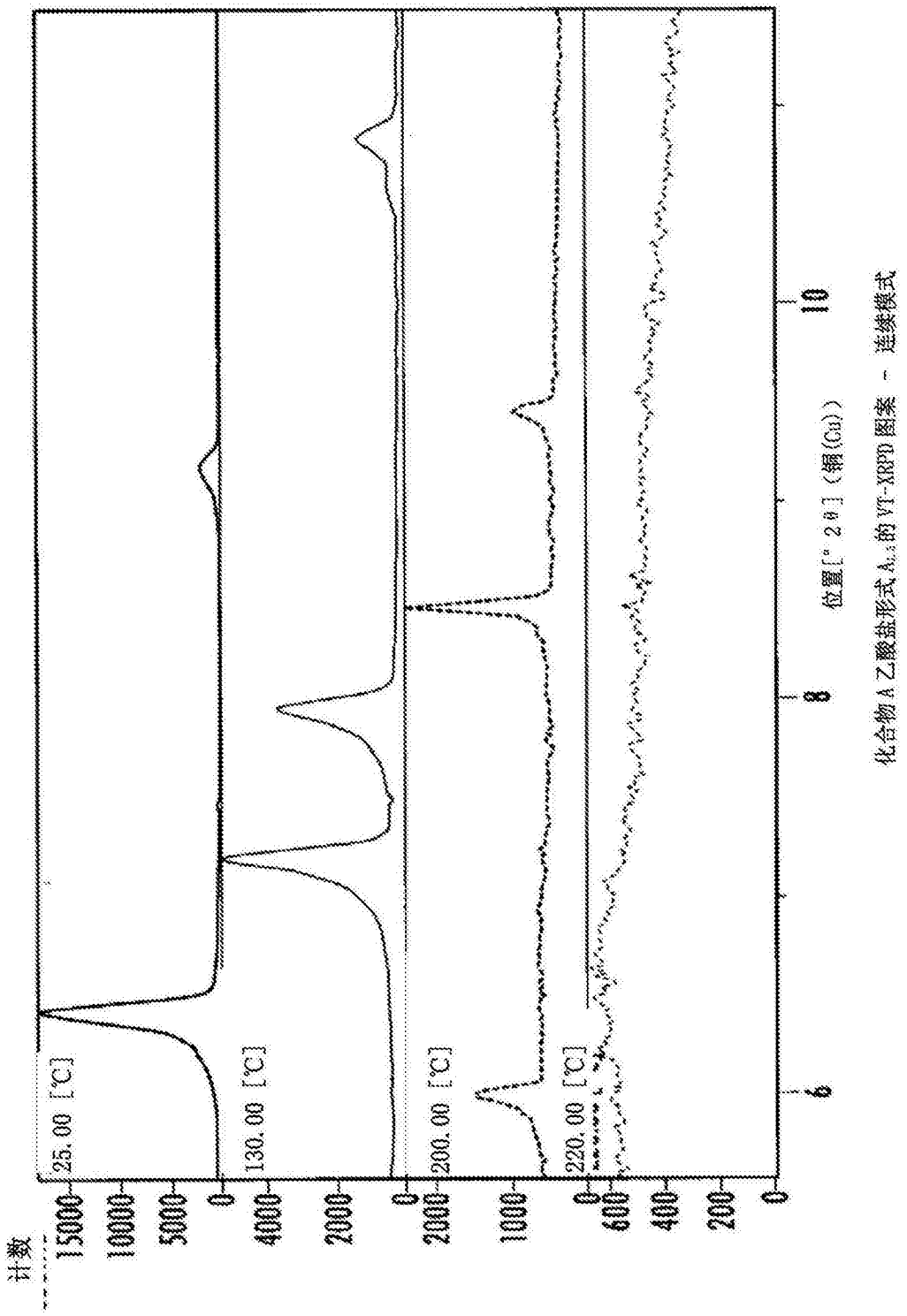
计数
15000
10000
5000
0
4000
2000
0
2000
1000
0
600
400
200
0
25.00 [℃]
130.00 [℃]
200.00 [℃]
220.00 [℃]
6
8
10
位置[°2θ](铜(Cu))
化合物A乙酸盐形式A1的VT-XRPD图案 - 连续模式

图5

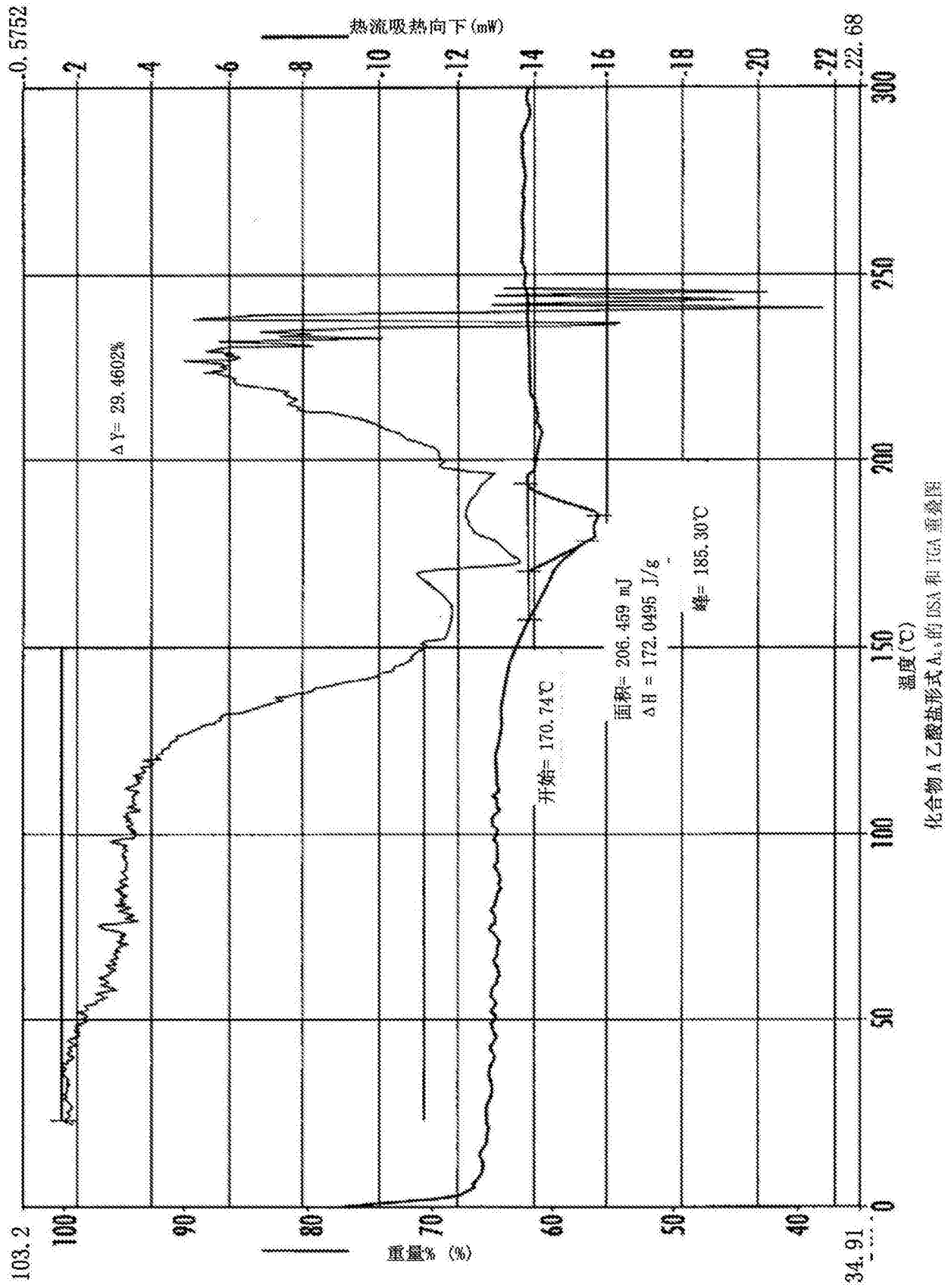
热流吸热向下(mW)
-0.5752
-2
-4
-6
-8
-10
-12
-14
-16
-18
-20
-22
22.68
ΔY= 29.4602%
面积= 206.459 mJ
ΔH = 172.0495 J/g
峰= 186.30℃
开始= 170.74℃
103.2
100
90
80
70
60
50
40
34.91
重量% (%)
0
50
100
150
200
250
300
温度(℃)
化合物A乙酸盐形式A1的DSA和TGA重叠图

图6

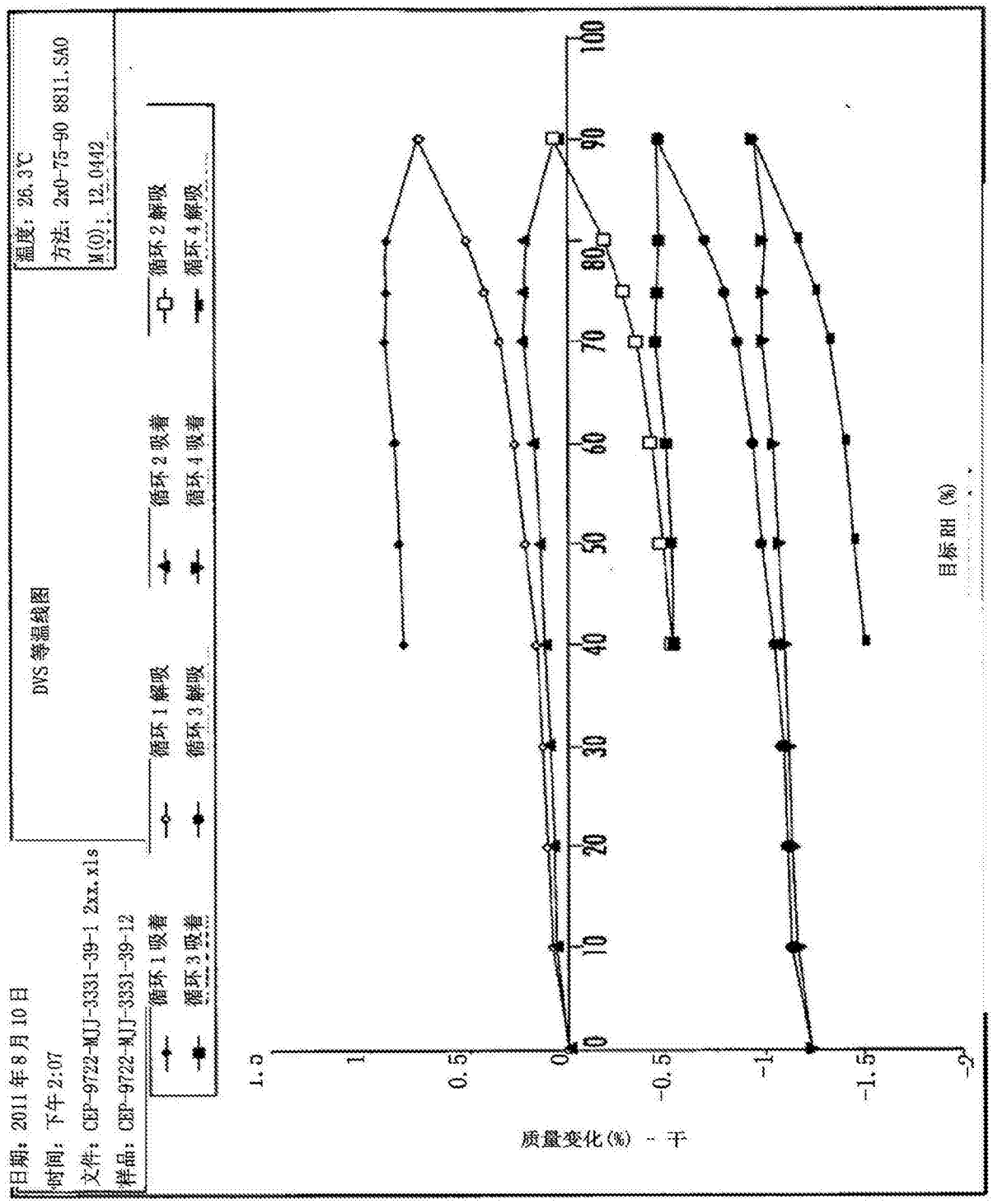
DVS 等温线图
温度：26.3℃
方法：2x0-75-90 8811.SAO
M(0)：12.0442
日期：2011年8月10日
时间：下午 2:07
文件：CEP-9722-MJJ-3331-39-1 2xx.xls
样品：CEP-9722-MJJ-3331-39-12
循环 1 吸着
循环 1 解吸
循环 2 吸着
循环 2 解吸
循环 3 吸着
循环 3 解吸
循环 4 吸着
循环 4 解吸
质量变化(%) - 干
目标 RH (%)
化合物 A 乙酸盐形式 A1.5 的 DVS 重叠图

图7

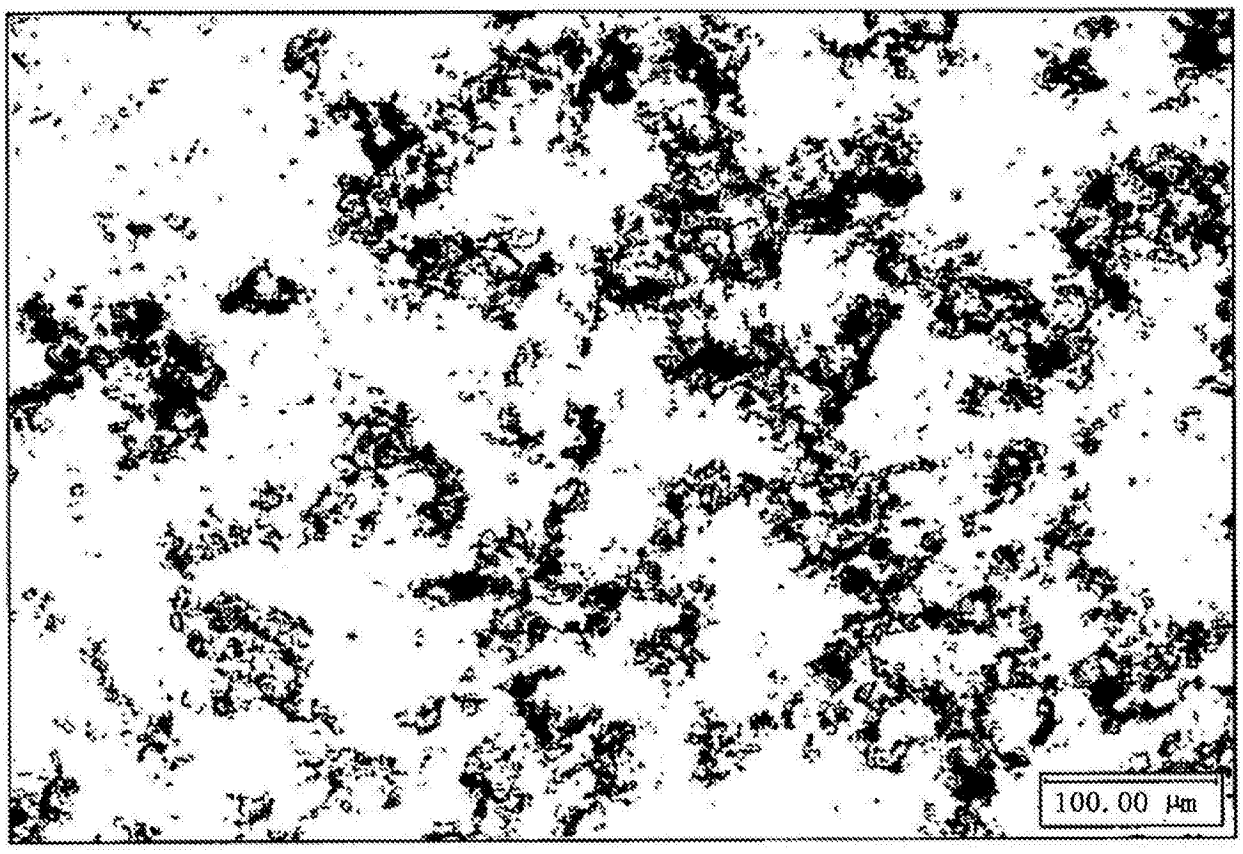

化合物 A 乙酸盐形式 $A_{1.5}$ 的显微照片

图8

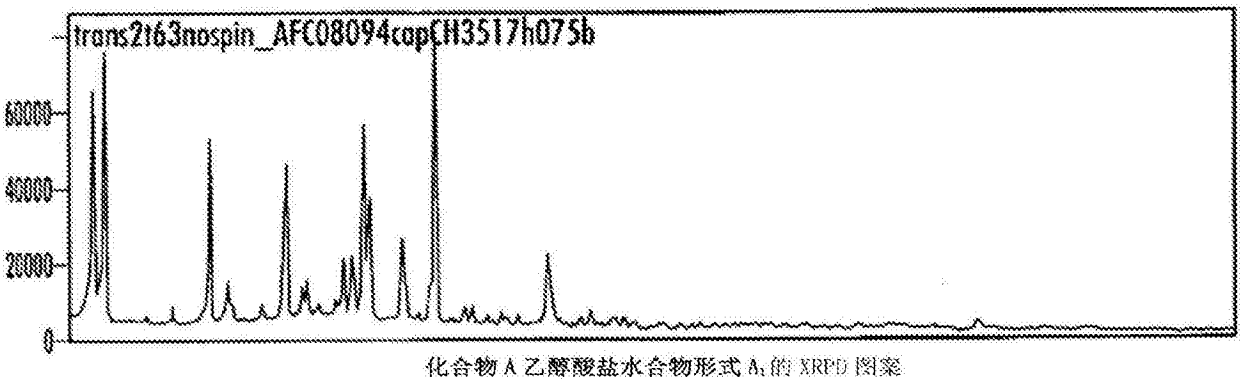

化合物 A 乙醇酸盐水合物形式 A_1 的 XRPD 图案

图9

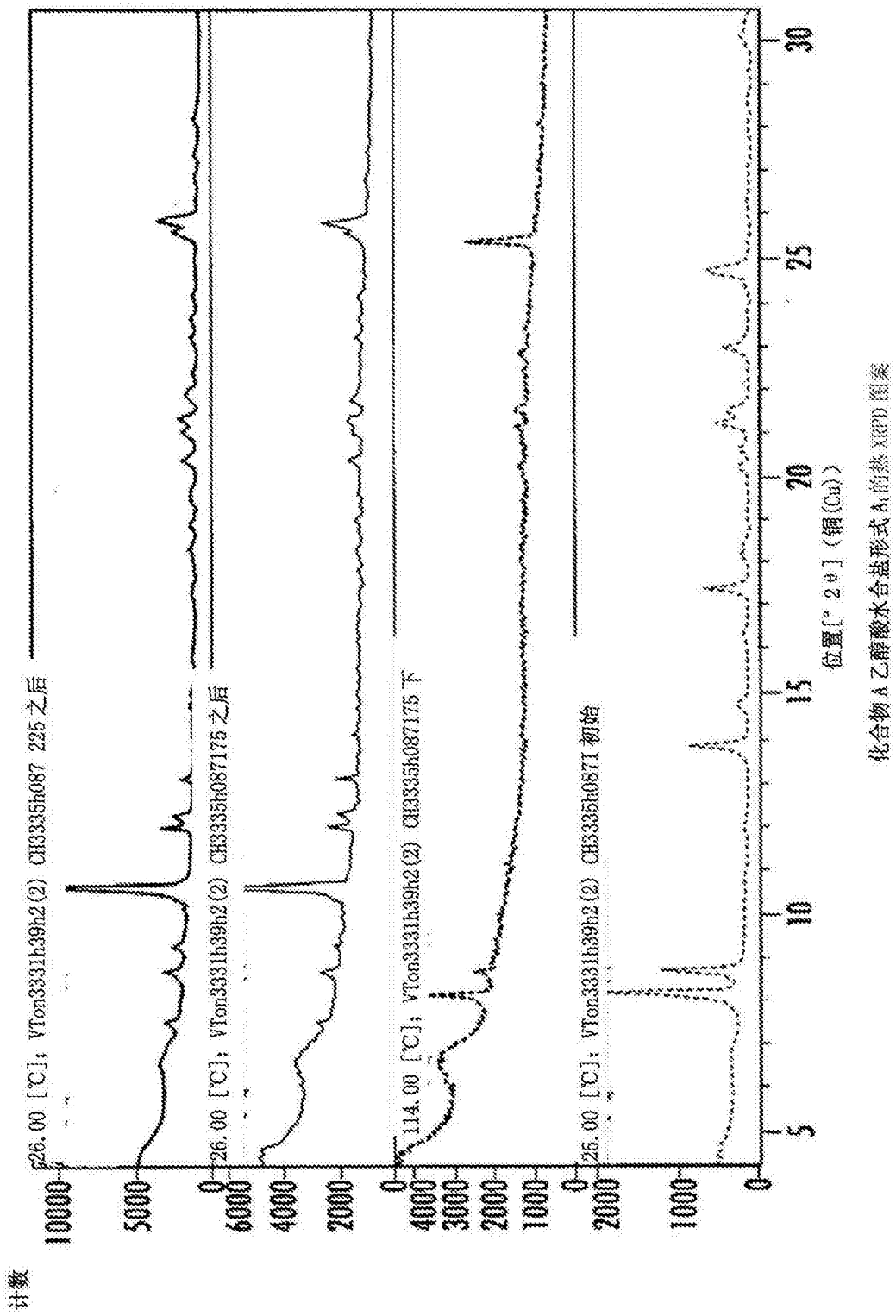
计数
26.00 [℃]; VTon3331h39h2(2) CH3335h087 225之后
26.00 [℃]; VTon3331h39h2(2) CH3335h087175之后
114.00 [℃]; VTon3331h39h2(2) CH3335h087175下
25.00 [℃]; VTon3331h39h2(2) CH3335h0871初始
位置[° 2θ] (铜(Cu))
化合物A乙醇酸水合盐形式A的热XRPD图案

图10

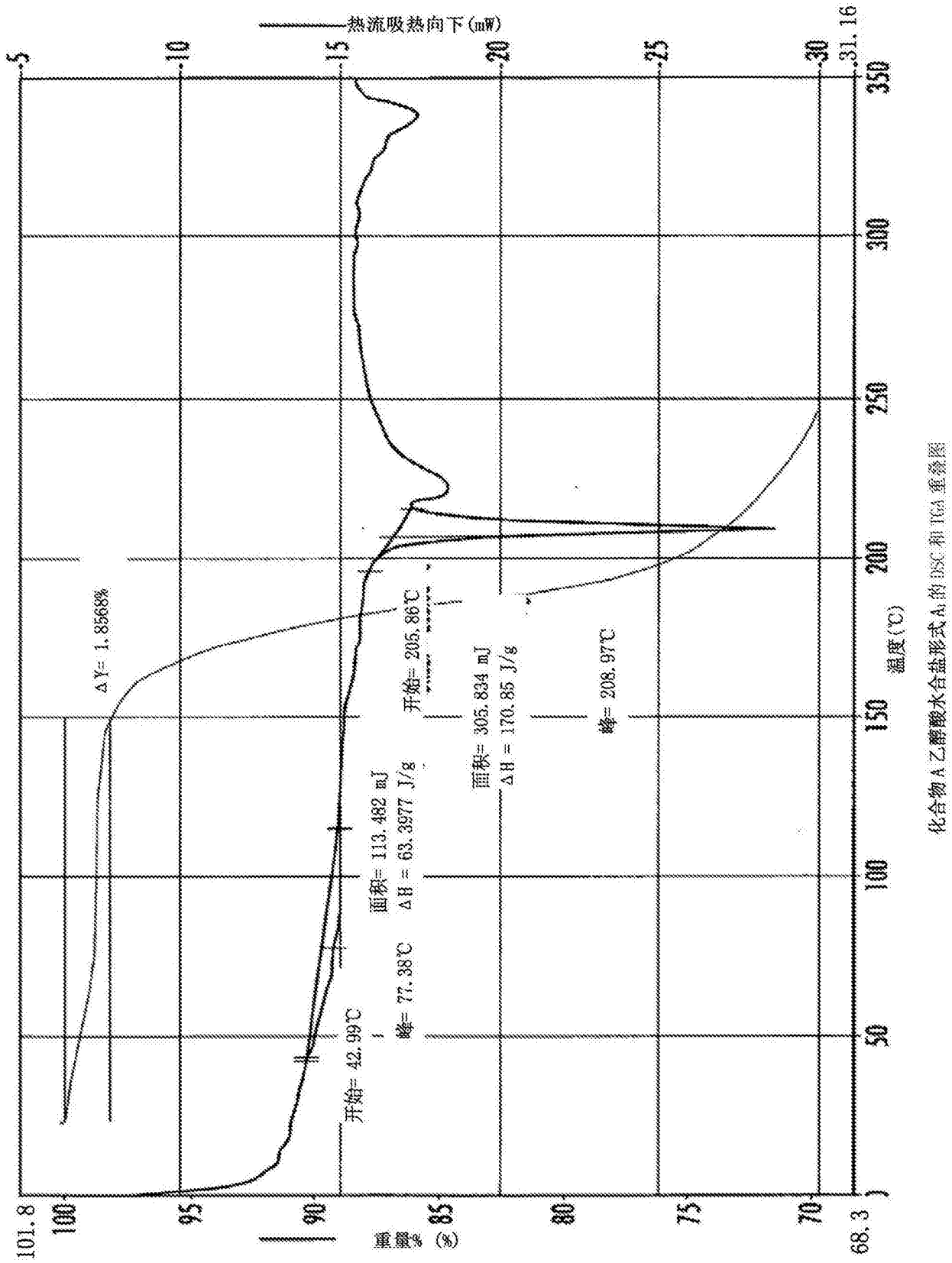
热流吸热向下(mW)
重量% (%)
温度(℃)
ΔY= 1.8568%
面积= 113.482 mJ
ΔH = 63.3977 J/g
峰= 77.38℃
开始= 42.99℃
面积= 305.834 mJ
ΔH = 170.85 J/g
开始= 205.86℃
峰= 208.97℃
101.8
68.3
31.16
化合物A乙醇酸水合盐形式A1的DSC和TGA重叠图

图11

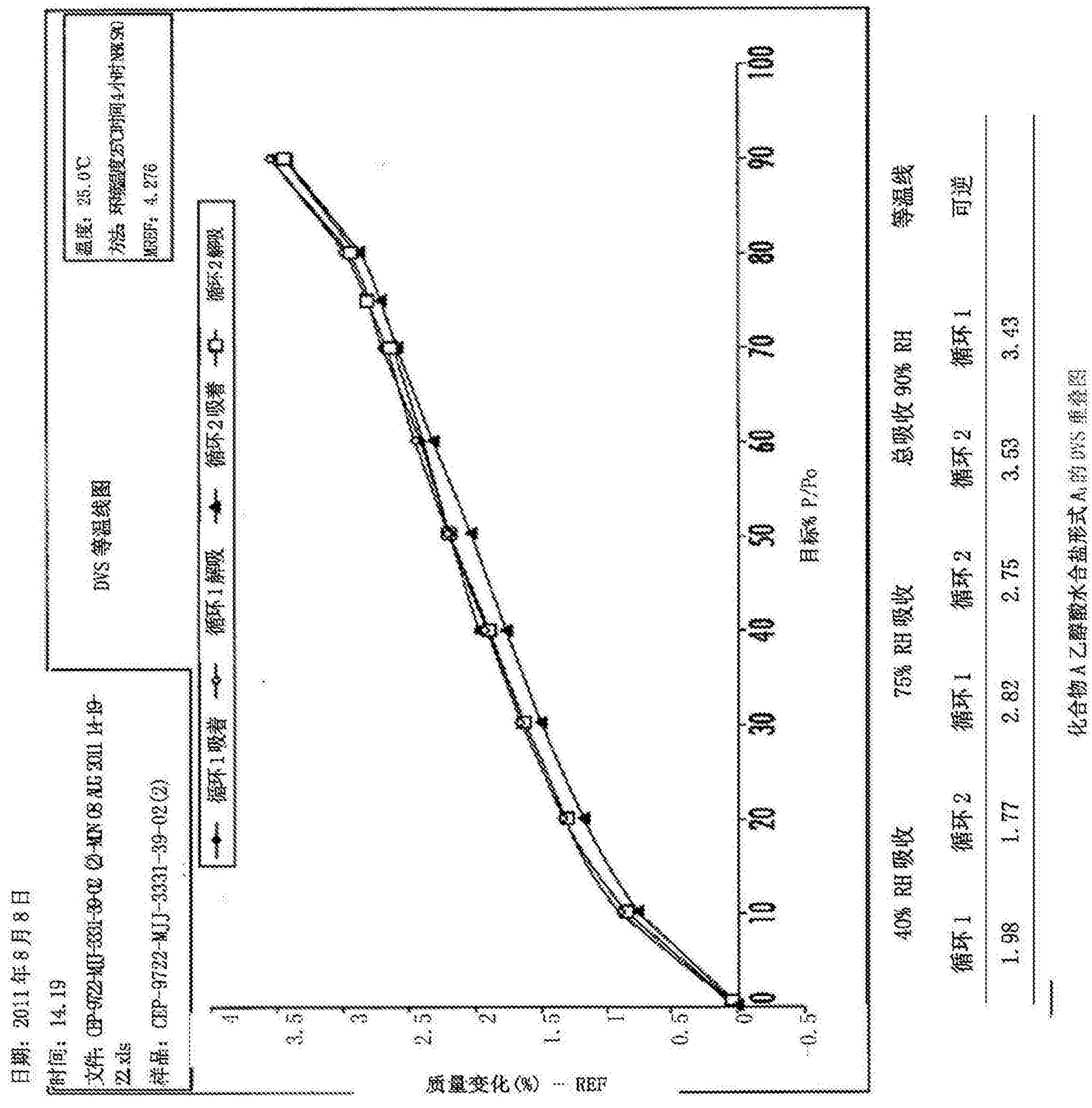
日期：2011年8月8日
时间：14.19
文件：CEP-9722-MJJ-3331-39-02 (2)-MON 08 AUG 2011 14-19-22.xls
样品：CEP-9722-MJJ-3331-39-02(2)
DVS 等温线图
温度：25.0℃
MSBF：4.276
循环1吸着
循环1解吸
循环2吸着
循环2解吸
质量变化(%) - REF
目标% P/Po
40% RH 吸收
75% RH 吸收
总吸收 90% RH
等温线
循环1
循环2
循环1
循环2
循环2
循环1
可逆
1.98
1.77
2.82
2.75
3.53
3.43
化合物A乙醇酸水合盐形式A的DVS叠图

图12

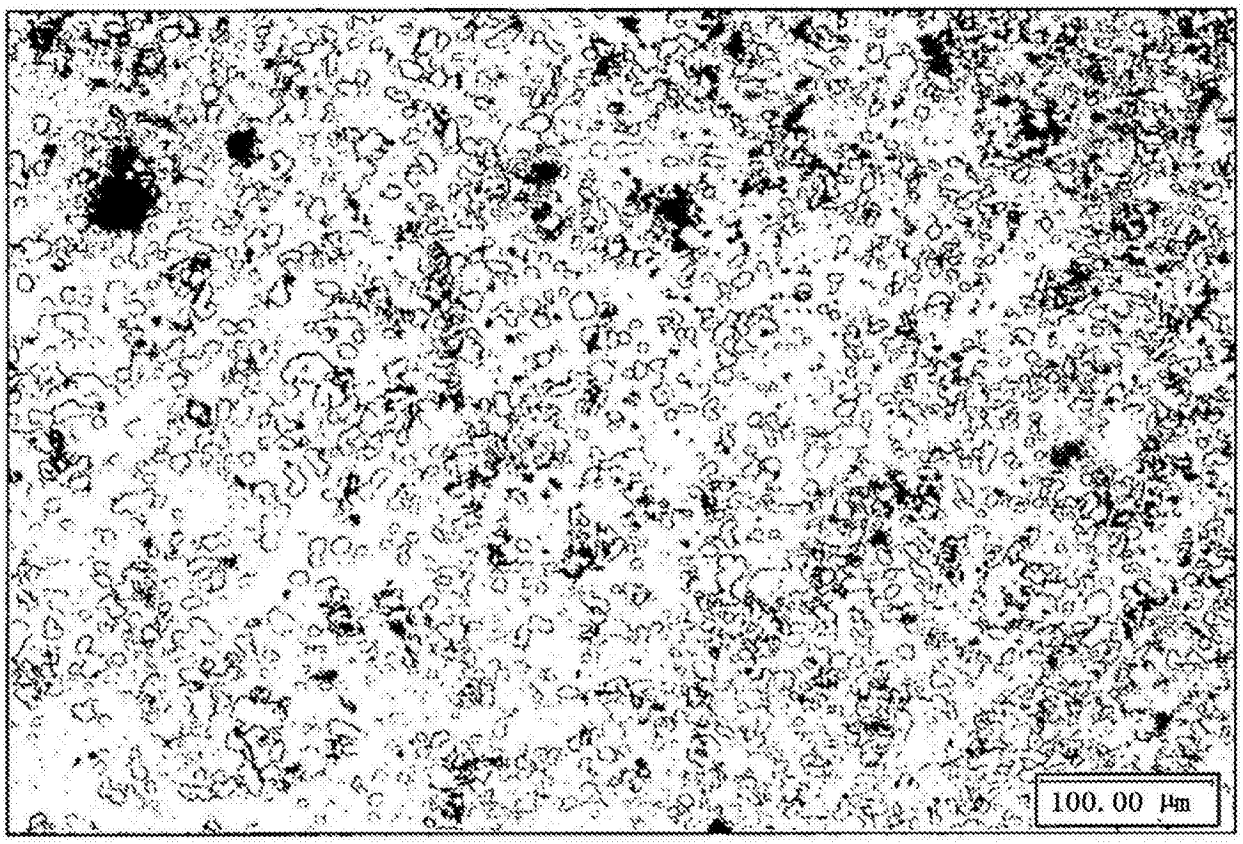

化合物A乙醇酸水合盐形式A1的显微照片

图13

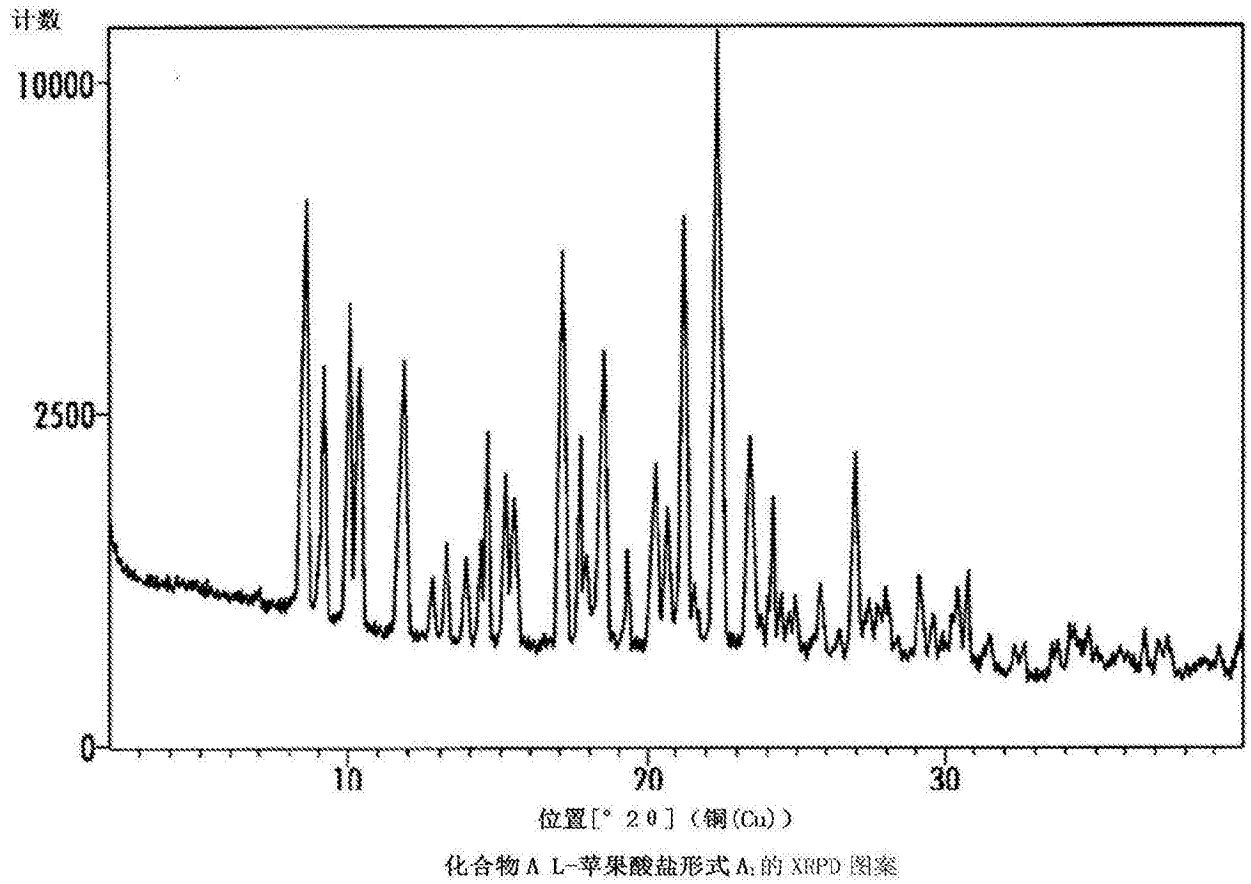

化合物A L-苹果酸盐形式A_1的XRPD图案

图14

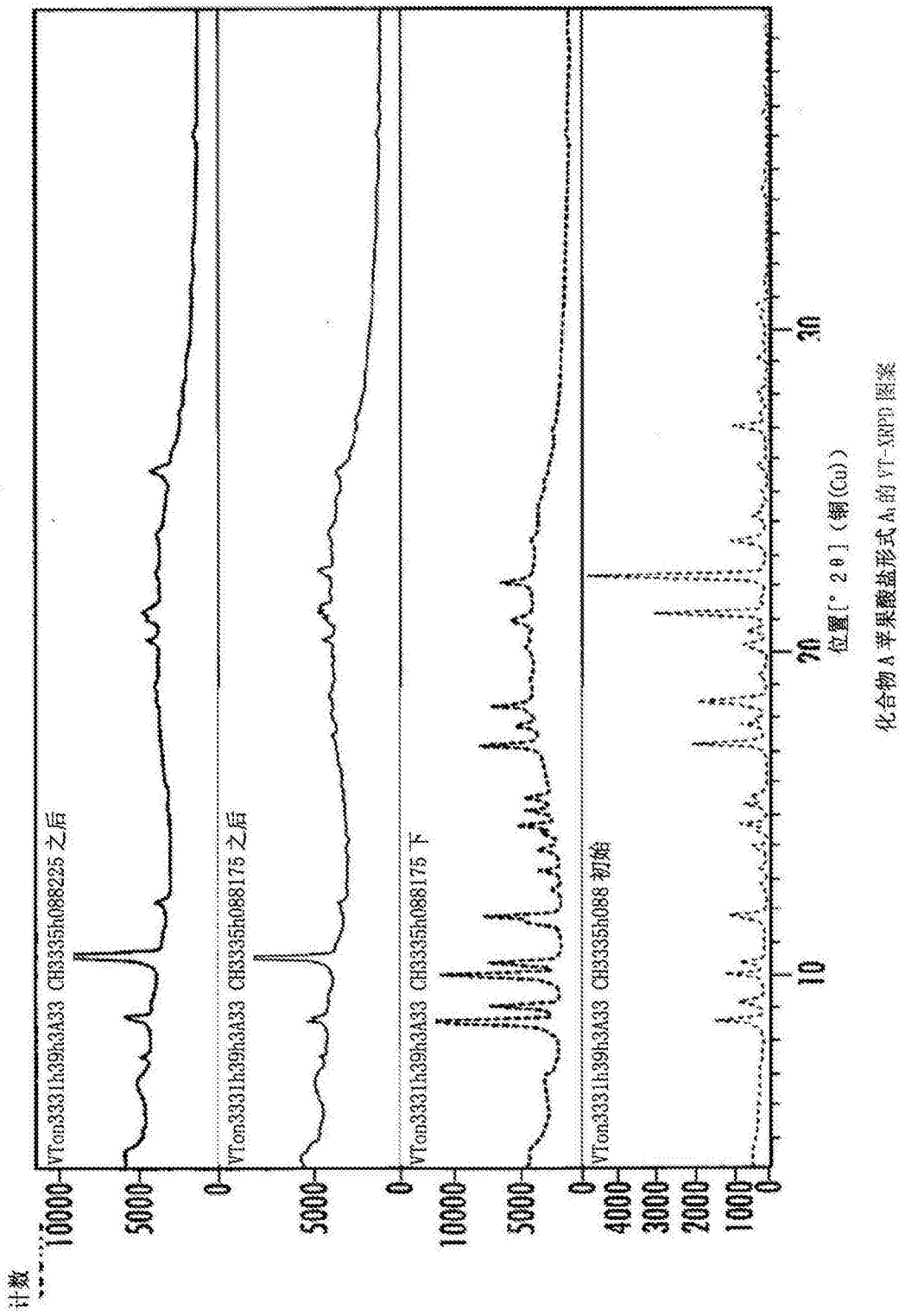
计数
VTon3331h39h3A33 CH3335h088225 之后
VTon3331h39h3A33 CH3335h088175 之后
VTon3331h39h3A33 CH3335h088175 下
VTon3331h39h3A33 CH3335h088 初始
10000
5000
0
5000
0
10000
5000
0
4000
3000
2000
1000
10
20
30
位置[° 2θ]（铜(Cu)）
化合物A 苹果酸盐形式A1的 VT-XRPD 图案

图15

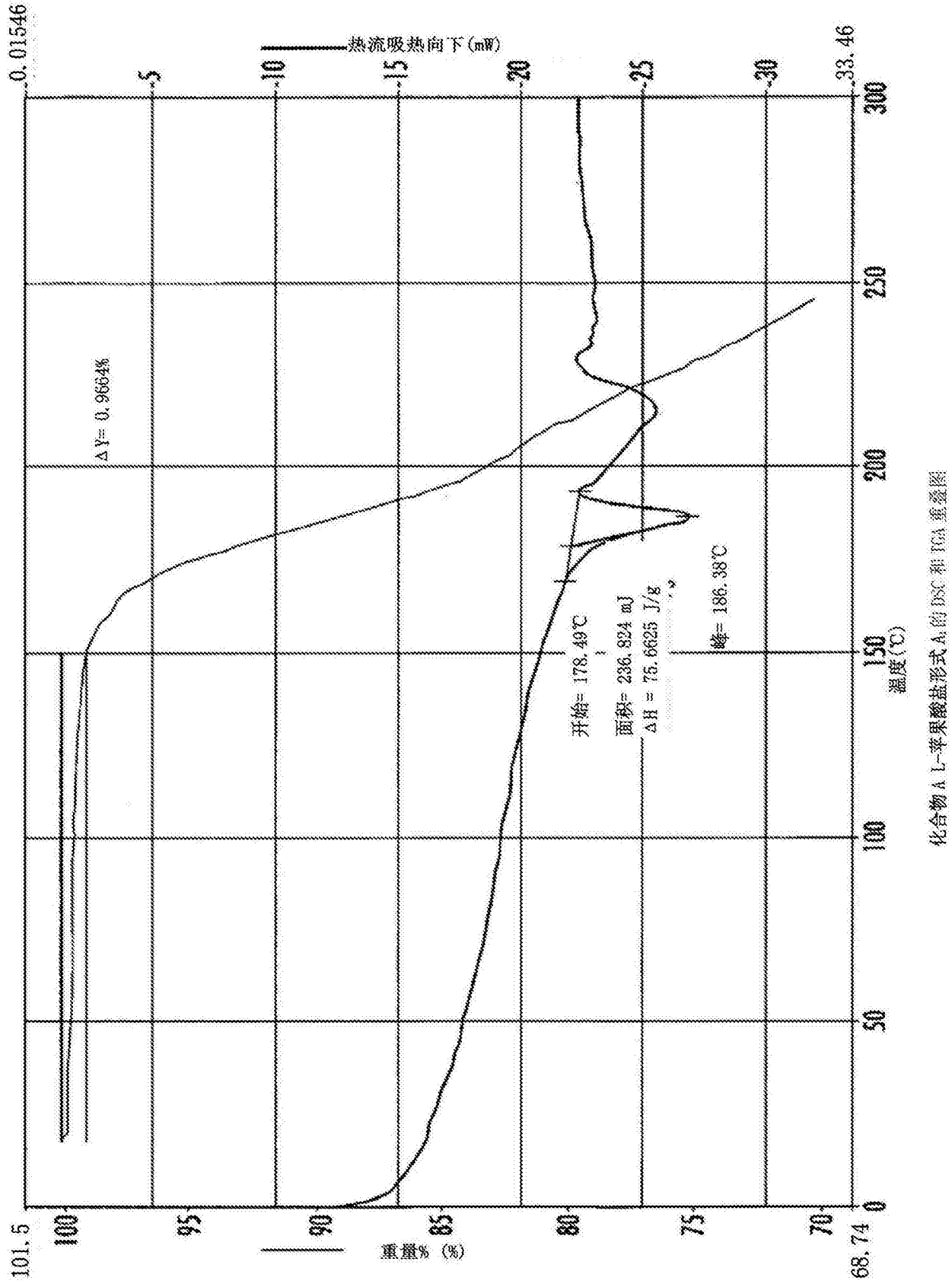
0.01546
热流吸热向下(mW)
33.46
ΔY= 0.9604%
开始= 178.49℃
面积= 236.824 mJ
ΔH = 75.6625 J/g
峰= 186.38℃
温度(℃)
101.5
重量% (%)
68.74
化合物A L-苹果酸盐形式A的DSC和TGA重叠图

图16

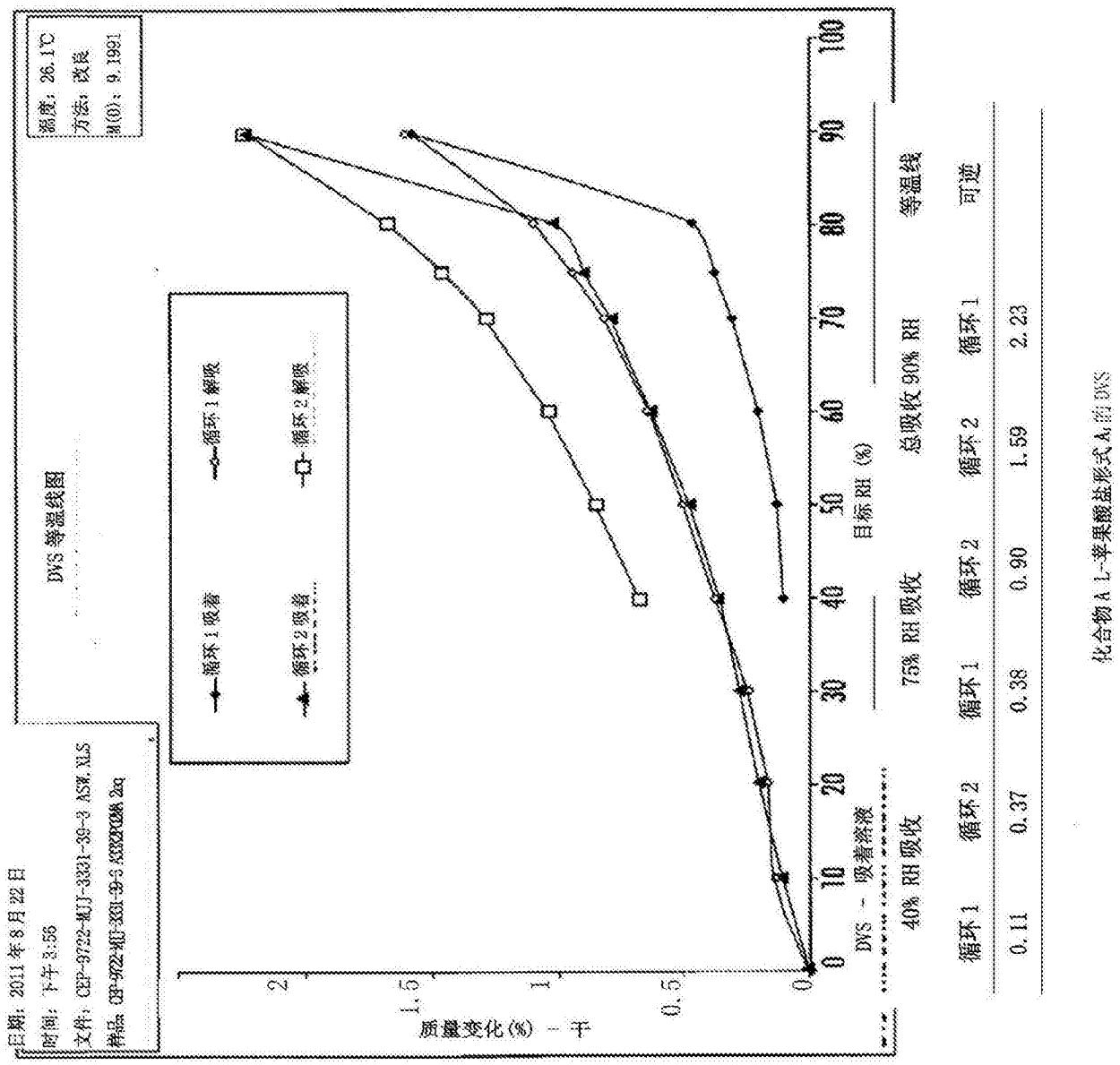
温度：26.1℃
方法：改良
m(0)：9.1991
DVS 等温线图
循环 1 吸着
循环 1 解吸
循环 2 吸着
循环 2 解吸
质量变化(%) - 干
目标 RH (%)
DVS - 吸着溶液
40% RH 吸收
75% RH 吸收
总吸收 90% RH
等温线
循环 1 循环 2 循环 1 循环 2 循环 1 可逆
0.11 0.37 0.38 0.90 1.59 2.23
化合物 A L-苹果酸盐形式 A 的 DVS

图17

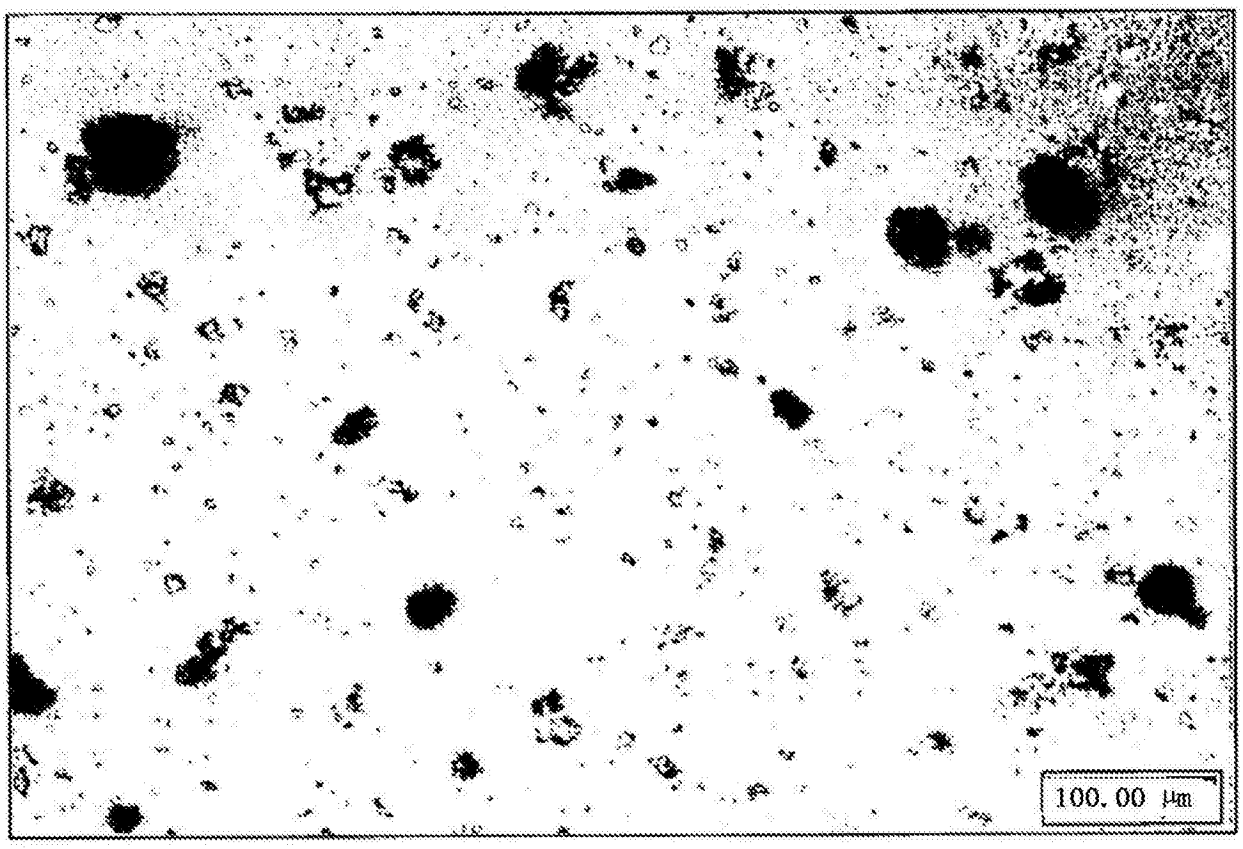

化合物A L-苹果酸盐形式A1的显微照片

图18

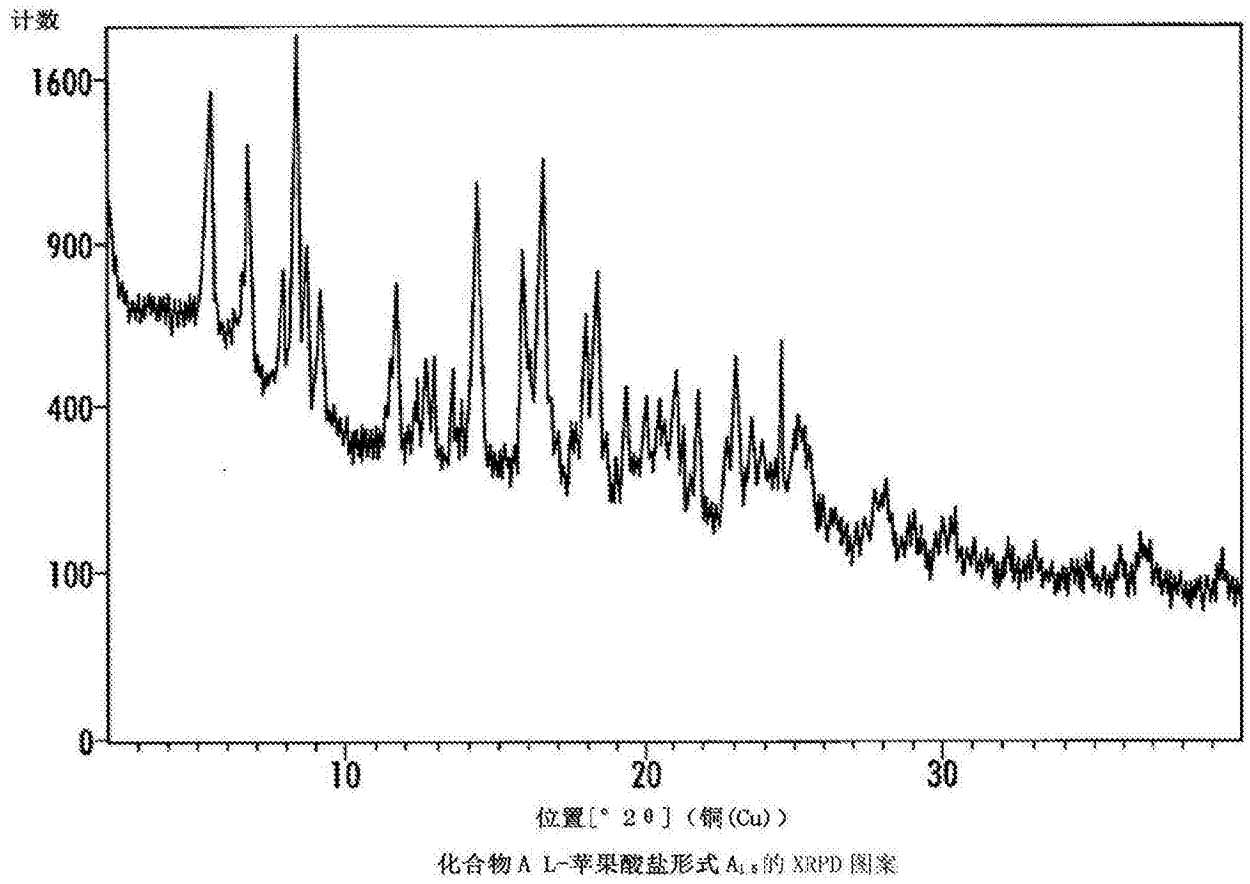

化合物A L-苹果酸盐形式$A_{1.8}$的XRPD图案

图19

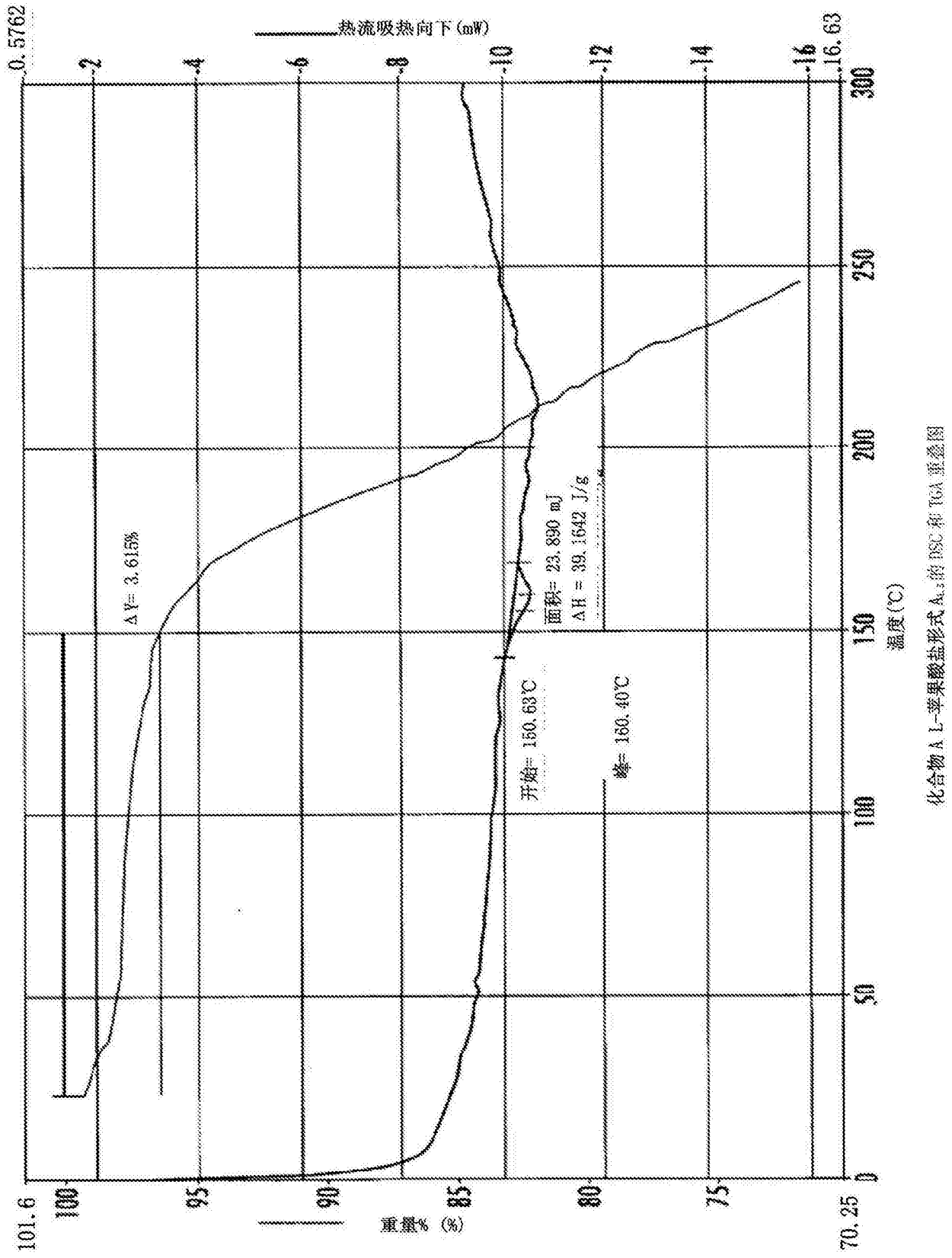
热流吸热向下(mW)
0.5762
-2
-4
-6
-8
-10
-12
-14
-16
16.63
300
250
200
150
100
50
0
温度(℃)
101.6
100
95
90
85
80
75
70.25
重量% (%)
ΔY= 3.615%
面积= 23.890 mJ
ΔH = 39.1642 J/g
开始= 160.63℃
峰= 160.40℃
化合物A L-苹果酸盐形式A1.3的DSC和TGA重叠图

图20

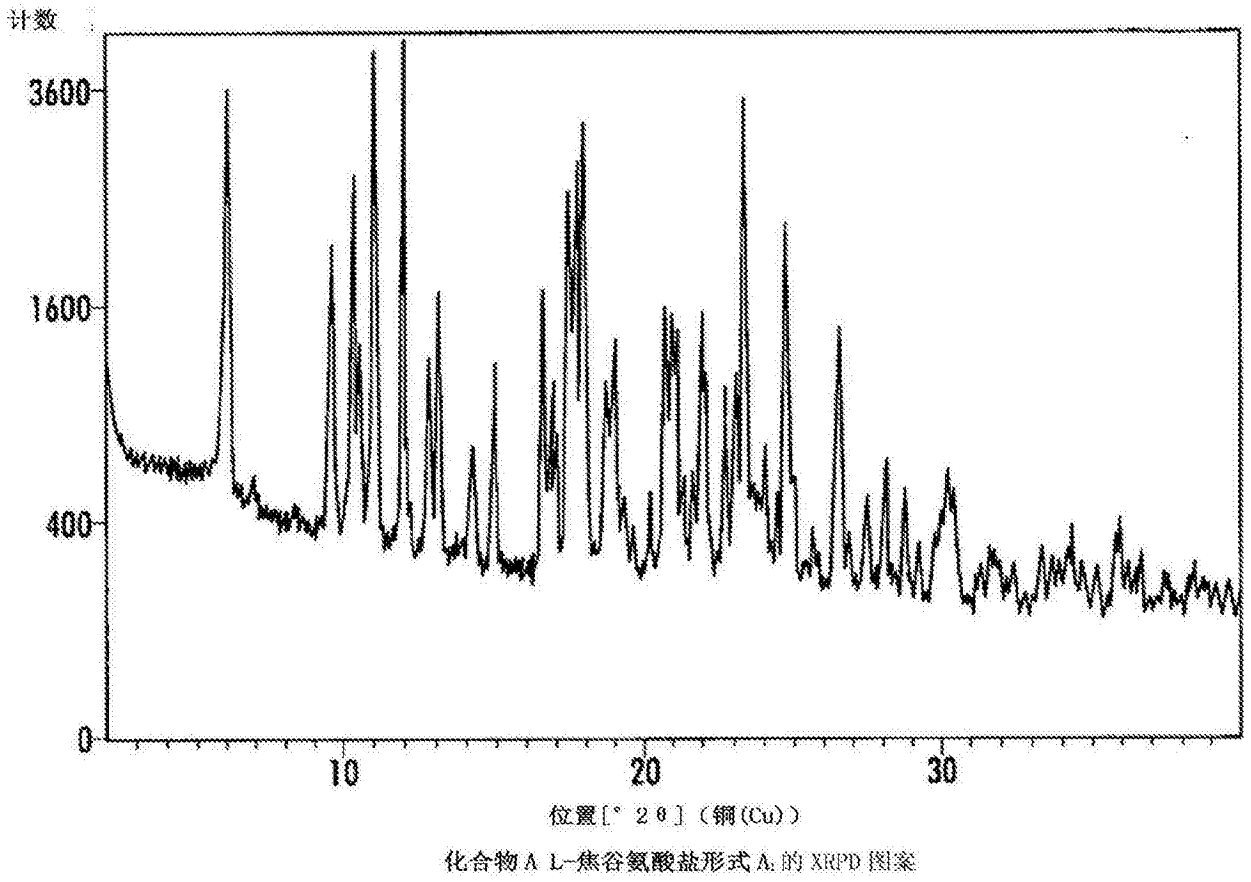

化合物A L-焦谷氨酸盐形式A1的XRPD图案

图21

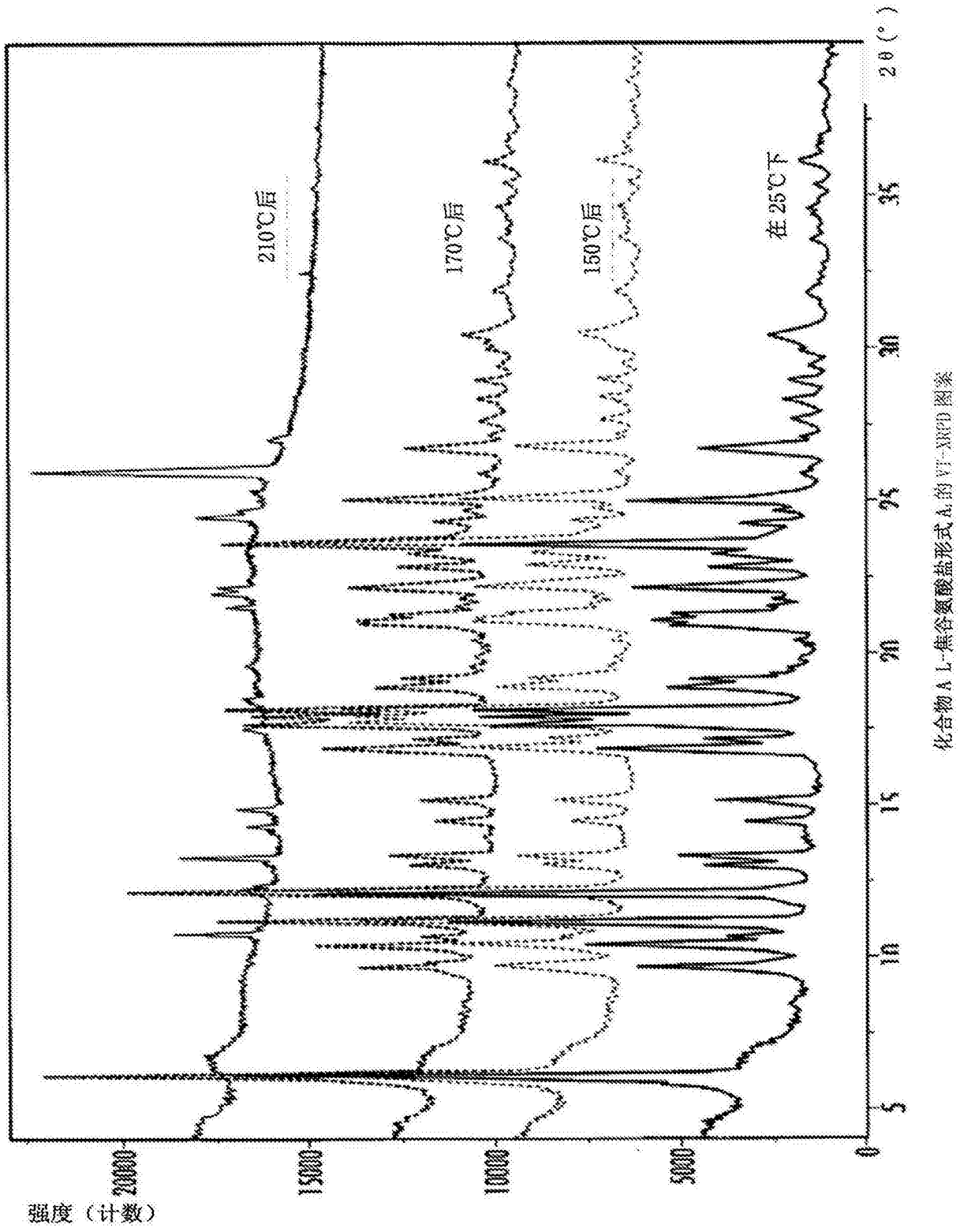
210℃后
170℃后
150℃后
在25℃下
强度（计数）
20000
15000
10000
5000
0
5
10
15
20
25
30
35
2θ(°)
化合物A L-焦谷氨酸盐形式A的VT-XRPD图案

图22

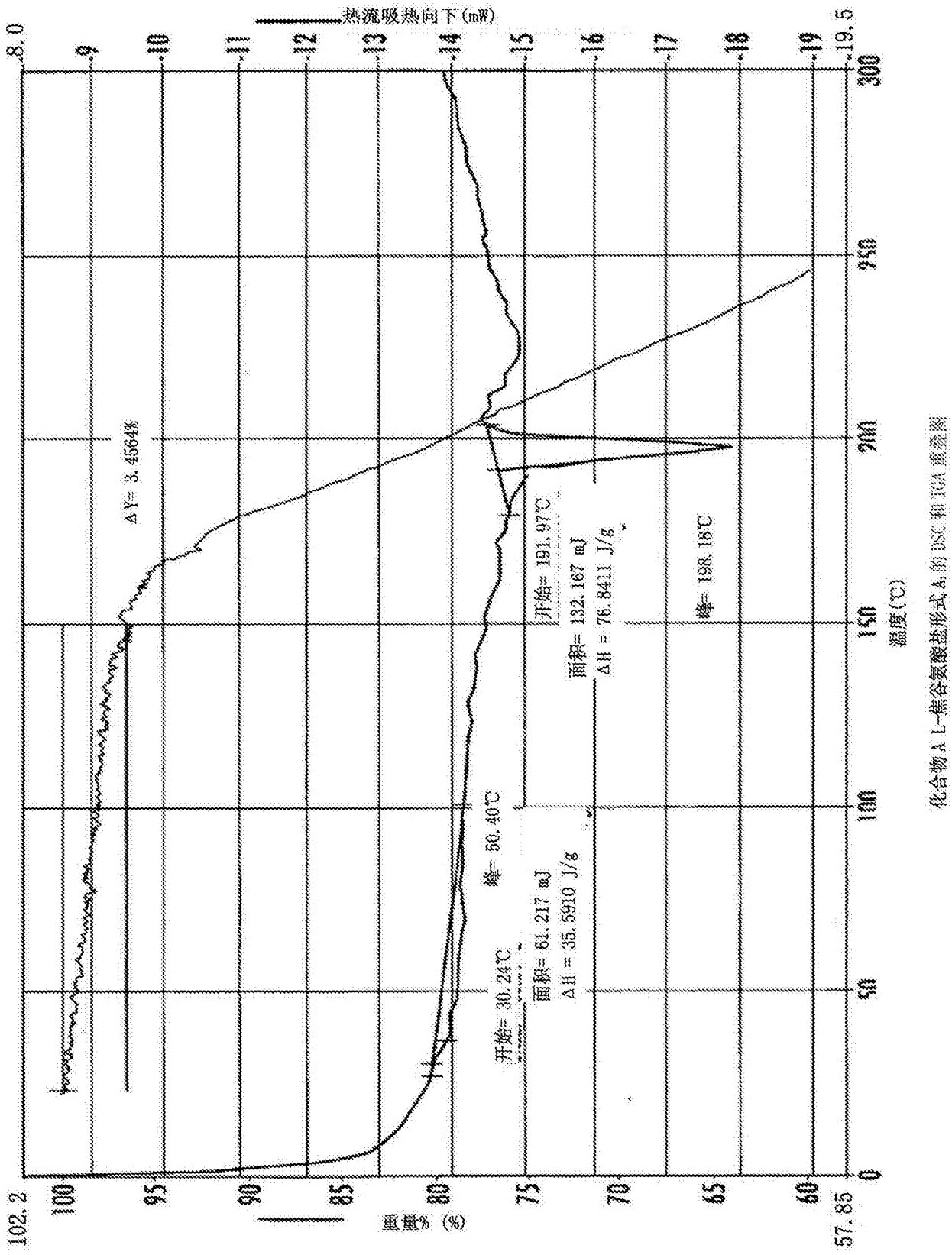
热流吸热向下(mW)
重量% (%)
温度(℃)
ΔY= 3.45648
开始= 30.24℃
峰= 50.40℃
面积= 61.217 mJ
ΔH = 35.5910 J/g
开始= 191.97℃
面积= 132.167 mJ
ΔH = 76.8411 J/g
峰= 198.18℃
化合物A L-焦谷氨酸盐形式A1的DSC和TGA重叠图

图23

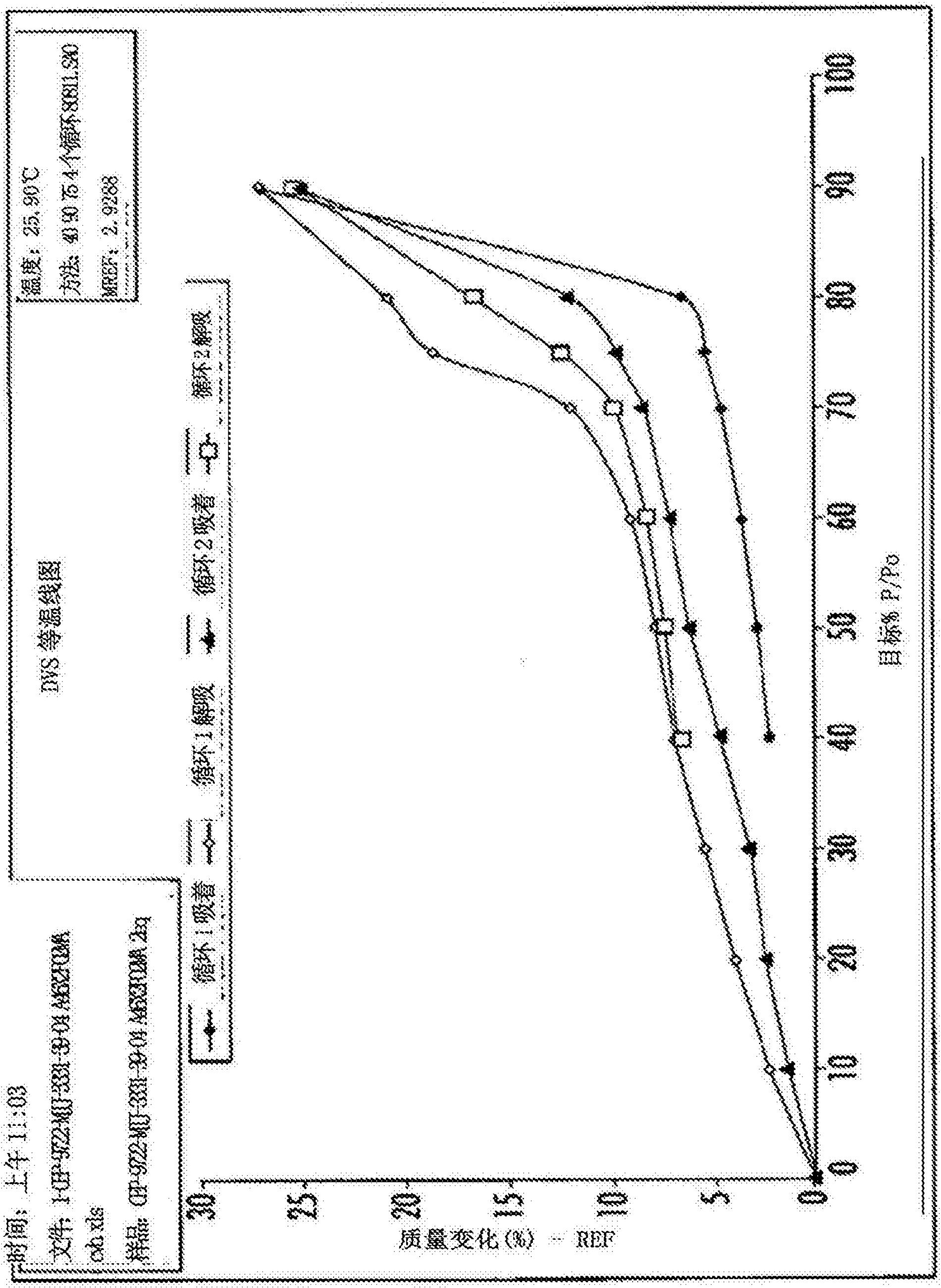

40% RH 吸收		75% RH 吸收		总吸收 90% RH		等温线
循环1	循环2	循环1	循环2	循环2	循环1	可逆
2.28	4.65	5.50	9.83	27.07	25.42	

化合物A L-焦谷氨酸盐形式A₁的DVS

图24

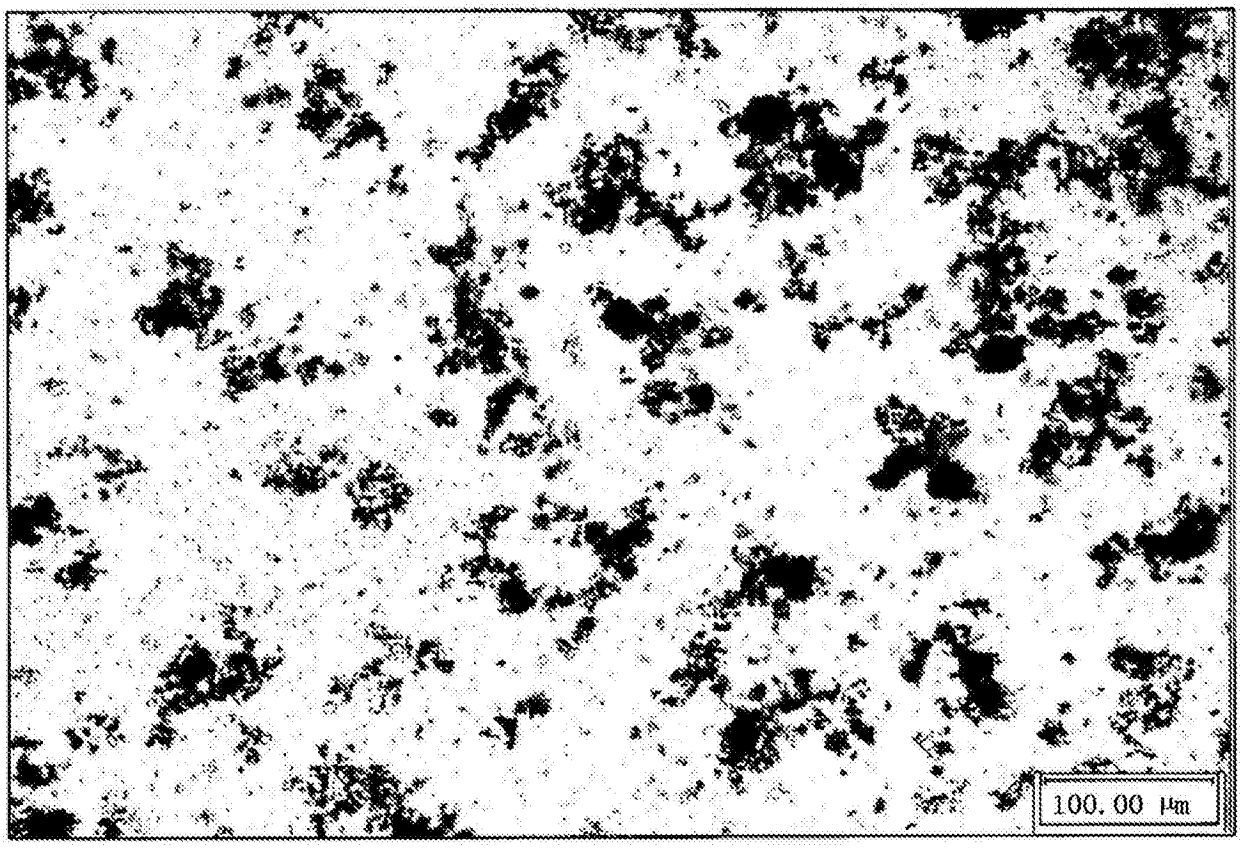

化合物A L-焦谷氨酸盐形式A1的显微照片

图25

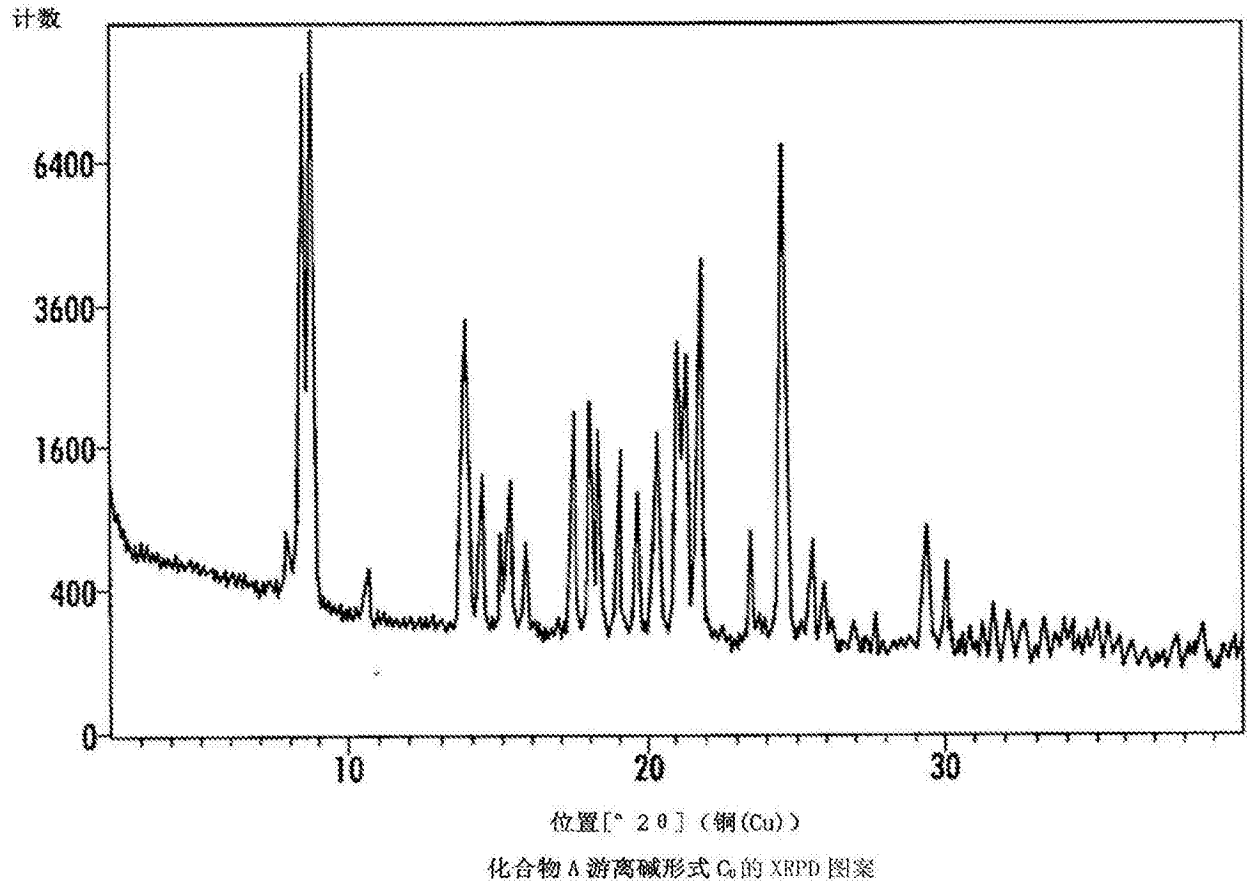

化合物A游离碱形式C_0的XRPD图案

图26

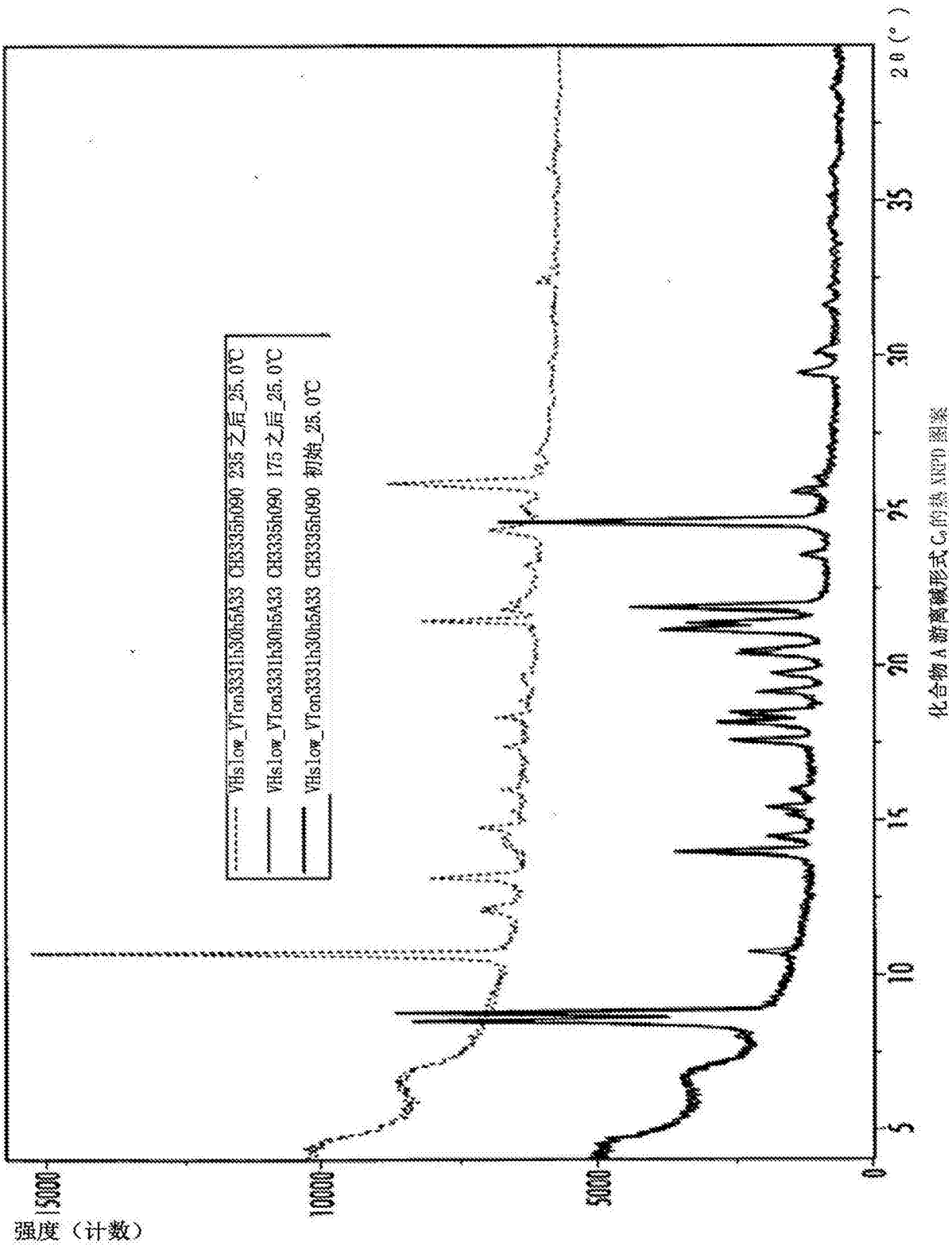
VHsLow_VTon3331h30h5A33 CH335h090 235 之后_25.0℃
VHsLow_VTon3331h30h5A33 CH335h090 175 之后_25.0℃
VHsLow_VTon3331h30h5A33 CH335h090 初始_25.0℃
强度（计数）
2θ(°)
化合物 A 游离碱形式 C_6 的热 XRPD 图案

图27

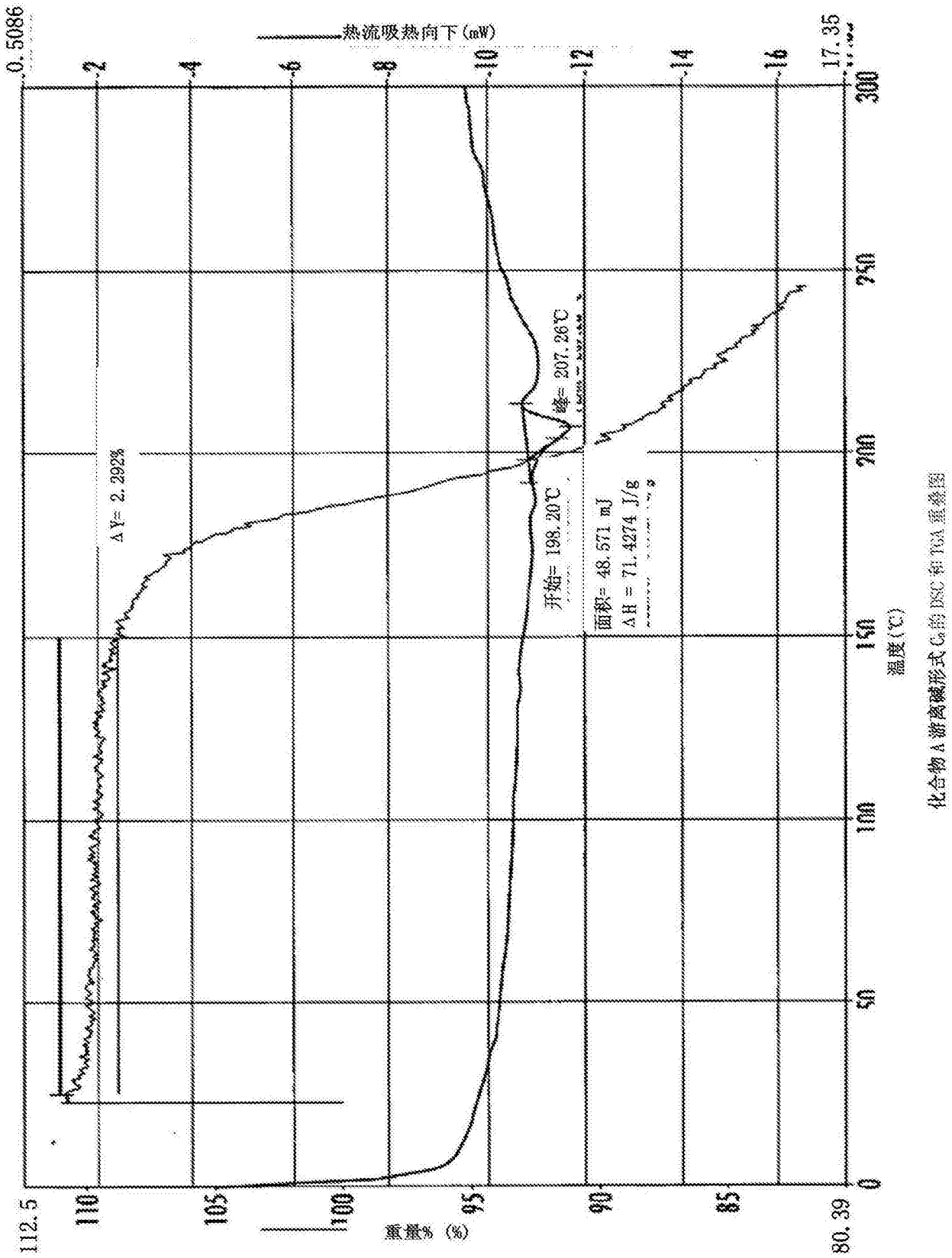
热流吸热向下(mW)
0.5086
17.35
ΔY= 2.292%
峰= 207.26℃
开始= 198.20℃
面积= 48.671 mJ
ΔH = 71.4274 J/g
112.5
80.39
重量% (%)
温度(℃)
化合物A游离碱形式C6的DSC和TGA重叠图

图28

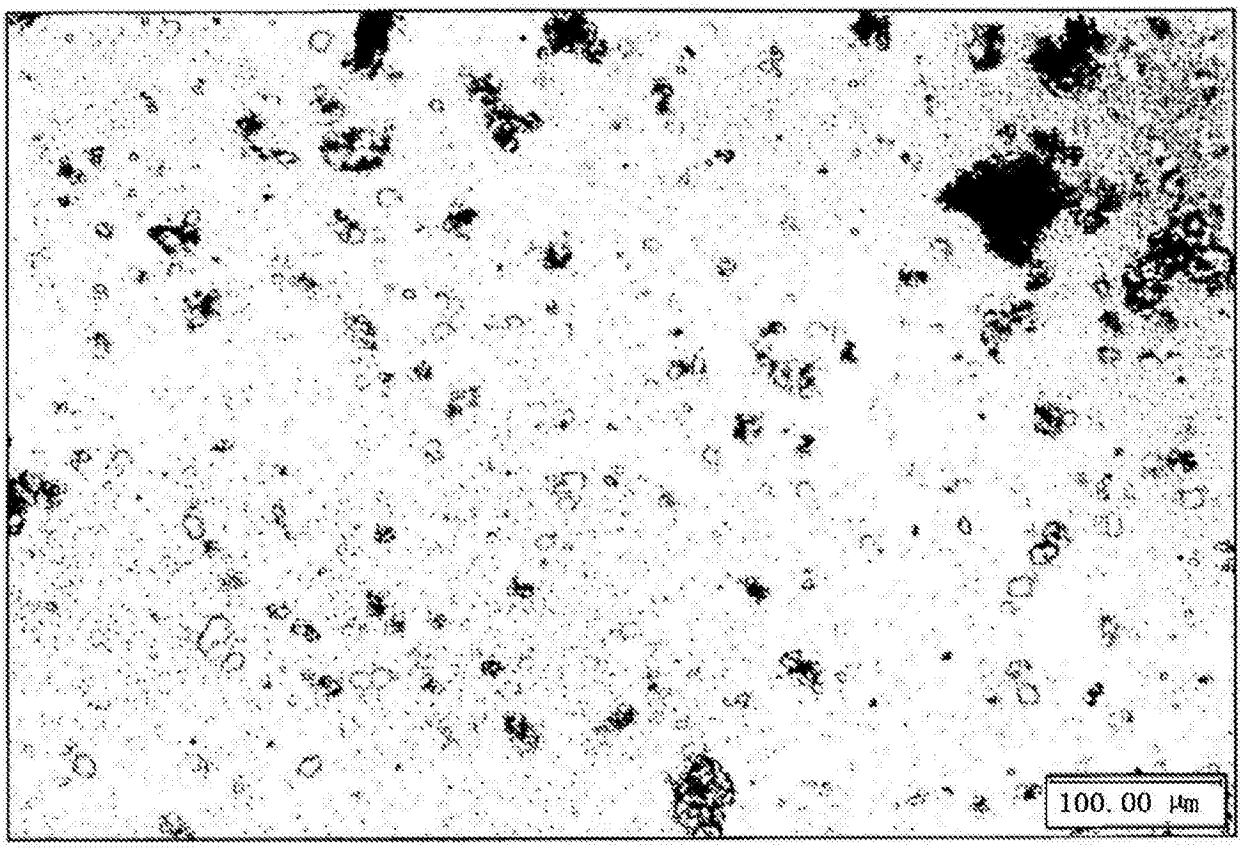

化合物A游离碱形式C₆的显微照片

图29

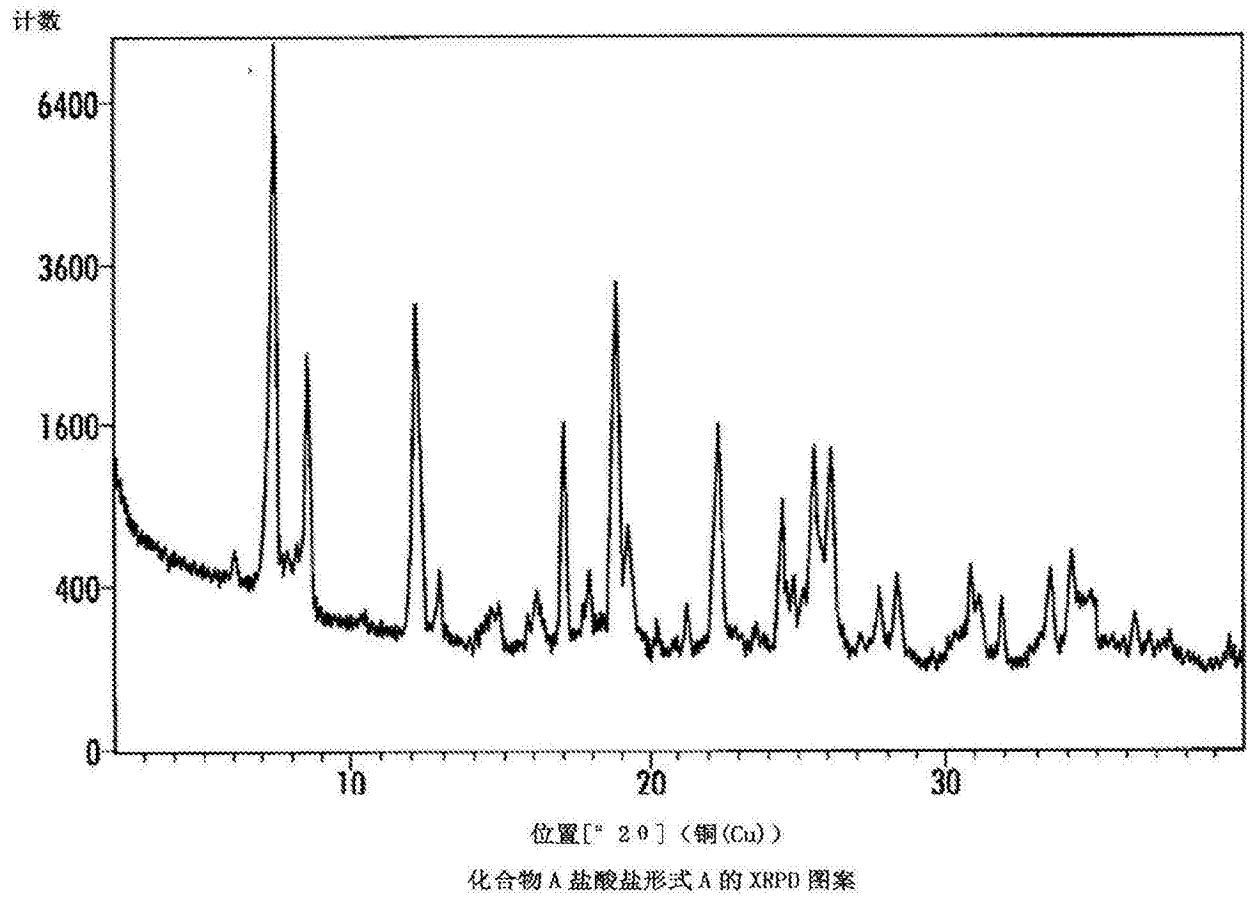

图30

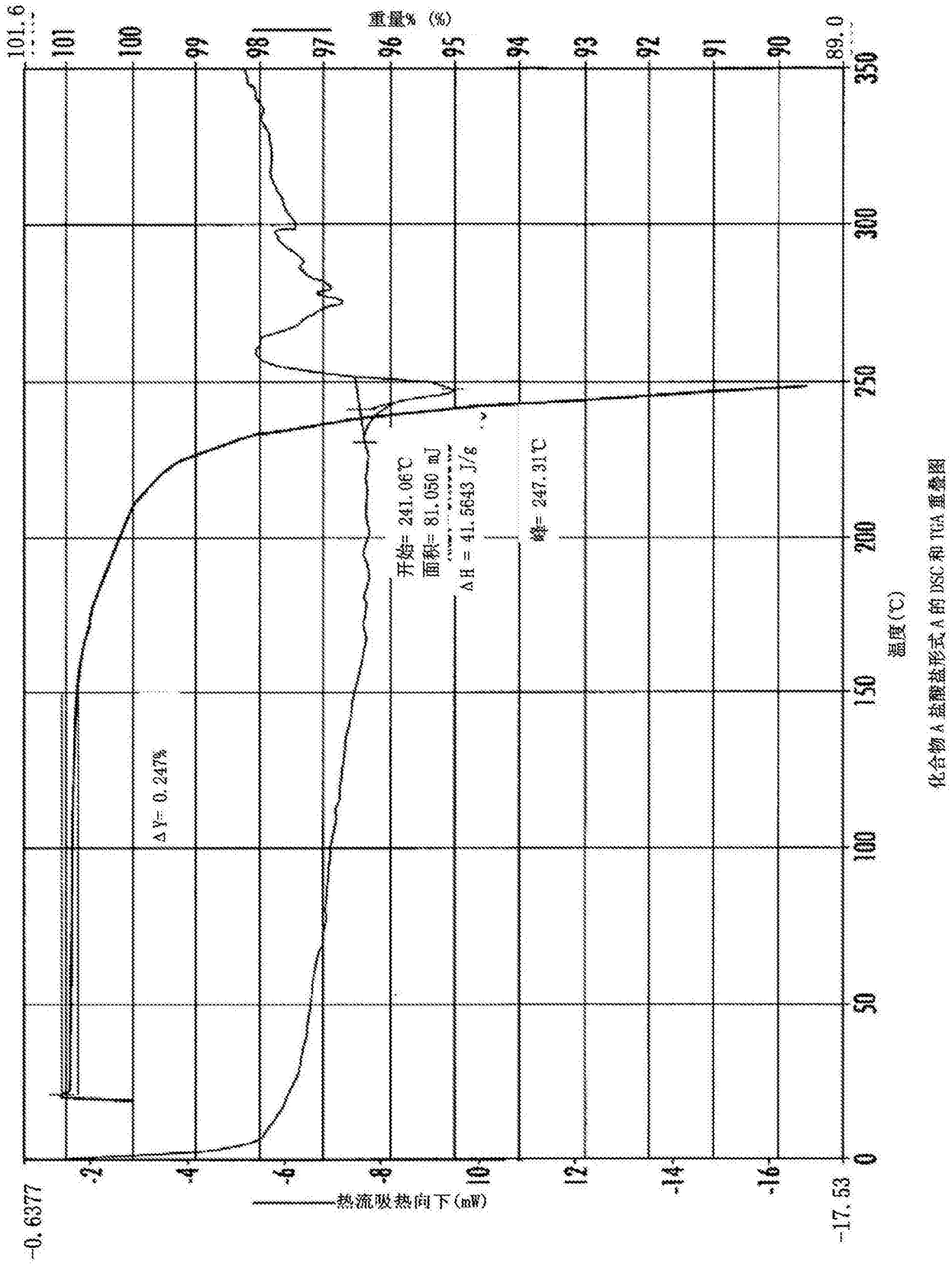
重量% (%)
101.6
101
100
99
98
97
96
95
94
93
92
91
90
89.0
350
300
250
200
150
100
50
0
温度(℃)
-0.6377
-2
-4
-6
-8
-10
-12
-14
-16
-17.53
热流吸热向下(mW)
ΔY= 0.247%
开始= 241.08℃
面积= 81.050 mJ
ΔH = 41.6643 J/g
峰= 247.31℃
化合物A盐酸盐形式A的DSC和TGA重叠图

图31

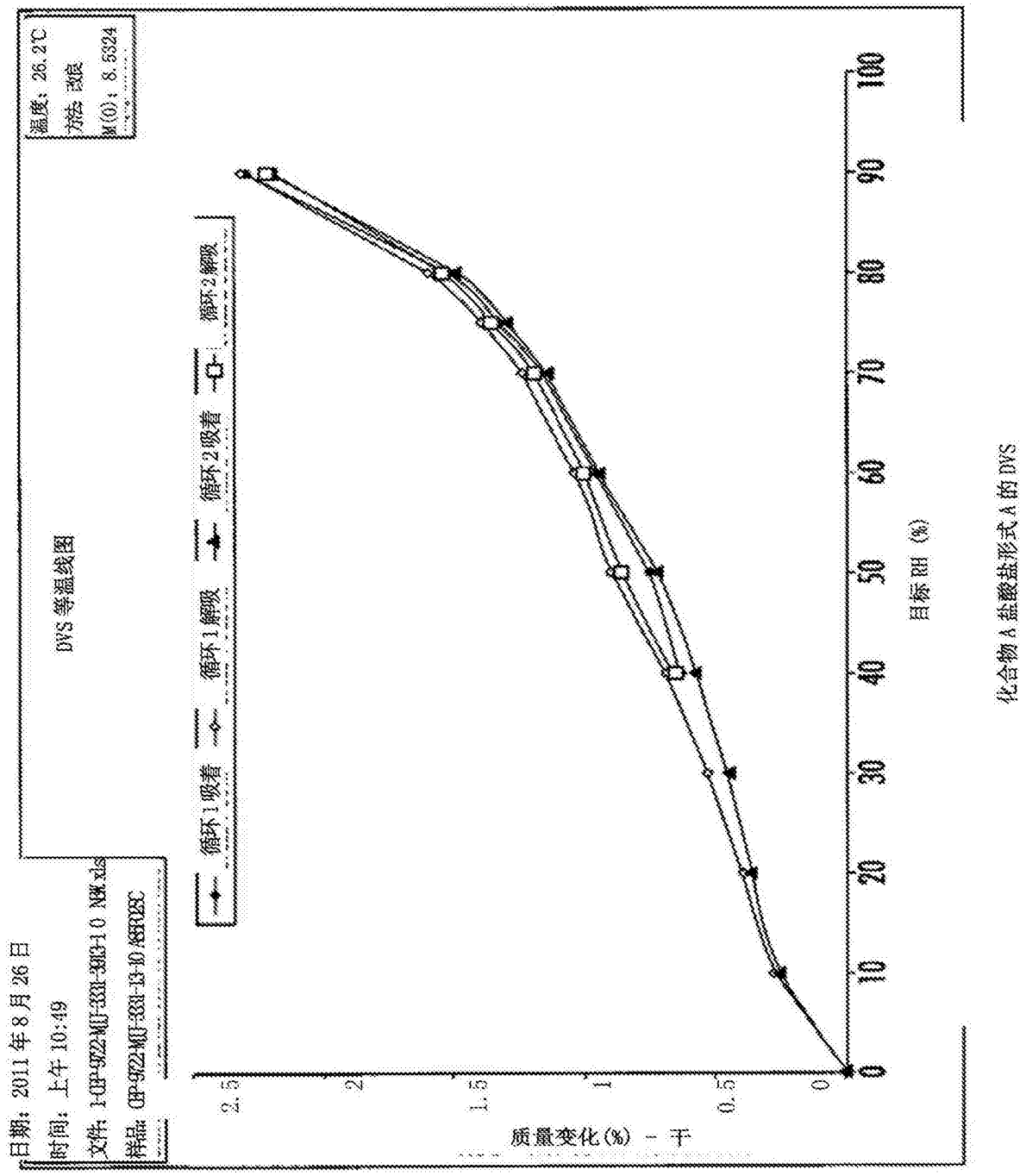
温度：26.2℃
方法 改良
m(0)：8.5324
DVS 等温线图
循环1吸着
循环1解吸
循环2吸着
循环2解吸
日期：2011年8月26日
时间：上午 10:49
文件：1-DP-9722-MJF-333I-303-1-0 NMX.xls
样品：DP-9722-MJF-333I-13-10 A6810SC
质量变化(%) - 干
目标 RH (%)
化合物A盐酸盐形式A的DVS

图32

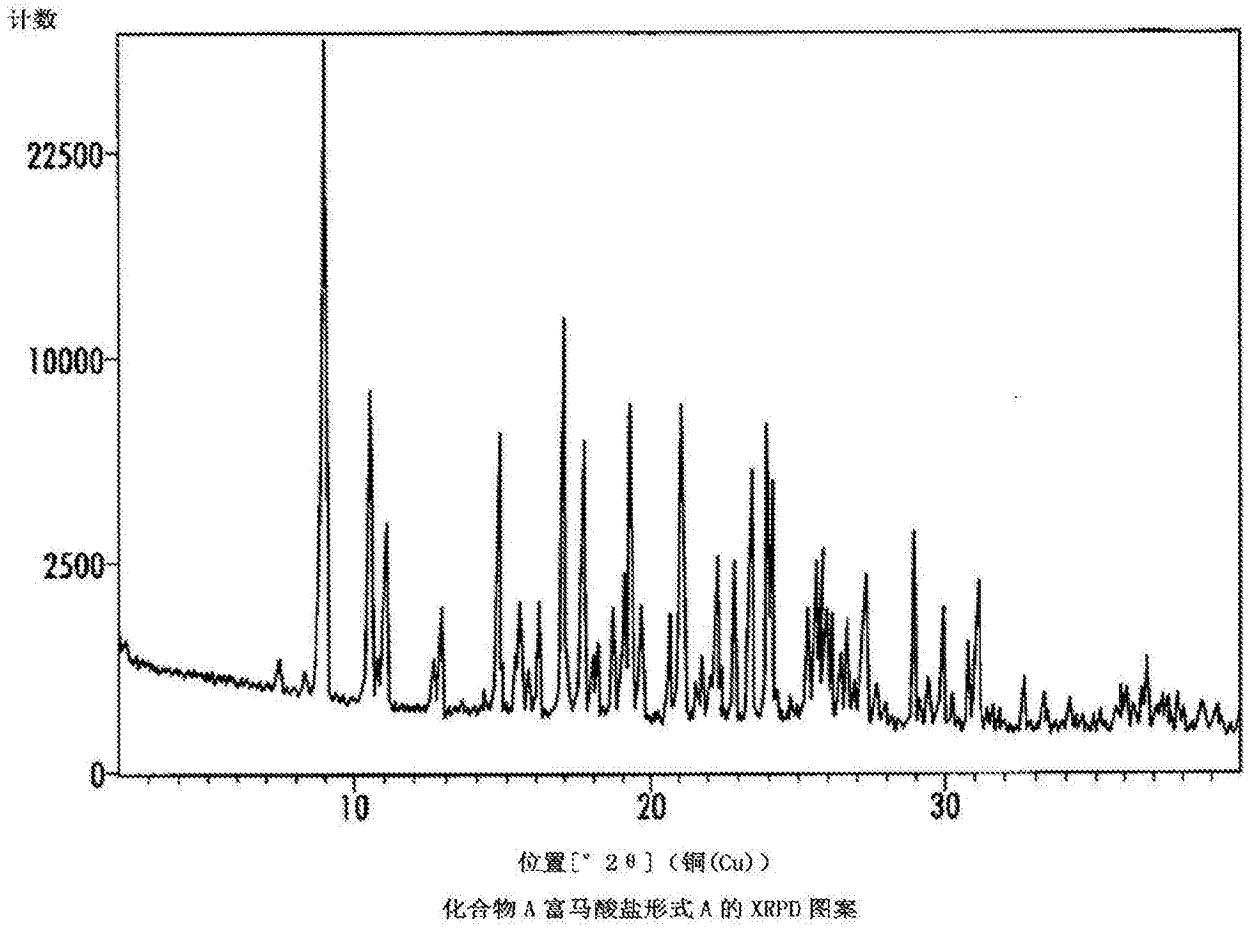

图33

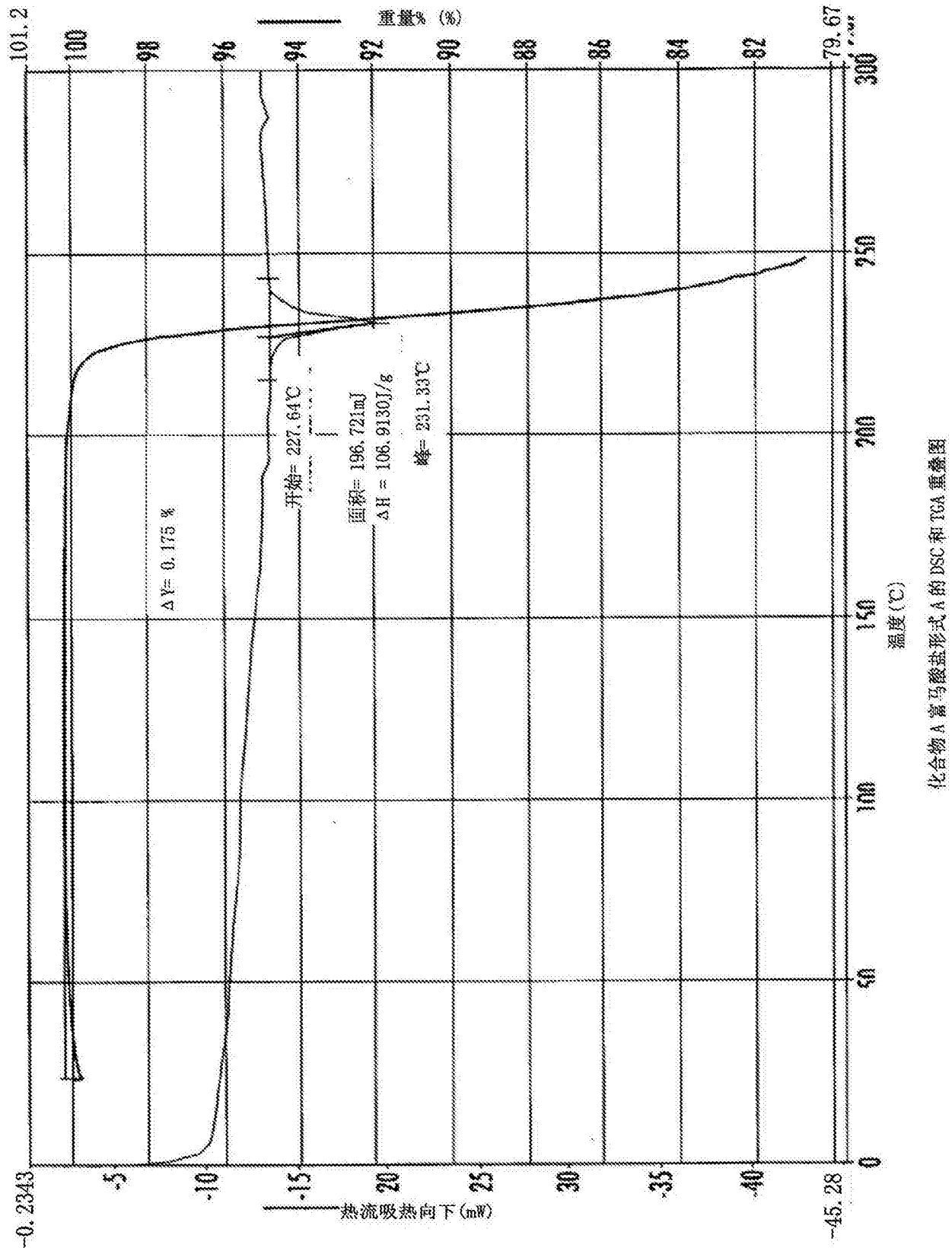
101.2
重量% (%)
79.67
ΔY= 0.175 %
开始= 227.64℃
面积= 196.721mJ
ΔH = 106.9130J/g
峰= 231.33℃
-0.2343
热流吸热向下(mW)
-45.28
温度(℃)
化合物A富马酸盐形式A的DSC和TGA重叠图

图34

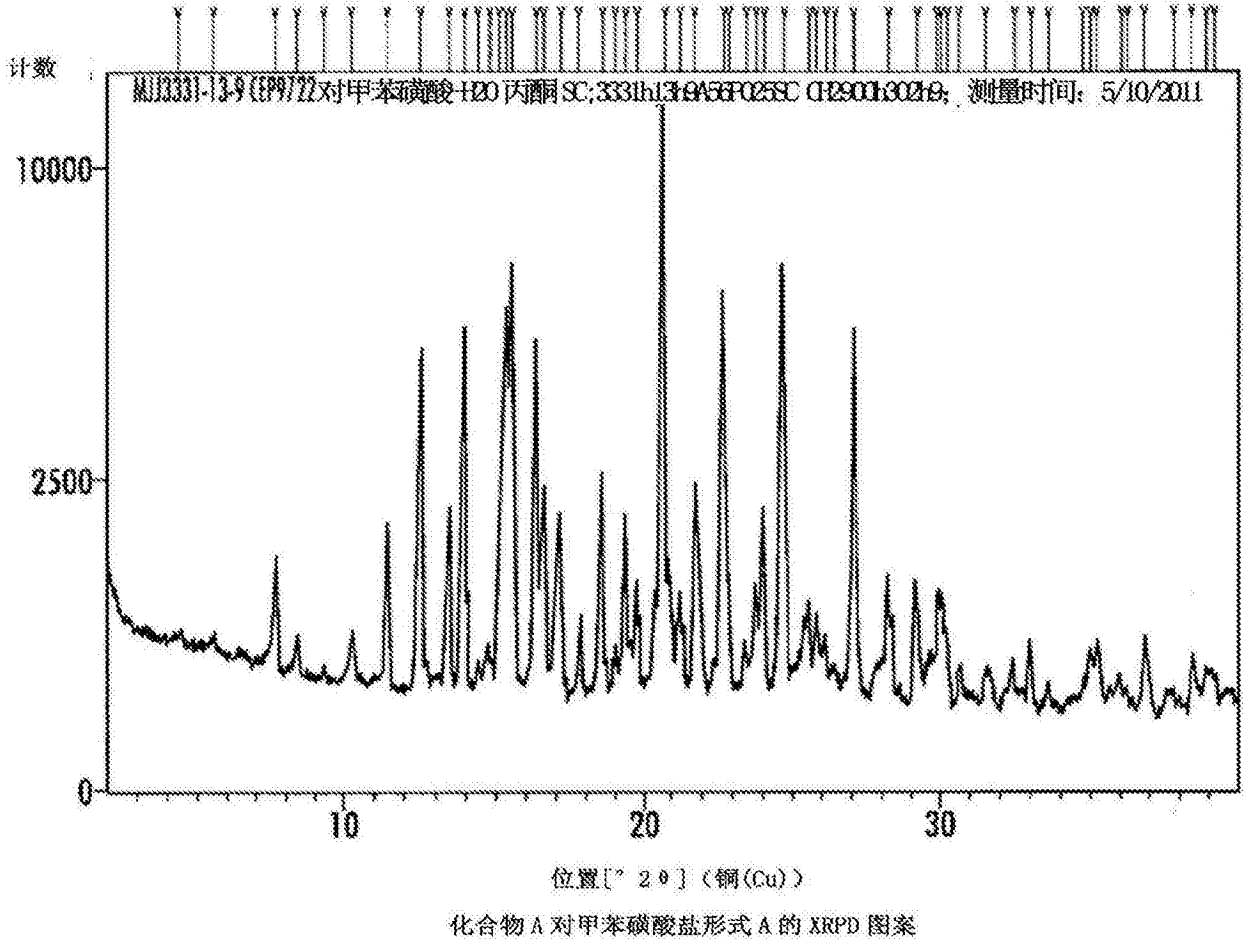

化合物A对甲苯磺酸盐形式A的XRPD图案

图35

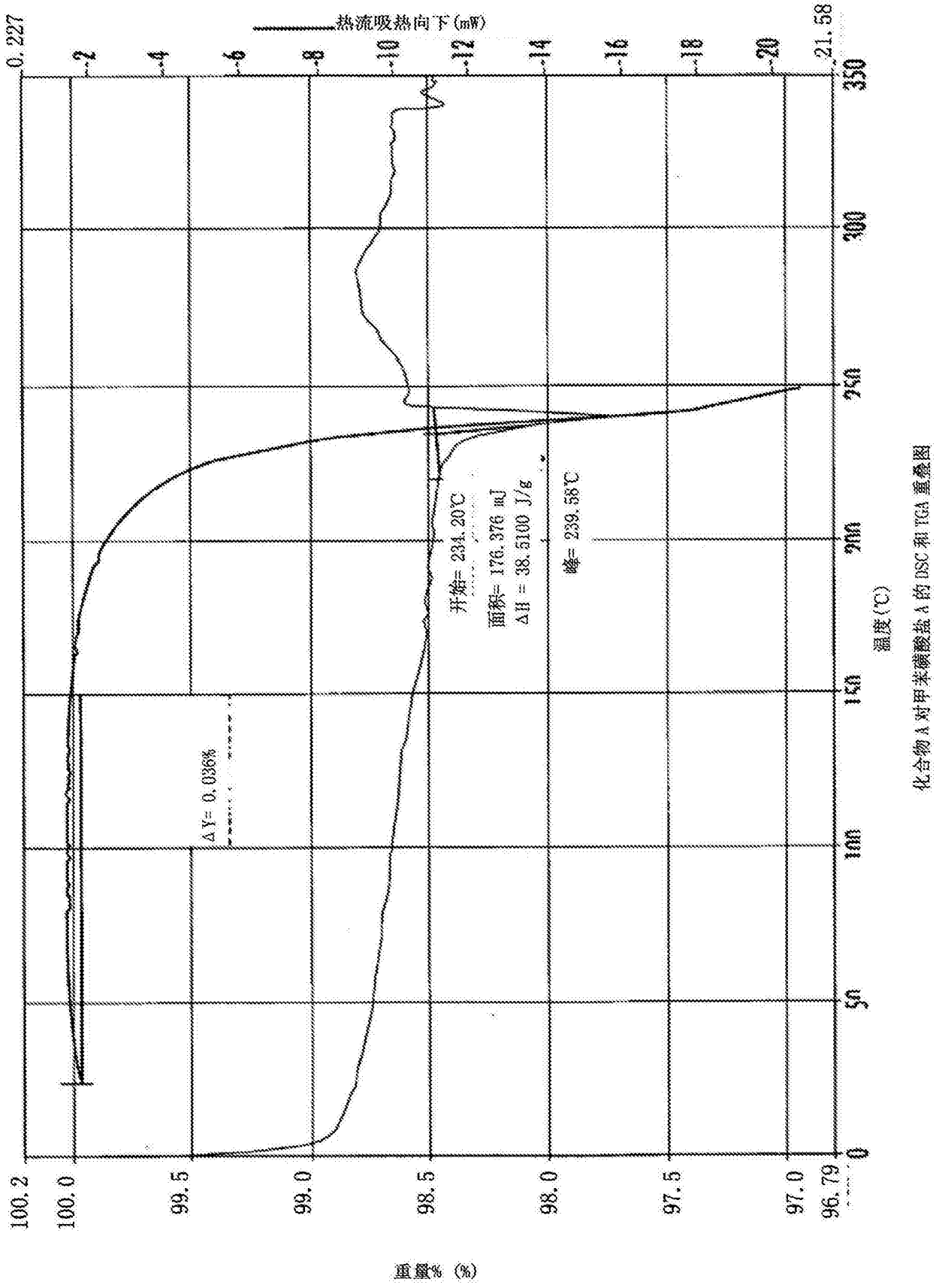
热流吸热向下(mW)
0.227
-2
-4
-6
-8
-10
-12
-14
-16
-18
-20
-21.58
开始= 234.20℃
面积= 176.376 mJ
ΔH = 38.5100 J/g
峰= 239.58℃
ΔY= 0.036%
温度(℃)
0
50
100
150
200
250
300
350
100.2
100.0
99.5
99.0
98.5
98.0
97.5
97.0
96.79
重量% (%)
化合物A对甲苯磺酸盐A的DSC和TGA重叠图

图36

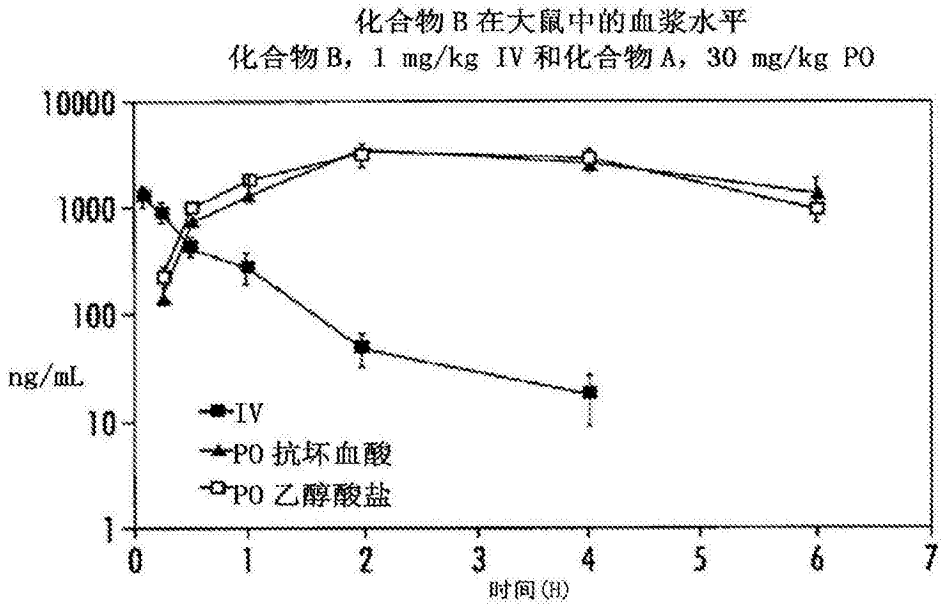

化合物 B	1 mg/kg I.V.	30 mg/kg P.O.	抗坏血酸	乙醇酸盐
t1/2，h	0.7 ± 0.2	C_{max}，ng/mL	3450 ± 377	3538 ± 809
$AUC_{0-\infty}$ ng*h/mL	889 ± 220	t_{max}h	2.3 ± 0.3	2.5 ± 0.5
AUC_{0-t}，ng*h/hmL	905 ± 224	AUC_{0-t} ng*h/mL	13365 ± 1754	13559 ± 2639
Vd，L/kg	1.2 ± 0.1	$AUC_{0-\infty}$，ng*h/hmL	ND	ND
CL，mL/min/kg	23 ± 4	t1/2，h	ND	ND

化合物 B（1 mg/kg 静脉内）、化合物 A 抗坏血酸盐（30 mg/kg 口服）和化合物 A 乙醇酸水合盐（30 mg/kg 口服）在大鼠中的血浆水平。

图37

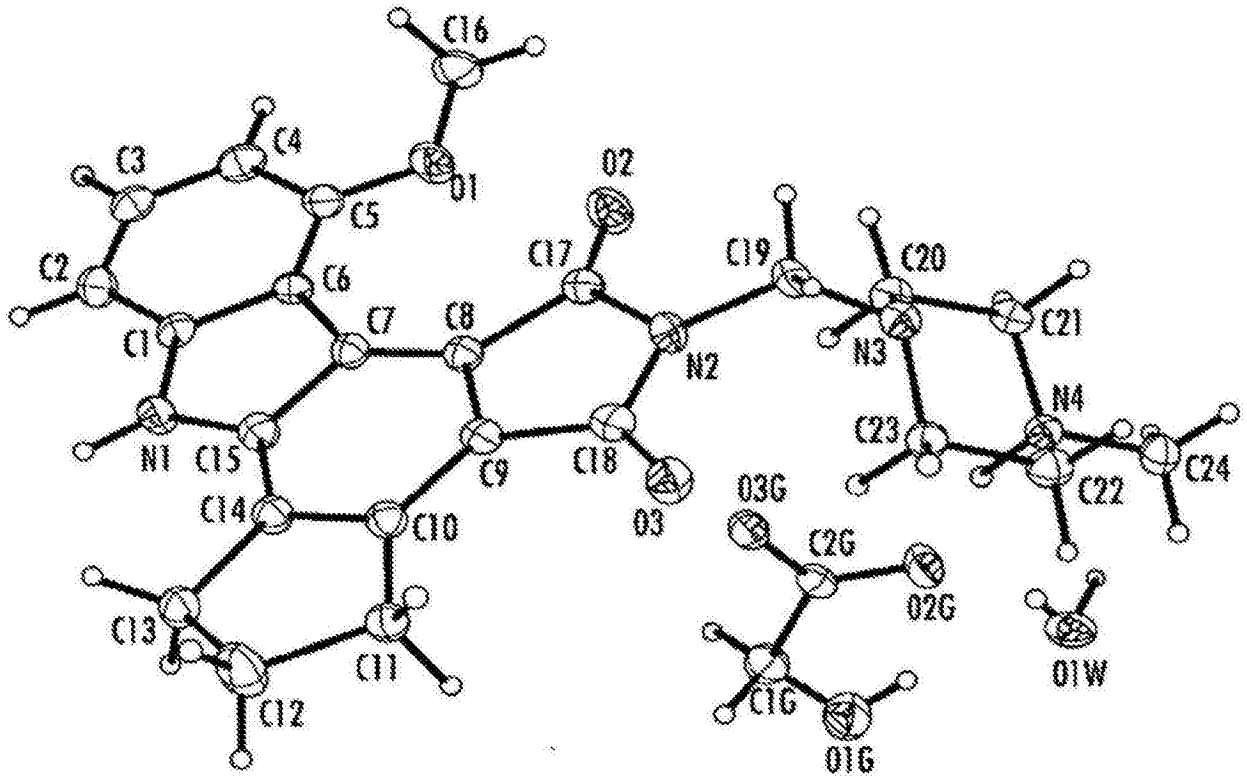

化合物 A 乙醇酸水合盐的单晶结构

图38